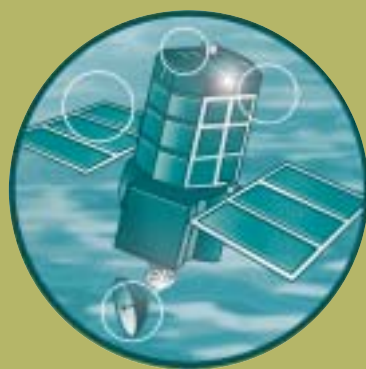# Rainfall-runoff and other modelling for ungauged/low-benefit locations

R&D Technical Report SC030227/SR1

Product Code: SCHO0307BMER-E-P

Environment Agency

defra
Department for Environment
Food and Rural Affairs

The Environment Agency is the leading public body protecting and improving the environment in England and Wales.

It's our job to make sure that air, land and water are looked after by everyone in today's society, so that tomorrow's generations inherit a cleaner, healthier world.

Our work includes tackling flooding and pollution incidents, reducing industry's impacts on the environment, cleaning up rivers, coastal waters and contaminated land, and improving wildlife habitats.

This report is the result of research commissioned and funded by the Environment Agency's Science Programme.

Science at the Environment Agency

Science underpins the work of the Environment Agency. It provides an up-to-date understanding of the world about us and helps us to develop monitoring tools and techniques to manage our environment as efficiently and effectively as possible.

The work of the Environment Agency's Science Group is a key ingredient in the partnership between research, policy and operations that enables the Environment Agency to protect and restore our environment.

The science programme focuses on five main areas of activity:

- **Setting the agenda**, by identifying where strategic science can inform our evidence-based policies, advisory and regulatory roles;

- **Funding science**, by supporting programmes, projects and people in response to long-term strategic needs, medium-term policy priorities and shorter-term operational requirements;

- **Managing science**, by ensuring that our programmes and projects are fit for purpose and executed according to international scientific standards;

- **Carrying out science**, by undertaking research – either by contracting it out to research organisations and consultancies or by doing it ourselves;

- **Delivering information, advice, tools and techniques**, by making appropriate products available to our policy and operations staff.

Steve Killeen

Head of Science

Executive Summary

Across England and Wales, the Environment Agency provides only a general Flood Watch service at locations that are ungauged and associated with low benefit from flood warning. Providing an improved, more targeted flood warning service is possible. But strategic guidance is needed on the technical possibilities available: both now as "best practice" and, through the identification of research opportunities, in the future.

Against this background, this report provides an overview of approaches for modelling at ungauged locations to guide operational practice both now and in the future. The emphasis is on the types of modelling problem commonly encountered and the general approaches that can be considered when addressing them. Whilst rainfall-runoff models are the main focus of attention, broader discussion encompasses hydrological channel flow routing models and hydrodynamic river models; simpler empirical models including level-to-level correlation methods are also considered.

Even for specific rainfall-runoff model types, it is unusual for a methodology to be sufficiently well established for its application to be routine for ungauged forecasting purposes. The overview first focuses on the nature of the ungauged problem and the modelling approaches available when considered at a generic level. Subsequent discussions of specific model types serve to illustrate how some of these approaches have been applied and their shortcomings. Possible opportunities for improvement are identified.

An important aspect of ungauged modelling is the ability to utilise digital spatial datasets on properties of the terrain, land cover, soil and geology that will influence the hydrological response. The more useful datasets for use in modelling are identified.

Although not a natural choice for application to ungauged locations, the scope for using purely statistical (empirical) modelling approaches, such as level-to-level and structure function methods, is considered. Similarly, the application of real-time updating techniques at ungauged locations is not immediately obvious, but a number of methods of transferred-error updating are considered as deserving of future attention.

More broadly, the opportunities for improved flood warning for ungauged locations relating to advances in monitoring and uncertain triggers for warning are considered. Topics addressed encompass improved methods of areal rainfall estimation, remote-sensing of land surface properties and river height and width, stage-discharge curve derivation, and flood warning trigger mechanisms incorporating uncertainty and costs of alternative actions.

The report closes with an overview of the operational guidelines for modelling at ungauged locations, providing a convenient synthesis of the main issues and approaches. It also provides, through reference to a more detailed appendix, case study illustrations of selected methods of model transfer to ungauged locations. A set of specific conclusions and recommendations are then identified. Some closing remarks highlight ongoing national and international research activities of relevance to flood forecasting and warning for ungauged locations.

Contents

List of Figures

List of Tables

1 Introduction

1.1 Introduction

Across England and Wales, the Environment Agency provides only a general Flood Watch service at locations that are ungauged and associated with low benefit from flood warning. Providing an improved, more targeted flood warning service is possible. But strategic guidance is needed on the technical possibilities available: both now as "best practice" and, through the identification of research opportunities, in the future.

Against this background, this report aims to provide an overview of approaches for modelling at ungauged locations that can help guide Environment Agency operational practice both now and in the future. The emphasis is on the types of modelling and forecasting problem commonly encountered and the general approaches that can be considered when addressing them. Whilst rainfall-runoff models are the main focus of attention, broader discussion encompasses hydrological channel flow routing models and hydrodynamic river models; simpler empirical models including level-to-level correlation methods are also considered.

Even for specific rainfall-runoff model types, it is unusual for a methodology to be sufficiently well established for its application to be routine for ungauged forecasting purposes. The overview first focuses on the nature of the ungauged problem (Section 2) and the modelling approaches available when considered at a generic level (Section 3). Subsequent discussions of specific model types in Section 4 serve to illustrate how some of these approaches have been applied and their shortcomings. Possible opportunities for improvement are identified.

An important aspect of ungauged modelling is the ability to utilise digital spatial datasets on properties of the terrain, land cover, soil and geology that will influence the hydrological response. The more useful datasets for use in modelling are highlighted in Section 5.

Although not a natural choice for application to ungauged locations, the scope for using purely statistical (empirical) modelling approaches, such as level-to-level and structure function methods, is considered in Section 6. Similarly, the application of real-time updating techniques at ungauged locations is not immediately obvious, but a number of methods of transferred-error updating are considered in Sections 7 and 8 as deserving of future attention.

In Section 9, the opportunities for improved flood warning for ungauged locations relating to advances in monitoring and uncertain triggers for warning are considered in broad terms. Topics addressed encompass improved methods of areal rainfall estimation, remote-sensing of land surface properties and river height and width, stage-discharge curve derivation, and flood warning trigger mechanisms incorporating uncertainty and costs of alternative actions.

Section 10 gives an overview of the operational guidelines for modelling at ungauged locations, providing a convenient synthesis of the main issues and approaches discussed in the report. Through reference to a more detailed appendix, Section 10 provides illustrations of the practical application of selected methods of model transfer to ungauged locations using case studies from upland and lowland Britain.

A set of specific conclusions and recommendations are identified in Section 11. Some closing remarks highlight ongoing national and international research activities of relevance to flood forecasting and warning for ungauged locations.

2 Classes of problem for ungauged locations

2.1 Introduction

An 'ungauged' catchment is usually taken to be one for which there are limited data available and no measurement of discharge. This usually implies that there is insufficient data for fitting a hydrological model, for updating the model with measured discharge, and for issuing a flood forecast.

2.2 Terminology and data considerations

Real-time flood forecasting for sites that are considered "ungauged" requires consideration of many different aspects. Flood forecast model accuracy is highly dependent on the availability of both historical and real-time data. When some or all of these data are missing, it can be helpful to look to similar sites nearby for which more data are available. The availability of data at *neighbouring sites* is then an additional consideration. Hence, the task of modelling for ungauged catchments requires consideration of data availability for more than one site.

It is useful to consider the availability of:

- on-site historical data for model calibration
- on-site real-time data for model updating
- historical and real-time data at a neighbouring site.

The availability or otherwise of different types of measurement at target and neighbouring sites can lead to a seemingly complex choice of modelling procedure. By way of guidance, Figure 2.1 presents a flowchart highlighting which modelling procedures make the best use of the available data at the target and neighbouring sites.

The recommendations are most straightforward when there is a full set of data available for model calibration and updating, as indicated in the left hand-side of the flowchart. However, this situation does not require the use of modelling techniques for ungauged sites, and has only been included for completeness.

When historical data are available but there is no on-site telemetry for real-time updating, the *process model* may be calibrated for the site, but the user may need to look to neighbouring sites (rivers) for real-time telemetry. If good quality telemetry is available nearby, on-site discharge estimates can be inferred leading to a pseudo-updating scheme for the site. Similarly, if there is no historical data on-site suitable for calibrating the process model, *process model* parameters may be inferred from a model fitted to a nearby catchment.

Although the flowchart indicates which set of modelling approaches makes best use of available data, it does not provide guidance on *which* model to use. This will be discussed in Section 3, which aims to provide guidance on the best model to use for different hydrological situations.
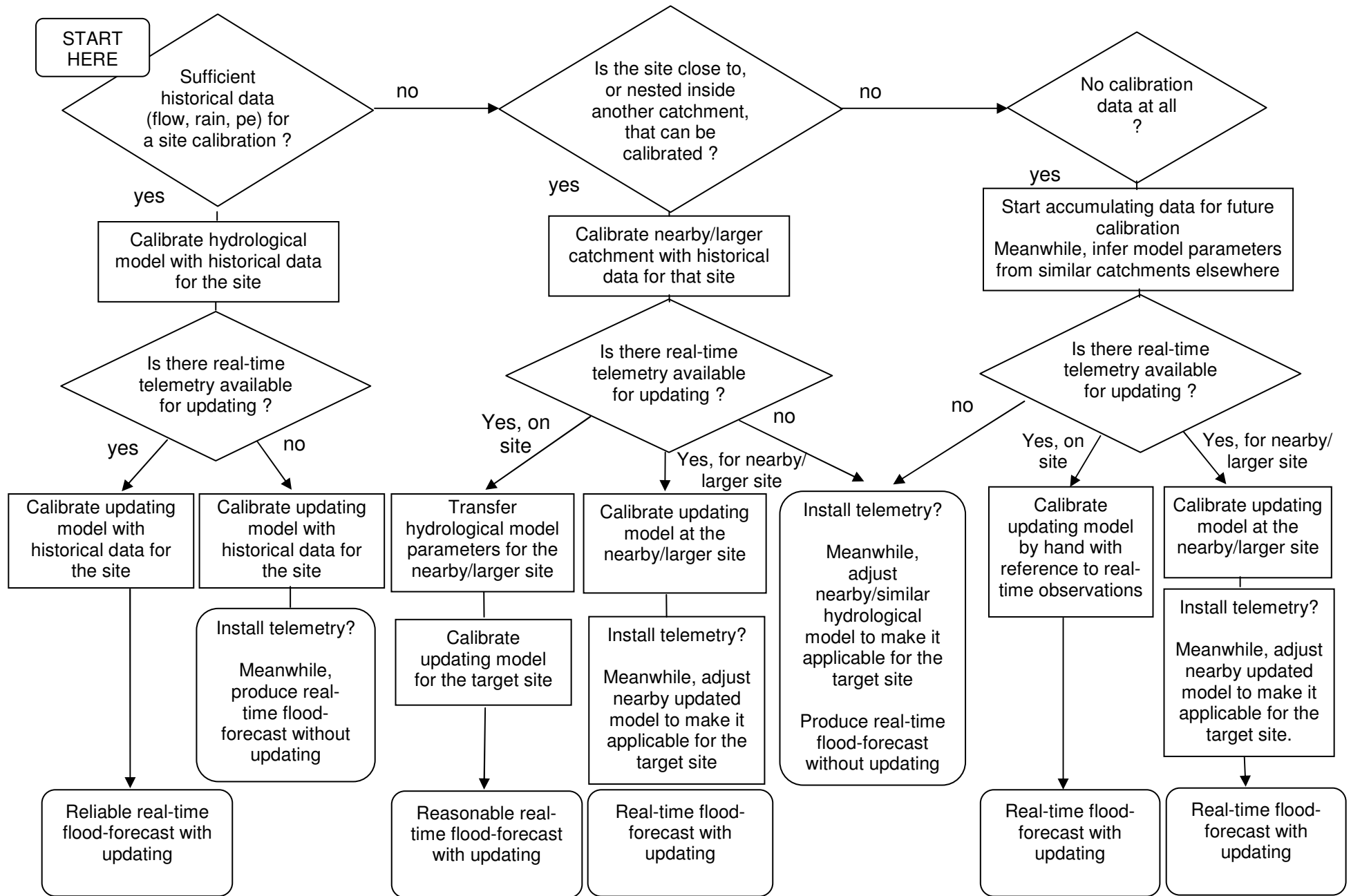
Figure 2.1 Flowchart highlighting modelling needs in response to different levels of data availability

A summary of data requirements and considerations is presented in Table 2.1. It is worth remembering that accurate measurement of all but river level is difficult to achieve, and that many of these data types may be considered to be 'ungauged'. However, in practice, sensible approximations leading to reasonable model accuracy is attainable.

Note that in hydrometric applications the terms "gauged" and "ungauged" can be used to distinguish sites where an adequate stage-discharge curve has been constructed. For real-time forecasting, this distinction is not an overwhelming consideration, as it is now common to fit an unknown stage-discharge relation as part of the model-calibration process. The calibration process ensures that good forecasts are obtained of directly observable quantities such as river level, while the model provides estimates of modelled flows.

Table 2.1 Data considerations for modelling ungauged catchments

Data requirement	Example data types	Issues/comments
Long-term data records for model calibration	- Flow - Level - Rainfall measurement from: - Nearby raingauges - Radar rainfall measurement - Other remotely sensed rainfall	Flow is less routinely measured directly but can be estimated using a stage-discharge relation. Catchment rainfall can be estimated from a number of sources by various methods.
Telemetered real-time observations for updating	- Levels - Flow derived from observed level - Flow (e.g. ultrasonic)	Routinely measured Less routinely measured

2.3 Modelling approaches

The need to consider data at neighbouring sites also impacts on the modelling, which must therefore be extended to include other sites. Transferring modelling information (parameters or data) from one site to another in this way leads to *indirect modelling* of the target site. In the context of forecasting for locations with poor data availability, the target site (catchment) may lie within the model extent of a larger site which has better data-availability. This approach can be useful when modelling river reaches affected by backwater effects, and is widely used in hydrodynamic modelling, where it is common to deal with many target sites within a single model. It has also been used, for example, within the River Flow Forecasting System configuration for Northeast Region to create a forecast of flow at a target location by abstracting the modelled flow at a node within a model calibrated over a longer reach. Figure 2.2(b) illustrates some of the possible ways in which model information can be transferred between sites. Information leading to a flood forecast at the target site (indicated by a cross) is assumed to be transferred from a neighbouring, nested, or larger site (indicated by a solid circle).

There is clearly considerable potential in extending the indirect modelling approach to distributed rainfall-runoff models which typically apply modelling concepts on a grid covering a region. Specifically, there is some hope that the physical conceptualisation
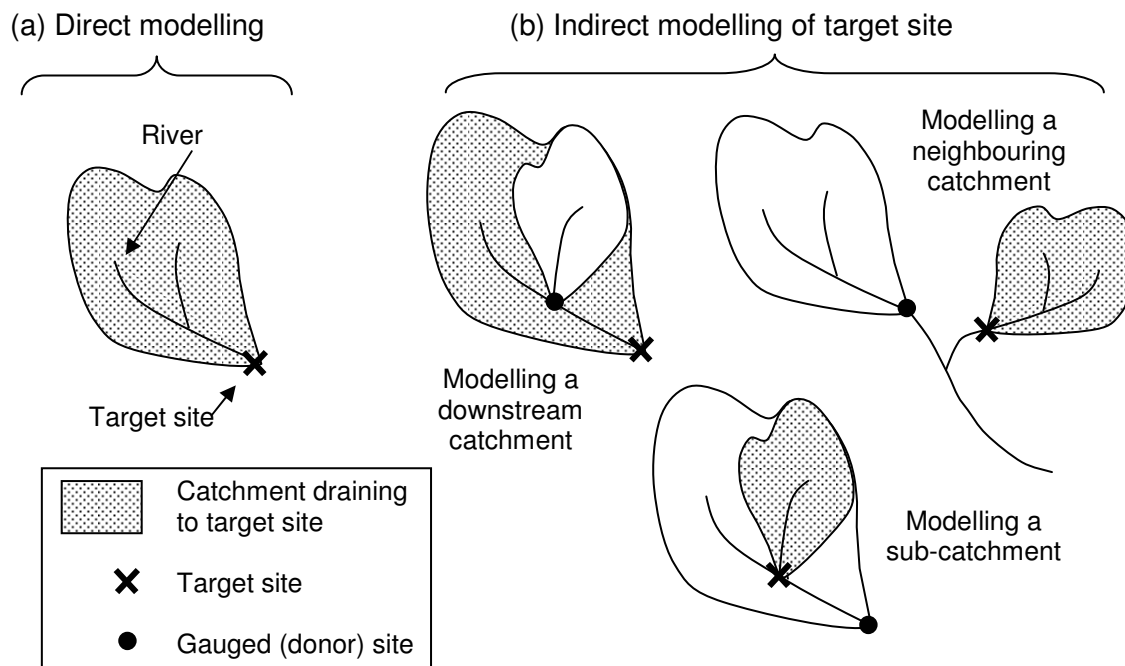
Figure 2.2 Direct and indirect modelling of a catchment, downstream catchment, neighbouring catchment or sub-catchment

of these models will allow modelled *flows* at internal locations to perform well. However, the creation of modelled *river-levels* can be more problematic. Although an indirect hydrological modelling approach may be used as an interim measure to overcome problems of data-availability, the longer-term aim should be to replace it with a dedicated model that has the target location as its outlet. This will, of course, require the accumulation of historical data for model calibration.

A summary of modelling considerations is presented in Table 2.2. This includes hydrodynamic and other models in addition to rainfall-runoff models. The table also highlights that the models can be applied directly to the target site, or indirectly, through measurement and model application at another site. The method used to transfer information, such as model parameters or data, from the indirectly modelled site to the target site has been termed the *Inference model*. Common examples of inference models include forms of parameter regionalisation (sometimes called parameter generalisation) discussed later in Section 3.3.2. The Thiessen polygon method, and other methods used for estimating catchment average rainfall from a network of raingauges, can also be thought of as inference models.

Table 2.2 also includes the idea of *inferred error prediction* which would be an extension of the basic error prediction approach. This arises in the context of indirect modelling in cases where there is no telemetry data for the target site but where telemetry data are available for updating the overall indirect model. Possibly the best approach in this situation would be to apply some form of internal state-correction across the model. Nonetheless, there is potential in the idea of making a more direct inference about the errors at the target location from model-errors at locations where telemetry exists. This methodology may be limited by the lack of data for calibrating the updating model in cases such as this. Another possibility is to use 'best-guess' values for the parameters of the updating model. These limitations suggest that inferred error prediction should employ heavily down-weighted errors, except where the target ungauged locations is close to a gauged one and where there is no intervening major source of lateral inflow.

Table 2.2 Modelling considerations for the ungauged case

Model type	Varieties
Process Model	• Direct Hydrological models (lumped rainfall-runoff, flow routing) • Indirect Hydrological models (distributed rainfall-runoff, flow routing) • Hydrodynamic models • Level-to level correlation of peaks • Black box models (e.g. transfer functions) • Simple combination of forecast-sources
Inference model	Model uses transfer information from one site to another • Parameter inference • Data inference (eg flow, rainfall) • Inferred error-prediction

Updating model	• Model-state correction, based on error of forecasts
	   o applied to internally represented storages
	   o applied to internally represented flows/levels
	• Error-prediction for Direct modelling
	   o applied to flows or levels, with forecasts converted to levels if necessary
	• Inferred Error-prediction for Indirect modelling
	   o applied to flows, with forecasts converted to levels if necessary
	   o applied to levels

When developing suitable modelling approaches, it is also important to consider whether the forecasts are needed specifically for flood warning purposes (emphasising forecasts of levels) or for use as model-inputs to drive forecasting models for other locations (emphasising forecasting of flows).

3 Modelling approaches for ungauged locations

3.1 Choice of modelling approach

Influence of catchment type

The nature of the catchment will influence the choice of modelling approach to use. Considerations include catchment size, location within a river basin (headwater, middle reach, lower reach), steepness and the influence of tides, backwater or river gate controls. Modelling options for a variety of catchment-types are presented in Table 3.1, working downstream from small headwater catchments to tidal regions. Major rivers are distinguished from minor tributaries, the latter being less likely to be gauged except near the confluence with major rivers. In addition, it is important to consider whether the catchment is rural or urbanised. It can be helpful to forecast the faster, more localised response of urban catchments separately to the rest of a catchment.

Headwater catchments of small or moderate size are natural candidates for rainfall-runoff models using transferred parameters, or scaled versions of model forecasts from neighbouring or similar catchments.

Techniques for use on the middle to lower reaches of more major rivers may vary from simple level-to-level correlation methods or hydrological storage-routing models (extrapolated from gauged sites), to hydrodynamic river models (using survey data for configuration and model parameters transferred from "similar" gauged reaches).

Tidally-influenced rivers may use hydrodynamic approaches or simpler tabular forecasts linked to observations and tide/surge predictions at gauged locations along the river, estuary or coast.

Distributed hydrological models have the ability to mix rainfall-runoff and routing models in an integrated way to allow a unified transfer of information from gauged to ungauged sites whilst using spatial datasets on terrain, soil, land use and geology to support model configuration. They are potentially flexible to the type of catchments being targeted but may not incorporate the detailed modelling capability of hydrodynamic river models developed for tidal- and backwater-influenced rivers.

Table 3.1 Choice of modelling approach

Catchment type	Suggested modelling approaches	Notes
Headwater (steep)- small upstream areas (<10 km^2)	Consider: *(i) lumped rainfall-runoff model with transferred parameters (ii) distributed hydrological modelling*	Less likely to have relevant gauged location nearby. Overflow from minor or major rivers likely to be limited by steep topography. Locations may be affected by overland flows and possible springs.
Headwater (steep)- moderately sized upstream areas (>10 km^2)	Consider: *(i) lumped rainfall-runoff model with transferred parameters (ii) scaling from nearby location with benefit of updating (iii) distributed modelling (iv) hydrological routing from gauged location upstream*	Fast response times to rain on rural catchment areas. Possibly have relevant gauged location nearby.
Middle and lower catchment	Minor tributaries: *In addition to treatments for headwater areas: (i) override forecast from upstream gauged flows with backwater curve estimate under influence of receiving stream level (ii) possible extension of hydrological models to incorporate backwater effects (iii) extend hydrodynamic model to include tributaries experiencing backwater effects* Major rivers: *(i) level-to-level correlations (ii) hydrological routing from gauged location upstream (iii) hydrodynamic models for special cases, in particular, for* urban reaches	Possibly have relevant gauged location nearby, but also possible backwater effects from major rivers. Likely to have gauged flows upstream.

Catchment type	Suggested modelling approaches	Notes
Mixed Fluvial/Tidal TIDE	Minor tributaries: *(i) tabular forecast based on forecasts for upstream flows and downstream levels* *(ii) empirical prediction rules constructed to fit results from a full hydrodynamic model* *(iii) hydrological simplification of full hydrodynamic model* *(iv) extend hydrodynamic model to include tributaries and use in real-time* Major rivers: *As (i) to (iii) for minor tributaries* *(iv) hydrodynamic model for use in real-time*	May have relevant gauged location upstream, but certainly tidal effects from major rivers or estuary. Typically will be a relevant gauged location upstream, but certainly tidal effects from estuary or sea.
Tidal Tidal limit Tidal limit	Need to decide if forecast for tributary should have any fluvial component. For minor tributaries: *(i) tabular forecast based on forecasts for estuary or coast* *(ii) empirical prediction rules constructed to fit results from a full hydrodynamic model* *(iii) hydrological simplification of full hydrodynamic model* *(iv) extend hydrodynamic model to include tributaries and use in real-time* For major rivers*: As (i) to (iv) for mixed fluvial/tidal case, but additionally:* *(v) consider 2D hydrodynamic models* *(vi) consider inclusion of wind run-up effects in hydrodynamic models*	Flooding mainly from tidal causes. Maps of area flooded if rivers reach given levels, forecasts based on models for coast or estuary. Hydrodynamic models including representation of extensive flood-plains and washlands. Gauged locations upstream less relevant than in mixed fluvial/tidal case but still need to be used to ensure proper coverage when fluvial conditions are extreme.

Influence of model type

In the five sub-sections that follow, a set of modelling approaches for flow forecasting at ungauged locations are identified for different types of model. Figure 3.1 provides a structural overview of these approaches. It serves as a quick guide to where more detail can be found, through number reference to specific sub-sections. It distinguishes between catchment models and river reach models and identifies a group of five methods of transfer that have applicability to both. Their support by property datasets is indicated. The five methods of transfer are discussed in Section 3.3, in relation to lumped conceptual rainfall-runoff models. However, they may have broader applicability as suggested in Figure 3.1. Models of distributed form, for both catchment areas and river reaches, more naturally make direct use of property datasets in their specification for flow forecasting at target ungauged locations, as indicated in the figure.
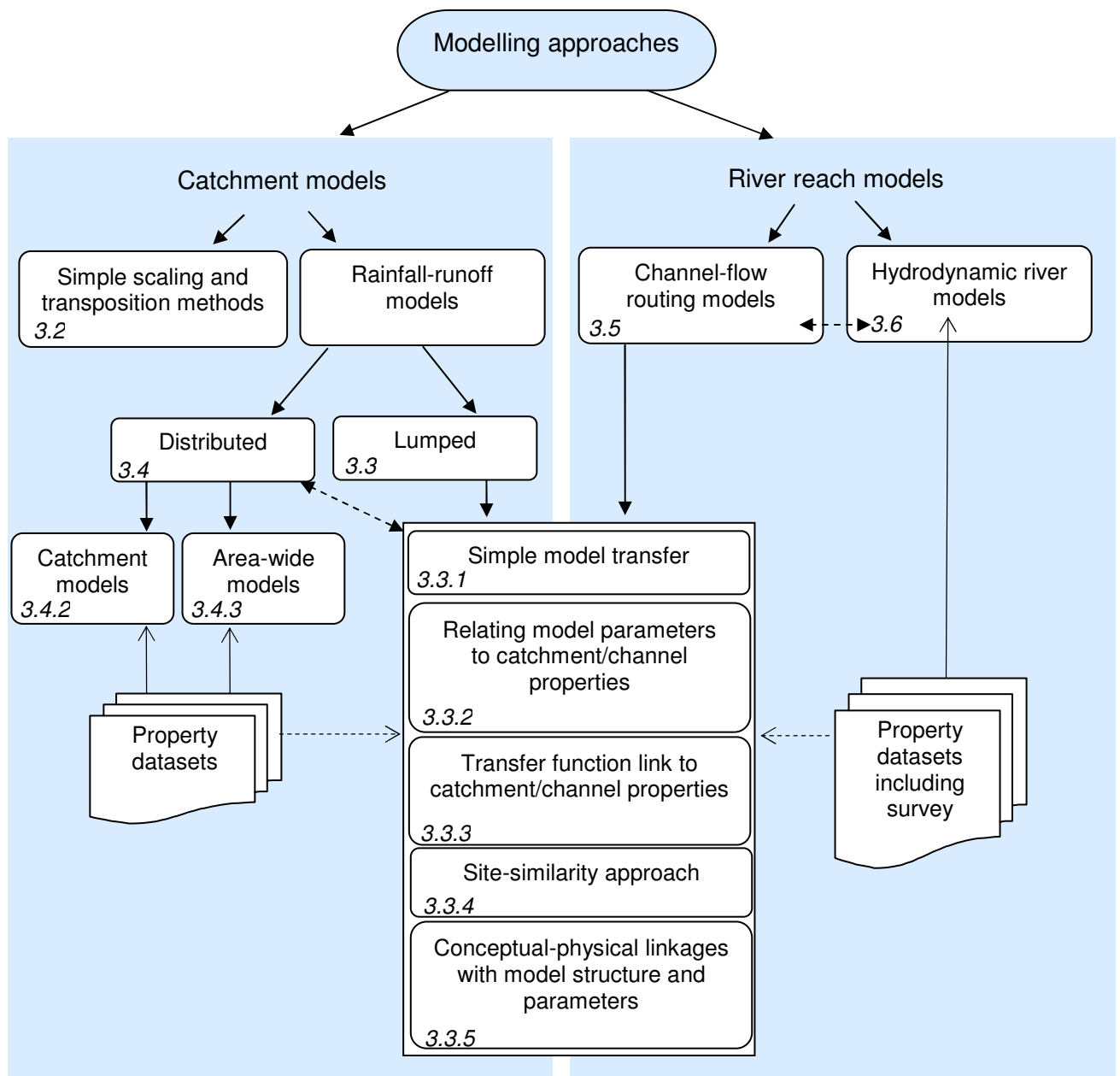
Figure 3.1 Modelling approaches for ungauged locations

3.2 Simple scaling and transposition methods

One of the apparently most straightforward ways of dealing with an ungauged location is to deploy a *simple scaling method*. Here, the forecast constructed at a nearby location is subject to a slight adjustment, usually related to catchment area, in order to forecast for the target location. This may seem so simple as to not deserve to be treated as a modelling approach at all. In many applications, the actual use of a scaling model may be disguised within the structure of the model for another site: for example, where such a model involves preparing input data-streams representing ungauged catchment areas. However, the scaling approach clearly does involve a model: specifically, that being used to transfer information from the "nearby location" to the required location. In addition, similar questions of using telemetered observations can arise as for other modelling approaches: the possibilities here may be missed if the topic is glossed over.

For completeness, it is convenient to identify *simple transposition methods* separately from scaling methods. In the case of simple transposition, the target location is very close to another location for which forecasts are also being created and for which there is a good modelling capability. It is to be expected that reasonable results for transposition methods would be obtained for target locations on the same river, immediately upstream and downstream of locations which are directly modelled. In the case of major rivers, river-flow may be reasonably modelled by direct transposition of flow values over reach lengths of several kilometres: this range is of course limited by any major tributary junctions or regions of backwater effects. Similarly, river-level might be transposed over much the same range, using a simple slope-related datum adjustment as necessary. In cases where simple transposition methods might be useable for an ungauged target site, the simplest overall approach to providing flood-warning would usually be one of using the nearby gauged site to trigger flood-warnings (Section 9.6), so that the additional forecast-construction steps involved in transposition are avoided. However, there may be a few circumstances where a flow modelled at the nearby gauge site can be converted to a level for a specific target site.

One reason for treating scaling methods separately from transposition methods is that this then allows the assumption that scaling methods will always be dealing with transferring information about river flows. In particular, scaling methods are an indirect modelling approach where the primary model deals with modelling flow at a location near the target site. In many cases, the primary target forecast quantity for a scaling model will usually be a river-flow for use as input to succeeding models whose purpose is to create forecasts for locations downstream of the target for the scaling model. However, scaling methods might also be used where the primary target forecast quantity is river-level at the target site: this requires that a stage-discharge relation can be used. In some other instances it may be worth treating the river-flow at the target site as the primary forecast quantity where experience can be built-up as to the flooding consequences of such flows.

The structure of the model used within a simple scaling approach is a rather simple one. The "input" data, on which the model is based, are the flows, Q_S, for the *source location*: these may be observed or forecasted flows, values of which are assumed to exist. Then the modelled flows, Q_T, for the *target location* are constructed as

$$Q_T(t) = f\, Q_S(t)\,,$$

for each time-point t within the forecast time-period. Here the factor f is a constant whose value is often determined by a simple calculation based partly on the catchment areas, A_T and A_S draining to the target and source locations. Several possibilities for specifying f exist. Firstly, depending on whether values for Standard Annual Average Rainfall (noted by R here), Annual Average Evaporation (E) and percentage runoff (P) are assumed known, f might be defined by any one of the following equations

$$A_T = f\, A_S$$
$$R_T A_T = f\, R_S A_S$$
$$(R_T - E_T)A_T = f\,(R_S - E_S)A_S$$
$$P_T R_T A_T = f\, P_S R_S A_S \,.$$

Secondly, where the constructed flow for the target location is used as an input to a model for a gauged location downstream, there is a possibility of specifying f by calibrating its value within the downstream model to produce good modelled values for the downstream location.

Several possible extensions of the simple scaling method can be proposed. One of these would replace the simple scaling relation by

$$Q_T(t) = b_T + f\left\{Q_S(t) - b_S\right\}^+ ,$$

where b_T and b_S represent estimated baseflow components for the two locations. Note the operator x^+ used in the above relation is defined as

$$x^+ = \begin{cases} x & x \geq 0 \\ 0 & x < 0 \end{cases} .$$

Such an extended form of scaling may be more relevant than the simple form where there are substantial artificial influences. Additional extensions can be proposed to try to represent (i) differences in timing and (ii) differences in attenuation: for example,

$$Q_T(t) = f\, Q_S(t - t_{TS}) ,$$
$$Q_T(t) = f\left\{w Q_S(t) + (1 - w)Q_S(t - 1)\right\}.$$

Here, t_{TS} denotes the time-lag needed to synchronise flows at the target and source locations and w is an attenuation factor applied to the source flows to align to the target flows.

The above equations have been written in terms of observed values at the gauged "source" location. Where a "simulation-mode" forecast for the gauged location is available, the usual practice is that the simulation-mode forecast can be transferred to the ungauged location using essentially the same equation. Thus, if the basic scaling model is established as

$$Q_T(t) = f\, Q_S(t) ,$$

and if a set of simulation-mode forecasts $\left\{\tilde{Q}_S(t)\right\}$ are available for the source location, simulation-mode forecasts for the target location would be constructed using the equation:

$$\tilde{Q}_T(t) = f\, \tilde{Q}_S(t)\,.$$

A similar equation can be used in a real-time context when forecast-updating for the gauged location can be achieved using telemetered observations at that site: this is discussed in Section 8.2.

3.3 Lumped conceptual rainfall-runoff models

3.3.1 Simple model transfer

It is a common occurrence that a set of rainfall-runoff models exist for gauged catchments within a river basin. An inspection of these catchments may suggest similarities with ungauged catchments for which forecasts are required. Similarities may include catchment area, terrain, proximity (including adjacent and nested catchments) as well as land-cover, soil and geology. A simple strategy is to simply use the model parameters of the most similar gauged site at the ungauged site, but use the actual catchment area. The rainfall input to the "transposed model" would also be estimated specifically for the ungauged site.

Variants of this basic approach clearly exist which involve consideration of more than one "similar gauged catchment" and possible weighted combinations of parameters based on "similarity distance measures".

Such methods of model transfer provide an alternative to the simple scaling methods described in Section 3.2. An advantage is that rainfall estimated specifically for the ungauged catchment is used as input to the model. This may prove better than the simple "Area/SAAR" factoring of the gauged catchment model flows used in the scaling approach. However, there may be less likelihood of being better if the rainfall estimate is based on raingauges over the gauged catchment.

3.3.2 Relating model parameters to catchment properties

The approach of trying to relate model parameters calibrated for a set of gauged catchments with the properties of these catchments is a common and popular method. Relations established between model parameters and catchment properties can subsequently be applied to an ungauged site to provide the estimates of model parameters required.

A straightforward application of this approach to a typical conceptual rainfall-runoff model is likely to encounter difficulties. This is because of the number of model parameters involved, a lack of independence between them, and a lack of data sensitivity to some of them. There are also problems arising from choosing and deriving catchment properties aggregated at the catchment scale and expecting these to be related in some way to conceptual model parameters. Since the relations are essentially empirical, being based on data analysis, meaningless relations can result.

The above problems normally lead to a reduced form of model being considered, employing fewer parameters and giving greater hope of establishing "stronger" relations. However, the reduced model structure may lose the original flexibility of the original full model and experience loss in performance as a result. The methodology used to arrive at a reduced model form may encompass use of hydrological insight to identify dominant modes of behaviour as well as tools for exploring parameter independence and sensitivity (objective function contour plots for selected parameter pairs and objective function dotty plots to explore single parameter sensitivity to data). Wagener *et al.* (2004) provides a useful review as well as introducing some new tools.

The approach overall involves three main considerations: (i) choosing a reduced form of model, (ii) choosing and calculating an appropriate set of catchment properties (typically involving topography, soil, land cover, and geology), and (iii) choosing a methodology for establishing the relations (typically some form of selective stepwise regression with variable transformation options). Examples of this approach are presented in Section 4.3.

3.3.3 Transfer function parameter link to catchment properties

A variant of the traditional approach described above, which has some appeal, is to impose the functional form of "transfer functions" that define the relationships between model parameters and catchment properties from the outset. The rainfall-runoff model is then calibrated to many catchments simultaneously. In this approach, it is the parameters of the transfer functions that are optimised directly rather than going though the traditional two-stage approach of estimating the model parameters and then the parameters of the catchment property relation. The functional form of the transfer function may take the linear form of a regression model, but may take more general forms. Hundecha and Bárdossy (2004) provide an example of this approach as applied to the HBV rainfall-runoff model.

3.3.4 Site-similarity approach

The site-similarity approach provides a means of combining model parameter estimates for gauged sites to obtain estimates for an ungauged site based on a measure of site-similarity. Consider N catchments of which P form a pooling group based on a similarity measure calculated from M catchment properties or characteristics ($C_{i,m}$, $m = 1,2,...,M$) for catchment i. A similarity or distance measure between catchments i and j can be defined as the Euclidean distance in the property space as

$$d_{ij} = \sqrt{\sum_{m=1}^{M} \lambda_m \left(\frac{C_{i,m} - C_{j,m}}{\sigma_m} \right)^2} \qquad (3.3.1)$$

where σ_m is the standard deviation of property m and λ_m is an "influence coefficient" assigned to this property. The P nearest-neighbours in this property space of the N catchments form a pooling group for each catchment, with P typically chosen as 10.

A calibrated model exists for each catchment in the pooling group. Consider any parameter θ which takes a value θ_i at catchment i within the pooling group. An estimate of this parameter for an ungauged catchment is given by the weighted average

$$\hat{\theta} = \frac{\sum_{i=1}^{P} w_i \theta_i}{\sum_{i=1}^{P} w_i}.$$

(3.3.2)

The weight w_i applied to the model parameter value at the i'th pooling group catchment is defined as

$$w_i = \frac{1 - (d_{ij}/d_{max})^{\beta}}{1 + k\sigma_i^2}.$$

(3.3.3)

This scheme incorporates distance-weighting via the numerator term and calibration uncertainty weighting via the denominator term. Here, d_{ij} denotes the distance measure calculated using equation (3.3.1) between the catchment i and the ungauged catchment of interest j. The statistic σ_i^2 here denotes the variance in the calibrated model parameters at catchment i. The quantity k is treated as a constant whose value can be estimated iteratively. With $k = 0$, distance-weighting only is invoked. The value of the exponent β can be set to invoke different distance-weighting schemes: 0, 1 and 2 gives equal, linearly decreasing and quadratically decreasing weights respectively.

3.3.5 Establishing conceptual-physical linkages with model structure and parameters

A more scientific approach to formulating rainfall-runoff models for ungauged sites aims to establish a model from the outset having a conceptual-physical structure and parameter set that that can be linked directly with spatial datasets on topography and physical properties of soil, land cover and geology.

It is usual to apply the model initially at gauged sites to establish a "regional" or "area-wide" calibration. Only a small set of "regional parameters" are involved but these may map onto a much larger set through the spatial datasets. Application to ungauged catchments in the area/region exploits both this calibration and the spatial datasets.

The methodology may be used to develop either lumped or distributed forms of model. Lumped models are normally a derivation of an initial distributed formulation which establishes the links to the spatial datasets. It is useful to distinguish between two types of rainfall-runoff model in this context. *Source-to-sink* models are essentially lumped models in that they simulate flow at a catchment outlet (the "sink"), translating runoffs from distributed source areas (grid cells or delineated sub-areas) directly to the source location. *Grid-to-grid* (or *cell-to-cell*) models, in contrast, route runoffs from cell to cell over an area with flows calculated for all cell outlets as a sequential procedure in a spatially-distributed way. Cell outlets corresponding to ungauged locations provide the model flow simulations required. Source-to-sink models are generally more computationally efficient but simplify the dynamics involved. The grid-to-grid models may be designated as *area-wide models* and can be configured for an area encompassing many river basins or countries. Both types of model employ a runoff production function within each delineated sub-area or cell.

3.4 Distributed hydrological models

3.4.1 Introduction

Distributed hydrological models are arguably the most natural way of obtaining flood forecasts at ungauged sites across a region. Such models normally encompass rainfall-runoff modelling and flow routing into a single unified framework capable of making forecasts at any location. The modelling domain can encompass any set of ungauged target locations requiring forecasts. Also the same domain can contain a set of gauged locations to support model calibration.

In the context of the classification of modelling approaches discussed in Section 2.3, distributed models deal with the ungauged target location via an indirect model provided by the distributed model formulation. Transfer of information for gauged sites in the modelling domain is achieved via indirect calibration of the target site by achieving a good model fit at the gauged locations. However, the distributed model formulation commonly aims to lessen the importance of calibration by using "physically-based" process representations that can be related directly to measurable properties of the process controls operating. This is discussed further below.

The distributed model formulation normally aims to provide a physical basis for supporting its configuration and behaviour. This is achieved through process formulations defined where possible via measurable properties of land cover, soil, geology and topography. However, in catchment systems there can be real problems relating to the relevance and availability of measurements. Problems include the real complexity of catchments above and below ground, the difficulty of measurement particularly of subsurface properties, and serious scaling issues relating to both the measurement and modelling domain. These problems, along with the difficulty of estimating spatial rainfall, have curtailed the adoption of distributed hydrological models for operational flood forecasting at gauged sites. In general, experience from model intercomparisons indicate that for a gauged site a calibrated lumped rainfall-runoff model often provides more robust, superior forecasts. However, the choice of distributed versus lumped catchment model is a much more open question when the target location is ungauged.

It is worth highlighting that when lumped rainfall-runoff models are used within flood forecasting systems, they normally feature as part of a network of models linking through to flow routing models downstream. In this sense, such model networks are using a *semi-distributed model* formulation. They also present a requirement for forecasts of ungauged tributary and distributed lateral inflows to river reaches.

3.4.2 Catchment versus area-wide approaches

An important distinction can be made between distributed models that employ a *source-to-sink* catchment approach and ones that employ a *grid-to-grid* (cell-to-cell) area-wide approach (for example, see Olivera *et al.*, 2000). In the grid-to-grid approach, a runoff production scheme operates within each grid and generated runoffs are translated from grid to grid using a routing scheme. Commonly there is no attempt to represent within-grid routing effects. Flow paths from grid to grid are delineated with reference to a digital terrain model (DTM). Errors in flow path delineation can occur as the DTM is normally degraded to the model grid size. This also means that any inference of catchment boundaries suffers from related errors. These errors may be overcome by reducing the model grid size but only at the cost of increased model

computation. It is more normal to devise manual and automated methods of correcting flow paths and catchments obtained from using degraded DTMs (for example, Soille, 2004). The grid-to-grid approach has been the first choice of land surface schemes developed for weather and climate models providing wide-area coverage extending from national to global scales. Here, the emphasis is on modelling the feedback of water and energy to the atmosphere and not estimation of catchment river flow *per se*. Evaporation under the control of soil moisture and areas of inundation is the water transport process of primary concern and area-wide estimation is essential.

In the source-to-sink approach to distributed hydrological modelling, the focus is on efficiently calculating the river flow at a catchment outlet of interest whilst at the same time representing the distributed nature of runoff formation and translation through the catchment system. This means that efficient calculation schemes can be devised that route flows directly to the catchment outlet without troubling with estimation of flows at intermediate locations. This can be accomplished by using a model grid over the catchment to generate runoffs from each grid-square (the source grids), but using a routing scheme that takes these distributed runoffs and translates them directly to the catchment outlet (the sink). Flows are not routed from grid to grid explicitly. The form of routing can account for the source location of runoff, with runoff from more distance source grids experiencing greater translation. A common form, used by the Grid Model (Section 4.4.2), employs an isochrone delineation of the catchment which is used to spatially configure a cascade of kinematic routing reaches. Essentially 2-D routing from grid to grid is simplified to a 1-D representation that preserves the effects of distance to catchment outlet when translating source runoffs. Because the spatial resolution of the routing scheme can be finer than the model grid used by the runoff production scheme, within-grid routing effects can be implicitly accommodated. Also the routing reaches defined via isochrone bands can be inferred from a DTM at it's base resolution, and not that of the model grid.

It is clear that the source-to-sink approach is catchment focussed. However, because the formulation is distributed in nature it can be configured and calibrated to a gauged catchment, and reapplied to a set of target ungauged catchments. This would most obviously be done for locations within the catchment used for calibration, or a little downstream but could be applied more widely. Note that the approach is using the topography of the ungauged catchment in configuring the routing model. It is also using any land cover, soil, geology and topography information that features in the formulation of the runoff production function operating within each grid-square. It thus provides a potentially powerful mechanism of information transfer from gauged to ungauged locations. This is also the case for the grid-to-grid area-wide approach.

The grid-to-grid approach is a natural one for providing full national coverage grid estimates of runoffs, routed river flows and inundated areas in support of Flood Watch activities. However, for targeted ungauged catchment estimates of an accuracy required for flood forecasting and warning, both approaches deserve consideration. In particular, the resolution of the DTM-inferred information may argue for finer scale grid-to-grid applications or the efficiency of the source-to-sink approach and its use of the DTM at its base resolution for flow path and catchment delineation.

Specific examples of source-to-sink and grid-to-grid forms of distributed model are discussed later in Section 4.4. Some further discussion of grid-to-grid area-wide models is given in Section 3.4.3 below.

The use of DTM-derived river network topology to configure grid-to-grid flow models can be taken a step further using *geomorphological relations*. These can take the form of power-law relations for estimating the discharge, width and depth at bankfull for any

river location from catchment characteristics, such as drained area and standard average annual rainfall. The grid-to-grid estimates of flow can be combined with estimates of bankfull discharge to provide indicative maps of flood inundation. Animations of these maps over time can show the propagation of flood flows down a river system and locations where bank overtopping may occur. Whilst only indicative - because of the weakness of the geomorphological relations and the exclusion of artificial controls on water movement – the approach can provide a useful mapping of flood inundation risk over time. An example of this first-alert approach is provided by Bell and Moore (2004).

3.4.3 Area-wide models

The need for a representation of the land surface within atmospheric models has formed an important driver for the development of area-wide models. Atmospheric models are configured on a grid with global coverage along with nested models where finer resolution is required. These atmospheric models are used for weather forecasting or climate prediction.

A common feature of many land surface models developed primarily to support better atmospheric modelling is that the description of land surface processes tends to emphasise vertical transfers of energy and moisture flux. The model descriptions began their development as essentially classic "point" or "big leaf" representations of the processes operating within a model grid box. They commonly employ flat surface representations, ignoring the control of topography on lateral transfers of water that can exert a strong influence on water movement at the catchment scale.

A detailed description of evaporation under atmospheric forcing and soil/vegetation control is a common feature of many schemes. However the soil component can vary from a very simple water-accounting "bucket model" to more complex solutions of Richard's equation representing vertical movements of water in a multi-layered soil. Often there is no explicit representation of groundwater or the routing of flows via rivers to the sea.

The main strength of land surface schemes for ungauged modelling is that serious consideration has often been given to their country- or global-wide application. Their formulation has normally considered the use of information on soil properties and land cover, making them applicable to any location and therefore to ungauged areas. However the scale of application has tended to be coarse with priority given to extensive coverage rather than spatial resolution. Topographic control on runoff production operating at the smaller catchment scales does not normally feature in the formulation of land surface schemes.

Section 4.4.4 discusses land surface schemes in more detail, taking the MOSES-PDM applied across the UK by the Met Office as an example of particular relevance.

3.5 Channel flow routing models

Channel flow routing models function to translate a flow hydrograph for an upstream site to a downstream location. Note, for the purposes here, we will deal with models that account for backwater effects - where the downstream flow/level influences flows upstream – under the heading of hydrodynamic models (Section 3.6). Typically, a routing reach is chosen where possible so that the upstream and downstream locations are gauged. This allows the flow routing model to be calibrated using the observed

upstream flow as input and the observed downstream flow as a reference for model fitting. The model reach may be sub-divided into sub-reaches with nodes at their boundaries; the detail of sub-reach definition in relation to model function will be considered later in Section 4.5. Assigning a boundary node to a target ungauged location provides the simplest example of the use of a channel flow routing for ungauged modelling via an indirect model approach (Section 2.3).

Even in this simple situation, lateral inflows in the form of concentrated tributary flows or distributed lateral inflows can complicate and lessen the accuracy of the routing model performance. Sometimes the main tributary inflows are gauged but the more diffuse sources of lateral inflow will not be, and require to be estimated as an ungauged problem. This might be accomplished, for example, using the simple scaling approaches of Section 2.3. This might employ Area/SAAR factors applied to a gauged tributary to the reach to account for source areas of ungauged lateral inflows. Inspection of the reach will allow major tributaries to be distinguished from diffuse sources and lateral inflows assigned to each node so as to respect their geographical location in an approximate way. Transfer of one or more rainfall-runoff models to represent the lateral inflow areas may be another way to proceed. It may be possible to refine the factors of the scaling approach, or the parameters of the rainfall-runoff models, as part of the overall calibration task of fitting the channel flow routing model to the gauged downstream river location.

A less extreme form of "ungauged problem" impacting on channel flow routing modelling is when the gauging station at the downstream end of the reach only records river stage and there is no stage-discharge relation. This "level-only station problem" can be addressed by embedding the stage-discharge relation within the overall channel flow routing problem. Modelled flows are converted to levels and the objective function minimised with reference to the observed levels by searching in the parameter space of the routing model and the rating relation. This requires to be done with care. The Guide to the KW Channel Flow Routing Model (CEH Wallingford, 2005a) provides practical guidance on how this should be done for a specific model. The same level-only station approach can be used for other observations sites that feature in the model, such as the reach inflow station or a tributary inflow station. However, only one such site can feature within a given flow routing model.

Some forms of channel flow routing model are linked directly to the St. Venant equations that underpin hydrodynamic river models and are characterised by measurable channel properties. In this sense, they offer a path of application to wholly ungauged rivers provided the information on channel properties are available. In practice, due to model simplification, the complexity of real flows, and difficulties with specifying certain channel properties (such as roughness), a degree of data transfer from gauged sites will be highly desirable if not essential. Further discussion of this is deferred to the next section which specifically addresses the application of hydrodynamic models to ungauged rivers.

Specific types of channel flow routing model are outlined in some detail in Section 4.5.

3.6 Hydrodynamic river models

The use of existing hydrodynamic models to deal with ungauged locations within their modelling domain is, at first sight, one of the most easily implemented. However, this may not necessarily be so straightforward. One immediate advantage that hydrodynamic models have over hydrological models is that they inherently provide modelled values of river-level which, for flood-warning purposes, is usually the quantity

of primary interest. In the present context, "hydrodynamic models" refers to typical models treating river-channels using one spatial dimension, with inclusion of tributaries and river bifurcations on a similar basis, and with representation of over-flows to flood-plains etc., which are themselves modelled as static or flowing on a one-dimensional basis.

In the simplest cases, the ungauged location for which a forecast is required is on a river-reach which is already explicitly included within the hydrodynamic model. If the location is not already at, or sufficiently close to, a river cross-section explicitly represented in the model, it would usually be fairly easy to introduce such a cross-section, possibly using interpolated data for the cross-section data. An alternative would be to interpolate the modelled levels at adjacent cross-sections, externally to the model: this would avoid the risk of affecting the numerical stability of the hydrodynamic model if the addition were done incautiously. The hydrodynamic model has an underlying representation of the basic physics of water flow and hence, on this basis, might be expected to perform reasonably well for ungauged locations in modelling both river-flow and river-level. However, hydrodynamic models generally do rely on the calibration of parameters such as channel-roughnesses or conveyances to achieve successful modelling of observed river-levels. In this context, modelling for ungauged locations is likely to be good for locations relatively close to sites for which calibration data are available, and less good for more isolated locations. Thus there is some minor uncertainty about how good the modelled values of river-level at ungauged locations will be and, in practice, the aim should be to provide check-observations for all such ungauged locations on a regular basis. An additional practical problem of using modelled levels obtained for ungauged locations is that the model provides levels with respect to a common underlying datum (typically, ordnance datum at Newlyn) for which there may be no local reference: this may make modelled values difficult to interpret in terms of consequences for flooding, and can make the use of local observations of river-level difficult to relate to the modelled values.

The next most simple cases arise where the ungauged locations are notionally not on any river reach, but on land, for example on flood-plains or washlands. Where an existing hydrodynamic model (used for forecasting) has been derived from one originally configured for flood-defence design purposes, important flood-plain locations should already be included within the model. The transfer from design purposes to forecasting purposes may have led to some simplification of the configuration of hydrodynamic model for reasons of computational speed, but the model should still be able to give a good indication of flooding-extent. There are cases where models configured for flood-defence design purposes do not include adequate representation of possible flooded zones: this would occur where the model was configured to establish defence-levels necessary to contain flooding within a restricted river corridor. Other models may have been established on an ad-hoc basis with the inclusion of flood-plains decided on what was necessary to encompass a limited number of past events, rather than on a more comprehensive basis. In such cases it would be necessary to extend the model configuration to include all relevant areas subject to possible flooding. Extension of the model configuration to include extra flood zones, etc., would not necessarily detract from the computational speed for forecasting in non-flood conditions, but this might depend on the particular "brand" of hydrodynamic model being used. Special consideration should be given to computational times under flood conditions to assess whether special arrangements are needed for modelling runs under such conditions, for example to prevent modelling for one area holding-up model-runs for other areas. In practice there is a limit to the geographical extent of flooding that should be dealt with by extending river-channel models onto flood-plains. When flooding is extensive enough, other classes of hydrodynamic model become necessary to allow representation of flood-flows over wide regions of the countryside.

These classes would include: (i) models having representations of water-flow in two spatial dimensions which are structured to cope with rapidly changing flooded regions; (ii) models capable of representing breaches in flood embankments.

A final set of cases arise where ungauged locations are on tributaries of reaches covered by existing hydrodynamic models. In many contexts, configurations of hydrodynamic models omit what are considered to be relatively minor tributaries to save surveying costs and computational time, particularly where the emphasis of the original purpose for the model is some way from the tributary location. Instead the tributary is treated either as a simple lumped input to the main river-reach being modelled, or using simple hydrological routing within the modelling package to represent delay and attenuation of the flow. In cases where the target location is likely to experience backwater effects from the main river-channel, one possibility for providing forecasts is to extend the set of reaches treated by hydrodynamic modelling to include such tributaries. Such model-extension is likely to suffer from problems with calibrating the model-reaches for the tributaries unless there do exist at least some locations on the tributaries having records of river-level for calibration purposes.

4 Some specific modelling tools

4.1 Introduction

This section aims to outline a selection of specific models with regard to their suitability for application to ungauged locations. The selection places emphasis on models in current use for operational flood forecasting by the Environment Agency. It also includes consideration of emerging modelling strategies that show promise for forecasting at ungauged locations.

The specific modelling tools are treated thematically under the headings: simple scaling methods, lumped rainfall-runoff models, distributed hydrological models, channel flow routing models, hydrodynamic river models and flood mapping tools. Figure 4.1 provides an overview of these specific tools within the structure of modelling approaches presented previously in Figure 3.1. Through numbered reference to sub-sections of this report, it serves as a useful guide to where information on a specific modelling tool can be found.
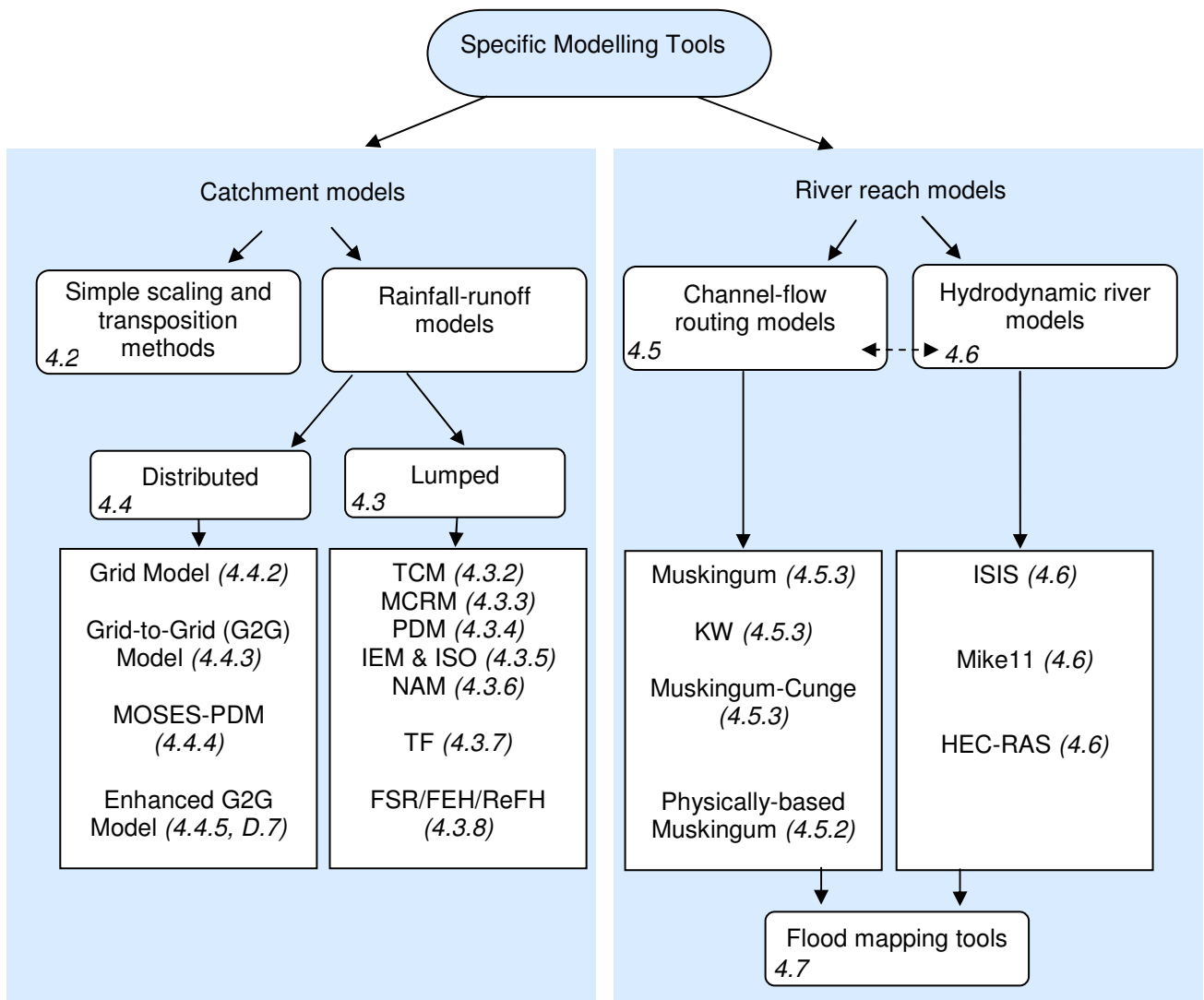
Figure 4.1 Some specific modelling tools

4.2 Simple scaling methods

These simple scaling methods have been adequately reviewed in Section 3.2. Simple Area/SAAR weighting of flow forecasts from a gauged catchment, that is similar and may be adjacent or nested with respect to the ungauged catchment of interest, is a popular method that has been widely applied in the UK. Good examples exist in the Agency's Northeast region.

4.3 Lumped rainfall-runoff models

4.3.1 Introduction

The rainfall-runoff models used operationally for flood forecasting by the Environment Agency are limited in number and normally lumped in form. The main ones are the Thames Catchment Model (TCM or CatchMod), the Midlands Catchment Runoff Model (MCRM), the PDM (Probability Distributed Model), the Isolated Event Model (IEM), the ISO (Input-Storage-Output) model, and forms of Transfer Function Models. The NAM model has also been introduced more recently via the AFFMS operated by Anglian Region.

A number of these models contain common elements. Guidance on applying these specific models to ungauged areas will be given in this section, drawing on the commonality of elements where possible to provide more generic, concise advice. The approach adopted in developing the required guidance is to address each model in turn, providing an outline of the model and then dealing more specifically with the prospect of applying it to a gauged catchment. A detailed mathematical formulation and review of each of these models has previously been provided by CEH Wallingford in the Agency's Technical Report W241 "Comparison of Rainfall-Runoff Models for Flood Forecasting. Part 1: Literature review of models". Only the main features of each model will be summarised here, sufficient to allow a commentary to be made on the prospect for application to ungauged areas. An additional group of models is reviewed at the end that, although developed for design use, pays special attention to application to ungauged catchments in the UK. This group of models is associated with the Flood Study Report rainfall-runoff method, the Flood Estimation Handbook restatement of it and the recent reformulation called the ReFH model.

4.3.2 Thames Catchment Model

Model Outline

The structure of the Thames Catchment Model, or TCM (Greenfield, 1984), is based on subdivision of a basin into different response zones representing, for example, runoff from aquifer, clay, riparian and paved areas and sewage effluent sources. Within each zone the same vertical conceptualisation of water movement is used, the different characteristic responses from the zonal areas being achieved through an appropriate choice of parameter set, some negating the effect of a particular component used in the vertical conceptualisation. The zonal flows are combined, passed through a simple routing model (optional), and go to make up the basin runoff. In this study the same, catchment-average, rainfall is used for all zones.

The conceptual representation of a hydrological response zone in the TCM is illustrated in Figure 4.2 using nomenclature appropriate to an aquifer zone. This zone structure is used for all types of response zone but with differing nomenclature; for example, percolation is better described as rainfall excess for zones other than aquifer. Within a given zone, water movement in the soil is controlled by the classical Penman storage configuration (Penman, 1949) in which a near-surface storage, of depth related to the rooting depth of the associated vegetation and to the soil moisture retention characteristics of the soil (the root constant depth), drains only when full into a lower storage of notional infinite depth. Evaporation occurs at the Penman potential rate whilst the upper store contains water and at a lower rate when only water from the lower store is available. The Penman stores are replenished by rainfall, but a fraction ϕ (typically 0.15, and usually only relevant to aquifer zones) is bypassed to contribute directly as percolation to a lower "unsaturated storage". Percolation occurs from the Penman stores only when the total soil moisture deficit has been made up.

The total percolation forms the input to the unsaturated storage. This behaves as a linear reservoir, releasing water in proportion to the water stored at a rate controlled by the reservoir time constant, k. This outflow represents "recharge" to a further storage representing storage of water below the phreatic surface in an aquifer. Withdrawals are allowed from this storage to allow pumped groundwater abstractions to be represented. A quadratic storage representation is used, with outflow proportional to the square of the water in store and controlled by the nonlinear storage constant, K.

Total basin runoff derives from the sum of the flows from the quadratic store of each zonal component of the model delayed by a time τ_d. Provision is also made to include a constant contribution from an effluent zone if required. A more recent extension of the model passes the combined flows through an additional channel flow routing component if required. This component of the model derives from the channel flow routing model developed by the Institute of Hydrology (Moore and Jones, 1978; Jones and Moore, 1980) which, in its basic form, takes the kinematic wave speed as fixed. The model employs a finite difference approximation to the kinematic wave model with lateral inflow. The delay and attenuation of the flood wave is controlled by the spatial discretisation used and a dimensionless wave speed parameter, θ. The parameters of the TCM are summarised in Table 4.1.

E_a

Actual Evaporation

P   Precipitation

$P' = \max(0, P-E)$

Soil surface

$(1-\phi)P'/100$

D_1

R_c

Direct percolation $\phi P'/100$

Soil Moisture Stores

D_2

percolation

total percolation

i

Unsaturated storage

s

Recharge

a

abstraction

$q = s/k$

Saturated storage

S

$Q = S^2/K$

Groundwater discharge to streamflow
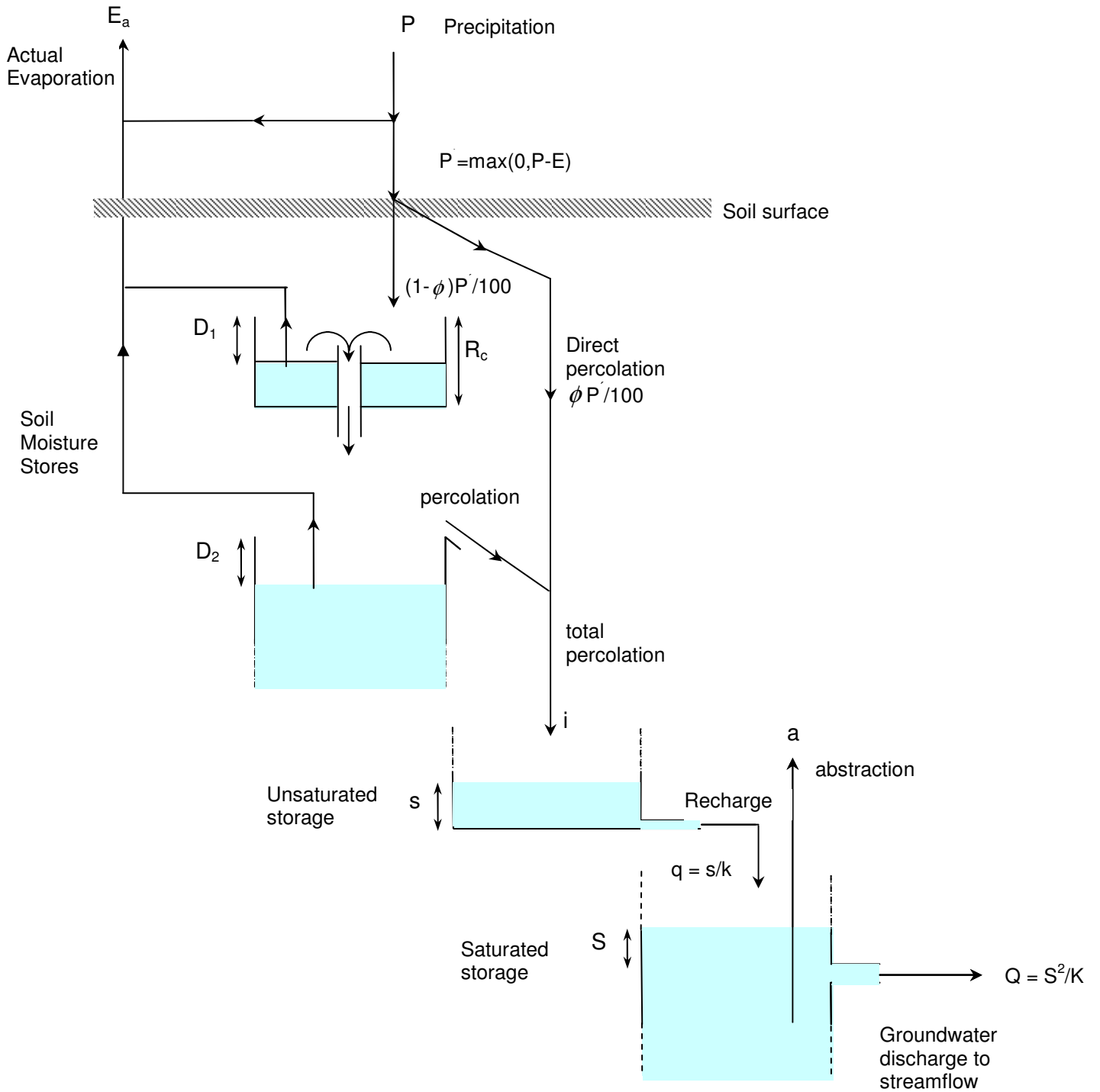
Figure 4.2 Representation of a hydrological response zone within the Thames Catchment Model

Table 4.1 Parameters in the Thames Catchment Model

Parameter name	Unit	Description
Zone parameters		
A	km^2	Area of hydrological response zone
γ	none	Drying rate in lower soil zone (usually γ =0.3)
R_c	mm	Depth of upper soil zone (drying or root constant)
R_P	mm	Depth of lower soil zone (notionally infinite)
ϕ	none	Direct percolation factor (proportion of rainfall bypassing soil storage
k	h	Linear reservoir time constant
K	mm h	Quadratic reservoir time constant
a	m^3 s^{-1}	Abstraction rate from quadratic reservoir
Other parameters		
n_z	none	Number of zones
q_c	m^3 s^{-1}	Constant flow (effluent or river abstraction)
τ_d	h	Time delay
N	none	Number of channel sub-reaches
θ	none	Dimensionless wave speed, $c\Delta t / \Delta x$

Suitability for ungauged catchments

The parameters listed in Table 4.1 indicate that the TCM has 6 zonal parameters that normally require adjustment to a particular catchment. Also a typical application may involve 2 or 3 zones: riparian and/or urban and rural. The routing component may typically be switched off for ungauged catchments, particularly smaller ones. Table 4.2 provides a guide for selection of response zone areas and parameters applicable to ungauged catchments. This indicates it is only the time constants of the linear and quadratic reservoirs applicable to the different response zones that are critical for estimation, once a zonal area configuration has been determined from map information. In many ungauged situations, a pragmatic two zone representation may be sought with the zones representing fast (urban/riparian) and slow (groundwater) pathways. Existing calibrated models within a region and site-similarity arguments may help considerably in choosing the zonal partitioning and appropriate parameters to use for an ungauged catchment. Guidance on the selection of zones and zonal parameters is provided in PSM User Guide (Penman Store Model incorporating the TCM and the IEM) within the component "A Practical User Guide to the PSM" (CEH Wallingford, 2005c).

Table 4.2 Setting parameter values in the Thames Catchment Model

Parameter name	Description	Suggested values
A	Area of hydrological response zone	Infer from maps eg. Urban: CEH Urban area Riparian:100 year flood risk map Other zones: WRAP (soil) & geology maps
γ	Drying rate in lower soil zone	γ =0.3 γ =0.0 for impervious (urban)
R_c	Depth of upper soil zone (drying or root constant)	R_c =75 Normal (short grass) R_c =25 or 30 Oolitic limestone R_c =1 Riparian R_c =0 Urban
R_P	Depth of lower soil zone	$R_P = \infty$ (always)
ϕ	Direct percolation factor (proportion of rainfall bypassing soil storage	ϕ =0 Normal ϕ =0.15 Aquifer zones
k	Linear reservoir time constant	k ~5% area in km^2 Fast zones k ~ 200-400 Aquifer zones
K	Quadratic reservoir time constant	K ~ 10-1000 Fast zones (K/A tends to be fairly constant for a given zone type) K ~ 10^6 Aquifer zones
a	Abstraction rate from quadratic reservoir	a =0 Normal Infer from pumping data
n_z	Number of zones	Infer from maps of land cover, soil, geology, flood risk
q_c	Constant flow (effluent or river abstraction)	q_c =0 Normal Infer from abstraction/return and reservoir compensation release data
τ_d	Time delay	τ_d =0
N	Number of channel sub-reaches	N =0 De-activates channel flow routing
θ	Dimensionless wave speed, cΔt/Δx	θ =0

4.3.3 Midlands Catchment Runoff Model

Model Outline

The Midlands Catchment Runoff Model (MCRM) (Bailey and Dobson, 1981; Wallingford Water, 1994) comprises three main stores: an interception store, a soil moisture store and a groundwater store (Figure 4.3). Rapid runoff is generated from the soil moisture store, the proportion of the input to the store becoming runoff increasing exponentially with decreasing soil moisture deficit. "Percolation" to the groundwater store occurs when the soil is supersaturated, increasing as a linear function of the negative deficit. When supersaturation exceeds a critical value, "rapid drainage" also occurs as a power function of the negative deficit in excess of the critical value (the so-called excess water). This rapid drainage along with rapid runoff forms the soil store runoff. Evaporation occurs preferentially from the interception store at a rate which is a fixed proportion of the catchment potential evaporation. A proportion of any residual evaporation demand is then met by water in the soil store, the proportion varying as a function of the soil moisture deficit. Drainage of the groundwater store to baseflow varies as a power function of water in storage, the exponent being fixed at 1.5. The total output, made up of baseflow and soil store runoff, is then lagged and spread evenly over a specified duration to represent the effect of translation of water from the ground to the catchment outlet. Finally, the flow is smoothed using two nonlinear storage functions, one for routing in-bank flow and the other out-of-bank flow, the two components being summed to give the catchment model outflow. A summary of the parameters involved in the MCRM are presented in Table 4.3.

Suitability for ungauged catchments

The parameters listed in Table 4.3 indicate that the MCRM has as many as 22 parameters. Midlands Region hydrologists have attempted to apply the approach of "regression of model parameters on catchment properties" to this model. They have identified a subset of parameters that are of highest and medium importance in terms of their sensitivity. The parameters in the highest category are: Runoff Coefficient, Runoff Exponent and Maximum Runoff Percentage; Lag Time, Duration of Response; Channel Routing Coefficient; Pr Routing Factor; and Bankfull Flow. Those allocated to the medium category are: Soil SM Surplus, S Function Coefficient and Soil Function Exponent; Maximum Percolation Rate and Baseflow Coefficient.

Table 4.5 presents a summary of the regression relations established for parameters in the high sensitivity category, and one in the medium category (S Function Coefficient). A stepwise regression procedure was used which allowed for variations in the catchment properties introduced; it also allowed selected catchments to be removed when judged to produce rogue outliers. Consideration was given to whether the outcome was conceptually acceptable. The procedure was applied to 8 catchments in the Severn basin: Clwedog, Dulus, Lake Vyrnwy, Banwy, Tanat, Perry, Rea Brook and Upper Tern. However, in practice, model calibration parameters were not available for 3 of these: Clywedog, Lake Vyrnwy and Banwy. Thus, while the R^2 Model Efficiency measures reported in Table 4.4 appear at times reasonable, they relate only to a small number of points used to establish the regression. With so many parameters involved, and so few catchments considered, it is difficult to place much credibility on the outcome of this analysis.
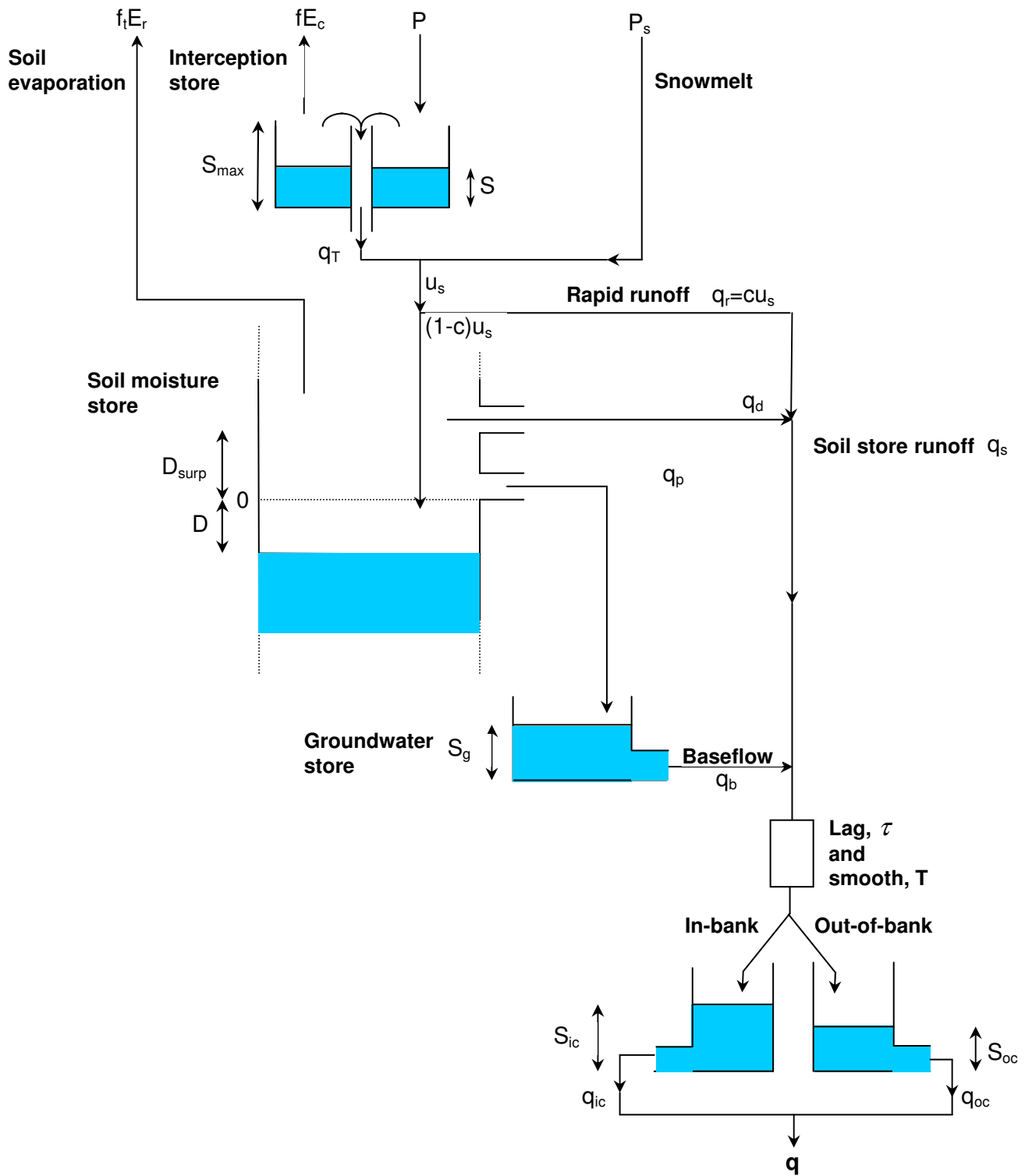
Figure 4.3 The Midlands Catchment Runoff Model

Table 4.3 Parameters in the Midlands Catchment Runoff Model

Parameter	Unit	Description
f_c	none	Rainfall factor
$S_{\max}$	mm	Capacity of interception store
f	none	Fraction of catchment evaporation potentially met by interception storage
c_0	none	Minimum value of rapid runoff proportion
c_1	mm^{-1}	Parameter in rapid runoff proportion function
$c_{\max}$	none	Maximum value of rapid runoff proportion
$q_p^{\max}$	mm h^{-1}	Maximum percolation rate
D_{surp}	mm	Maximum soil store moisture surplus
γ_d	none	Soil function exponent controlling rapid drainage
k_d	h mm$^{\gamma_d - 1}$	Soil function coefficient controlling rapid drainage
T_p	none	Potential transpiration factor
T_m	none	Minimum transpiration factor
$E_{\max}^D$	mm	Deficit below which potential transpiration factor applies
$E_{\min}^D$	mm	Deficit above which minimum transpiration factor applies
K_g	h mm$^{0.5}$	Time constant in baseflow storage function
τ	h	Time lag applied to total runoff
T	h	Duration of time spread applied to total runoff
S_{bf}	mm	Channel storage at bankfull
k_{cr}	h^{-1} mm$^{1-\gamma_{cr}}$	In-channel routing storage coefficient
γ_{cr}	none	In-channel routing storage exponent
k_{or}	h^{-1} mm$^{1-\gamma_{or}}$	Out-of-bank channel routing storage coefficient
γ_{or}	none	Out-of-bank channel routing storage exponent

Table 4.4 MCRM model parameter regressions on catchment properties

Parameter Name	Parameter Symbol	Const.	Area	CAAR	LENG	MSL	CHAN1	CHAN2	STRMFRQ	Slope	RELF	ALT	PFORM	SOIL	Geol1	R^2
Runoff Coefficient	PSRC	0.0148										0.0005		0.9321	-0.0113	0.828
Runoff Exponent	PSRS	-0.015												0.132		0.3394
Max runoff percentage	PRPM		-0.0012	0.0003	0.0038	-0.0094								1.1545		0.81
S Function Coefficient	PDRF	147.6				-1.067				-6.58				-122.5		0.52
Lag Time	PLAG	6.99			-0.018				-0.995				-0.21			
Duration response	PDUR	16.656				0.661					-0.026			-47.331		0.765
Channel Routing Coefficient	PC1F	0.047				-0.002	-0.58×10^{-4}	0.66×10^{-4}			-0.72×10^{-4}				0.001	0.645
Pr Routing factor	PCOF	0.0252				0.0006			0.0114						-0.0034	0.474
Bankfull Flow	PCBF	-10.638			0.0977				13.41			0.07				0.817

It is noteworthy, that an earlier study by Midland Region hydrologists (Pirt and Bramley, 1984) recognised at the outset the difficulty of establishing reliable regression relations of model parameters with catchment properties for models having many parameters. They recognised similarities between the MCRM (then the Severn-Trent CRM) and the simpler Isolated Event Model and developed a model of intermediate complexity embracing certain useful sophisticated features whilst retaining much of the simplicity. This model would then be more appropriate for application to ungauged catchments using a regression of model parameters on catchment properties approach. We will refer here to this model as the "Simple MCRM". This model has only 8 parameters: the coefficient and exponent of an equation related to soil moisture deficit that controls the proportion of rapid (quick) runoff entering the channel system for positive deficits and the proportion percolating to a groundwater reservoir for negative deficits; two threshold parameters that constrain rapid runoff and percolation to maximum rates under saturated conditions, the time constant of a nonlinear reservoir representing groundwater storage (with an exponent of 1.5, rather than 2 used in the IEM), the rate constant of a nonlinear storage representing channel flow routing (with an exponent of 1.66) together with a channel time delay parameter, and a pure time delay parameter defining the delay between rainfall and the hydrograph response.

The model was calibrated to 14 catchments in the Severn and Trent basins, each catchment having 10 events for calibration covering a range of conditions. Stepwise regression of the 8 model parameters was performed on a set of 17 catchment properties, subsequently reduced to 10 after taking account of colinearity. Relations were required to be conceptually acceptable. The resulting regression relationships are summarised in Table 4.5 and the catchment properties considered are set down in Table 4.6. The Dry Weather Flow (DWF) Index requires DWI Maps to be available. For relations involving DWFI, alternative ones were developed using a Geological Index to remove the dependence on the availability of such maps. The r^2 correlation coefficients obtained for all model parameters are reasonably good, all being above 0.84.

An independent assessment of the model for forecasting ungauged catchments was carried out using 4 different catchments and 3 flood events. Two of the 4 catchments gave very good results with average peak error and total runoff volume error being 2.5 and 6.6% respectively; timings of the peaks were also accurate. Performance was less good for the other two catchments, but only 2 of the 6 events had major errors: for example peak errors of -35 and -22%. The results, whilst encouraging, are not convincing for operational use. There was also no attempt to assess against simpler alternatives such as scaling/similarity/analogue approaches.

Table 4.5 Simple MCRM model parameter regressions on catchment properties

(a) Using Dry Weather Flow Index

Parameter Name	Parameter Symbol	Const.	Variable 1	Variable 2	Variable 3	Variable 4	Variables in Regression	r^2
Runoff Coefficient	ROC	0.3693	-0.0082	0.01			DWFI, MSL	0.9144
Runoff Exponent	ROE	0.018	0.0545	455×10^{-7}			SOIL, CHAN	0.8888
Max runoff percentage	MRO	0.747	-0.0047				DWFI	0.9124
Max Percolation Rate	MPR	0.9761	-0.4134				STMFRQ	0.8469
Groundwater time constant	GWF	-32891.45	291.535				RELF	0.9380
Rainfall time delay	LAG	-2.522	0.176	0.0027	-65.3631	4.4293	MSL, RELF, CFORM, SOIL	0.9580
Channel Routing Delay	DUR	25.5768	-0.0713				ALT	0.8612
Channel Routing Rate constant	CRF	0.0682	1.222×10^{-6}	-0.0001			CHAN, ALT	0.8780

(b) Using Geological Index

Parameter Name	Parameter Symbol	Const.	Variable 1	Variable 2	Variable 3	Variable 4	Variables in Regression	r^2
Runoff Coefficient	ROC	0.5258	-0.1107	0.2253			GEOL, XSWP	0.9055
Max runoff percentage	MRO	7.222	-0.0646	0.0959			GEOL, STMFRQ	0.9035

Table 4.6 Catchment properties used in Simple MCRM parameter regionalisation scheme

Symbol	Description	Units
GEOL	Geological index	-
PERM	Catchment average permeability	
DWFI	Catchment dry weather flow index (yield)	Mld/km^2/100 km^2
SOIL	Catchment winter rainfall acceptance potential	-
MSL	Main stream length	km
CFORM	Catchment circularity (shape)	-
AREA	Catchment area	km^2
SHAPE	Catchment shape	-
RELF	Catchment fall (relief)	m
ALT	Average altitude	m
SLOPE	Slope of the main stream	-
STMFRQ	Stream frequency	junctions/km^2
LENG	Total stream length	km
XSEC	Channel cross-sectional area	m^2
XSWP	Channel Hydraulic radius	m
MANN	Channel roughness	
CHAN	Channel volume index	m^3

4.3.4 Probability Distributed Model

Model Outline

The Probability Distributed Moisture model, or PDM, is a fairly general conceptual rainfall-runoff model which transforms rainfall and evaporation data to flow at the catchment outlet (Moore, 1985, 1999, 2006; CEH Wallingford, 2005b). Figure 4.4 illustrates the general form of the model. The PDM has been designed more as a toolkit of model components than a fixed model construct. A number of options are available in the overall model formulation which allows a broad range of hydrological behaviours to be represented.

Runoff production at a point in the catchment is controlled by the absorption capacity of the soil to take up water: this can be conceptualised as a simple store with a given storage capacity. By considering that different points in a catchment have differing storage capacities and that the spatial variation of capacity can be described by a probability distribution, it is possible to formulate a simple runoff production model which integrates the point runoffs to yield the catchment surface runoff into surface storage. The standard form of PDM employs a Pareto distribution of store capacities, with the shape parameter b controlling the form of variation between minimum and maximum values c_{min} and c_{max} respectively. Drainage from the probability-distributed moisture store passes into subsurface storage as recharge. The rate of drainage is in proportion to the water in store in excess of a tension water storage threshold.

The subsurface storage, representing translation along slow pathways to the basin outlet, is commonly chosen to be of cubic form, with outflow proportional to the cube of the water in store. An extended subsurface storage component (Moore and Bell, 2002) can be used to represent pumped abstractions from groundwater; losses to underflow and external springs can also be accommodated.
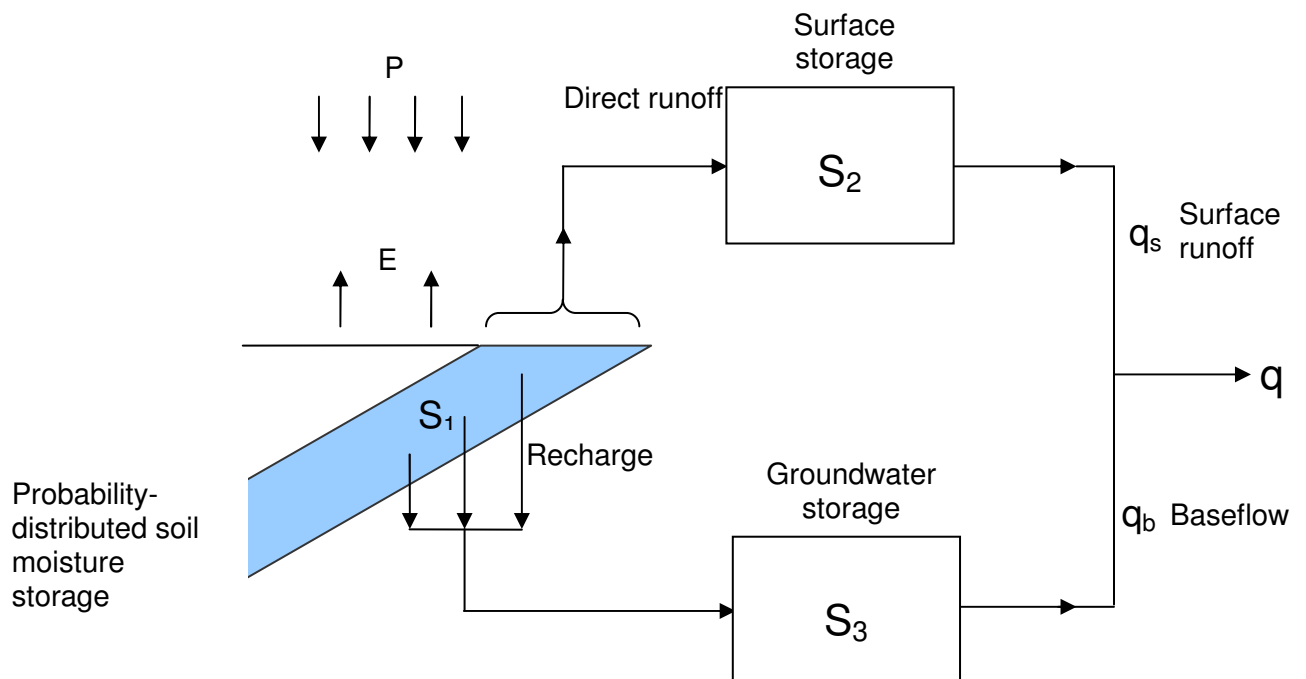
Figure 4.4 The PDM rainfall-runoff model

Runoff generated from the saturated probability-distributed moisture stores contribute to the surface storage, representing the fast pathways to the basin outlet. This is modelled here by a cascade of two linear reservoirs cast as an equivalent transfer function model (O'Connor, 1982). The outflow from surface and subsurface storages, together with any fixed flow representing, say, compensation releases from reservoirs or constant abstractions, forms the model output. The parameters involved in the standard form of PDM model are summarised in Table 4.7.

Suitability for ungauged catchments

The physical-conceptual nature of the PDM and the model's level of intermediate complexity offer some hope of successful application to ungauged sites. Each of the model parameters has a clear physical meaning that invites attempts to establish physically-based linkages with data on soil and geological properties, land cover, topography and stream network topology. However, to date, there has been no systematic attempt to do this. Some related first steps are discussed later.

Table 4.7 Parameters of the PDM model

Parameter name	Unit	Description
f_c	none	rainfall factor
τ_d	h	time delay
Probability-distributed store		
c_{min}	mm	minimum store capacity
c_{max}	mm	maximum store capacity
b	none	exponent of Pareto distribution controlling spatial variability of store capacity
Evaporation function		
b_e	none	exponent in actual evaporation function
Recharge function		
k_g	h mm$^{b_g-1}$	groundwater recharge time constant
b_g	none	exponent of recharge function
S_t	mm	soil tension storage capacity
Surface routing		
k_1, k_2	h	time constants of cascade of two linear reservoirs
Groundwater storage routing		
k_b	h mm^{m-1}	baseflow time constant
m	none	exponent of baseflow nonlinear storage
q_c	m^3 s^{-1}	constant flow representing returns/abstractions

Review of work to date

There has been extensive work on applying regression of model parameters on catchment properties to a reduced form of the PDM: see, for example, Lamb (1999) and Calver *et al.* (2001). This work has been undertaken in the context of the continuous simulation approach to flood (and drought) frequency analysis for design and climate/land-use impact assessment applications. For such applications, there is not the same concern with simulating an actual flood event as precisely as possible that exists with real-time flood forecasting. It is the reproduction and extension of the frequency curve, and the estimation of return periods of flow exceedences this implies, that is the main objective. The reduced form of model is arrived at with the aim of having a small number of model parameters that can be reliably linked with catchment properties via a set of regression models. Thus the accuracy of simulation that might be achieved with the full PDM model for a gauged catchment is compromised by strengthening the regression models linking model parameters to catchment properties. The overall intent is that the reduced PDM model, together with the regression models for its parameters, provides a reasonable way of transferring the model to ungauged sites.

The reduced form of PDM is illustrated in Figure 4.5. This model is invoked directly from the full PDM toolkit of model structures (CEH Wallingford, 2005b). Its main distinguishing features can be summarised as follows. The probability-distributed store assumes a uniform distribution, with capacities ranging from 0 to $c_{\max}$ with an equal frequency of occurrence $1/c_{\max}$. Runoff for translation to the basin outlet is only generated as overflow from the saturated elemental stores, these being closed at the bottom prohibiting drainage. The splitting function of the PDM is invoked to partition the runoff into two parallel pathways to the basin outlet, a fraction α going via a fast store and $1-\alpha$ via a slow one. (Note that interdependence of parameters, seen when the PDM's soil drainage to recharge function is invoked, can be circumvented through the use of the PDM's splitting function.) The fast pathway (the "surface storage") is represented by a single linear store whilst the slow pathway (the "groundwater storage") employs a cubic store, with time constant k_1 and k_b respectively. Summing the fast and slow (base) flows output from these stores gives the discharge at the catchment outlet. The rainfall factor f_c applied to scale the catchment average rainfall input is used as a volume adjustment to compensate for water transfer losses/gains, having ensured that raingauge representativity issues have been dealt with directly in forming the rainfall input to the catchment. The PDM in this reduced form thus has only 5 parameters: f_c, $c_{\max}$, α, k_1 and k_b.

Model parameter regressions on catchment properties (from over 50 available) were established using an hourly dataset encompassing 40 catchments across England, Wales and Scotland. A sequential regression procedure on catchment properties in linear and log space was used to arrive at a set of regression relations. The model parameter regressions and the catchment properties involved are summarised in Figure 4.5. One parameter, the splitting factor α, is pre-determined from standard percentage runoff given by the HOST soils dataset. The fast and slow time constants of the routing stores have model parameter regressions with R^2 Efficiencies of 0.8 and 0.6 respectively. The rainfall factor and maximum soil store capacity regressions both have R^2 values of 0.7. Average errors in simulated flood magnitudes, obtained from the reduced-form PDM model using the regression-derived model parameters, are of the order of $\pm 25\%$ for a spread of British catchments.

(a) Reduced-form PDM
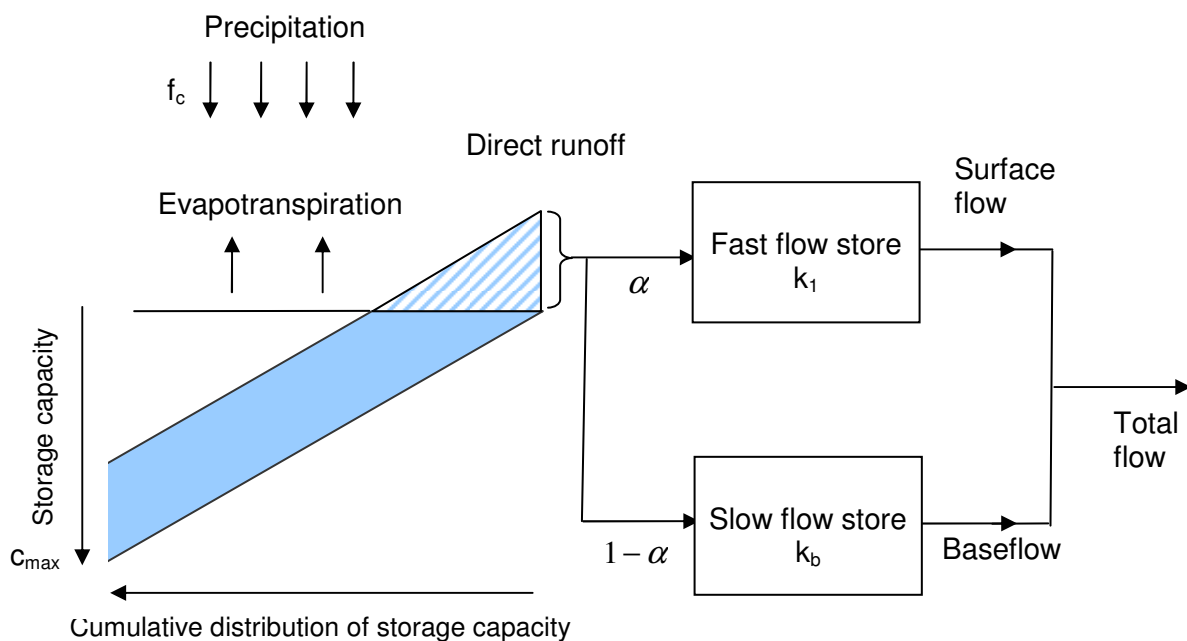
(b) Model parameter regressions

Regression equation	R^2
f_c = 0.71 + 0.00066 DPSBAR + 0.0016 MEDWET − 0.4 HOSTP	0.71
c_{max} = -96.6 + 10.6 SKEW + 4.97 DPLBAR + 0.056 $SAAR_{6190}$ − 1175.3 URBFRAC	0.67
k_1 = -42.7 + 62.4 HOSTBFI + 14.8 SDIST + 1.1 RESIDM − 19.9 SUBFRAC	0.76
k_b = 32.2 − 224.5 HOSTBFI + 0.33 PORO + 550.1 HOSTP	0.61
α = 0.01 HOSTSPR	n/a

(c) Catchment properties

Catchment property	Description
DPLBAR	Mean drainage path length [km]
DPSBAR	Mean slope of drainage paths [m/km]
HOSTBFI	Baseflow index, as weighted average of values inferred from HOST
HOSTP	Index of soil porosity as weighted average of values inferred from HOST
HOSTSPR	Standard percentage runoff, as weighted average of values inferred from HOST
MEDWET	Median length of spells where SMD < 6 mm during 1961-90 [days]
PORO	Total soil porosity, derived from SEISMIC and HOST [%]
RESIDM	Residual soil moisture, derived from SEISMIC and HOST [%]
$SAAR_{6190}$	Standard average annual rainfall, 1961-90 [mm]
SDIST	Proportional distance from outlet at which the number of channels is maximum
SKEW	Skewness of the ln(area/tan B) topographic index distribution
SUBFRAC	Suburban fraction of catchment area
URBFRAC	Urban fraction of catchment area

Figure 4.5 The reduced-form PDM, model parameter regressions and catchment properties

Recent work has refined and reviewed the approach with the benefit of an extended dataset (Calver *et al.*, 2005). The outcome was that for the PDM model the site-similarity approach, reviewed here in Section 3.3.4, was found to be slightly superior to the catchment property regression approach. The catchment properties that feature in both approaches are substantially different to those that appear in Figure 4.4 summarising the earlier work. The catchment properties that feature in both parameter estimation approaches are presented in Table 4.8 whilst the new regression equations are summarised in Table 4.9. Table 4.10 provides a summary of the catchment properties that feature in this revised analysis. The performance of the new site-similarity approach is similar to the earlier sequential regression formulation (when target sites are excluded for fairness).

Table 4.8 Catchment properties used for each model parameter in the regression and site-similarity methods. Properties in red are used in both methods whilst those in blue are where correlated properties are used in the other method.

Method	f_c	c_{max}	k_1	k_b
Univariate regression	√DPSBAR √(HOSTGMIN/100) √(HOSTPEAT/100) HOSTNG √(LANDA/100)	PROPWET SPRHOST √URBEXT HOSTNG FIELDC	√ALTBAR DPLBAR √(1-FARL) PROPWET SPRHOST √URBEXT	BFIHOST DPLBAR √DPSBAR √URBEXT √(HOSTPEAT/100) DRAIN2
R^2	0.51	0.46	0.68	0.51
Site-similarity	√AREA BFIHOST √DPSBAR √SAAR √(LANDB/100) √(LANDC/100)	PROPWET √URBEXT HOSTNG √HOSTP √(LANDA/100)	BFIHOST DPLBAR √(1-FARL) √URBEXT √(LANDB/100)	BFIHOST √URBEXT HYDC √(LANDC/100) DRAIN2
R^2 (inc. target)	0.78	0.70	0.82	0.74
R^2 (exc. target)	0.55	0.41	0.66	0.50

Table 4.9 Regression equations used for reduced-form PDM parameter estimation

f_c=-0.241+0.021√DPSBAR+0.668√(HOSTGMIN/100)+0.919√(HOSTPEAT/100)+0.0093HOSTNG+0.217√(LANDA/100)

c_{max}=-70.46-231.1PROPWET-2.588SPRHOST-270.3√URBEXT+0.399HOSTNG+11.62FIELDC

Log(k_1)=4.270-0.049√ALTBAR+0.023DPLBAR+1.479√(1-FARL)-1.595PROPWET-0.016SPRHOST-2.423√URBEXT

Log(k_b)=3.237+2.154BFIHOST+0.015DPLBAR+0.085√DPSBAR+1.852√URBEXT+0.986√(HOSTPEAT/100)-0.845DRAIN2

α=0.01 SPRHOST

Table 4.10 Definitions of catchment properties used for reduced-form PDM parameter estimation

CP Name	Range, units	Source	Notes
AREA	$[0,\infty]$ km^2	FEH	DTM-derived
ALTBAR	$[0,\infty]$ m	FEH	Mean altitude
BFIHOST	$[0,1]$ -	FEH	Base flow index, calculated from weighted average of HOST classes over the catchment
DPLBAR	$[0,\infty]$ km	FEH	Mean drainage path length
DPLCV	$[0,\infty]$ -	FEH	CV drainage path length
DPSBAR	$[0,\infty]$ m/km	FEH	Mean slope of DTM drainage paths to site
FARL	$[0,1]$	FEH	Index of flood attenuation due to reservoirs and lakes
PROPWET	$[0,1]$ -	FEH	Proportion of time catchment wet (SMD<6mm)
SAAR	$[0,\infty]$ mm	FEH	Standard average annual rainfall, 1961-90
SPRHOST	$[0,100]$ -	FEH	Standard percentage runoff derived from weighted average of HOST classes over catchment
URBEXT	$[0,1]$ -	FEH	Extent of urban/suburban land cover (URBEXT=URB$_{FRAC}$+0.5×SUBURB$_{FRAC}$)
HOSTGMIN	$[0, 100]$ %	HOST	% of catchment area covered by HOST 1-10,13,14 (mineral soils with underlying groundwater)
HOSTPEAT	$[0, 100]$ %	HOST	% of catchment area covered by HOST 11,12,15 ('peat soils with groundwater')
HOSTNG	$[0, 100]$ %	HOST	% of catchment area covered by HOST classes 16-29 (essentially 'non-groundwater')
HOSTP	$[0,1]$	HOST	Index of porosity as a weighted average of values inferred from HOST classes.
FIELDC	$[0,100]$ %	SEISMIC/HOST	Volumetric soil water content at 5 kPa, as weighted average of values inferred from HOST classes.
RESIDM	$[0,100]$ %	SEISMIC/HOST	Residual soil moisture, as weighted average of values inferred from HOST classes.
PORO	$[0,100]$ %	SEISMIC/HOST	Total soil porosity, as weighted average of values inferred from HOST classes.
HYDC	$[0,\infty]$ cm/d	SEISMIC/HOST	Saturated soil hydraulic conductivity, as weighted average of values inferred from HOST classes
LANDA	$[0, 100]$ %	ITE	% of catchment area covered by grassland based on ITE land cover data (classes 5-8,19,23)
LANDB	$[0, 100]$ %	ITE	% of catchment area covered by upland based on ITE land cover data (classes 9-13,17,24,25)
LANDC	$[0, 100]$ %	ITE	% of catchment area covered by trees based on ITE land cover data (classes 14-16)
LANDD	$[0, 100]$ %	ITE	% of catchment area covered by 'arable' based on ITE land cover data (class 18)
DRAIN2	$[0,\infty]$ km/km^2	DTM	Drainage density (total length of river (km) divided by the catchment area (km^2)

Notes on sources:

FEH — Properties appearing on the FEH CD-ROM or based on FEH catchment properties

HOST — Properties derived from the HOST soil classification system (Boorman *et al.*, 1995)

SEISMIC/HOST — Properties derived from the SEISMIC soils characteristics database for each HOST class

ITE — Properties derived from the ITE 1990 land cover classification (Fuller, 1993)

DTM — Properties derived from the CEH-Wallingford 'Integrated Hydrological Digital Terrain Model' (IHDTM) (Morris and Flavin, 1990)

Future opportunities

It is clear that the approach of model simplification and regression of model parameters on catchment properties is unsatisfactory from many points of view. This also applies to the related empirical site-similarity pooling approach. However, are there better ways to develop the PDM model for application to ungauged catchments? This question can be addressed by looking at the constituent components of the PDM. The main components relate to runoff production and flow routing and these will be discussed in turn. The discussion that follows is also relevant to other models considered here, such as the TCM and IEM, that employ components common to those used in the PDM.

Runoff Production in the PDM

The runoff production mechanism is controlled by the frequency distribution of absorption capacity over the basin to be modelled. Soil storage is seen as the dominant capacity although vegetation canopy storage and surface depression storage are also acknowledged. How can the capacity distribution be estimated for ungauged basins? The simplest conjecture is to assume a relation between topographic slope and capacity, with steeper slopes having least capacity to absorb water. This combines notions of thin soils, sparse vegetation and effects of gradient enhancing runoff production for steep slopes. A basic relationship is that the storage capacity at a point, c, is linearly related to topographic slope (or gradient) g by

$$c = \left(1 - \frac{g}{g_{max}} \right) c_{max} \tag{4.3.1}$$

where c_{max} and g_{max} are the maximum regional storage capacity and gradient values.

For a given distribution of gradient within a catchment, equation (4.3.1) can be used to derive the distribution of storage capacity over the catchment in terms of the parameters defining the distribution of topographic slope. For a power distribution of slope

$$F(g) = \text{Prob(slope} \le g) = \left(\frac{g}{g_{max}} \right)^b \qquad 0 \le g \le g_{max} \tag{4.3.2}$$

with the exponent c related to the mean slope $\bar{g}$ by

$$b = \frac{\bar{g}}{g_{max} - \bar{g}} \ , \tag{4.3.3}$$

it can be shown that the distribution function of storage capacity takes the Pareto distribution form

$$F(c) = 1 - \left(1 - \frac{c}{c_{max}} \right)^b \qquad c \le c_{max} \ . \tag{4.3.4}$$

The maximum catchment storage capacity, $S_{max} = c_{max} / (b + 1)$, is also the mean store capacity $\bar{c}$ over the catchment given by

$$\bar{c} = S_{\max} = c_{\max} \left(1 - \frac{\bar{g}}{g_{\max}} \right).$$

$$(4.3.5)$$

Soil moisture storage S and volume of direct runoff V are readily calculated at each time-step using algebraic expressions that form part of the PDM methodology (Moore, 1985, 1999).

The relevance to ungauged catchment modelling is that a DTM can be used to obtain catchment estimates of mean and maximum slope, $\bar{g}$ and $g_{\max}$, to obtain the Pareto shape parameter b. The maximum store capacity within the catchment, $c_{\max}$, is primarily a soil property with canopy storage a secondary consideration. This provides a physics-based path for application to ungauged catchments that has still to be explored. The Integrated Air Capacity of the Soil Survey provides one source to investigate, whilst depth and porosity estimates are alternatives. Land cover maps combined with estimates of canopy storage for different cover types provides a secondary avenue to explore.

Whilst the above has focussed on topographic control of absorption capacity and the use of DTM data, a natural alternative is to begin with soil property data if available. The Integrated Air Capacity (IAC) dataset provides an attractive point of departure. The simplest approach is to assume that the catchment store capacity is proportional to the integated air capacity value, I, estimated as an average for the catchment such that

$$S_{\max} = \gamma I$$

$$(4.3.6)$$

where γ is an adjustment factor allowing values other than 1 if appropriate. A generalisation of this to incorporate gradient explicitly assumes that catchment storage capacity is dependent on both the average gradient and the integrated air capacity, such that

$$S_{\max} = \gamma (1 - \bar{g} / g_{\max}) I$$

$$(4.3.7)$$

with γ having a similar interpretation as before. Ideas of this kind have been explored in a Grid Model context by Bell and Moore (1998) and found to be of some benefit where soil dominates over topographic control: typically in low relief catchments with some soil heterogeneity.

Depending on the spatial resolution and heterogeneity of the IAC soil data relative to catchment area, it is also possible to obtain empirical distribution functions of IAC and use these to formulate new forms of probability-distributed runoff production function. Combinations of IAC and topographic slope data considered in a probability-distributed modelling context provide other possibilities to explore.

Flow routing in the PDM

The flow routing component of the PDM uses the Horton-Izzard equation (Dooge, 1973; Dooge and O'Kane, 2003) as its primary ingredient. This considers a nonlinear storage having an outflow rate per unit area q that is a power function of the storage per unit area S such that $q = kS^m$ where k is a rate coefficient and exponent m is a parameter. If the rate of water input per unit area is u, then continuity gives

$dS/dt = u - q$ which combined with the nonlinear storage equation results in the Horton-Izzard equation

$$\frac{dq}{dt} = a(u - q)q^b, \quad q > 0, b < 1, \tag{4.3.8}$$

where $a = mk^{1/m}$ and $b = (m-1)/m$ are two parameters. The PDM provides recursive solutions suitable for forecasting for various values of m (or b), assuming the input rate is constant over the time-interval. Application for the ungauged case involves making a suitable choice for m and k (or b and a).

There is a body of theory that can guide a suitable choice for the power exponent m depending on the hydrological process being represented. In turn, this can provide a basis for determining a suitable value for k through links to relevant hydrological properties. For example, Horton (1945) considered nonlinear storage models as descriptors of the overland flow process. Considering turbulent sheet flow from a slope of unit width, Manning-Strickler gives the velocity as

$$V = n^{-1} \sqrt{s_0} R^{2/3}, \tag{4.3.9}$$

where n is Manning's roughness, s_0 is the slope, and R is the hydraulic radius which for sheet flow is the depth of water storage, S. Therefore the discharge is given by

$$q = VS = k \, S^{5/3} \tag{4.3.10}$$

where $k = \sqrt{s_0}/n$, and consequently the exponent m for fully turbulent flow is $m = 5/3$. This provides a basis for defining the rate coefficient k from slope and roughness information if the process mechanism is appropriately viewed as approximating turbulent overland flow, or a wide channel with Manning roughness, for which $m = 5/3$ ($b = 2/5$). Clearly, because the PDM is using a catchment-scale conceptualisation of the nonlinear storage, such relationships may not be immediately applicable and require consideration of scale and within-catchment variability to arrive at appropriate aggregate values of slope and roughness. However, this theoretical background for investigating sensible relations that can be applied to ungauged catchments may have value.

For fully laminar flow the exponent of the power relation can be shown to be 3 (for example, see Eagleson 1970). This type of flow is also associated with overland flow and is equivalent to steady, uniform flow in a wide channel. Velocity is given by

$$V = C\sqrt{s_0} S^{1/2} = \left(\frac{2g}{c_f}\right)^{1/2} \sqrt{s_0} S^{1/2} \tag{4.3.11}$$

where C is the Chezy coefficient ($L^{1/2}T^{-1}$), c_f is a resistance coefficient (dimensionless) and S is the depth of flow. For laminar flow

$$c_f = \frac{4}{R_e} = \frac{4\nu}{VS} \tag{4.3.12}$$

where v is the kinematic viscosity ($L^2 T^{-1}$), so

$$V = \frac{g s_0}{2v} S^2 . \tag{4.3.13}$$

Since $q = VS$ then

$$q = \frac{g s_0}{2v} S^3 = k S^3 . \tag{4.3.14}$$

This indicates that the rate coefficient for laminar flow is dependent on slope but independent of roughness.

Horton defined an "index of turbulence":

$$I_T = \frac{3}{4}(3 - m) \tag{4.3.15}$$

ranging from $I_T = 1$ for turbulent flow ($m = 5/3$) to $I_T = 0$ for laminar flow ($m = 3$). Horton (1938) found that $m = 2$ was a reasonable choice for overland flow on most naturally occurring surfaces. The exponent $m = 2$ corresponds to $I_T = 0.75$ and referred to as the "75% turbulent flow" case.

Although Horton considered overland flow, and S to be the depth of overland flow, it is reasonable to extend the idea to any input-storage-output system, so S could, for example, be the average depth of water stored over a basin as channel storage. Ding (1967) related the $m = 2$ case to an "unconfined or non-artesian" storage element, following Werner and Sundquist's (1951) theoretical analysis of flow from a deep non-artesian aquifer based on Darcy's law and Dupuit's assumption. The Thames Catchment Model (TCM) uses this quadratic storage element to represent release from groundwater storage (Greenfield, 1984).

The quadratic storage function was used by Mandeville (1975) as the basis of the Isolated Event Model (IEM) used in the UK Flood Study (NERC, 1975) as a method for deriving design flood hydrographs. The IEM's efficient parameterisation (the one parameter, k) and sensible response shape offered the prospect of successful regionalisation of the model to obtain design hydrographs for ungauged catchments. Mandeville found that its recession behaviour was too steep for larger, lowland basins, although it performed well on smaller, upland catchments. The IEM has been used in modified form for real-time flow forecasting as part of a microprocessor based flood warning system at Haddington in Scotland (Brunsdon and Sargent, 1982).

For $m = 1$ ($b = 0$) the Horton-Izzard equation reduces to the linear reservoir model. This is used in the Thames Catchment Model to represent unsaturated soil storage. The theoretical work of Werner and Sunquist (1951) and Ding (1967) suggests the use of the linear form for confined (artesian) aquifers. Note that a standard implementation of the PDM employs a cascade of two linear storages to represent the surface storage, primarily thought of as representing routing of water via channel pathways to the basin outlet. The relation of the rate constants to channel properties can be considered with the benefit of an understanding of the theoretical underpinnings of the Transfer Function model equations involved.

When $b = 1$ ($m \rightarrow \infty$) then Moore (l983) shows that the model derives from the storage equation $\log q = \gamma + aS$ or $q = \exp(\gamma + aS)$ where a is the same parameter as appears in the Horton-Izzard equation and γ is an intercept parameter (that cancels out in the solution). This is the "log-storage" model, or more properly the exponential storage model, derived by Lambert (l972), and which is used for flood forecasting on the River Dee (Central Water Planning Unit, l977).

Horton remarked in his 1938 paper about the insensitivity to the value of the exponent m, provided k could be adjusted to compensate; subsequent workers have therefore tended to choose an appropriate value of m and optimised k in some manner to avoid the problem of interdependence between k and m. For example, the cubic form (m =3) has commonly been adopted for representing the groundwater storage component in PDM applications. This choice has been motivated by the shape of the hydrograph often being initially steep but subsequently sustained and slowly decreasing (Moore and Bell, 2002).

A summary of the different types of nonlinear storage (as defined for different values of m), and the process mechanism they can be related to, is presented in Table 4.11. It is clear from the above discussion that there is a body of theory available to support an approach that moves away from pure empiricism in determining model parameters for an ungauged catchment. However, the application to an essentially lumped model such as the PDM will be associated with problems of scaling, aggregation and conceptualisation. Such problems are arguably least with the probability-distributed absorption capacity formulation which allows spatial datasets to be used in a natural way. The catchment-scale aggregation implicit in the routing formulations presents greater conceptual difficulties in the sensible use of spatial data. Starting from a model formulated from the outset in distributed form - and capable of using spatial datasets on topography, soil, land cover and geology more directly - appears most rational as a way to proceed for ungauged forecasting. Aggregated forms of such models can be developed as and if required.

Table 4.11 Nonlinear storage model process mechanisms

Exponent		Storage type	Storage mechanism
m	b		
0	-	constant	Infinite storage
½	-1	square root	Orifice
1	0	linear	Confined or artesian aquifer
3/2	⅓		Rectangular weir
			Wide channel (Chezy formula)
5/3	2/5		Turbulent overland flow
			Wide channel (Manning formula)
2	½	quadratic	Unconfined or non-artesian aquifer
5/2	3/5		Triangular weir
3	⅔	cubic	Laminar overland flow
$\rightarrow \infty$	1	exponential	Transient storage

4.3.5 Isolated Event and ISO function models

Model Outline

The Isolated Event Model, or IEM, was originally developed for design applications as part of the UK Flood Studies Project (NERC, 1975). In many respects it is very similar to the single zone representation of the Thames Catchment Model in using the Penman stores concept and a quadratic reservoir for routing. However, the use of the Penman stores concept is not done as part of an explicit soil moisture accounting procedure as is the case with the TCM. Rather, the soil moisture deficit it provides is used as an index of catchment wetness within an empirical equation which relates the proportion of rainfall that becomes runoff - the runoff coefficient - to the soil moisture deficit, D. Specifically the runoff coefficient is defined by the exponential function, $f = \alpha \exp(-\beta D)$, where β is a parameter with units (mm water)$^{-1}$ and α is a dimensionless parameter. Note that the IEM uses as standard a Penman upper store of depth 75 mm, the root constant for short grass, with no bypassing (ϕ=0). Because the original formulation was event-based and for design, the runoff coefficient, f, was applied to the whole storm and D was the soil moisture deficit at the start of the storm. The parameter α can be interpreted as a "gauge representativeness factor" since, with zero deficit (saturated conditions), a proportion α of the rain becomes runoff. The storm rainfall time series is multiplied by the factor f to give an "effective rainfall" series. This is then subject to a time delay before being used as input to the quadratic storage reservoir, the outflow from which forms the IEM model flow prediction.

For real-time flood forecasting applications the concept of an "event" is an awkward notion to work with. The IEM has been modified for real-time use by redefining the runoff coefficient, f, to be a time variant function of the deficit D. Thus, we have $f_t = \alpha \exp(-\beta D_t)$. The calculation of D_t is calculated continuously, within and between storm events, using the Penman stores water accounting procedure. No use is made by the IEM of the outflows from the Penman stores, only the deficit as an index of catchment wetness and its impact on the ensuing volume of flood runoff.

Further modifications of the classical IEM formulation resulted from trials undertaken in the context of the study by Moore *et al.* (1993). The first is to replace rainfall by net rainfall (rainfall less evaporation) prior to applying the factor f_t to yield effective rainfall. The second modification is to replace the simple time delay on the effective rainfall by a triangular time delay function. Thus the inflow to the quadratic storage is a weighted combination of delayed effective rainfalls up to the current time, with the weighting defined by a triangular function. The final modification is that a constant flow, q_c, can be added to the outflow from the quadratic storage to give the total basin outflow.

The similarity between the IEM and a single zone of the TCM has been exploited by implementing the IEM as a variant on the TCM, with the overall model code being referred to as the PSM (Penman Store Model). The IEM parameters are as for a TCM zone with n_z=1, A equal to the catchment area, R_c=75, R_p=999 and ϕ, k, a, τ_d and N set to zero. The remaining parameters, together with additional parameters specific to the IEM, are listed in Table 4.12.

Table 4.12 Parameters of the Isolated Event Model

Parameter name	Unit	Description
α	None	Coefficient in runoff proportion equation
β	None	Exponent in runoff proportion equation
K	mm h	Quadratic storage constant
τ_s	h	Delay to start of smoothing triangle
τ_p	h	Delay from start to peak of smoothing triangle
τ_e	h	Delay from start to end of smoothing triangle
q_c	m³ s⁻¹	Constant flow

Suitability for ungauged catchments

The IEM model as developed within the Flood Studies Report or FSR (NERC, 1975)), and referred to as IEM4, had the four parameters α, β, K and τ_s (a simple delay rather than a delayed smoothing triangle was assumed). It was recognised in the FSR that regressions of these parameters on catchment characteristics could be undertaken for application to ungauged catchments. However, this was not undertaken.

4.3.6 The NAM Model

Model Outline

The NAM Model is a classical lumped conceptual model of the rainfall-runoff process. NAM as an acronym stands for Nedbør-Afstrømnings-Model, Danish for precipitation-runoff-model. It was developed originally as a daily simulation model at the Technical University of Denmark (Nielsen and Hansen, 1973). A schematic of the main features of the model is shown in Figure 4.6.

Figure 4.6 highlights that the model is made up of three main storage elements:

(i)   *upper zone storage* representing vegetation, depressions and near surface (cultivated) soil;
(ii) *lower zone storage* representing the root zone and the main soil horizons; and
(iii) *groundwater storage* representing water bearing rocks.

Overland flow, together with interflow generated from the upper zone storage and baseflow generated from the groundwater storage, experience additional routing and are summed to give the total model flow at the basin outlet.

Evaporation, E_a, occurs at the potential rate, E, given sufficient water in the upper storage, and then at a reduced rate proportional to the degree of saturation of the lower storage. Net rainfall is computed from rainfall P reduced by evaporation, E_a, interflow, q_i, and an addition to storage. Infiltration to the lower zone storage, i, is net rainfall less overland flow. Overland flow, q_o, only occurs when the saturated fraction of the
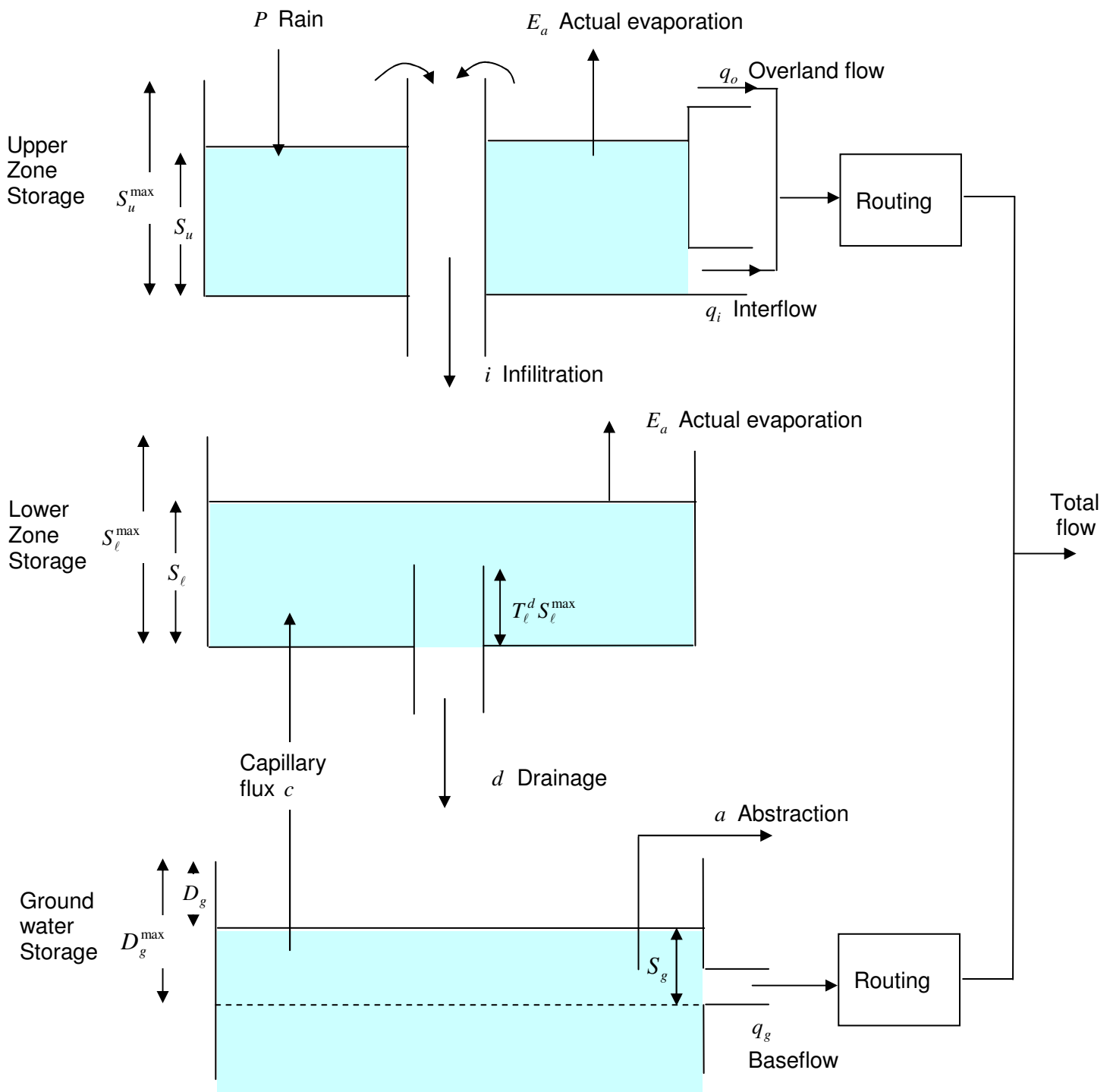
Figure 4.6 The NAM rainfall-runoff model

lower storage exceeds a threshold proportion, T_ℓ^o. The magnitude is proportional to the degree of excess and the net rainfall; the parameter of proportionality, f, is called the overland flow runoff coefficient.

Again, interflow only occurs when a critical saturation fraction of the lower storage is exceeded, the threshold in this case being denoted T_ℓ^i. The magnitude is directly proportional to the degree of excess, with the proportionality parameter k_i called the interflow storage coefficient. There must be sufficient water available to the upper store to sustain this interflow, although the NAM documentation does not make this clear. An alternative conjecture is that interflow is actually generated from water in the lower storage and that the model schematic is wrong.

Groundwater recharge, d, is the drainage of water from the lower storage into the groundwater storage. It is directly related to the infiltration entering the lower storage, i, and its degree of saturation in excess of a critical threshold for drainage to occur, T_ℓ^d. The lower zone storage is added to by infiltration and depleted by drainage to groundwater recharge. The groundwater storage releases water as baseflow according to one of two schemes. The simple scheme uses a linear reservoir conceptualisation relating baseflow q_g to S_g, the water in groundwater storage above a zero reference (negative values are possible); k_g is the time constant parameter of the linear reservoir. The second scheme aims to conceptualise a shallow reservoir typical of lowland catchments with little topographic variation and the potential for waterlogging. In this case baseflow is proportional to the water table depth, D_g, above the maximum drawdown of the groundwater reservoir, D_g^{max}; the proportionality parameter is the time constant k_g. The specific yield of the groundwater reservoir, Y_s, is used to convert from depth to a water equivalent depth.

Water can transfer upwards from the groundwater reservoir to the lower zone storage by capillary action. The capillary flux, c, is proportional to the square root of the deficit in the lower zone storage and inversely proportional to a power of the drawdown in the groundwater reservoir. The power exponent α is related linearly to a quantity D_g^1, defined as the depth of the groundwater table at which the capillary flux is 1 mm day^{-1} when the lower zone storage is empty. In updating the depth to the water table, an allowance for pumped abstractions, a, is made.

Overland flow and interflow are summed and routed to represent translation through the catchment using two linear reservoirs in series with time constants k_1 and k_2. To accommodate a linear response for near surface flows and a kinematic response for above surface flows (classic overland flow) at higher flow rates, the time constants are modified above a threshold q_o^{min} to vary as an inverse power function of the flow with the exponent parameter β set to 0.4 mm hr^{-1} and 0.33 respectively.

As a final step all the lateral components of streamflow – overland flow, interflow and baseflow – are routed together through a final linear reservoir to obtain the total flow response at the basin outlet. This step is not made clear in the model schematic in the NAM Reference Manual. The NAM model also allows for feedback effects within the catchment where irrigation water from groundwater and/or river water can form an input to the model in addition to rainfall. This features within the irrigation module available for modelling catchments with major irrigation schemes.

A summary of the model parameters used in the NAM Model is presented in Table 4.13.

Suitability for ungauged catchments

The NAM model has 16 parameters to be estimated. Advice on setting these parameters for an ungauged catchment is not given in the User Guide.

Table 4.13 Parameters of the NAM Model

Parameter	Unit	Description
S_u^{max}	mm	Maximum capacity of upper zone storage
S_ℓ^{max}	mm	Maximum capacity of lower zone storage
D_g^{max}	mm	Maximum capacity of groundwater storage
T_ℓ^o	none	Critical saturation fraction of lower storage above which overland flow occurs
f	none	Overland flow runoff coefficient
T_ℓ^i	none	Critical saturation fraction of lower storage above which interflow occurs
k_i	mm h^{-1}	Interflow storage coefficient
T_ℓ^d	none	Critical saturation fraction of lower storage above which drainage occurs
k_g	h^{-1}	Baseflow time constant
Y_s	none	Specific yield of groundwater reservoir
D_g^{max}	mm	Maximum depth of water table below zero datum
D_g^1	mm	Depth of water table at which capillary flux is 1 mm day^{-1} when the lower zone storage is empty
k_1 , k_2	h^{-1}	Time constants of two linear reservoirs in series used to route the sum of overland flow and interflow
q_0^{min}	mm h^{-1}	Threshold above which kinematic overland flow occurs
β	none	Exponent in kinematic overland flow threshold function

4.3.7 Transfer Function Models

Model Outline

Transfer Function or TF models are a class of time-series models popularised by Box and Jenkins (1970). They are linear models with which an output variable can be forecast as a linear weighted combination of past outputs and inputs. In a rainfall-runoff context the output is usually flow (or baseflow separated flow) and the input rainfall (or effective rainfall). Any residual model error can be represented through a noise model which is normally of autoregressive moving average (ARMA) form. The overall model is termed a Transfer Function Noise, or TFN, model.

A linear transfer function model relates an output at time t, y_t, to r previous values of the output and s previous values of an input with delay b, u_{t-b}, such that

$$y_t = -\delta_1 y_{t-1} - \delta_2 y_{t-2} - \dots - \delta_r y_{t-r} + \omega_o u_{t-b} + \omega_1 u_{t-b-1} + \dots + \omega_{s-1} u_{t-b-s+1}$$

where $\{\delta_i\}$ are r autoregressive parameters and $\{\omega_i\}$ are s moving average parameters operating on the past outputs and inputs respectively. With y_t as basin runoff (or baseflow separated runoff) and u_t as rainfall (or effective rainfall) this TF model can be used as a simple rainfall-runoff model. The notation TF(r, s, b) is used to indicate the order of the model in terms of the number of parameters and the time delay.

The TF model is equivalent in form to the linear model

$$y_t = v_o u_{t-b} + v_1 u_{t-b-1} + v_2 u_{t-b-2} + \dots.$$

where the weights v_0, v_1, v_2, … define the model's impulse response function (equivalent to the unit hydrograph for effective rainfall as input and baseflow separated runoff as the output). In general the number of parameters $r+s$ in the transfer function representation is far fewer than in the impulse function representation: this is strictly infinite although in practice can be treated to correspond to a significant memory length. The transfer function model thus offers a parsimonious parameterisation of a linear system response.

The model output, y_t, can be related to the observed output, Y_t, though the relation

$$Y_t = y_t + \eta_t$$

where $\eta_t = Y_t - y_t$ is the simulation-mode model error. This model error may be represented by an ARMA error predictor (discussed later) to obtain real-time updated forecasts. In this form, the overall model is referred to as a Transfer Function Noise (TFN) model as popularised by Box and Jenkins (1970).

A special case of the TFN formulation, referred to as AutoRegressive Moving Average on eXogenous inputs or ARMAX, is given by

$$Y_t = -\delta_1 Y_{t-1} - \delta_2 Y_{t-2} - \dots - \delta_r Y_{t-r} + \omega_o u_{t-b} + \omega_1 u_{t-b-1} + \dots + \omega_{s-1} u_{t-b-s+1} + \xi_t$$

where ξ_t also represents model error and can be represented by an ARMA noise model structure. If possible dependence in the model error is not explicitly represented then the above can be used to justify the TF prediction equation

$$ y_t = -\delta_1 Y_{t-1} - \delta_2 Y_{t-2} - ... - \delta_r Y_{t-r} + \omega_o u_{t-b} + \omega_1 u_{t-b-1} + ... + \omega_{s-1} u_{t-b-s+1}. $$

It is this TF predictor that is most commonly used as the basis of operational forecasts by the Environment Agency regions using TF models. The predictor simply operates to form a forecast as a weighted sum of present and past flows and lagged rainfall inputs. (The flows may be baseflow separated with baseflow taken as the flow at the start of an event. This possible distinction is assumed below without further comment.) Observed values of flow are used in the right hand side of the above equation but as the forecast lead time increases the latest forecast value replaces the not-yet-available observed flow at future times. This forecast formulation in which observed flow values are used directly can be referred to as "full state correction".

With the input-output pair of a TF model being rainfall-runoff then the nonlinearity known to exist by hydrologists is clearly not represented explicitly. The state correction formulation is one way of reducing the effect of this weakness. Allowing the model parameters to be time-variant and tracking the variation using a recursive estimation scheme provides other opportunities for improvement. For example, Cluckie and Owens (1987) employ a TF model in such a way that a single model gain parameter, G_t, controlling the proportion of rainfall that becomes runoff, is recursively estimated. Specifically, they use the reparameterised TF model

$$ y_t = -\delta_1 Y_{t-1} - \delta_2 Y_{t-2} - ... - \delta_r Y_{t-r} + G_{t-1}\left(\omega_o u_{t-b} + \omega_1 u_{t-b-1} + ... + \omega_{s-1} u_{t-b-s+1}\right) $$

for forecasting, with the time-varying model gain parameter calculated as

$$ G_t = \mu\, G_{t-1} + (1-\mu)\frac{Y_t + \delta_1 Y_{t-1} + ... + \delta_r Y_{t-r}}{\omega_0 u_{t-b} + \omega_1 u_{t-b-1} + ... + \omega_{s-1} u_{t-b-s+1}}. $$

Here, μ is a smoothing factor in the range (0,1) used to dampen out erratic fluctuations in G_t. This form of TF model with time-varying model gain is included here in the assessment of models using catchment data. It has been used operationally for flood forecasting in Anglian (Page, 1991), and Southern (Pollard, undated) regions of the Environment Agency. In Anglian region the output has been taken to be baseflow separated runoff. Also two sets of model parameters are sometimes used to cope with different responses under "fast response" and "average" conditions. In the assessment that follows the output is taken to be total flow and only a single set of model parameters has been used. This arises from the use of continuous long records in the assessment, typically of eight months duration, and where the concept of an event required to define baseflow has no place.

A related approach in focussing on real-time tracking of the model gain is used in the Nith flood forecasting system in Scotland (Lees *et al.*, 1993). In this case the model gain is tracked using recursive least squares, assuming a random walk process for the parameter variability. A drawback of such approaches involving recursive parameter updating is that the variation is merely "tracked" and not "anticipated". Our understanding of hydrological science, for example, tells as that antecedent wetness can influence the gain or runoff proportion and that soil moisture accounting model components can be

used to anticipate this effect. This leads one to recognise that the role of the transfer function is primarily that of a linear routing operation and can be incorporated as such into a conceptual model as merely one component form. However, an important purpose of this study is to establish whether TF models used in practice provide acceptable model performance when compared to other models.

Another approach to accommodating nonlinear effects in a linear TF model is through the use of a nonlinear loss function to transform rainfall to "direct runoff" or "effective rainfall" and using this as the input variable u_t. Functionally, the transfer function serves as a simple linear routing function. Alternatively, a parallel system of two transfer function models can be envisaged together with a partitioning rule which directs rainfall to the two functions which operate as slow and fast translation pathways. A variety of nonlinear loss functions and parallel TF model functions were investigated in the UK for use in flood forecasting (Moore, 1980, 1982). Most recently, improved estimation schemes for this class of parallel TF model have been developed (see, for example, Young, 1992, Jakeman *et al.*, 1990) which overcome some of the problems encountered in this earlier work. These modified forms of TF model are not used by the EA operationally at the present time.

A form of Transfer Function model deserving of special mention is the *Physically Realisable Transfer Function (PRTF) Model* (Han, 1991). The basic idea in formulating the PRTF model is to choose a parameterisation which constrains the impulse response function to have a physically realistic form in a hydrological context. Principally, this means that it should be positive and not exhibit oscillatory behaviour (it is stable). The basic idea in the PRTF formulation is to replace the set of autoregressive parameters, $\delta_1, \delta_2, \delta_3,...$, by a single parameter, β, related to them by

$$\delta_i = (-\beta)^{-i} C_r^{r-i},$$

where the combinatorial has the standard definition

$$C_k^r = \frac{r!}{(r-k)!\, k!} = \frac{r(r-1)...(r-k+1)}{k!}.$$

This is referred to as an "equal root" parameterisation and gives a stable impulse response function for $\beta > 1$. An important feature of the equal root parameterisation is that it allows the r autoregressive parameters of the TF model to be reduced to one, the root β, through the use of the above relation. However, the form of TF model is restricted as a result.

It is of interest to note special cases of the above. For dependence on one past output ($r = 1$) we have $\delta_1 = -1/\beta$ and for two past outputs ($r = 2$) $\delta_1 = -2/\beta$ and $\delta_2 = 1/\beta^2$. The impulse response function for a single, unlagged input ($s = 1$, $b = 0$) is $v(t) = \beta^{-t}$ for $r = 1$ and $v(t) = (1+t)\beta^{-t}$ for $r = 2$. Han (1991) suggests that choosing r to be 2 or 3 provides sufficient flexibility of the impulse response function, provided the moving average parameters $\{\omega_i\}$ can take on negative values so as to lower the recession limb. To make the model more physically intuitive the equal root parameterisation β is substituted by the time-to-peak, t_{peak}, of the impulse response function. For $r = 2$ when $v(t) = (1+t)\beta^{-t}$ we have for the reparameterisation

$$\beta = \exp\left\{\frac{1}{\left(1 + t_{peak}\right)}\right\}.$$

Note that t_{peak} is actually the time-to-peak of the impulse response function corresponding to the autoregressive part of the PRTF model, excluding moving average and pure time delay effects. Unless the moving average parameters are constrained to be positive then the parameter is better interpreted as indexing the rate at which the tail decays and fails to be indicative of the time-to-peak.

Han (1991) recognises that the TF model, with its fixed impulse response function, will not provide an adequate representation of the rainfall-runoff process which is both nonlinear and time variant. He chooses to address this problem by adjusting the form of the impulse response function to reflect each flood situation as it is encountered in real-time. To ease this task Han introduces three types of adjustment factor designed to alter the volume, shape and time response of the TF model. For volume adjustment the moving average parameters, $\{\omega_i\}$, are scaled using a factor α, the proportion of volume change, such that the adjusted parameters are given by

$$\omega_i^* = (1 + \alpha)\omega_i \qquad i = 0,1,..,s-1.$$

Note that the autoregressive parameters, $\{\delta_i\}$, are not affected by this adjustment.

The shape of the impulse response function is changed with reference to a shift in the position of the peak of the autoregressive part of the impulse response function. The shape adjustment factor, γ, is defined as

$$\gamma = t_{peak}^* - t_{peak}$$

where t_{peak}^* denotes the adjusted peak time. For $r = 2$ this may be expressed in terms of the equal root parameterisation, β of the original model and the adjusted model β^*, to give

$$\beta^* = \exp\left\{\left(\gamma + \frac{1}{\ln\beta}\right)^{-1}\right\}.$$

It follows that the adjusted autoregressive parameters are obtained by substituting the above in

$$\delta_i^* = \left(-\beta^*\right)^{-i} \ C_{r-i}^r.$$

The third form of adjustment is to time shift the impulse response system. This simply involves a change to the pure time delay parameter, b, used to delay the rainfall inputs to the transfer model.

Practitioners can encounter difficulties in implementing such simple adjustments, especially for fast responding catchments and where forecasts from many catchments may be required. Presently, the PRTF model is used in Northwest and Southwest regions in a form that requires the user to manually adjust the three factors controlling

the volume, shape and time response of the model as the flood develops to gain better agreement between past observed and forecast flows. The approach is not automatic or objective. The PRTF model can be used in conjunction with two forms of forecast updating: ARMA error prediction and state updating (full state correction with model gain updating).

The selection of the optimal TF model structure is a further issue with this modelling approach which requires careful consideration.

Suitability for ungauged catchments

The TF model when viewed as a pure black-box model is arguably the antithesis of a suitable model for ungauged catchments. However, because simple forms of TF model can be related to physical-conceptual models - for example representing the storage and release of water in soils, groundwater and channel reaches - they have relevance to the ungauged problem. The underpinning conceptual-physical equations, providing links to physical properties of these storages, can be invoked to help support parameter estimation. Also a small number of basic characteristics of simple forms of transfer function, including forms used in unit hydrograph analysis such as the triangle, can be linked to catchment properties through the traditional empirically-derived relations. The former approach is conceptually more appealing whilst the latter has proved of practical use, at least for design studies, starting with the pioneering work of Nash (1960). However, progress on the ungauged problem for flood forecasting is likely to be limited following this approach in a purely black-box, empirical way.

4.3.8 FSR/FEH/ReFH Rainfall-Runoff Models

The lumped rainfall-runoff models reviewed up to now have been used in some form for operational flood forecasting. Another category of rainfall-runoff model has been developed specifically with design applications in mind and are of interest here because of the attention given to addressing the ungauged site problem. Of particular interest to UK application is the rainfall-runoff method associated with the Flood Study Report, the restatement of it in the Flood Estimation Handbook and the recent reformulation known as the ReFH model. These developments are reviewed next with particular reference to their relevance for forecasting at ungauged locations.

FSR/FEH Model Outline

The Flood Study Report (NERC, 1975) developed a simple form of rainfall-runoff model for design use which has some relevance to the ungauged modelling problem. Essentially the same model formulation features as the basis of the FEH rainfall-runoff method (Houghton-Carr, 1999). The model adds a constant event baseflow to storm runoff derived from storm rainfall via a proportional loss model and a unit hydrograph (UH) routing model.

The form of instantaneous unit hydrograph (IUH) used is of particular interest. A triangular form is assumed characterized by a time-to-peak, T_p, and duration, T_b, with $T_b = 2.525 T_p$. The ordinate of the IUH at the peak, U_{T_p}, is fixed by the requirement that the area under the triangle is $0.5 T_b U_{T_p}$. For a unit volume (area) IUH $U_{T_p} = 2/T_b$.

However, the FSR considers an IUH resulting from 10 mm effective rainfall falling on an area of 100 km^2. Noting that 10 mm falling on 100 km^2 is equivalent to $10 \times 100/3.6 = 277.78$ m^{3}s^{-1} h , then for this volume $U_{T_p} = 220/T_p$ (utilising the relation

between T_b and T_p). The IUH is scaled to a specific catchment of area A using the factor $Q_p = 2.2A/T_p$ m³ s⁻¹ per 10 mm effective rainfall. Thus the IUH is characterised by a single parameter, the time-to-peak T_p .

For gauged catchments T_p was estimated from the observed catchment lag L (the time from the hyetograph centroid to the hydrograph peak) using the relation $T_p = 0.879 L^{0.951}$. For ungauged catchments a relation with catchment properties was derived:

$$T_p = 4.27 DPSBAR^{-0.35} PROPWET^{-0.8} DPLBAR^{0.54} (1 + URBEXT)^{-5.77}$$

An addition $0.5\Delta t$ was made for a UH of data interval Δt .

The proportional loss model is a simple "Percentage Runoff" P_r transforming storm rainfall to effective rainfall for UH routing. This is made up of 3 parts: $P_{r,s}$ the standard part reflecting the capacity of the catchment to generate runoff and the dynamic parts $P_{r,cwi}$ and $P_{r,rain}$ reflecting the catchment wetness prior to the storm and the storm magnitude itself. Specifically, $P_r = P_{r,s} + P_{r,cwi} + P_{r,rain}$. For ungauged catchments, $P_{r,s}$ is estimated as a linear weighting of the 29 HOST class values, $P_{r,cwi} = 0.25(CWI - 125)$ where *CWI* is the Catchment Wetness Index and $P_{r,rain} = \max(0, 0.45(P - 40)^{0.7})$ where P is the catchment rainfall in mm. For urban catchments, the Percentage Runoff P_r is adjusted using the transformation $P_r(1 - 0.615\,URBTEXT) + 70(0.615\,URBTEXT)$.

Finally, baseflow for ungauged catchments is estimated as the constant value $Q_b = \{33(CWI - 125) + 3\,SAAR + 5.5\}10^{-5}A$. Total catchment runoff is obtained as the sum of this baseflow and the routed effective rainfall at each time-step within the flood event.

Relevance for ungauged catchments

The direct relevance to ungauged flood forecasting of the FSR/FEH event-based rainfall-runoff model developed for use in design is limited. Probably the most relevant aspect of the formulation is the efficient parameterisation of the routing component of the rainfall-runoff process as a triangle defined via one parameter, the time-to-peak T_p . The relation of T_p with catchment properties provides an easy way of characterising the translation phase of fast response runoff for ungauged catchments. The expression for T_p might also be used to guide the choice of a simple TF (Transfer Function) model that reproduces this time-to-peak. For example, if the form of TF model is chosen to be conceptually equivalent to a cascade of two linear reservoirs (as used in the PDM model) with equal time constants, these time constants can be chosen to give an IUH (impulse response function) with this time-to-peak.

ReFH Model Outline

The FSR introduced the UH theory with a definition sketch of a simple IUH of triangular form but with a kink (break in slope) in the recession limb. However a simple triangle was used in practice as outlined above. The FSR rainfall-runoff method (and FEH

restatement of it) has recently undergone a substantial review leading to a new method referred to as the ReFH model (Kjeldsen *et al.*, 2005). This retains use of the UH method but is extended to allow for a kinked triangle form of IUH, with the kink located at time ordinate $2T_p$, and the S-curve approach is used to obtain UHs of a required duration. The proportional loss model is replaced by a probability-distributed soil moisture accounting procedure with store capacities assumed to follow a rectangular distribution (constant frequency of occurrence between zero and a maximum value c_{max}); it thus uses a component special case of the PDM model for soil moisture accounting. A baseflow model is invoked of linear reservoir form, characterised by a baseflow lag b_l, receiving recharge as input which is a fraction, b_r, of the total flow less the baseflow. In contrast to the isolated event formulation of the FSR method, the ReFH model can be used as a continuously accounting rainfall-runoff model. The method has been developed for application to ungauged basins using the regression of model parameters on catchment properties approach. The model structure in parameter-reduced form is defined by four model parameters (c_{max}, T_p, b_r and b_l) and two initial conditions (initial baseflow b_f and initial wetness C_0). The regression relations obtained are summarised below:

$$c_{max} = 589 BFIHOST^{0.94} PROPWET^{-0.26}$$
$$T_p = 1.492 PROPWET - 1.24 DPLBAR^{0.66}(1+URBEXT) - 5.02 DPSBAR^{-0.36}$$
$$b_r = 3.751 BFIHOST^{1.08} PROPWET^{0.36}$$
$$b_l = 25.47 BFIHOST^{0.47} DPLBAR^{0.21} PROPWET^{-0.53}(1+URBEXT)^{-3.01}$$

$$b_f = (53.7(C_0 - 126.4) + 5.56 SAAR)10^{-5} AREA \qquad \text{for winter}$$
$$b_f = (27.0(C_0 - 92.56) + 3.23 SAAR)10^{-5} AREA \qquad \text{for summer}$$

Relevance for ungauged catchments

The regression relations with catchment properties are generally weak with r^2 values below 0.5, except for c_{max} and T_p (0.56 and 0.83 respectively), suggesting unreliable model performance at ungauged sites. The relation for T_p, whilst similar to that in the FEH, is an improvement on it and might have value for inferring UH or TF forms for ungauged catchments. The expression for c_{max} may have value for PDM applications at ungauged sites, provided a rectangular distribution of store capacity is invoked (equivalent to a Pareto distribution with unity shape parameter).

4.4 Distributed hydrological models

4.4.1 Introduction

The classical *physically-based distributed models* employ nonlinear partial differential equation descriptions of key physical processes that are solved numerically using, for example finite difference or finite element schemes. Well-known brand name examples are the SHE (Système Hydrologique Européen) and the IHDM (Institute of Hydrology Distributed Model). The former employs a grid-square structure and finite difference solutions whilst the latter focuses on a hillslope representation solved on a finite element mesh. Both employ the same fundamental equations (but differing in application dimension): the St. Venant equations for overland and channel flow, Richard's equation for subsurface flow and the Boussinesq equation for groundwater flow. Models of this type are complex to use, require detailed spatial data for configuration and can demand significant computer resources to run. Their performance will necessarily be constrained by the real complexity of hydrological systems above and below ground, the data support available, and the approximations involved in process representation and numerical solution. Experience with models of this type indicates that their value is greatest where there is a need to understand the impact of some future change within the catchment, particularly relating to land cover or land management. This form of planning or policy-setting application benefits most from their "physical-basis". The application of such models for real-time forecasting under present conditions is less likely to prove worthwhile. For gauged catchments where model calibration is possible, simpler models are easier to apply and can give as good if not better performance. Even for ungauged catchments, the complexity of model formulation can raise false expectations of model accuracy. For these reasons, more extensive treatment of "physics-based" distributed models will not given here. For further information on this type of model, the reader is referred to the useful reviews given by Beven (1985) and contained in Singh (1995).

The limitations of classical "physics-based" distributed models for flood forecasting discussed above have led to simpler forms of distributed hydrological model being developed. Commonly the partial differential equation representations are replaced by, or reduced to, simpler ordinary differential equations that represent the processes in a physical-conceptual way at a simpler, aggregate level. Examples of such *physical-conceptual models* are presented in this section. The first example is the Grid Model, developed by CEH with Environment Agency funding support for use in flood forecasting and exploiting weather radar and supporting spatial datasets, especially DTMs. The second is the Grid-to-Grid Model representing a development of the former for area-wide modelling with support via the Met Office from the Ministry of Defence and Defra. These represent examples of grid-based distributed models, the first based on a source-to-sink formulation and the second on a grid-to-grid area-wide formulation (see Section 3.4.2). Similar runoff production functions operating within each grid-square are available for use within the present standalone versions of these models. Section 4.4.4 that follows discusses the relevance of land surface schemes used as grid-based runoff production schemes (and providing evaporation and soil moisture estimates) coupled to atmospheric models. This is done with specific reference to the Met Office MOSES-PDM scheme developed in collaboration with CEH. An operational trial version of this is coupled to the routing scheme employed by the Grid-to-Grid Model for UK-wide indicative estimation of river flows. Lastly, emerging ideas are outlined on new distributed runoff production functions and flow routing formulations that combine controls from topography with soil, land cover, and channel properties.

The suitability of a particular modelling approach to the ungauged flood forecasting application is discussed for each model in turn.

It should be noted that whilst the examples of distributed model presented here are configured on a regular square grid, this need not be the case. For example, a number of models are formulated to use *representative elementary areas* (REAs) as spatial building blocks within which hydrological response is judged to be reasonably homogeneous. When combined with flow routing models of channel links the overall configuration can be described as *tree-and-leaf*, with the leafs being REAs and the tree branches and trunks the channel links. Such a configuration can provide a more efficient way of representing catchment processes when compared to a fixed grid, whilst the regularity of the grid coverage has appeal particularly for area-wide application.

4.4.2 The Grid Model

Model outline

The Grid Model was developed by the Institute of Hydrology for the Environment Agency to exploit the distributed nature of radar data and new digital datasets on elevation, land use and soils (Moore *et al.*, 1992; Bell and Moore, 1998). It is configured to share the same grid as that used by the weather radar. Each radar grid square area is conceptualised in the catchment as a storage which receives water in the form of precipitation and loses water via overflow, evaporation and drainage. The storage used in the basic form of model is a simple store (tank or bucket) having a finite capacity S_{max}. This capacity can be thought of as an absorption capacity characterising the area of the square grid encompassing surface detention, soil moisture storage, and the interception capacity of vegetation and other forms of land use. A fundamental idea used in the basic form of model is that absorption capacity is controlled by the average gradient, $\overline{g}$, of the topography in the grid square which can be calculated readily from a digital terrain model (DTM).

Specifically, for a given grid square, the following linkage function is used to relate the maximum storage capacity, S_{max}, and the average gradient, $\overline{g}$, within a grid square:

$$ S_{max} = \left(1 - \frac{\overline{g}}{g_{max}} \right) c_{max} , \qquad (4.4.1) $$

for $\overline{g} \le g_{max}$. The parameters g_{max} and c_{max} are upper limits of gradient and storage capacity respectively and act as "regional parameters" for the basin model. A measurement of the mean gradient within each grid square of the river basin is obtained from the DTM. Values of S_{max} for all grid squares are determined using only the two model parameters, g_{max} and c_{max}, together with measurements of $\overline{g}$ for each square.

A grid storage loses water in three possible ways. If the storage is fully saturated from previous rainfall then any net addition of water spills over and contributes to the fast catchment response. Drainage from the base of the store is controlled by the volume of water in store and contributes to the slow catchment response. Thirdly, water is lost via evaporation to the atmosphere.

Figure 4.7 (a) illustrates a typical grid storage and the components of the water balance involved. Evaporation loss occurs at the rate, E^a, which is related to the potential evaporation rate, E, and the store water deficit, D, through a simple linear decrease from the potential rate as a threshold deficit, D^*, is exceeded. The value of D^* is common across grid squares. Drainage from the grid storage, which contributes to the slow catchment response, occurs at a rate controlled by a power function of the water in store. Finally, the updated water storage is given by continuity taking into account the initial storage and losses to evaporation and drainage. The direct runoff rate contributing to the fast basin response is calculated as the rainfall less loss to any storage left available.

Water is routed from each grid square storage to the catchment outlet using DTM-derived isochrone pathways. The construction of isochrones – lines joining points of equal time of travel to the basin outlet – is achieved by assuming that water travels with only two velocities depending on whether the pathway involves a hillslope or a river channel. In this way it is relatively easy to construct isochrones by direct inference from the distance of a point to the basin outlet and the nature of the pathways involved. The catchment is subdivided into reaches according to these isochrones and water is routed along the reaches to the catchment outlet using a discrete kinematic wave routing procedure. This not only advects water between the reaches but also incorporates a diffusive component seen in observed hydrographs.

Figure 4.7 (b) shows an idealised catchment with isochrones overlaid onto the grid squares: it highlights for grid-square j the area of each isochrone strip within it with $A_{\tau+1,j}$ denoting the area bounded by isochrones $\tau+1$ and τ and the grid-square (and the catchment boundary where this intersects). The water input to each isochrone strip can be readily calculated as an area weighted summation of the outflow rates from the grid squares encompassed by the strip. The outflow can be the direct runoff rate, q, or the drainage rate, d, depending on whether the routing scheme relates to the fast or slow response pathway to the catchment outlet.

The n isochrone strips are represented by a cascade of n reaches, with each reach represented by a discrete kinematic wave equation with lateral inflow. The number of strips, n, together with a dimensionless wave speed parameter, θ, controls the lag and attenuation of water movement through the reaches (Moore and Jones, 1978). The lateral inflow, r_t^k, can be defined as direct runoff or drainage which are routed separately using two parallel discrete kinematic wave models, characterised by different wave speeds θ_s and θ_b respectively. A schematic depicting the overall structure of this basic form of Grid Model is shown in Figure 4.7 and Table 4.14 provides a summary of the model parameters.

The Grid Model exists in a basic form and as a number of variants. The variants encompass alternative forms of runoff production and flow routing scheme. The variants of runoff production scheme include: (i) the distribution of slope within a grid square to underpin a probability-distributed store formulation, (ii) a topographic index control, and (iii) an integrated air capacity control based on soil survey data. Also, land use classification of urban area can be used to delineate the fraction of each grid square that can be considered to have zero storage capacity. A variant of the flow routing scheme allows drainage from each grid square to travel to the basin outlet in a way governed by a separate set of isochrones, representing the slow response pathway, which is determined by the path length and a Darcy velocity of flow. This velocity is estimated from the local gradient of the terrain (calculated from the DTM) as

(a) Water balance within a grid
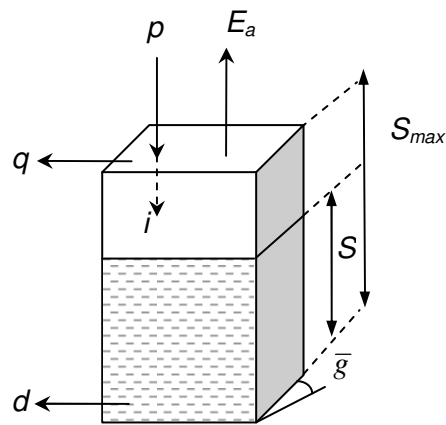
p	rainfall
E_a	evaporation
q	direct runoff
d	drainage
I	infiltration
$\overline{g}$	average gradient
S, S_{max}	water storage and maximum storage capacity

(b) Catchment with superimposed weather radar grid and inset showing isochrone areas in grid square j
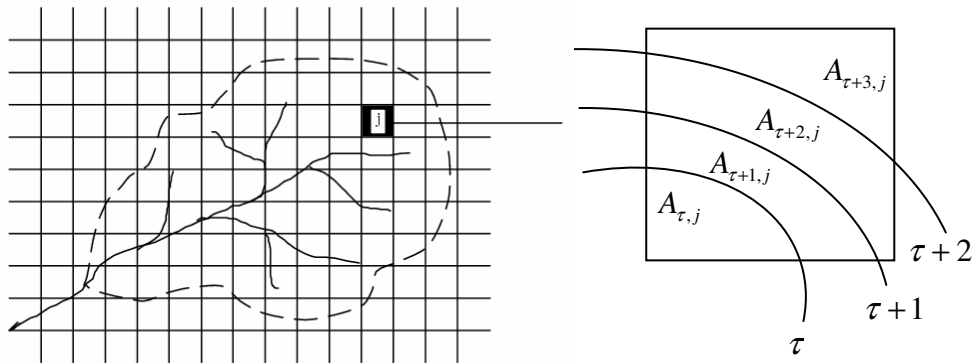
(c) Grid Model configuration
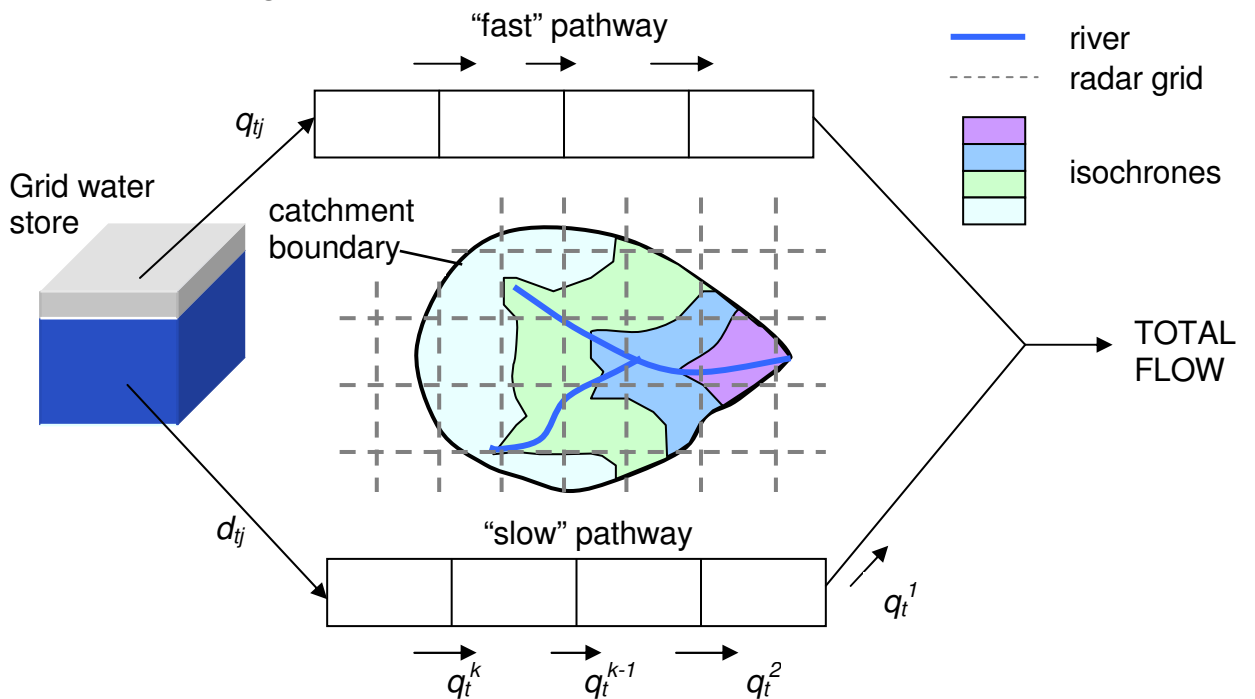
Figure 4.7 The Grid Model

Table 4.14 Parameters of the Grid Model

Parameter	Description	Unit
f_r	Rainfall correction factor	-
D^*	Storage threshold deficit (or root constant) in evaporation function	mm
S_0	Proportion of total storage capacity initially full	-
g_{max}	Regional upper limit of gradient	-
c_{max}	Regional upper limit of storage capacity	mm
i_{max}	Maximum infiltration rate	mm h^{-1}
k_d	Storage constant of (cubic) drainage function	h^{-1} mm^{-2}
θ_s	Wave speed parameter for routing direct runoff	-
θ_b	Wave speed parameter for routing drainage	-
v_L	Advection velocity of flow along land path	m s^{-1}
v_R	Advection velocity of flow along river path	m s^{-1}

an approximation to the hydraulic gradient. More detail of the basic and probability-distributed runoff production schemes is given in Appendix A. Appendix B provides further details of the flow routing scheme.

Suitability for ungauged catchments

The Grid Model development reported in NRA R&D Note 252 (Moore *et al.*, 1994) included assessments of its application to the ungauged case using paired and nested catchments for evaluation. Good results were obtained when the Silk Stream model parameters were used for the neighbouring Yeading Brook (R^2 =0.79) and when the Rhondda at Trehafod parameters were applied to the nested Tynewedd catchment (R^2 =0.8). However poor results for the Rhondda to Cynon and Kinnersley Manor (Mole) to Gatwick model transfers were obtained. In hindsight, incorporating a return flow component representing water transfers between the slow and fast routing pathways might have provided more robust model transfers. This extension of the Grid Model is still to be trialled.

In general, the Grid Model has a structure well suited to the ungauged problem as it provides a natural way of incorporating topographic effects on runoff production and flow routing. Variants of the model also allow considerations of soil (for example, integrated air capacity) and land cover (for example, urban area) properties to be incorporated in a physically sensible way.

4.4.3 The Grid-to-Grid Model

Model Outline

The Grid-to-Grid Model has been configured to represent spatial variability in catchment response and to make full use of the spatially-distributed rainfall data derived from networks of radars and raingauges. The model can be configured for use at (almost) any spatial resolution, with the temporal resolution determined by stability criteria. At present, it is typically run at a 1 km resolution and for a 15 minute time-step. The model employs Digital Terrain Model (DTM) data to support its configuration and parameterisation. A modular formulation allows model revisions/extensions to be made. Through adopting an area-wide formulation, in contrast to a catchment-based one, it is well suited to support forecasting at any set of locations within a defined area. As a consequence, the model is able to be calibrated to groups of gauged locations within an area and forecasts extracted for any ungauged location within the same area. It will also support modelling of nested and parallel catchments

The model structure is summarised in Figure 4.8. Currently the model employs a simple terrain-based runoff production scheme, based on methodology used in the CEH Grid Model (Bell and Moore, 1998a,b), to derive surface and sub-surface runoffs from gridded rainfall and potential evaporation inputs. The grid-to-grid water routing component employs a kinematic wave formulation that is equivalent in conceptualisation to a network cascade of linear reservoirs. Surface and sub-surface runoffs are routed via parallel fast and slow response pathways linked by a return flow component representing stream-soil-aquifer interactions. The terrain-following flow paths are configured using the DTM. Further details can be found in Appendix A and Appendix B.
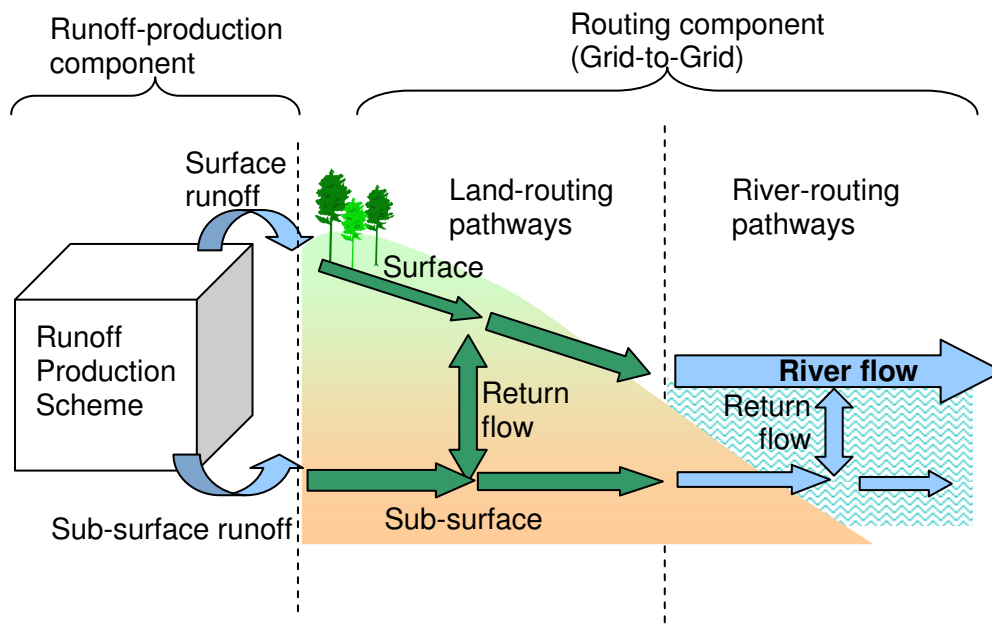
Figure 4.8 Schematic of the Grid-to-Grid Model structure

Suitability for ungauged catchments

The Grid-to-Grid Model development has particular appeal for the ungauged case where forecasts at many locations across a wide area are required. For this reason it was developed initially as a suitable routing scheme for use with grid-square runoffs from the Met Office Unified Model in numerical weather prediction (NWP) and regional climate model (RCM) forms. It can provide routed flows at any location across the UK and Europe, and potentially globally.

Shortcomings in the Unified Model runoffs and the need for higher resolution, more precise estimates for flood forecasting have led to the current prototype self-standing form. This presently uses the runoff production scheme of the CEH Grid Model and rainfall inputs from (spatially interpolated) raingauge and/or radar estimates. Alternative runoff production schemes are under trial, including that outlined in the next section (Section 4.4.4) which provides a way of incorporating a combination of soil property and topographic information. A prototype application of this is presented in Appendix D.

Note that it contrasts with the source-to-sink form of the Grid Model. This is calibrated to a chosen outlet point to obtain its "regional" parameters. The model is re-applied to the ungauged location of interest (a nested, paired and/or similar catchment) using these regional parameters but configured using the topography (and any other supporting information) and rainfall for the ungauged catchment area. The area-wide form of the Grid-to-Grid Model allows a regional parameter set to be established providing reasonable performance across a number of gauged sites, and at the same time allows forecasts for the ungauged sites within the delineated area to be output.

There are advantages to the Grid Model approach in providing a much simpler routing scheme in which the 2D grid-to-grid routing is replaced by an essentially equivalent 1D cascade of channel reaches. This is defined as a cascade of reaches delineated by isochrone strips identified from terrain data and wave speed parameters. However, it lacks the flexibility of the grid-to-grid approach for forecasting the flow out of any set of grid-squares over the defined model domain.

4.4.4 Land surface scheme models: the MOSES-PDM example

Model Outline

The need for a representation of the land surface within atmospheric models has formed an important driver for the development of area-wide models. Atmospheric models are configured on a grid with global coverage along with nested models where finer resolution is required. These atmospheric models are used for weather forecasting or climate prediction. In the UK, the Met Office employ a "Unified Model" formulation which underpins different model configurations serving these two purposes. The nested Mesoscale Model operates presently at a resolution of circa 12 km over the UK in support of weather forecasting.

The land surface component of the Unified Model is the Met Office Surface Exchange Scheme, or MOSES. In common with many land surface models developed primarily to support better atmospheric modelling, the description of land surface processes emphasises vertical transfers of energy and moisture flux. The model descriptions began their development as essentially classic "point" or "big leaf" representations of the processes operating within a model grid box. Essentially they are flat surface

representations which ignore the control of topography on lateral transfers of water that can exert a strong influence on water movement at the catchment scale. A detailed description of evaporation under atmospheric forcing and soil/vegetation control is complemented by the use of Richard's equation representing vertical movements of water in the soil. The scheme generates estimates of surface and subsurface runoff, the latter being bottom drainage from the soil column; there is no explicit representation of groundwater. A schematic of the MOSES land surface component is presented in Figure 4.9.
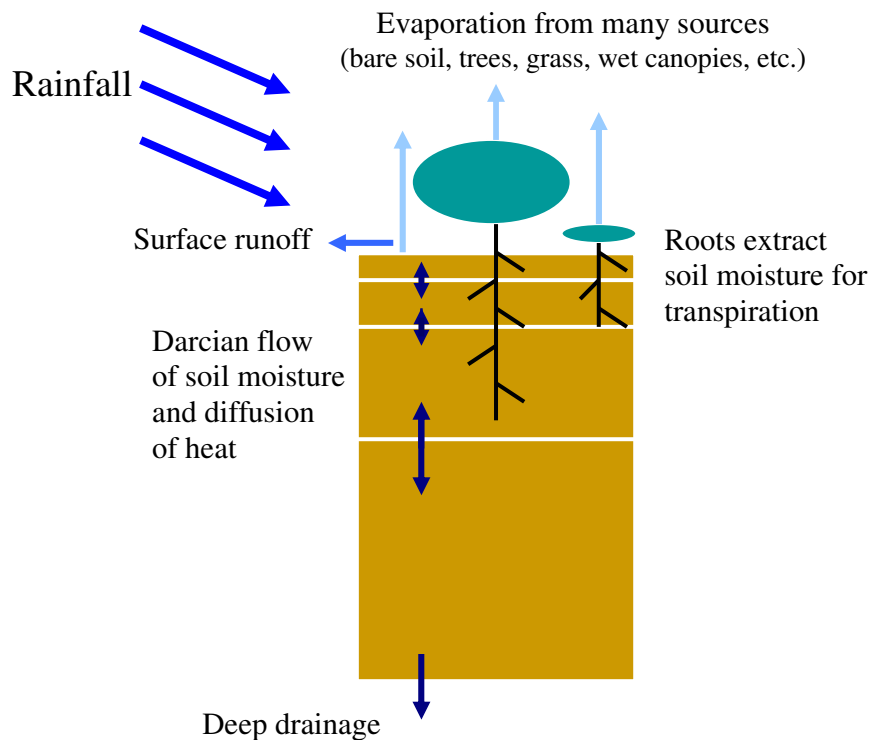
Figure 4.9 Schematic of the MOSES land surface component

Recent work with CEH Wallingford has extended MOSES in two ways that are relevant to its hydrological use. The first has modified the representation of soil moisture and runoff production to allow the soil water capacity to vary within the model grid. This has been done using the PDM (Probability Distributed Moisture) concept that represents capacity as varying as a Pareto distribution across the grid box. The result is more runoff is generated from areas of lower capacity and soil moisture is reduced. This new representation, called MOSES-PDM, can be viewed as an indirect way of introducing topographic variation via its effect on soil capacity (Blyth, 2002; Smith *et al.*, 2004).

The second development has been to couple MOSES to the grid-to-grid routing scheme used in the Grid-to-Grid Model outlined in Section 4.4.3 and Appendix B. The scheme is used to translate surface and subsurface runoffs from MOSES along fast and slow pathways respectively (Bell and Moore, 2004; Bell *et al.*, 2004). The direction of movement of water from grid to grid is determined by flow paths delineated using a Digital Terrain Model. A kinematic routing scheme is employed which allows transfers of water between the slow and fast pathways, for example representing in a simple way any stream/aquifer interactions. Flows can be extracted at the outlets to model grids that correspond to gauged or ungauged catchment locations. The model grid used for routing is currently 1 km.

MOSES and MOSES-PDM Runoff production schemes

MOSES (Met Office Surface Exchange Scheme) conceptualises the production of surface runoff and subsurface runoff within a grid cell as a simple vertical flow process through four soil layers controlled by Richards' equation. A simplified description is given here that assumes no frozen water and omits the detail of the evaporation calculation as a function of land cover and soil layer.

Consider a layer of soil of thickness Δz containing a water volume per unit depth of soil θ which at saturation has a value θ_s, so that $S = \theta / \theta_s$ is the soil wetness as a fraction of that at saturation. Then the soil moisture content (in terms of water mass per unit area, kg m^{-2}) is $M = \rho_w \Delta z \theta = \rho_w \Delta z \theta_s S$ where ρ_w is the density of water. Let W denote the diffusive water flux with W_{in} and W_{out} the values in and out of the layer respectively. Then mass balance for the layer gives

$$\frac{dM}{dt} = W_{in} - W_{out} - E \tag{4.4.2}$$

where E denotes the evaporation flux out of the layer.

The water flux is given by Darcy as

$$W = K\left\{ \frac{\partial \psi}{\partial z} + 1 \right\} \tag{4.4.3}$$

where ψ is the soil water suction and K the soil hydraulic conductivity. These are related to soil wetness through the Clapp and Hornberger (1978) approximations $\psi = \psi_s S^{-B}$ and $K = K_s S^{2B+3}$, with the suffix s denoting values at saturation and B is a parameter.

For the top soil layer, if P is effective surface precipitation (rainfall, throughfall, snowmelt) then if Q_s denotes surface runoff, $W_{in} = P - Q_s$ provides the upper boundary condition. For the bottom soil layer, free drainage is assumed so that the subsurface runoff $W_{out} = K$ provides the lower boundary condition. Equation (4.4.2) is solved for the four layers by invoking a forward time-step weighting scheme to obtain 4 simultaneous equations forming a tridiagonal set solved by Gaussian elimination. Any excess soil moisture in a soil layer is assumed to contribute to surface runoff. A fixed layer configuration is assumed for all grid cells with thicknesses from the top being 0.1, 0.25, 0.65 and 2 m, giving a fixed total depth of 3m.

The MOSES-PDM extension (Blyth, 2002; Smith *et al.*, 2006) considers that the soil down to a depth Δz (taken to be the 1 m depth of the top three layers) has a capacity to hold water, c, that varies from point to point in the grid-square. Specifically, it is probability distributed according to the Pareto distribution function

$$F(C) = prob(c \le C) = 1 - (1 - C / c_{max})^b \tag{4.4.4}$$

used in the PDM model (Moore, 1985, 1999). Parameter b controls the shape of the distribution between zero and the maximum capacity at a point, c_{max}. The original implementation of the scheme was rather simple with parameter b fixed at 1, which

meant that the capacity c varied between 0 and c_{max} with a uniform frequency of occurrence equal to $1/c_{max}$. Parameter b is now set at 0.5.

The point water capacity c and the total water capacity S_{max} are taken here to have units of kg m^{-2} for the MOSES grid-square. (Note that S and S_{max} now have different meanings in this PDM context.) The relation between c and θ is provided by equating the maximum storage capacity in the PDM to that at saturation in MOSES giving

$$S_{max} = c_{max}/(b+1) = \rho_w \Delta z \theta_s = M_s,$$

so that

$$c_{max} = (b+1)\rho_w \Delta z \theta_s. \tag{4.4.5}$$

The critical capacity below which stores are full C^* is related to θ by equating the total water in storage

$$S = S_{max}\left\{1 - (1 - C^*/c_{max})^{b+1}\right\} \tag{4.4.6}$$

in the PDM to the soil water content in MOSES $M = \rho_w \Delta z \theta$, which yields

$$C^* = c_{max}\left\{1 - (1 - \theta/\theta_s)^{b+1}\right\}. \tag{4.4.7}$$

Note that $F(C^*)$ is the fraction of the grid-square that is saturated and capable of generating surface runoff.

If P is the effective rainfall rate over the next interval of duration Δt, then at the end of the interval the critical capacity becomes $C^* + P\Delta t$ (constrained to an upper limit of c_{max}) and a new total water storage S' calculated based on equation (4.4.6). Continuity then gives the mass volume of surface runoff generated over the interval as

$$V_S = P\Delta t - (S' - S) \tag{4.4.8}$$

and Q_s is taken as equal to $V_S/\Delta t$.

Suitability for ungauged catchments

The main strength of MOSES-PDM for the "ungauged case" is that its physical formulation naturally requires information on soil properties and land cover and is thus immediately applicable to ungauged areas to obtain runoff estimates. MOSES-PDM derives from its roots in supporting atmospheric modelling. Its representation of water movement emphasises the vertical dimension in support of energy transfer calculations: it would not be the natural choice for estimating runoff at the grid or basin scale. However, the formulation supports the use of soil and land-cover information and provides a simple way of treating sub-grid heterogeneity of soil capacity. Unfortunately, the data support to the formulation as applied over the UK can be weak: for example a constant soil depth is assumed everywhere and there is no topographically determined control on runoff production changing with grid location.

The link to a grid-to-grid routing scheme, using the MOSES-PDM runoffs as inputs, allows flows to be estimated approximately for any grid outlet within the modelling domain, and therefore supports ungauged location modelling. Initial trials point to shortcomings in the runoff volumes generated by MOSES-PDM. The Nimrod rainfall, used as input to MOSES-PDM, can be a source of error that particularly affects some grid locations and to which runoff estimates are sensitive.

A more tailored approach to flood forecasting for the ungauged case would clearly be preferable. However, MOSES-PDM has real value in a Flood Watch context by providing UK-wide coverage and indicative grid-square estimates of soil moisture, evaporation, runoffs and routed river flows.

4.4.5 A simplified kinematic wave model soil- and topography-controlled approach to rainfall-runoff modelling

Introduction

This section considers a general approach to rainfall-runoff modelling based on a simple kinematic wave model foundation. The formulation involves physically-based linkages with topography through the influences of terrain slope and water pathway topology. The resulting nonlinear storage model equations also allow the influence of soil physical properties and land cover to be introduced in a physically-based way. The approach is used to develop model formulations for lateral soil drainage, surface runoff (saturation overland flow) and channel flow processes within and between cells of a model grid. A discussion of the suitability of the approach for flood forecasting at ungauged locations concludes the section.

Runoff production scheme with lateral soil water drainage

Consider a sloping soil column of depth L and slope s_0 subject to precipitation falling at a rate p (ms^{-1}). It will be assumed that the transient phase of vertical infiltration can be neglected and the horizontal transfer of water dominates. Continuity of mass according to a kinematic wave model is given by

$$(\theta_s - \theta_r)L\frac{\partial \Theta}{\partial t} + \frac{\partial q}{\partial x} = p .$$
(4.4.9)

Here, the effective soil moisture content, $\theta_e = \theta_s - \theta_r$, is the difference of the content at saturation, θ_s, and the residual content, θ_r. The soil moisture content θ (a volumetric fraction) is scaled over the interval (0,1) to give the reduced soil moisture content

$$\Theta = \frac{\theta - \theta_r}{\theta_s - \theta_r} .$$
(4.4.10)

The actual and maximum water contents (m) are given by

$$S = (\theta_s - \theta_r)L\Theta = (\theta - \theta_r)L$$
(4.4.11)

$$S_{\max} = (\theta_s - \theta_r)L .$$
(4.4.12)

The horizontal flow per unit width (m²s⁻¹), q, is approximated by the momentum equation

$$q = T(\Theta)s_0 = s_0 k_s L\Theta^\alpha .$$ (4.4.13)

where the horizontal transmissivity, $T(\Theta) = k_s L\Theta^\alpha$, derives from considering the Brooks and Corey (1964) relation for point relative permeability integrated over the depth of soil (Todini, 1995; Benning, 1995). Here, k_s is the saturated hydraulic conductivity (ms⁻¹) and α is a pore size distribution factor.

Equation (4.4.13) can be written in the form of a nonlinear reservoir function as

$$q = CS^\alpha$$ (4.4.14)

with $C = \dfrac{Lk_s s_0}{S_{max}^\alpha}$ interpreted as a local conveyance.

Since

$$\frac{\partial S}{\partial t} = (\theta_s - \theta_r)L\frac{\partial \Theta}{\partial t}$$

then from equation (4.4.9) the following kinematic wave model is obtained:

$$\frac{\partial S}{\partial t} = p - \frac{\partial q}{\partial x} = p - \frac{\partial CS^\alpha}{\partial x} .$$ (4.4.15)

This continuous equation in time, t, and space, x, can be applied to a grid cell of length Δx. Let $V_i = \Delta x^2 S_i$ denote the volume of water stored in the i th cell. Approximating the space derivative by $\partial S^\alpha / \partial x = (S_i^\alpha - S_{i-1}^\alpha)/\Delta x$, then simple substitution and consideration of inflows from multiple upstream cells gives

$$\frac{dV_i}{dt} = p\Delta x^2 + Q_i^I - Q_i^D .$$ (4.4.16)

Here, Q_i^I is the inflow to cell i from contributing upstream cells and Q_i^D is the lateral drainage from the cell, given by

$$Q_i^D = \frac{C_i \Delta x}{\Delta x^{2\alpha}} V_i^\alpha .$$

The inflow will be zero for source cells and elsewhere made up of surface and subsurface contributions from the upstream contributing area. For a single inflow originating as lateral drainage from cell $i-1$ the inflow to cell i is given by $Q_i^I = Q_{i-1}^D$.

A soil water balance for a time-step $(t_0, t_0 + \Delta t)$ gives the outflow discharge in the form of lateral soil drainage as

$$Q_i^D = p\Delta x^2 + Q_i^I - \frac{V_i'(t_0 + \Delta t) - V_i(t_0)}{\Delta t},$$

the saturation excess flow volume as

$$q_i = \max\{[V_i'(t_0 + \Delta t) - \min(V_i'(t_0 + \Delta t), V_i^{max})], 0\}$$

where V_i^{max} is the saturated soil water storage, and the storage at the end of the interval as

$$V_i(t_0 + \Delta t) = \min(V_i'(t_0 + \Delta t), V_i^{max}) - E_a\Delta x^2,$$

where E_a is the actual evaporation.

The model formulation is such that it can be related directly to topographic slope and soil physical properties. A digital terrain model can be used to provide estimates of terrain slope s_0 applicable to each grid cell. Soil survey datasets can provide cell values for the effective soil moisture content, θ_e, the saturated hydraulic conductivity, k_s, and soil depth, L. The parameter α is linked to the Brooks and Corey relation for hydraulic conductivity $k = k_s\Theta^\alpha$ with $\alpha = (2 + 3B)/B$ and B is a pore size distribution index; whilst the linkage strictly applies at a point, it may approximately hold for the integrated form particularly for a uniform soil. Smith and Hebbert (1983) indicate that α typically lies between 3 and 4, although a value of 2.5 has been used for the integrated application considered here.

Percolation, recharge and groundwater flow

Equation (4.4.16) defining the continuity equation for a grid cell dominated by a lateral flow regime can be extended to incorporate percolation (a vertical downward flow, m³s⁻¹), Q^P, such that

$$\frac{dV}{dt} = p\Delta x^2 + Q^I - Q^D - Q^P. \tag{4.4.17}$$

The grid cell identifier subscript i is omitted for notational simplicity. Representing percolation as a simple power law function of the soil water volume V, expressed as a fraction of the saturated water volume V_{max}, gives

$$Q^P = k_P\Delta x^2\left(\frac{V}{V_{max}}\right)^{\alpha_P} \tag{4.4.18}$$

where k_P is the vertical saturated hydraulic conductivity of the soil (ms⁻¹) and α_p is the exponent of the percolation function. Clapp and Hornberger (1978) indicate, on the basis of soil experiments, that α_P can vary from circa 11 for sand to 25 for clay.

The simplest representation of recharge to groundwater is to assume that percolation freely drains as recharge to the groundwater saturated zone (for the cell), so that

recharge $Q^R \equiv Q^P$. Let V^g denote the groundwater volume (m^3) stored in the cell, V_{max}^g its maximum value and s_b the slope of the underlying bedrock in the flow direction. Then Darcy's law gives the lateral groundwater flow out of the cell to a reasonable approximation by the linear relation

$$Q^G = \frac{k_g s_b}{\Delta x} V^g \qquad (4.4.19)$$

where k_g is the horizontal hydraulic conductivity of the aquifer. Continuity for the groundwater volume is

$$\frac{dV^g}{dt} = Q^R + Q^H - Q^G \qquad (4.4.20)$$

where Q^H is the lateral groundwater flow into the cell. Note this a linear reservoir equation and can be solved analytically for an assumed constant rate of input over the time interval. Alternatively, the KW model formulation can be invoked directly recognizing its basis as a discrete space-time approximation to a linear reservoir of the above form. Note, in particular, that the dimensionless wave-speed is given by $\theta = \kappa \Delta t = k_g s_b \Delta t / \Delta x$.

A more complex formulation, due to Liu *et al.* (2005), assumes that percolation feeds a lower soil layer that limits the percolation flow rate Q^P to be no greater than that allowed by the saturated soil hydraulic conductivity of this lower layer, $k_g \Delta x^2$. Let this lower soil layer have a maximum groundwater volume V_{max}^g of which V^g contains saturated water in store and V^u contains unsaturated water in store. Then recharge to groundwater is now given by

$$Q^R \equiv Q^P \left(\frac{V^u + V^g}{V_{max}^g} \right)^{\alpha_R} . \qquad (4.4.21)$$

The saturated groundwater volume V^g can be related to the water table depth above the bedrock, h, via the effective soil porosity, ρ, such that $h = V^g / (\rho \Delta x^2)$. If the bedrock depth below the surface is d, then the depth down to the water table is $d - h$. Since the depth from the surface down to the top of the lower soil layer is L, then $V_{max}^g = (d - L)\rho \Delta x^2$.

Surface and channel flow models

The form of kinematic wave model for soil water storage given by equation (4.4.15) can be invoked in a similar way to represent surface flow (saturation excess overland flow) and channel flow processes within a river basin. In this case the momentum equation is given by the Manning equation $q = CS^\alpha$. This is the form of equation (4.4.14) but now with S being the water depth (m), $\alpha = 5/3$ and the conveyance $C = \sqrt{s_0}/n$ where n is Manning's roughness coefficient (m$^{-1/3}$s). Without change of notation, to simplify

presentation, these models are developed below for a generic grid cell within a river basin.

Surface flow model

Assuming a Manning friction law and constant water depth over the cell, the rate of change of surface flow volume is given by

$$\frac{dV_i}{dt} = q_i - \frac{C_i \Delta x}{\Delta x^{2\alpha}} V_i^{\alpha} = q_i - q_{si} \qquad (4.4.22)$$

where q_i is the saturation excess runoff generated by the cell soil water storage and q_{si} is the surface runoff output from the cell. The local conveyance parameter is now given by the Manning type formula $C_i = \sqrt{s_0}/n_i$, with n_i the Manning surface roughness coefficient (m$^{-1/3}$s) and $\alpha = 5/3$. Digital land cover maps and standard tables of Manning's n (for example, Chow, 1959) can be used to assign values to each cell.

Channel flow model

Assuming a tree network structure of channel reaches with wide rectangular cross-sections of width, w_i, increasing downstream, then the kinematic wave model for a reach is

$$\frac{dV_i}{dt} = q_i - \frac{C_i w_i}{(\Delta x w_i)^{\alpha}} V_i^{\alpha} = q_i - q_{ci}. \qquad (4.4.23)$$

Here, V_i is the volume stored in the reach, and the flow input q_i is made up of three components: the surface runoff q_{si}, the soil drainage q_{di} and the channel inflow from upstream q_{ci}^u. Local conveyance is now $C_i = \sqrt{s_0}/n_i$ with s_0 the channel bed slope, assumed equal to the cell slope, n_i is the Manning surface roughness coefficient for the channel (m$^{-1/3}$s) and $\alpha = 5/3$. Standard tables of Manning's n can be used to assign values to each cell if information on the type of channel is available. A channel ordering system, such as that due to Strahler, can be invoked with the support of a digital terrain model and used to allow roughness to decrease with increasing stream order.

Solution schemes

The kinematic wave models for interflow, surface flow and channel flow given by equations (4.4.16), (4.4.22) and (4.4.23) take the general nonlinear reservoir form

$$\frac{dV}{dt} = a - bV^{\alpha} \qquad (4.4.24)$$

where V is the water volume of concern and the quantities a and b are constants within a time-step. The exponent α is equal to 5/3 for surface flow and channel flow or fixed for a given soil type in the case of interflow.

The following cases are relevant for an arbitrary time interval $(t, t + \Delta t)$:

Case 1: $a = 0$

This case has the analytical solution

$$V_{t+\Delta t} = [V_t + b(\alpha - 1)\Delta t]^{\frac{1}{1-\alpha}}$$ (4.4.25)

where V_t is the water volume at time t.

Case 2: $a \neq 0$

For this case, an analytical solution can be obtained by introducing the approximation $V^\alpha = c_1 V + c_2 V^2$, where the coefficients c_1 and c_2 are determined by least squares regression for a given value of α.

With this approximation, equation (4.4.24) may be written as

$$\frac{dV}{dt} = A(V^2 + BV + C)$$ (4.4.26)

with $A = -bc_2$, $B = c_1/c_2$, and $C = -a/(bc_2) = a/A$. Integrating gives

$$\int_{V_{t-\Delta t}}^{V_t} \frac{1}{V^2 + BV + C} dV = A\int_{t-\Delta t}^{t} dt \quad .$$ (4.4.27)

This gives

$$\frac{1}{p_1 - p_2} \log\left(\frac{V_t - p_1}{V_t - p_2}\right)\left(\frac{V_{t-\Delta t} - p_2}{V_{t-\Delta t} - p_1}\right) = A\Delta t$$ (4.4.28)

where $p_1 = [-B + (p_1 - p_2)]/2$, $p_2 = [-B - (p_1 - p_2)]/2$ and $p_1 - p_2 = \sqrt{B^2 - 4C}$ for $B^2 \geq 4C$; note that $p_1 \geq 0$ and $p_2 \leq 0$. Rearranging gives the required solution

$$V_t = \frac{p_1 - p_2 F}{1 - F} = p_2 + (p_1 - p_2)(1 - F)^{-1}$$ (4.4.29a)

where

$$F = \left(\frac{V_{t-\Delta t} - p_1}{V_{t-\Delta t} - p_2}\right)\exp[(p_1 - p_2)A\Delta t].$$ (4.4.30a)

This solution applies for a recession period when $V_{t-\Delta t} \geq p_1$.

For a rising flow period when $V_{t-\Delta t} \geq p_1$, then the required solution is

$$V_t = \frac{p_2 - p_1 R}{1 - R} = p_1 - (p_1 - p_2)(1 - R)^{-1}$$ (4.4.29b)

where

$$R = \left(\frac{V_{t-\Delta t} - p_2}{p_1 - V_{t-\Delta t}}\right)\exp\left[(p_1 - p_2)A\Delta t\right].$$ (4.4.30b)

The approximation $V^\alpha = c_1 V + c_2 V^2$ is a reasonable one over the range $1 \le \alpha \le 2$. For $\alpha > 2$, equation (4.4.24) can be transformed by making the substitution $U = V^{-(\alpha-1)}$ to give an equation in U

$$\frac{dU}{dt} = b(\alpha-1) - a(\alpha-1)U^{\frac{\alpha}{\alpha-1}}$$ (4.4.31)

with the exponent α replaced by $\alpha/(\alpha-1)$ which falls in the range 1 to 2 required of the approximation. This substitution is needed for interflow when α typically falls between 2 and 4. This solution scheme follows that of Liu and Todini (2002); the published paper contains typesetting errors which are corrected here.

An alternative approach, as used in the PDM model (Moore, 1999; Moore and Bell, 2002), is to develop an approximate recursive solution based on the piecewise linear difference equation solution suggested by Smith (1977, p213) for solving the general nonlinear differential equation

$$\frac{dx}{dt} = f(x,t).$$ (4.4.32)

The solution, for a constant input over an interval $(t, t+\Delta t)$ of duration Δt, is

$$x_{t+\Delta t} = x_t + J_t^{-1}\left(\exp\left(J_t\Delta t\right)-1\right)f_t.$$ (4.4.33)

where the Jacobian $J_t = \partial f/\partial x\,|\,x_t$. Application to equation (16) gives $J_t = -\alpha b V_t^{\alpha-1}$ and the required approximate solution is

$$V_{t+\Delta t} = V_t - \frac{1}{\alpha b V_t^{\alpha-1}}\left(\exp\left(-\alpha b V_t^{\alpha-1}\Delta t\right)-1\right)\left(a - b V_t^\alpha\right).$$ (4.4.34)

Conversion from distributed to lumped formulations

It is possible with the above simple distributed kinematic wave model formulation to integrate over all cells within a basin to obtain a lumped version of the model. The result is a set of zero-order nonlinear reservoir equations representing the basin as a whole. However the separation of surface runoff from soil water components has not proved analytically tractable in lumped form. This separation can be achieved by invoking a Beta distribution function to describe the proportion of the basin that is saturated and generating surface runoff. The form of the function is fitted at each time-step using the saturated cell fraction computed from the distributed form of the model. Despite this shortcoming, the resulting lumped model formulation still preserves strong physically-based linkages with measurable terrain and soil physical properties. Clearly the lumped formulation cannot hope to represent the response to rainfall that is

strongly varying over space, but may provide a good approximation to the distributed model response during more spatially uniform rain. Further details of the type of lumped model formulation that can be achieved are presented by Todini (1995) and Liu and Todini (2002). The need to develop equivalent lumped representations is arguably less strong for the intended application of forecasting at ungauged sites where the original distributed formulation offers considerable flexibility to forecast at many ungauged locations. Computational constraints on running simple distributed models are also becoming less of an operational issue.

Discussion of application for forecasting at ungauged locations

For forecasting at ungauged locations, the simplified physical-basis of models formulated using the above types of kinematic representations of lateral soil drainage, surface runoff and channel flow offer considerable appeal. Their strength lies in the simple but physically-based linkage with topography, soil physical properties and land cover that is achieved. A model may be configured for a river basin for forecasting at ungauged interior locations. Alternatively, the simple cell descriptions of volume water-accounting and runoff-generation and -translation may be used as the basis of area-wide models with cell-to-cell transfers of water to forecast at any cell outlet location encompassed by the model grid.

The approach is clearly more scientifically appealing than regionalising procedures based on model simplification and empirical regression of model parameters with basin-integrated properties. Models may also prove less time-consuming to develop for a region or country of interest as the approach does not rely on the exhaustive model calibration at gauged sites required in developing regression relations. Much scope exists for exploring models of this general type and to employ new sources of digital spatial datasets on terrain, soil/geology physical properties and land cover.

It is clear that the development concerned with interflow on sloping terrain can be used as a "runoff production" module that accounts in a physically-based way for topographic and soil controls on runoff generation. For example, the scheme can be used to develop variants of the Grid Model and Grid-to-Grid Model presented in early sections. These variants will allow soil properties (effective soil moisture content, saturated hydraulic conductivity, soil depth) and topographic slope (as measured from a DTM) to be introduced in a way that has some physical basis. Similarly, the surface and channel flow routing schemes can be used to develop variants of the land and channel routing phases; note the grid-based models already employ a kinematic wave routing formulation. What is provided is a physics-based way of introducing slope and roughness information explicitly into the routing scheme. Links to aquifer properties provide further opportunities for investigation in relation to representation of slow and return flow pathways. Whilst there is no guarantee that such added spatial complexity will lead to better forecasts, there is a prospect of more robust transfer to ungauged basins where spatial variation in these properties exert a significant influence on flood response. Appendix D.7 presents preliminary results from a prototype extended Grid-to-Grid embracing these ideas that illustrates more robust transfer in catchments where contrasting soil controls are important to flood generation.

4.5 Channel flow routing models

4.5.1 Introduction

There is a rich literature on channel flow routing methods that derive from the St. Venant equations for open channel flow and their simplifications. At one end of the spectrum are hydraulic models based on flow hydrodynamics whilst simpler formulations are commonly referred to as hydrological routing methods. The latter are based on simple mass balance storage accounting principles combined with a simplified momentum equation normally linking channel storage or water level to flow discharge. Whilst the distinction between hydraulic and hydrological approaches has convenience, it is largely artificial with the formulations linked to a common basis in the St. Venant equations and their simplification.

Because of this link back to the St. Venant equations and a definition of a channel flow routing model in terms of channel properties, concerning geometry and resistance (roughness), the basis of application to ungauged river reaches is relatively well founded. However, channel geometry simplification and the essentially empirical nature of roughness means that there is real benefit in model calibration even for the most refined hydraulic models.

For a review of both simple and more complex channel flow routing schemes, the reader is referred to Fread (1985) and the textbooks of Chaudhry (1993) and Sturm (2001). Here, a specific exposition will be given that first defines the St Venant equations and develops a specific solution that has attraction for application to ungauged river reaches. This is intended not to condone this method to the exclusion of others. Rather the intention is to introduce the St. Venant equations and give an example of how they can be simplified to provide a practical methodology for application to ungauged rivers

There is a plethora of other schemes, developed particularly as variants of the Muskingum and kinematic wave routing methods, that are reviewed in the texts previously cited. Section 4.5.3 presents the Muskingum-Cunge method as an example - developed from a consideration of Muskingum, kinematic and diffusion wave methods – that is of particular relevance for application to ungauged rivers. A reader requiring a simpler exposition of practical flood routing methods, starting from hydrological reach storage principles, might go directly to this section.

4.5.2 Development of a Muskingum-type routing scheme from the St. Venant equations

The St. Venant equations and their simplification

The St. Venant equations comprise the equations of continuity and momentum which are defined below.

Continuity equation

$$\frac{\partial A}{\partial t} + \frac{\partial Q}{\partial x} = q \qquad (4.5.1)$$

where A is cross-sectional flow area, Q is discharge, q is lateral inflow or outflow, S_0 is the channel bottom slope and S_f is the friction slope; t denotes time and x the distance along the channel length.

Momentum equation

$$\frac{1}{g}\frac{\partial v}{\partial t} + \frac{v}{g}\frac{\partial v}{\partial x} + \frac{\partial h}{\partial x} = S_0 - S_f \qquad (4.5.2)$$

where v is the flow velocity, h the depth of flow and g the acceleration due to gravity. The first two terms of this *dynamic equation* are inertia terms (local and convective acceleration); these terms relate to the Froude number F_r which varies with channel roughness and slope but is independent of flow. Neglecting the two inertia terms is the basis of *diffusion routing* whilst retaining only the slope terms (so $S_0 = S_f$) gives the *kinematic routing* simplification.

Development of a Muskingum-type routing scheme

For a trapezoidal channel of bottom width B_0, and lateral section slope α then the St. Venant equations reduce to

$$\frac{\partial h}{\partial t} = \frac{q}{B_0 + 2\alpha h} - \frac{1}{B_0 + 2\alpha h}\frac{\partial Q}{\partial x} \qquad (4.5.3)$$

$$p\frac{\partial h}{\partial x} = S_0 - S_f . \qquad (4.5.4)$$

with

$$p = \left(1 - \frac{F_r^{\,2}}{4}\frac{B_0 + \alpha h}{B_0 + 2\alpha h}\right). \qquad (4.5.5)$$

Chezy's equation with roughness C_z gives the friction slope as

$$S_f = \frac{Q^2}{C_z h^3 (B_0 + \alpha h)^2} .$$

These equations combine to give the nonlinear convection-diffusion equation for a trapezoidal channel (Wang *et al.*, 2006):

$$\frac{\partial Q}{\partial t} = \frac{pQ}{2p_1 S_f} \frac{\partial^2 Q}{\partial^2 x} + f(Q,h)\frac{\partial Q}{\partial x} + g(Q,h) \qquad (4.5.6)$$

where

$$f(Q,h) = -\left(\frac{F_r^2 \alpha B_0}{8 pp_1^2} \frac{S_f - S_0}{S_f} + \frac{3}{2h} + \frac{\alpha}{B_0 + \alpha h} \right) \frac{Q}{p_1} \qquad (4.5.7)$$

and

$$g(Q,h) = \frac{(3B_0 + 5\alpha h)qQ}{2p_1(B_0 + \alpha h)h} + \frac{S_0 - S_f}{S_f}\left(h - \frac{F_r^2 B_0 q}{8 pp_1} \right)\frac{\alpha Q}{p_1^2} \qquad (4.5.8)$$

with $p_1 = B_0 + 2\alpha h$.

Using the Taylor series expansion approximation

$$\frac{\partial Q}{\partial x} = \frac{Q_i - Q_{i-1}}{\Delta x} - \frac{\Delta x}{2}\frac{\partial^2 Q}{\partial^2 x} \qquad (4.5.9)$$

where i is a space-index and with the constraint that the reach length

$$\Delta x = \frac{pQ}{p_1 S_f f(Q,h)} \qquad (4.5.10)$$

then equation (4.5.6) simplifies to

$$\frac{\partial Q}{\partial t} = f(Q,h)\frac{Q_i - Q_{i-1}}{\Delta x} + g(Q,h). \qquad (4.5.11)$$

This has eliminated the physical and numerical diffusion terms leaving a first-order non-linear ordinary differential equation. Elimination of the diffusion term by selecting an optimal space interval Δx is called the "mixing-cell method". Imposition of the Δx constraint results in a characteristic channel reach with a unique relation between reach storage and lower section discharge such that

$$Q = C_z \sqrt{S}(B_0 + \alpha h)h^{3/2}.$$

Applying a four-point finite difference scheme with weighting coefficients X in time and Y in space gives the difference equation

$$Q_i^{k+1} = c_1 Q_i^k + c_2 Q_{i-1}^{k+1} + c_3 Q_{i-1}^k + c_4 q \qquad (4.5.12)$$

with coefficients

$$c_1 D = \frac{X}{\Delta t} + \frac{(1-Y)f(Q,h)}{\Delta x}$$

$$c_2 D = -\frac{1-X}{\Delta t} - \frac{Yf(Q,h)}{\Delta x}$$

$$c_3 D = \frac{1-X}{\Delta t} - \frac{(1-Y)f(Q,h)}{\Delta x} \tag{4.5.13}$$

$$c_4 D = g(Q,h)$$

with denominator

$$D = \frac{X}{\Delta t} - \frac{Yf(Q,h)}{\Delta x}.$$

This formulation is structurally similar to the Muskingum-Cunge method but derives from the St. Venant equations in a radically different way. The difference equation is solved for each reach in sequence, solving for all time-steps in an iterative manner yielding estimates of Q, h and Δx at each time. Since Δx can change at each time, linear interpolation is used to calculate flow for a required fixed space interval ΔL.

Relevance to the ungauged problem

In contrast to the traditional Muskingum method which requires calibration to observed outflow data, the above scheme is parameterised by properties of the river channel. These channel properties are bottom slope, roughness, cross-section shape and reach length. Digital terrain data and/or surveys can be used to estimate the geometrical properties of the channel whilst roughness can be inferred from standard sources: for example, see Chow (1959) and Barnes (1967). Note that the Chezy coefficient is related to Manning's n via the relation $C_z = R^{1/6}/n$ where R is the hydraulic radius. The weighting factors X and Y of the finite difference scheme are not prescribed, lie between 0 and 0.5 with $X + Y = 1$, and with lower values of Y reducing the hydrograph peak; however, sensitivity is typically low.

The scheme, due to Wang *et al.* (2006), is clearly attractive as a methodology for application to ungauged sites. As with all solutions to the St. Venant equations, however exact, there is benefit from calibration especially due to the simplified channel geometry assumed and because of the essentially empirical nature of roughness as conventionally defined. Ideally, experience should be gained on similar gauged reaches in configuring the model geometry and in estimating roughness, allowing this experience to be transferred in a rational way to the ungauged reaches of interest. A feature of the scheme is the imposition of a characteristic reach length that imposes for each time-step a unique stage-discharge relation at its outfall. This may allow the scheme to represent a looped rating (at a fixed location for all time-steps) arising from backwater effects induced by river gates, junctions and tides.

4.5.3 Muskingum, Kinematic Wave and Muskingum-Cunge routing

Muskingum Routing

The basis of Muskingum routing is the combination of the continuity equation, expressed as the storage equation for a river reach

$$\frac{dS}{dt} = I - O \, , \tag{4.5.14}$$

and the momentum equation simplified to the Muskingum equation

$$S = K[XI + (1 - X)O] \tag{4.5.15}$$

where S is the reach storage, I the reach inflow rate, O the reach outflow rate, K is a time constant and X is a weighting factor (<1).

A finite difference approximation to the storage equation is

$$\frac{S_2 - S_1}{\Delta t} = \frac{I_1 + I_2}{2} - \frac{O_1 + O_2}{2} \tag{4.5.16}$$

where the subscripts 1 and 2 denote the start and end of a time interval of duration Δt. Eliminating the storage terms using the Muskingum equation gives

$$O_2 = c_0 I_2 + c_1 I_1 + c_2 O_1 \tag{4.5.17}$$

with routing coefficients

$$c_0 = \frac{-KX + 0.5\Delta t}{K - KX + 0.5\Delta t}$$

$$c_1 = \frac{KX + 0.5\Delta t}{K - KX + 0.5\Delta t} \tag{4.5.18}$$

$$c_2 = \frac{K - KX - 0.5\Delta t}{K - KX + 0.5\Delta t}$$

and $c_0 + c_1 + c_2 = 1$.

It is convenient to express the above in the more normal finite difference notation as the Muskingum difference equation

$$Q_{i+1}^{k+1} = c_0 Q_i^{k+1} + c_1 Q_i^k + c_2 Q_{i+1}^k \tag{4.5.19}$$

where Q_{i+1}^{k+1} and Q_i^{k+1} denoting the outflow and inflow rates at time $k+1$ respectively; that is, subscripts i and k denote discrete positions in space and time with separations Δx and Δt being the reach length and time-step. A stretch of river can be modelled as comprising of a number of river reaches and calculations performed over

the required number of time-steps using this generalised formulation. Without loss of generality, it is easy to see how lateral inflows (assumed to enter at reach boundaries) can be added to the outflow of one reach to give the inflow to the next reach.

The time constant K and weighting factor X are conventionally regarded as model parameters to be calibrated using inflow and outflow records for the stretch of river. In this sense, a classical application of Muskingum routing to ungauged rivers would be based on a "reach similarity" parameter transfer principle. However, the Muskingum-Cunge extension to be discussed next provides a more physically-based method of application to ungauged rivers.

Muskingum-Cunge routing

The Muskingum-Cunge method aims to allow for the true wave attenuation by matching the numerical and physical diffusion. Numerical diffusion is first quantified with reference to a numerical discretisation of the kinematic wave equation

$$\frac{\partial Q}{\partial t} + c_k \frac{\partial Q}{\partial x} = 0 \tag{4.5.20}$$

where c_k is the absolute wave celerity. This is discretised using a four-point difference scheme with weight factors X and Y, with Y fixed at a value of 0.5, to yield the Muskingum difference equation with routing coefficients redefined as

$$c_0 = \frac{0.5C_n - X}{1 - X + 0.5C_n}$$

$$c_1 = \frac{0.5C_n + X}{1 - X + 0.5C_n} \tag{4.5.21}$$

$$c_2 = \frac{1 - X - 0.5C_n}{1 - X + 0.5C_n}$$

where $C_n = c_k \Delta t / \Delta x$ is the Courant number. Note that K in the Muskingum equation is related to c_k in the kinematic wave equation through the identity $K = \Delta x / c_k = \Delta t / C_n$.

The approximation error in the difference equation form of the differential equation for the kinematic wave is determined from a Taylor series expansion of the function $Q(i\Delta x, k\Delta t)$ about the point $(i\Delta x, k\Delta t)$ to give the remainder

$$R = c_k \Delta x^2 (0.5 - X)\frac{\partial^2 Q}{\partial x^2} + c_k \Delta x^2 \{(1 - C_n)[0.5(X + 0.25) - (1 + C_n)/3]\}\frac{\partial^3 Q}{\partial x^3} + O(\Delta x^3).$$

The coefficient on the second derivative, $c_k \Delta x^2 (0.5 - X)$, functions as a numerical diffusion due to the approximation itself, as it is absent from the kinematic wave equation. Cunge (1969) equates this coefficient to the apparent physical diffusion coefficient, $Q/(2BS_0)$, in the diffusion routing equation for a rectangular channel of width B

$$\frac{\partial Q}{\partial t} + c_k \frac{\partial Q}{\partial t} = \frac{Q}{2BS_0} \frac{\partial^2 Q}{\partial x^2} \qquad (4.5.21)$$

to give the following expression for the Muskingum weighting factor

$$X = 0.5(1 - \lambda) \qquad (4.5.22)$$

with

$$\lambda = \frac{Q}{BS_0 c_k \Delta x} \, . \qquad (4.5.23)$$

For stability, $X \le 0.5$.

This method where, for $Y = 0.5$, X is chosen to equate the numerical diffusion to the physical diffusion is referred to as the Muskingum-Cunge method. The two routing parameters X, as defined above, and $K = \Delta x / c_k$ depend in a known way on the flow characteristics and channel properties. It is therefore immediately applicable to ungauged rivers although, as previously mentioned, calibration will invariably have a beneficial effect on model performance.

When c_k and λ are calculated as a function of a reference discharge, then this gives the constant-parameter form of the Muskingum-Cunge method. When they are calculated to vary with the discharge Q, then this gives the variable-parameter form in which routing coefficients are time-variant. Both forms involve the approximation of using a uniform flow formula with dependence on bed slope with actual depth assumed to be normal. The variable-parameter form suffers from volume loss, particularly for very mild slopes, and is best applied to moderate to large slopes. The constant-form has merit in its simplicity, often without great loss in accuracy relative to the variable form. This is particularly true for application to ungauged rivers.

Application to the ungauged problem

An application to an ungauged river site would first calculate the kinematic wave speed using Manning's equation for a reference discharge, say chosen to be about midway between the baseflow and typical peak discharge for an upstream site. Consideration of channel properties would identify the reach length, L, and bed slope, S_0, with, say, a typical trapezoidal cross-section of given bottom width B and side-slope ratio m. A Manning's n estimate would be based on field inspection, experience and guidance from standard literature sources. The normal depth y_0 is calculated by applying Manning's equation for a trapezoidal channel of side-slope ratio m so (for SI units)

$$\frac{\left[\frac{y_0}{B} \left(1 + \frac{my_0}{B}\right) \right]^{5/3}}{\left[1 + \frac{2y_0}{B}(1 + m^2)^{1/2} \right]^{2/3}} = \frac{AR^{2/3}}{B^{8/3}} = \frac{nQ}{S^{1/2}B^{8/3}} \, . \qquad (4.5.24)$$

This is solved iteratively for the normal depth using the given reference discharge and channel geometry; the normal velocity is then given by $V_0 = Q/A$ with $A = y_0(B + my_0)$.

To a first approximation for a very wide channel then the kinematic wave speed can be calculated as $c_k = (5/3)V_0$. The time-step may be chosen in relation to the time-to-peak of the inflow hydrograph as an integer divisor of it, typically 4. The space-step Δx is chosen in relation to a criterion to ensure accuracy and consistency (ie. reduced sensitivity to the choice): this is $C_n + \lambda \geq 2$ with $\lambda = Q/(BS_0 c_k \Delta x)$ which translates to $\Delta x \leq 0.5[c_k \Delta t + Q/(BS_0 c_k)]$. This criterion in relation to the reach length L is used to determine the number of sub-reaches and the final choice of Δx, whilst ensuring the Courant number $C_n = c_k \Delta t / \Delta x$ takes a satisfactory value. The Muskingum weighting factor is calculated as $X = 0.5(1 - \lambda)$.

The Muskingum difference equation with Muskingum-Cunge routing coefficients is used to calculate the outflow from the first sub-reach for each time-step in turn, with the outflow then becoming the inflow to the next sub-reach, repeating this in a recursive fashion for all sub-reaches until the reach outflow hydrograph (at the ungauged site) is calculated.

4.6 Hydrodynamic models

Information about hydrodynamic modelling programs and packages in use by the Environment Agency may most conveniently be found in reports from the "Benchmarking of Hydraulic Models" project, ongoing from 1993 to 1997 during the time of the National Rivers Authority (NRA) and restarted for the Environment Agency in 2002. The Stage One Final report by Harpin *et al.* (1995) identified 6 programs for hydrodynamic modelling in then current use by NRA regions, and this list would be extended to 7 to include all models known to be in use by consultants. Additional programs were identified for backwater modelling applications. The report listed 6 hydrodynamic models (a slightly different list) as requiring inclusion in the Benchmarking project, with an additional 9 models listed as being potentially suitable. In the most recent report of the present project (Crowder *et al.*, 2004), the list of hydrodynamic models supported by the Environment Agency, and identified for inclusion in the Benchmarking study, has been reduced to only 3: ISIS, Mike11 and HEC-RAS. Note that while HEC-RAS was previously a package dealing only with backwater calculations, it does now include hydrodynamic modelling.

Given that the target of the present project is catchment modelling for ungauged catchments, it is not appropriate here to try to provide details of specific differences between hydrodynamic models as implemented in particular packages, as this information can be difficult to access and is subject to rapid change. The main concern of the present project with hydrodynamic models is the potential need to include in such models flow contributions from ungauged areas: the same concern arises for all such models. However, the following is a brief list of potential differences between hydrodynamic models, constructed on the basis of background knowledge and without necessarily referring to the above list of candidate models.

> (a) The way that flows entering or leaving the river channel are treated. In particular, different models may have different ways of calculating the momentum adjustment associated with flows over river embankments, or with flows at river junctions. Models may have different capabilities for representing diffuse sources or sinks along river reaches, as distinct from point sources and sinks.

> (b) The treatment of "sinuosity". In the mathematical model, a reach has a fixed length whereas water in a river will travel over varying distances depending on

whether the river is in nearly dry, normal or out-of-bank flow conditions. Adjustments to both the mass and momentum balance equations can be made to allow for this type of effect. One result of allowing for sinuosity can be a change in the way that the model outcomes show varying speeds of wave-travel for different river conditions.

(c) Representation of non-flowing parts of river cross-sections. Certain models can include a distinction between areas of a river cross-section, even in in-bank flow conditions, where the river is treated as "still" rather than "flowing". These two types of area would make different contributions to the mass and momentum equations.

(d) Representation of channel roughness. There are several formulae for calculating the drag effects of the channel and different implementations may provide different choices or defaults. In addition the extent to which roughness can be allowed to vary may differ between implementations. If the effects of weed growth are considered, roughness effects can vary with both the speed and direction of river-flow, while if the surfaces in contact with river-flow are considered, roughnesses should be allowed to vary with river-height.

(e) Inclusion of wind-drag. Some hydrodynamic modelling packages will allow the effects from wind on the momentum balance of river-flow to be taken into account in the modelling. Such effects may be important on relatively wide (greater than 30m say) and straight river reaches where the effect of wind may change river levels by 10's of centimetres. Within a 1-dimensional model the effect would be restricted to being an "along the river" effect and it may require a 2-dimensional model to fully represent wind effects. Note that the concern here is with water-levels built-up by wind-shear, rather than wind-induced waves.

(f) The range of river-structures. Hydrodynamic models usually include specific representation of the hydraulic effects of a number of common but special types of river structures such as specific designs of river-weirs, control-gates and bridges. The list can also include short and long culverts. A specific representation within a hydrodynamic model of river-structure provides a convenient way of configuring the model to include that type of structure. River-structures not specifically represented within a package may need to be dealt with by a more general approach which makes the model more difficult to configure.

(g) Out-of-bank conditions and flood-plains. Different hydrodynamic modelling packages may be able to treat out-of-bank conditions with varying degrees of realism. In some instances a package may include representation of flows on floodplains via a parallel version of the 1-dimensional flow equations used for channel flow whereas, in others, floodplains would be treated as a collection of storages linked notionally by weir-type structures. A full treatment of floodplains involving modelling in 2 spatial dimensions is usually counted as outside the scope of a 1-dimensional river-modelling component within a hydrodynamic modelling package. Certain packages may allow 1- and 2-dimensional components to be joined, but it is not clear what the implications of this would be for real-time applications where the models are "usually" run in non-flood conditions.

(h) Computational methodology. Different hydrodynamic modelling packages may implement different computational approaches to solving the partial differential equations once their basic form has been established. While there are

some aspects to this question that relate to how the computations for different river reaches and flood-plains are undertaken jointly, the most important consideration arises in the computational treatment within individual river-reaches. Solution of the partial differential equations within a river reach is usually accomplished using a finite-difference scheme but there can be differences in the schemes by which this is undertaken. Such schemes are based on specifying a number of modelling nodes along a river reach at which the "solution" for river-flow and height may be sought: one type of scheme involves dealing with both flow and height at every such node, while a second scheme deals with either flow or river-height at any node, alternating along the reach. These two types of schemes can have different properties in terms of computational resources and the behaviour of responses to sharp changes in river-flow, including river-bores. Other types of scheme are specifically suited to treating such sharp changes in particular.

Since hydrodynamic models are derived from sound principles of physics, albeit with some approximations, it might be thought that they can be applied without any requirement for calibration of the model. Unfortunately, the model requires specification of channel roughnesses and, while it may be adequate to set these by experience or by reference to books of photographs showing typical cases for design-type applications where calibration data are not available, such parameters of the model really should be calibrated against observed data records. In some instances it may be wise to treat certain other model-specification values as parameters to be adjusted to ensure a good correspondence with reality: an example of such a parameter is the "contraction coefficient" associated with the hydraulic effects of weirs, bridges and gates. Calibration of hydrodynamic models demands records of river-levels at several points along each reach or tributary being modelled.

When an existing configuration for a hydrodynamic model is being transferred from an off-line design type application to real-time use, special reconsideration of the original calibration is required. Often such calibration for off-line use will have been concentrated on high-flow events and on matching river levels when the levels are highest. Use of the model for real-time forecasting may shift the emphasis of the calibration to include good performance when river-levels are rising. For some ways of implementing real-time forecasting schemes involving hydrodynamic models, it may be required that these models are run under all flow conditions. This then means that the hydrodynamic model needs to be calibrated across a full range of flow conditions, including both very low river-levels and the recession from high river-levels. Attempts at such calibrations can reveal that important aspects of the river environs have been omitted since they are not important during flood conditions.

It is unfortunate that the computational problems associated with the numerical algorithms in hydrodynamic models are very likely to arise either during low flow conditions or during the immediate response to a sharp rise in flows into the model, starting from low flow conditions. Thus the transfer to real-time use may require re-configuration of the model, possibly by adding modelling nodes or else by including river-structures that have no important effect during high river-level conditions. In some circumstance it may be necessary to accept that a hydrodynamic model will not run with very low flows and to use it operationally by artificially modifying the inflows used so as to be larger than some acceptable minimum: when such flow-modifications were in effect, the model results would need to be discounted.

In contrast to the possible need to complicate an existing model for real-time use in order to deal with low river-levels, the transfer may allow other parts of the model to be simplified. Thus, a flood-design study may require a complicated set of flood

compartments to be modelled to achieve adequate precision and spatial resolution in computed water-levels over a flood-plain: real-time uses would typical not require this precision and resolution, allowing a simplified set of flood compartments to be used.

4.7 Flood mapping tools

It is convenient to group some comments about tools for mapping flood extent under a separate section-heading, since a number of radically different products can be encompassed under this term. The on-screen appearance of the different products can be very similar, and they will often be presented as overlays on similar types of GIS datasets. Once again the scope of this report does not include a full review of these products.

The tools fall naturally into two groups. In the first of these, the visual display product is based directly on observations of flood extent, usually based on satellite telemetry, and no modelling is involved: thus there is no question of modelling ungauged areas. In the second group fall products where modelling is specifically involved and the configuration of implementations of these products may or may not take account of flows from ungauged areas. This group of flood extent modelling tools can be sub-divided into categories based on the type of model and the degree of linkage between the model and visual output. In all cases it is assumed that modelling takes place in a dynamic framework rather than a static one, as would be the case for backwater calculations where flood extent mapping tools are also useful. The categories can be summarised as follows.

(i) Tools in which levels inferred from hydrological or hydrodynamic modelling of flows in river channels are used as the basis of inferred levels away from the river. Here a simple approach is to predict that all areas upstream of a modelled location which have a land elevation below the modelled level at the river will be flooded. Clearly here there is an assumption that effectively any time lag and diffusion effects involved in water movement across the land are small compared with the time-scale over which changes in river level occur.

(ii) Tools linked to a quasi-1D hydrodynamic model of river-channels. Here out-of-bank river conditions can be represented as either static or flowing storage of water within model-compartments along the river banks. The hydrodynamic model then provides modelled levels for each of these model-compartments which can be made the basis of a mapping scheme.

(iii) Tools based on 2D (two-dimensional) modelling of flows across flood plains. Here water-levels and flows across a flood plain would be modelled using a hydrodynamic approach and the modelled levels would be directly available for mapping, often at a finer resolution than would be obtained from quasi-1D modelling. In cases where modelling of flow in the main river channels is based on established 1D models, suitable procedures for interfacing the two types of modelling are required.

It seems that much of the emphasis in the development of flood extent mapping tools has been for cases where the problem is flooding arising from overflow of river-channels and from the coast. Flows from ungauged areas can sometimes be treated by modelling ungauged tributaries by the approaches outlined earlier in this section, provided that such ungauged tributaries or point sources are represented in the model. More problematic can be the occurrence of substantial overland flows not associated with river channel sources (as in the floods near Northampton during Easter 1998) and

from overflow of groundwater aquifers (Chichester in January 1994 and Malton in March 1999). While flows of such types can potentially be included within the above types of modelling scheme, this would assume that their possible occurrence is known in advance. It is notable that the events mentioned above had not previously been foreseen for these locations. One solution to this problem should be sought by attempting to extend the capabilities of distributed catchment modelling to improve the representation of possible overland flows, springs and groundwater-overflows, while providing interfaces to hydrodynamic channel and floodplain flow modelling capabilities.

5 Digital datasets to support modelling ungauged locations

5.1 Introduction

The current generation of hydrological models used for flood forecasting tend to have a relatively simple structure which is tailored to a particular catchment through the use of model parameters. These are used in place of detailed knowledge of local conditions, and a single parameter can be used to represent one, or more than one attribute, or a distribution of catchment attributes. Where a parameter represents a single catchment attribute, or a distribution of an attribute within a catchment, there is considerable scope for using digital datasets to support model parameterisation. Such datasets can include information on topography, land-cover, hydraulic soil properties at different horizons, and geology. The aim of this section is to provide an overview of digital data resources available to support the development of process-based catchment models for ungauged locations.

The widespread use of remote sensing techniques to monitor earth systems is leading to a profusion of digital datasets for different regions and grid resolutions. Many of these are available for download from the World Wide Web, or can be bought online. The information presented here is focussed on datasets with coverage over the UK, and those currently available to CEH. Global-scale datasets (~1º resolution) have not been documented here as their poor spatial resolution is less likely to be of value for detailed catchment-based modelling. Example images of available datasets have been included by way of illustration.

Some attempt has been made to identify datasets which are freely available to all (sometimes following online registration), and these tend to originate from government organisations in the USA. European institutions (including those in the UK) tend to view digital datasets as a valuable source of income and often only make the data available under licence, with restrictions on their use. Licence fees for datasets vary according to the way they are used and whether the user belongs to a commercial organisation. As a result, it has been impossible to document the cost or availability of datasets originating from many EU sources. The datasets summarised in the tables are available from either the World Wide Web or under licence to the owner of the dataset. A number of the datasets listed are available to CEH staff for research purposes; they are also likely to be available to other organisations under licence.

5.2 Digital datasets currently available

Tables 5.1 to 5.3 present a summary of digital datasets currently available for supporting model application to ungauged sites. Currently-available soil and geology datasets are listed in Table 5.1. Data relating to soils are more easily available than those for geology, although some soil datasets include a reference to hydro-geology. Figure 5.1 shows soil types over Europe obtained from the European Soil Database (version 2). Although maps of soil type such as these are interesting, they are of limited

Table 5.1 Soil and geology datasets

Dataset	Coverage	Resolution	Description
IGBP (International Geosphere Biosphere Programme)	Global	5 arc minutes (~9km)	Numerous datasets including • Soil field capacity (mm) • Soil bulk density (g/cm^3) • Soil wilting-point (mm) • Profile Available Water Capacity (mm) • Groundwater depth • Hydraulic conductivity at specific suctions • Van Genuchten soil hydraulic parameters Available from website or by ordering a CD. Registration required. Arc-Info ASCIIGRID format available http://www.daac.ornl.gov/ Other IGBP datasets at lower resolutions include ISRIC-WISE: a 50 km resolution (0.5 degree) dataset of available water capacity (mm/m)
FAO	Global	5 arc minutes (~9km)	Digital Soil Map of the World (DSMW) CD-ROM based on the FAO/UNESCO Soil Map of the World. Also contains derived soil properties including • soil depth • soil moisture storage capacity • soil drainage class Format: ARC/INFO Export vector files and two raster formats. http://www.fao.org/ag/agl/agll/dsmw.HTM CDROM costs $44.
EEA (European Environment Agency)	Europe	1km	• Soil-type (CORINE) • Waterbase-groundwater: groundwater pressures and "physical characteristics of groundwater bodies" All datasets available to download. http://dataservice.eea.eu.int/dataservice/
ESD European Soil Database (European Soil Bureau Network)	Europe	10km	Data available from the JRC (Joint Research Centre). ESRI GRID format. Includes: • Parent material hydro-geological type • Depth to a gleyed horizon • Depth to an impermeable layer • Hydro-geological class • Available water capacity of topsoil and subsoil The JRC site is impossible to navigate, try the "Soil & Waste Unit" instead: http://eusoils.jrc.it/
HYPRES Macaulay Institute	Europe	1-2km	Availability under licence (not free of charge) through the European Soil Bureau (ESB). The database appears to be extensive and includes: • Soil type • Soil horizons • Hydraulic properties • Water capacities http://www.macaulay.ac.uk/hypres/index.html

Table 5.1 (continued) Soil and geology datasets

Dataset	Coverage	Spatial Resolution	Description
NatMap from NSRI (National Soil Resources Institute)	England and Wales	1, 2 or 5km	NRSI sells a number of products including "Profile" data: • HOST class • Depth to gleyed layer • Hydrological rock type • Integrated Air Capacity "Horizondata": • Saturated hydraulic conductivity • Water content at field capacity • Pore space • % of clay, sand, silt • Van Genuchten parameters "SEISMIC" 5km data (typically used to model impact of chemicals on soil) • Soil type • Aquifer type Formats include ArcView and ascii Charges vary according to the licensing agreement http://www.silsoe.cranfield.ac.uk/nsri/services/natmap.htm
HOST (Hydrology of Soil Types)	UK	1km	The derived quantity called the HOST class is available at CEH. This classification has 29 classes and encompasses soil type, hydrological response and substrate hydrogeology. A database of derived soil attributes supports the derivation of these classes and consists of • Air capacity • Parent material • Peaty topsoil • Depth to gleying • Depth to slowly permeable layer These derived soil attributes are not generally made available, but may be available under licence. http://www.macaulay.ac.uk/hypres/index.html
BGS Geology datasets	UK	various	A number of digital datasets are available under licence. http://www.bgs.ac.uk/

value for hydrological modelling in themselves unless the user has a detailed knowledge of how water interacts with the different soil types. Hence the particular value of datasets for physical soil properties such as water capacity, porosity and hydraulic conductivity.

Digital datasets for soil are likely to be of value to ungauged modelling in two ways: (i) for determining which soils are most likely to be saturated and producing surface runoff following rainfall, and (ii) to determine sub-surface travel pathways and travel times between sites of recharge and discharge. While both applications require some knowledge of soil-type and geology, determination of water pathways below ground is particularly dependent on the interaction between subsurface geology, topography and soil. subsurface pathways also depend on antecedent conditions, as the pattern of past rainfall and evapotranspiration will affect the position of the water table and the occurrence of fissures.
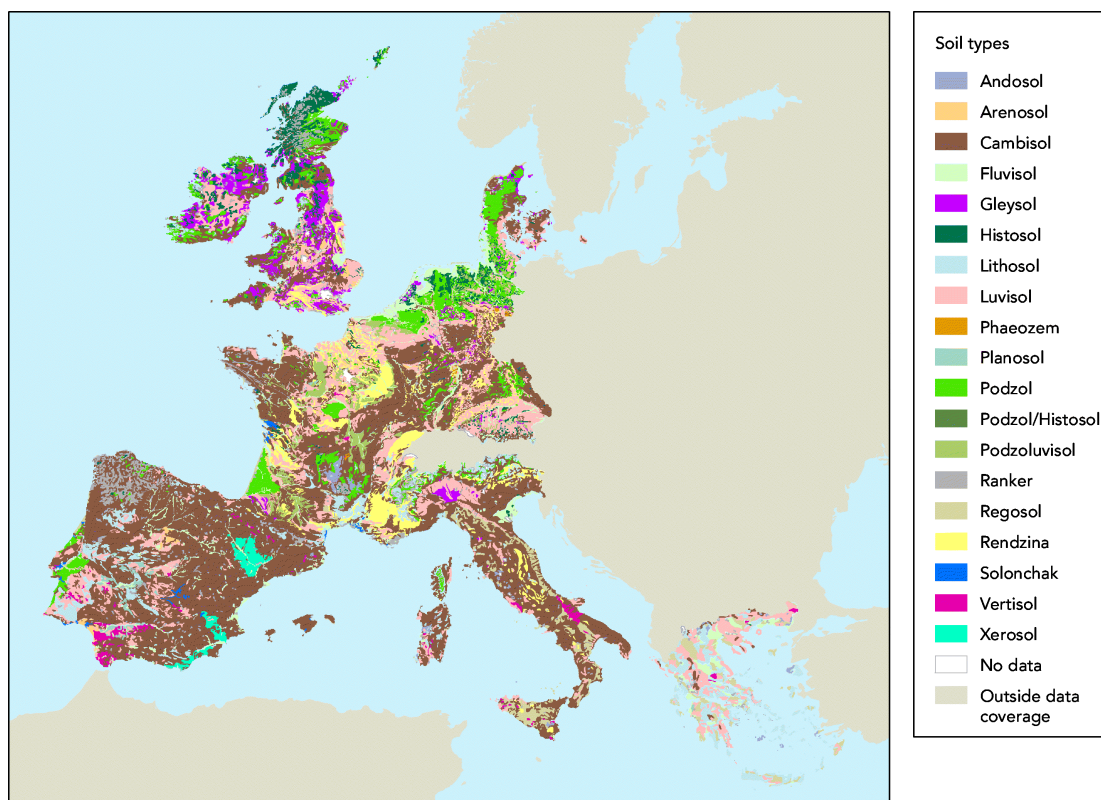
Figure 5.1 Map of soils over Europe: European Soil Database version 2. Soil units of Europe at a scale of 1:1000000 were digitised during the CORINE project.

The relative usefulness of the datasets listed here will depend on their spatial resolution, accuracy, and relevance to the application. For example, the FAO soil depth and storage capacity data may be of value for providing estimates of soil storage effects on runoff production for large catchments, or they could be used to provide a mean regional value as part of a probability-distributed soil-moisture model. The traditional approach of estimating model parameters from catchment characteristics via empirical regression, possibly with model simplification, might also benefit from new datasets as they become available.

The availability in recent years of soil datasets with global coverage has been capitalised upon by the global land-surface modelling community. Such properties include saturated hydraulic conductivity, pore space, wilting point, and parameters for functions of soil behaviour (for example, Van Genuchten (1980)). Land-surface models such as the Met Office Surface Exchange Scheme, MOSES, (Cox *et al.*, 1999) and (Essery *et al.,* 2003) make use of global datasets such as the IGBP (International Geosphere Biosphere Programme), which associates the Van Genuchten soil parameters with each of the 106 soil types it uses to categorise soils on a global scale. It is important to remember that these properties are aggregated and scale-dependent, and their usefulness for detailed modelling studies needs to be considered carefully.

Table 5.2 Land cover datasets

Dataset	Coverage	Spatial Resolution	Description
USGS US Geological Survey	Global	1km	• Land cover (253 types over Europe) • Forest cover http://edcdaac.usgs.gov/glcc/glcc.asp Available in binary raster for input to ArcGrid
GLCF Global Land Cover Facility	Global	1km, 8km or 1º	Products derived from satellite imagery: • MODIS-derived vegetation (500m) • AVHRR Global Land Cover • AVHRR Continuous Fields Tree Cover Format: compatible with ESRI products http://glcf.umiacs.umd.edu/data/
EEA (European Environment Agency)	Europe	1km (PELCOM) and 250m (CORINE)	• PELCOM (Pan-European Land Cover Monitoring project) 1km land-cover database 16 land classes. Predominantly broad vegetation types but also includes wetlands, urban areas and permanent ice and snow Format .BIL grid format. • CORINE Land Cover 250 m grid - version2 44 land classes including 11 types of urban area ranging from airports to construction sites. Various crops and vineyards are identified in addition to beaches, marshes and peat-bogs. Various formats including Arc-Info export. Data can be downloaded following registration. http://dataservice.eea.eu.int/dataservice/
CEH Land Cover	Great Britain	25m and 1km	The Land Cover Maps (LCMs) comprise 25 or 27 classes, including: • sea and inland waters • bare, suburban and urban areas • arable farmland, pastures and meadows • rough grass, grass heaths and moors, bracken • dwarf shrub heaths and moorland • scrub, deciduous and evergreen woodland • upland and lowland bogs Data are supplied under Licence http://www.ceh.ac.uk/data/lcm/

Online compendiums described in Rossiter (2004) and online at http://www.itc.nl/~rossiter/research/rsrch_ss_digital.html#europe provide a useful summary of currently available datasets.

Compared to soil and geology, land-cover and vegetation can be observed by satellites with comparative ease. Table 5.2 presents a selection of land-cover datasets freely available, together with details of the CEH land-cover map of Great Britain. Figures 5.2 and 5.3 show example maps of the different types of land-cover that can be identified by remote sensing (with varying degrees of confidence).
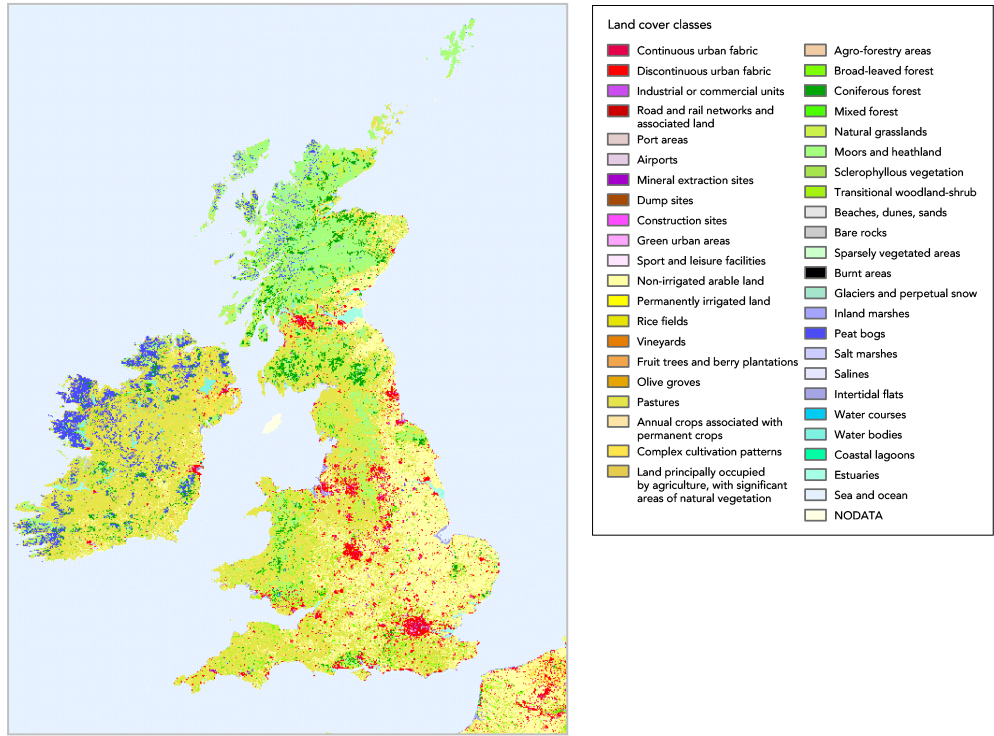
Figure 5.2 Map of UK land-cover based on CORINE Land Cover 250 m grid - version2 (12/2000)
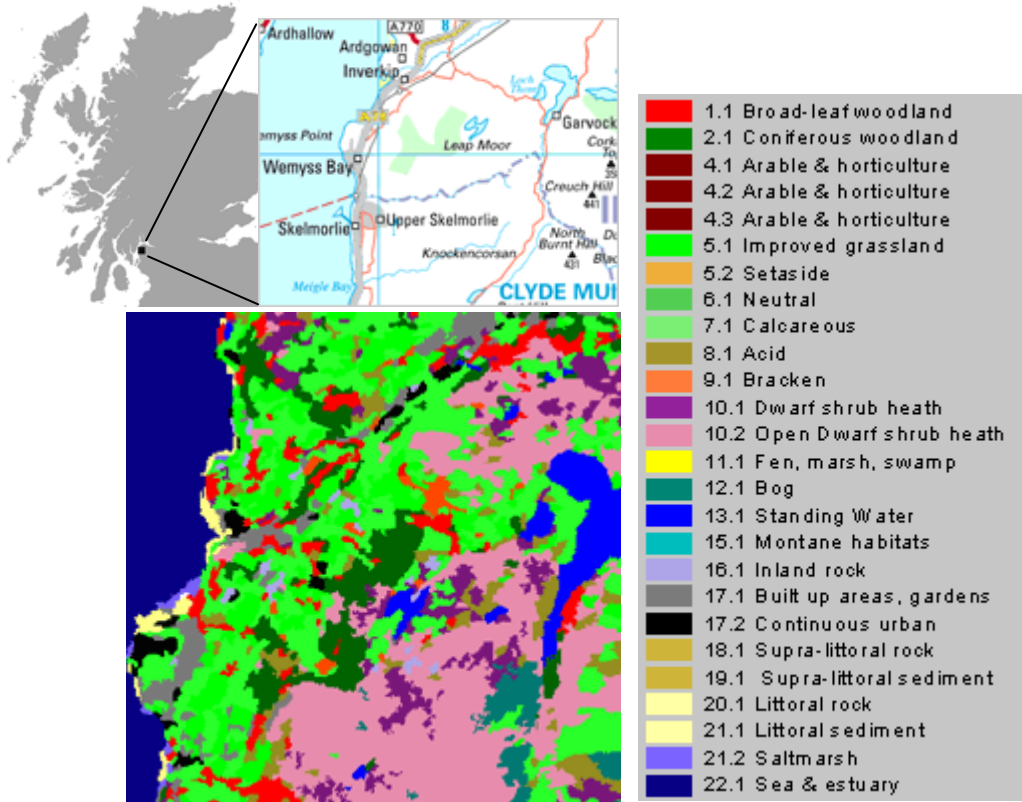
Figure 5.3 Sample of CEH Land Cover (LCM2000) for a small area west of Glasgow

Table 5.3 Digital terrain data

Dataset	Coverage	Spatial Resolution	Description
USGS (US Geological Survey) HYDRO1K	Global	1km	HYDRO1k provides global coverage of topographically derived datasets, including streams, drainage basins and ancillary layers derived from the USGS' 30 arc-second digital elevation model of the world GTOPO30. It aims to provide hydrologically correct DEMs along with ancillary datasets. http://lpdaac.usgs.gov/gtopo30/hydro/ Data freely available in a variety of formats including Arc-Info export format.
USGS Shuttle topography	Eventually Global	90m	Shuttle radar topography http://srtm.usgs.gov/ Available in a variety of formats, but at present, data are only available for the USA. Other parts of the globe will become available when processing is complete. Australia is next, followed by Europe.
Elevation Europe	Europe	1, 3, and 9km	Based on GTOPO30 from USGS. Freely available following acknowledgement of source. http://dataservice.eea.eu.int/dataservice/metadetails.asp?id=650
IHDTM Integrated Hydrological Digital Terrain Model	UK	50m	Based on Ordnance Survey 1:50000 Landranger maps. The complete dataset consists of 5 components representing • elevation, • inflow and outflow directions • cumulative drainage area • surface type (indicating land, river, lake or sea). Available from CEH in a variety of formats under license: http://www.nwl.ac.uk/ih/www/products/iproducts.html
Landmap	UK	30m	Hosted by MIMAS (University of Manchester), Landmap is a satellite data information and download system offering high quality Landsat-7 ERS1 and ERS2 raster images and the Landmap DEM product. UK tiles can be downloaded in Arc Grid format. http://www.landmap.ac.uk/products/dem.html
Nextmap	UK, USA, & selected other countries.	5m	NEXTMap Britain utilizes Intermap's IFSAR Technology (InterFerometric Synthetic Aperture Radar). Products consist of: • Orthorectified Radar Imagery (1.25m) • Digital Surface Model • Digital Terrain Model. http://istore.intermaptechnologies.com/nm_britain.cfm This product will soon be available to CEH
Environment Agency LIDAR (Light Detection and Ranging)	UK	2m	A database listing is downloadable, and LIDAR (elevation) data for selected OS tiles can be obtained from the Agency. http://www.environment-agency.gov.uk/science/monitoring/131047/?lang=_e

The datasets listed in Table 5.2 are based on satellite imagery from Landsat (e.g. CORINE), AVHRR (e.g. USGS landcover and PELCOM) and MODIS (e.g. GLCF MODIS-derived vegetation). An extended discussion of remote-sensing data and applications is provided in Section 5.3.

Digital terrain data, also known as DTM (Digital Terrain Model) or DEM (Digital Elevation Model) data, are becoming available at ever-greater resolutions as shown in Table 5.3. A number of global 1km datasets, (for example GTOPO30 from which Hydro1K has been derived), are readily available and have been composed from various sources of topographic data. These sources range from national datasets (such as the New Zealand DTM and the Map of Peru) to the Digital Chart of the World (which is itself based on US military aeronautical charts.). For European coverage, DTM data are only available at resolutions higher than 1km for individual countries. Table 5.3 presents a selection of well-known datasets which have UK coverage. The inclusion of 90m resolution USGS shuttle topography is an exception as coverage does not currently extend to Europe, however, data for Europe is next in line for processing after the EROS Data Centre have finished Australia and the US. Environment Agency Lidar data provides some of the highest resolution data for selected Ordnance Survey (OS) tiles; this is likely to be of particular benefit for high resolution flood inundation modelling. Airborne Lidar is a laser device that makes "profiles" of the earth's surface. The Lidar beam is reflected from both the vegetation cover and the ground surface; the difference between the two provides information on the height of vegetation (ranging from grassland to forests). Lidar data can be used to determine elevation, slope, aspect, and slope length of ground features. It can also measure coastal waters (water depth and subsurface topography), oil spills and organic pigments including chlorophyll.

DTM (elevation) data are useful in support of flood modelling for ungauged catchments at both a qualitative and quantitative level. Catchment or regional visualisation in 2 or 3 dimensions is reasonably straightforward using GIS packages, such as ArcInfo, to display DTM and other digital datasets. Information such as land-cover and digitised river networks can be overlaid on digitised terrain to produce a visual representation of the catchment/region.

GIS tools are also useful for determining average values of catchment properties such as slope, or for estimating percentage coverage for different land-cover classes in a region/catchment. Quantities such as channel slope and length, distribution of elevation or percentage land-cover are immediately useful as input parameters to a range of models. Spatially-distributed models such as the CEH Grid Model (Bell and Moore, 1998), and SHE (Système Hydrologique Europèen, Abbott *et al.,* 1986) are heavily dependent on DTM data for their basic configuration. Wide-area models such as MOSES (Met Office Surface Exchange Scheme), the EFFS (European Flood Forecasting Scheme; De Roo *et al.*, 2003) and other runoff-production (and routing) models are similarly configured using DTM data. Flow-routing models (both source-to-sink and grid-to-grid) require knowledge of the flow pathways from every point on the landscape to the river. GIS tools specifically developed for hydrological applications can be used to transform DTM data into a grid of flow-directions (determined from the steepest descent to neighbouring grid-squares) which can be 'joined-up' to form flow paths from every point to a natural sink (for example, the sea or a lake). Grid cells with a large number of cells draining to them often correspond to natural rivers, although there can be major discrepancies, particularly in areas of low relief, and in areas of high relief where the topography varies on a scale that cannot be detected at the resolution of the grid-cells. Figure 5.4 shows the Hydro1K elevation dataset for Europe, together with inset maps of slope and derived river network.
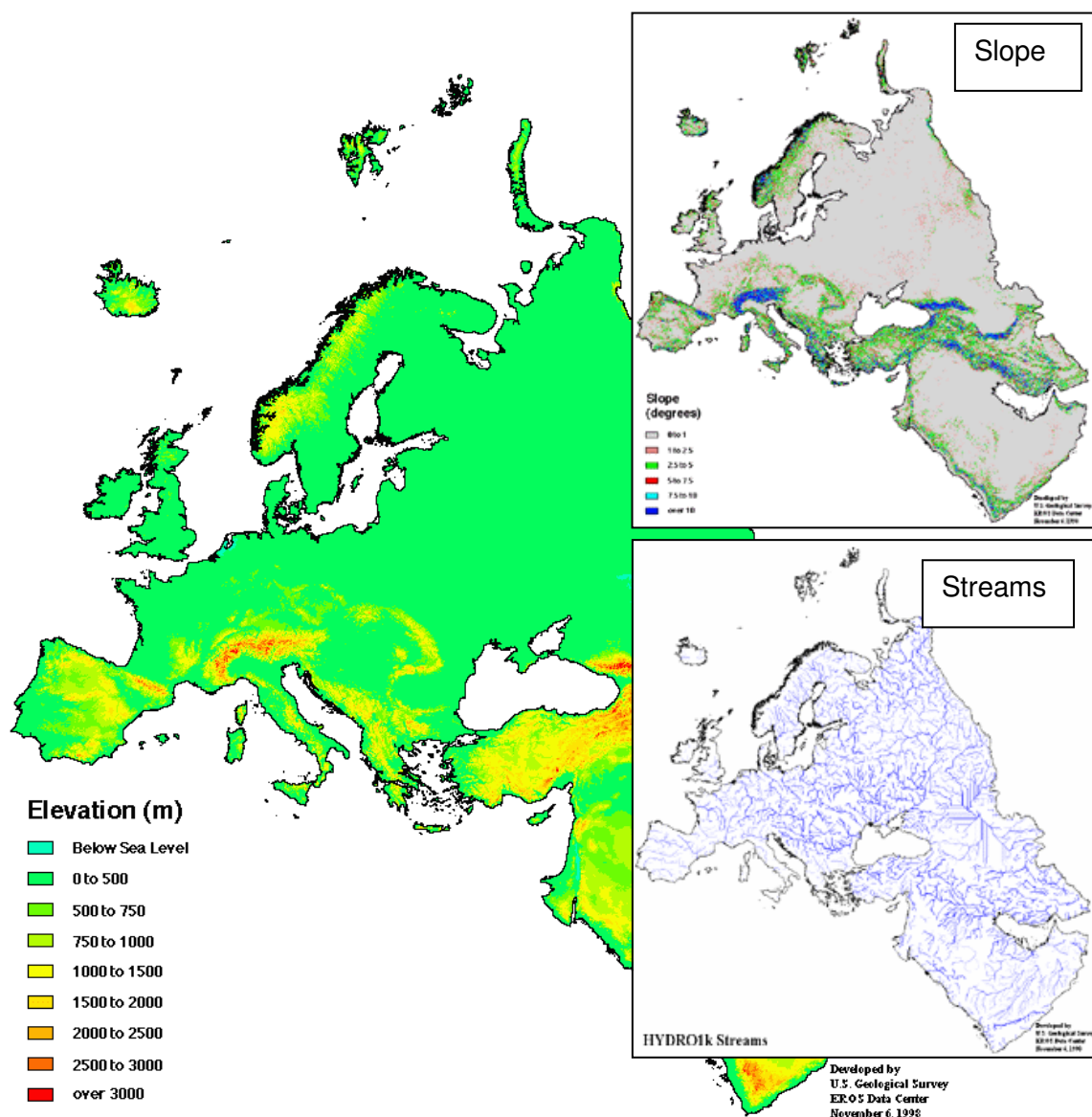
Figure 5.4 Hydro1K elevation, slope and streamflow maps for Europe (USGS - NASA Distributed Active Archive Centre).

Similar (and often more accurate) datasets of flow directions can also be produced using a fine scale DTM, for example the IHDTM (Integrated Hydrological Digital Terrain Model, Morris and Flavin, 1990) which has been constructed from 1:50000 (50m) Ordnance Survey data for the UK. This dataset consists of 5 components representing elevation, inflow and outflow directions, cumulative drainage area and surface type (indicating land, river, lake or sea). Figure 5.5 presents an example map of elevation for South Wales. These data have been used in support of the development of flood-risk maps for Great Britain, the FEH (Flood Estimation Handbook) CDROM, and a variety of modelling applications.
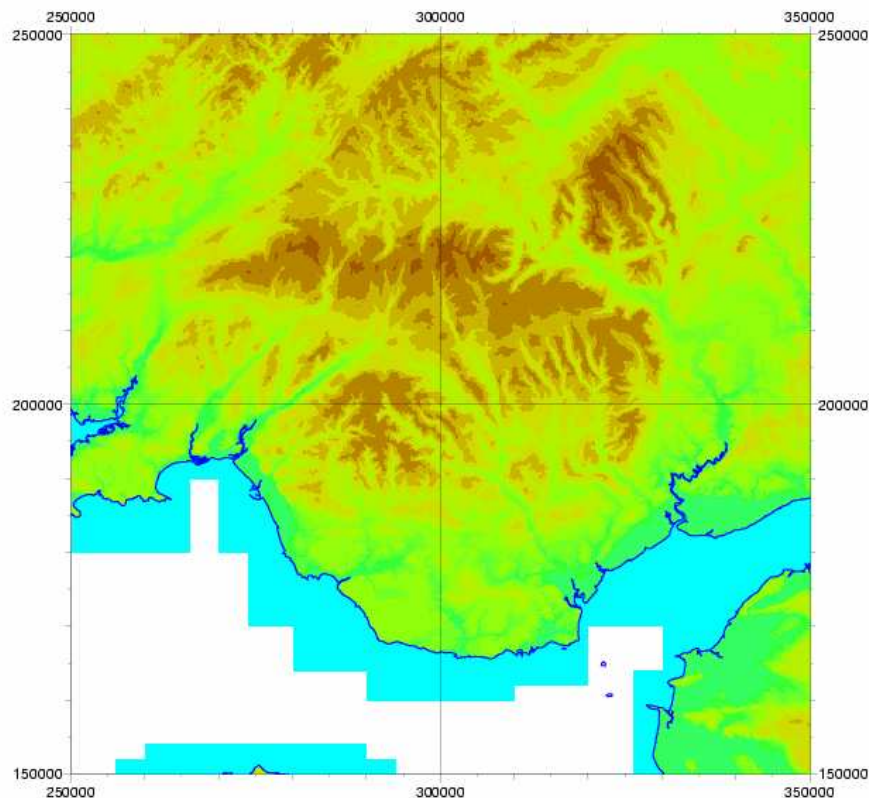
Figure 5.5 Map showing the IHDTM (50m resolution) for South Wales

5.3 Satellite-derived products

Although satellite-derived and other remote-sensing datasets have already been included in the summary tables (5.1 to 5.3), it is worth specifically discussing recent developments, and datasets that will soon be available. There is already a large body of remote-sensing data available from a variety of satellite-based sources. These are summarised, so far as is possible, by numerous websites, for example Leeds University Remote Sensing Resource website (http://www.geog.le.ac.uk/cti/rs.html) and NASA's Land Processes Distributed Active Archive Center (LP DAAC) (http://edcdaac.usgs.gov/main.asp).

Satellite products from European and NASA satellites are most likely to be useful for UK applications, although there are other sources. The NASA satellite TERRA obtains images of every point on the globe every 1-2 days. It contains a number of instruments and products, of which the most relevant are summarised in Table 5.4.

Among the datasets originating from MODIS is the Leaf Area Index (LAI). This quantifies the total leaf area (one side only) per unit ground area. Various soil-vegetation-atmosphere models use LAI, which varies globally from 0 to >10, as shown in Figure 5.6 which presents the MODIS/Aqua LAI over Northern Europe for the period 28 July to 4 August 2003. This is a 1 km global product updated every 8 days.

Table 5.4 Summary of TERRA satellite sensors and data products relevant for ungauged hydrological modelling.

Acronym	Product	Description
ASTER	Advanced Spaceborne Thermal Emission and Reflection Radiometer	Stereoscopic images and detailed terrain height models. Monitors: • Land-surface temperature • Emissivity • Reflectance • Elevation
MISR	Multi-angle Imaging Spectro-Radiometer	Monthly, seasonal, and long-term trends in: • the amount and type of atmospheric aerosol particles, • the amount, types, and heights of clouds; and • the distribution of land surface cover, including vegetation canopy structure
MODIS	Moderate-resolution Imaging Spectroradiometer	Useful for monitoring large-scale changes in the biosphere: • Vegetation Indices (eg LAI) • Snow • Albedo • Surface temperature • Land-cover and land-cover change

The European Space Agency (ESA) has two Earth observation 'missions', ERS (launched 1991 and 1995) and ENVISAT (launched in 2001). ERS-2 is the current operational satellite (ERS-1 ceased operation in March 2000). A radar scatterometer on board ERS-2 measures wind fields over the ocean surface in all weathers. It can generate real-time 'nowcasts' of the current climate state as well as more reliable short-range weather forecasts.

ENVISAT (ENVIronmental SATellite) is an advanced polar-orbiting Earth observation satellite which can provide measurements of the atmosphere, ocean, land, and ice over a five year period. The C-band ASAR (Advanced Synthetic Aperture Radar) instrument aboard ENVISAT provides 25m resolution, with superior coverage to the ERS. The reflected SAR beam is sensitive to linear and geometric features on the ground: different wavelengths are sensitive to vegetation or to ground surface phenomena, particularly in dry, porous soils, where the radar can penetrate the surface.

SAR can also be used to estimate soil moisture, particularly for bare or sparsely vegetated areas; regions with significant vegetation cover can decrease the sensitivity of the reflected beam to soil moisture. Figure 5.7 shows an ASAR 'multitemporal' colour composite image for a 100 km^2 region covering London. The Thames estuary can be seen on the right. The picture is composed of three images acquired on
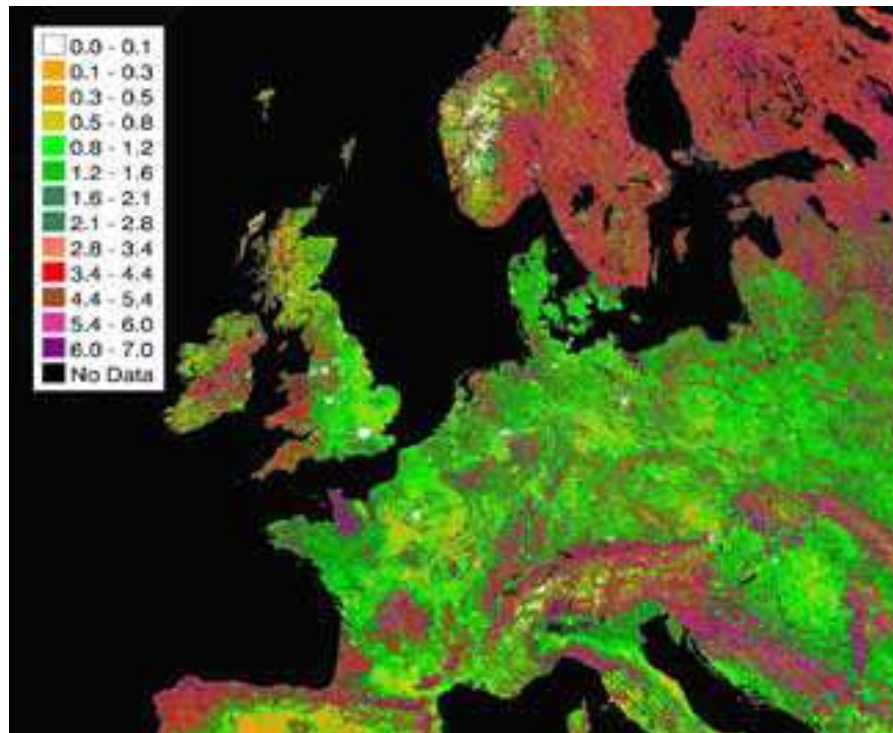
Figure 5.6 MODIS/Aqua Leaf Area Index (LAI) over Northern Europe: July 28 to August 4, 2003.
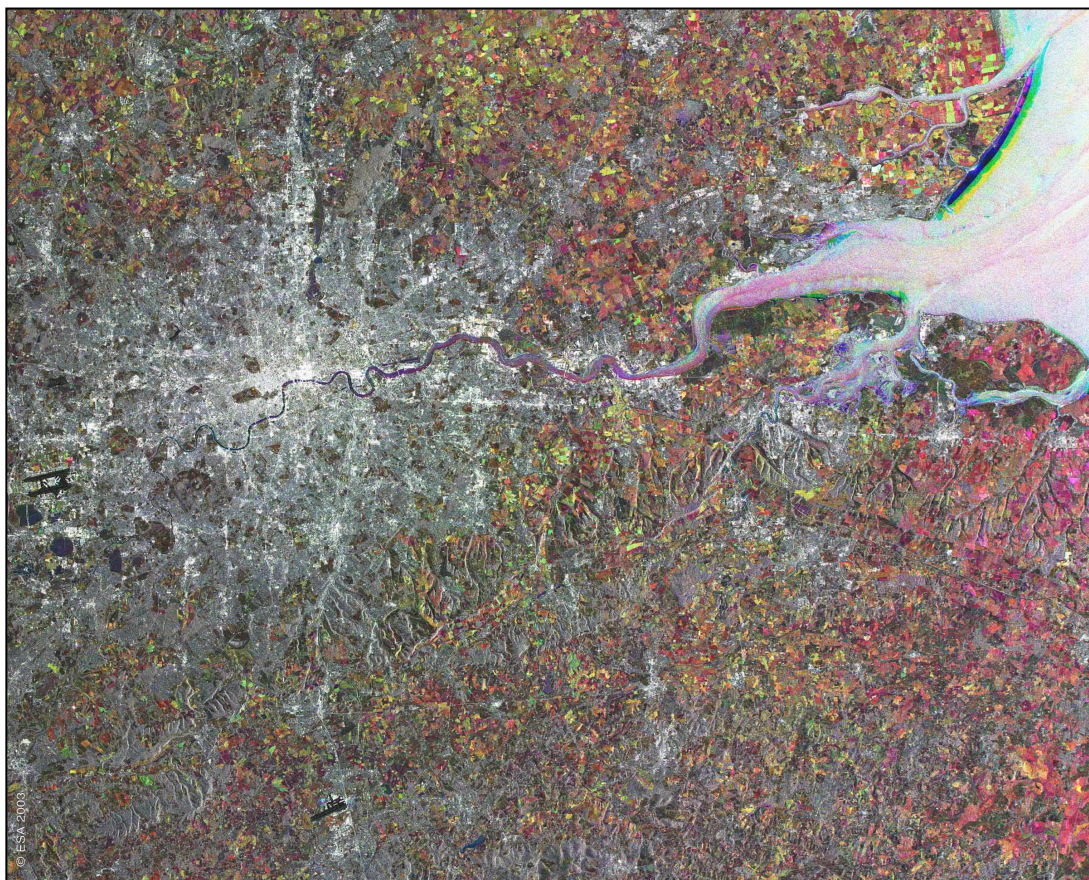
Figure 5.7 An ASAR multi-temporal colour composite image for London and the Thames Estuary. The image is composed of three images acquired on different dates. RGB colours are assigned to each (Red: 13 December 2002, Green: 02 May 2003, Blue: 15 August 2003).

different dates. RGB colours are assigned to each (Red: 13 December 2002, Green: 02 May 2003, Blue: 15 August 2003). White pixels indicate areas unchanged over period. The prevailing magenta colour in the river indicates that the 13 December and the 15 August were windy days. The green, orange and red areas seen over the entire image correspond to agricultural fields with a high variation from one season to another. MetOp is a series of three satellites to be launched sequentially over 14 years, starting in 2005.

ESA is also developing a new Polar-orbiting Meteorological Satellite, 'MetOp', which will be Europe's first polar-orbiting satellite dedicated to operational meteorology. The satellite will be launched in co-operation with the US agency NOAA and will provide data that will be used to monitor climate and improve weather forecasting. New instrumentation will provide:

- temperature and humidity measurements
- wind speed and wind direction measurements, particularly over the ocean, and
- profiles of ozone in the atmosphere

Finally, it is worth mentioning the Dartmouth Flood Observatory website. This site aims to detect, measure, and analyse extreme flood events world-wide using satellite remote sensing. Microwave and optical satellite imaging of selected river reaches are used to detect overbank and extreme low flow conditions. The Observatory also provides yearly catalogues, maps, and images of river floods, from 1985 to the present. By way of example, Figure 5.8 shows the MODIS satellite image for 5 January 2003 and the processed image of estimated flooded areas.

Prolonged heavy rainfall in the New Year caused the Thames to reach extremely high levels, with flows in some places the highest since the 'great flood of 1947'. Areas shaded in red are the flooded areas detected from the satellite image shown; the blue areas represent the previous 'reference flood' recorded at the flood observatory (likely to be 2001).

The Flood Observatory also describes a prototype system for 'satellite gauged reaches', a "Global Hydrographic Array" (Brackenridge at al., 2003), which appears to consist of 710 reaches worldwide that are constantly monitored using a combination of different satellite products. These consist of SRTM (Shuttle Radar Topography Mission) 90m topographic data, clear-sky ASTER multispectral images (at spatial resolution of 15 m), and a variety of in-situ measurements. Various orbital sensors are used to detect and map temporal changes in surface water. These currently consist of two MODIS sensors aboard NASA's Terra and Aqua satellites.
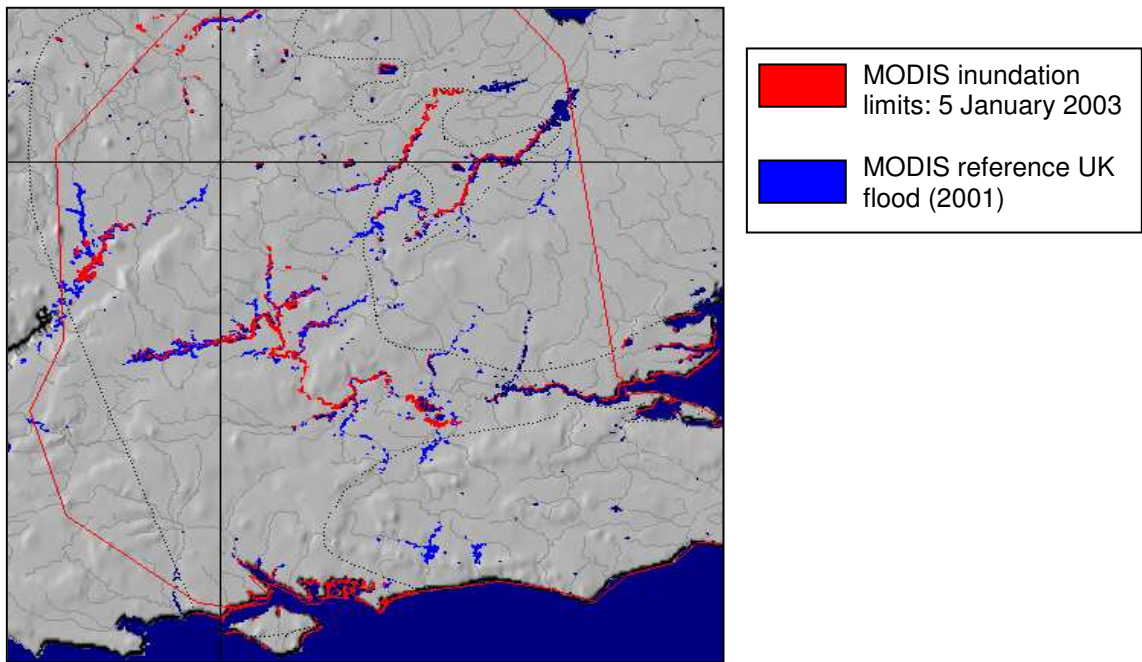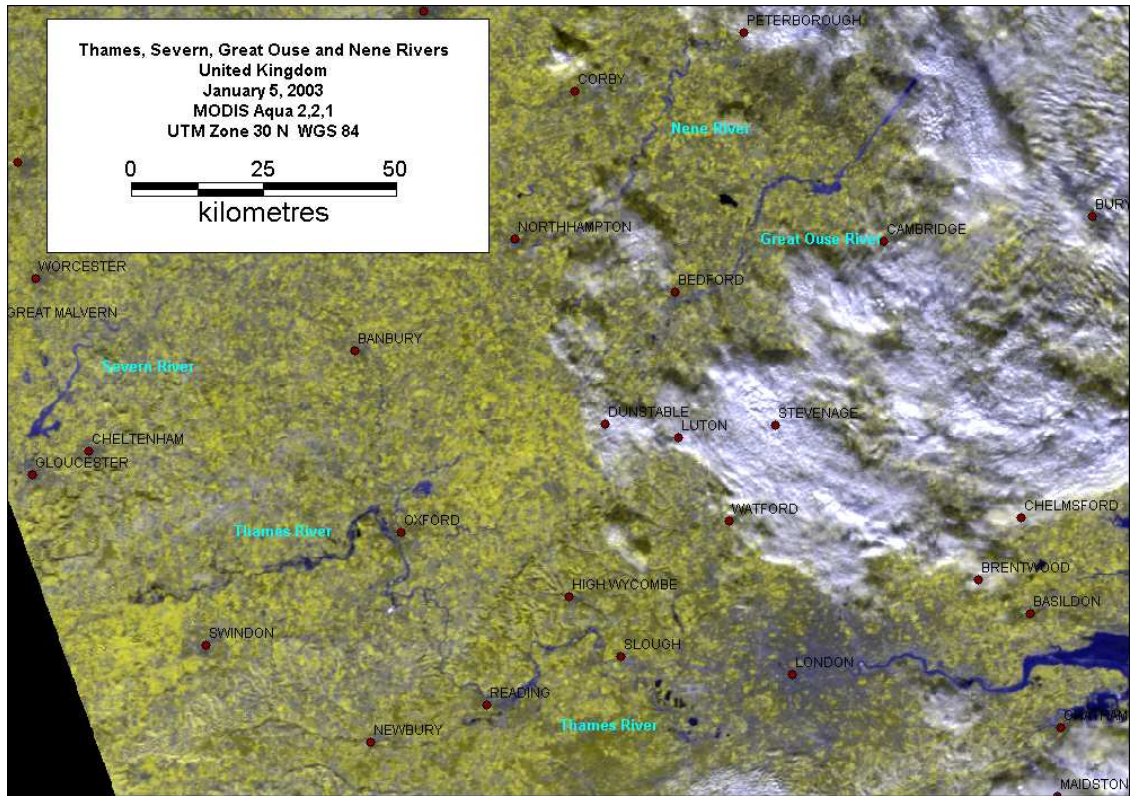
Figure 5.8 MODIS satellite image for 5 January 2003 and the processed image of estimated flooded areas over Southern England (prepared by the Dartmouth Flood Observatory)

6 Statistical methods for forecasting

6.1 Introduction

This section outlines some possibilities for forecasting which arise from approaches that do not rely directly on using models that represent hydrological or hydrodynamic processes mathematically. It is not entirely clear that the descriptor "statistical" is appropriate here, since the approaches do not involve statistical models in the sense of models including details of probability distributions. Rather they involve a type of empirical model building that relies on formulating a simple but flexible forecasting rule and then calibrating the parameters of this rule using available data. In some fields of application they would be called empirical methods. Since these approaches place considerable reliance on calibrating against past datasets for the quality of their forecasts, statistical methods do not obviously have any usefulness for problems of forecasting for ungauged locations. While these methods are partly described here for the sake of completeness, the following subsections do outline some ways in which statistical methods may still be useful for forecasting at ungauged locations.

6.2 Level-to-level correlations

A standard and well-known form of simple-to-apply forecasting technique is based upon the regression of peak river-levels at the target site on peak river-levels at some upstream site. Part of the data-analysis involves identifying a time-of-travel, τ_{peak}, for the flood-peak between the two locations. A collection of pairs of values of peak levels at the two sites $\left\{ L_1^{(j)}, L_2^{(j)} \right\}$ is prepared, where, for example, $L_1^{(j)}$ denotes the peak-level at the upstream site for the j'th pair of peaks. Typically the levels at the two sites are recorded with respect to the individual gauge-zero for the sites. A predictive relationship of the form

$$L_2^{(j)} \approx a + bL_1^{(j)}$$

is then established: this may be done using a formal approach such as least-squares regression or using a simple visually-fitted line, having plotted the data graphically. This stage of the analysis can also give some information about the likely size of errors in forecasts constructed by this method. The approach can be applied in two ways. Firstly, it can be applied to individual flood-peaks at the upstream site, to transfer a peak-level L_1 (which may be observed or derived from a mixed observation-and-forecast time-series) to a forecast for the downstream site, $\hat{L}_2$, using

$$\hat{L}_2 = a + bL_1 .$$

This forecast of the downstream peak-level would be associated with an estimated time of arrival for the peak derived from τ_{peak}. Secondly, the approach can be applied to create a continuous series of forecast values for the downstream site, with the understanding that only the peaks are to be used as true forecasts (because that is the

way the model is fitted). Such a series (i.e. forecast values at a number of different time-points t) would be constructed using the formula

$$\hat{L}_2(t) = a + bL_1(t - \tau_{peak}).$$

More general forms of predictive equations can be formulated and fitted. Some of these approaches avoid the question of identifying flood peaks and simply fit the predictive equation across the whole range of levels available in the calibration dataset. An example for such an equation follows. Let τ_{step} be the length of the basic time-step between observations and let a, b_1 and b_2 be real-valued parameters, while n is an integer-valued parameter. Then a possible predictive equation might be

$$\hat{L}_2(t) = a + b_1 L_1(t - n\tau_{step}) + b_2 L_1(t - (n+1)\tau_{step}).$$

An automatic scheme for estimating the parameters of such a predictor could readily be established.

Level-to-level correlation schemes may in some cases be useful for forecasting at ungauged locations if they can be used to establish calibrated forecasts of level at sites both upstream and downstream of the target site, or for only one site if levels can be forecasted for the other by some other means. The overall scheme would involve converting the level forecasts for the two sites to relate to the same gauge zero, for example using ordnance datum, interpolating these levels between the sites and then possibly converting to a local datum for the target site. The interpolation scheme could take into account the typical difference in timings between the two calibrated sites.

6.3 Empirical forecasting schemes

The simple level-to-level forecasting schemes outlined above can be made more complicated and more general. In order to achieve an overall scheme to create forecasts for a range of time-points it is possible to consider, for each such time-point, the relative times at which observations might be available for the construction of a forecast-value. In practice the "best" such set would be used, but as the target time-point advances into the future, the relative time of available telemetered observations changes. A separate forecast-rule can be constructed for each such relative timing of available data. For example, suppose that telemetered observations of flow $\{Q_T(t)\}$ at the target site are available up to a time τ_T, and that telemetered observations of flow $\{Q_U(t)\}$ are available up to a time τ_U for an upstream location. Then for a given target time τ use could be made of an empirical forecasting rule of the form

$$\hat{Q}_T(\tau) = a_{\tau-\tau_T, \tau-\tau_U} Q_T(\tau_T) + b_{\tau-\tau_T, \tau-\tau_U} Q_U(\tau_U),$$

where the coefficients $\{a_{ij}\}, \{b_{ij}\}$ would be determined by calibrating the forecast rule using historical data, separately for each relative pattern of data availability, indexed by $i = \tau - \tau_T$, $j = \tau - \tau_U$. In practice it would probably be necessary to construct a modified version of τ_U for use in the empirical rule to control the time point used relative to τ: for example $\tau_U{}^* = \max(\tau - \delta, \tau_U)$.

This type of approach is clearly not limited to forecast rules based on linear functions. Forecast-rules constructed by a neural-network modelling approach form further sets of examples.

6.4 Statistical simplification of hydrodynamic models

Where inter-site level and flow relationships cannot be estimated using observed data because of a lack, or shortage, of observed data for the target site, it may instead be possible to establish some simple statistical relationships based on modelled values obtained from a hydrodynamic model calibrated to the reach in question. Of course, given that such a hydrodynamic model would have to exist or be created, that model could itself be used to create the requisite forecasts. Nonetheless, simple predictive relationships may prove useful where savings in computational time need to be made, or where a back-up procedure for generating manual forecasts is required in the event of an unexpected failure of a main forecasting system.

In fact simple predictive relations for peak river-level have already proven useful operationally on the Tidal Thames in the form of tabular "Structure Functions" derived from a hydrodynamic model for the tidal zone from Moseley to Southend. Use of such tables is well-suited to those who wish, or need, to avoid access to extensive computational equipment. In this instance, the structure function tables yield the predicted peak river-level at a given location on the basis of two items of information: the river-flow at the upstream end of the tidal reach (nominally at Teddington: the flow is assumed to be slowly changing so that a current or recent flow-value will do) and the peak tidal level at the downstream end of the reach (nominally Southend or Sheerness: this might be an observed value or a predicted value obtained for example from the STWS). The structure function tables were obtained from multiple runs of the hydrodynamic model driven by profiles of upstream river-flow and downstream tidal-level with the right selection of characteristics. Note that the structure functions were originally derived for other purposes concerned with joint-probability calculations involving operations of the Thames Barrier.

The above example of structure functions illustrates one way in which predictive relationships can be obtained using a hydrodynamic model. In particular, it is an instance where the hydrodynamic model is run over a range of conditions more extreme than those actually experienced over the period for which continuous observations are available. It is also an instance where the predictive relationships used are not restricted to the type of linear predictive relationship used in most level-to-level correlations. However, it is not necessarily an example that can be followed in many cases, since the approach relies on there being no strong need to account in the predictions for the relative timings of peak-flows and tidal-peaks.

In general, the basic approach for a new application would be as follows:

(i) Decide the important causative factors for river-levels at the target site:

> (a) determine, for each important factor, one or more descriptors for the time-profile of each factor, including also descriptors of relative timings of the important factors;
> (b) establish ranges of values for the descriptors of each factor, starting first from observed data but extending this range to cover more extreme conditions also;

(c) for relatively unimportant factors (other boundary conditions on the hydrodynamic model) decide how these are to be treated (for example, minor flows might be set in proportion to important river flows).

(ii) Decide what should be the quantity being forecasted for the target site: possibilities are the maximum river-level in the response to a given flow-event or tidal cycle, or the river-level at a particular time.

(iii) Decide what quantities should be the basis of the predictive relationship for each potential target site:

(a) consider basing predictions on the causative factors decided on in (i), for general background forecasts;
(b) consider also basing predictions on river-levels or flows that will be available in real-time via telemetry, or for which simple forecasting models can be predicted, with a possible emphasis on telemetry locations closer to the target location;
(c) consider basing predictions for targets on tributaries on river-levels at the junction of the tributary with the more major river;
(d) depending on the decision made for (ii), decide on the specific quantities to use as the basis of the prediction: possibilities are maximum river-level, average flow or levels and flows for particular times relative to the target forecast time.

(iv) Undertake multiple runs of the hydrodynamic model for various combinations of the different causative factors, decided on in (i).

(v) As part of a careful analysis of the response of the river-level within the hydrodynamic model at a particular location:

(a) examine the responses to changing one or two factors systematically in order to determine suitable structures for predictive relationships;
(b) consider further runs with either systematic or randomly varying selections of the causative factors, or with profiles corresponding to historical events;
(c) establish parameters for the predictive relationships.

It is clear from the above that considerable research is necessary for the construction of simple statistical relationships based on hydrodynamic models. Apart from the "structure function" examples already mentioned, which were not specifically constructed for real-time forecasting purposes and which are relatively simple, there has been no work on constructing such relationships. In principle, the approach could be applied to observational rather than modelled data and in this instance practical examples mostly arise as level-to-level correlations. The use of the hydrodynamic model is to effectively increase the amount of data available for model-fitting and to extend the range of extremes experienced. The increased amount of data allows consideration of predictive relations which are more complicated that the simple level-to-level correlations and which allow more causative factors to be taken into account.

The major difficulty with implementing the approach discussed here is that is relies on the existence of an adequately configured hydrodynamic model, which are known to be expensive to create. Once the hydrodynamic model exists, forecasts directly from the model are very likely to be better than those obtained from any statistical simplification of the model. Considerable effort would be required for initial trials of structuring statistical simplifications for forecasting within particular reaches, but experience gained on such trials would then reduce the effort required for later applications. This

suggests that the best way forward would be to undertake research into statistical simplifications of hydrodynamic models using a case where the immediate target is to construct back-up forecasting procedures in event of a major computer-system failure: this research should be allowed to consider procedures that are somewhat more complicated than could be implemented using purely manual calculations so that some idea of the gain of accuracy with complexity can be obtained.

6.5 Statistical simplification of hydrological models

Once the idea of statistical simplification of hydrodynamic models has been posed, it is natural to consider applying the same idea to distributed hydrological models, to collections of lumped hydrological models setup in a semi-distributed fashion or even to individual hydrological routing or rainfall-runoff models. While there may be some circumstances in which this would be profitable, it seems unlikely that statistical simplification can provide anything useful in these cases. This is primarily because these classes of model do not contain typically a sufficient modelling of physics to be able to represent variations of river-level at ungauged locations with any degree of confidence. Secondly, hydrodynamic models can be viewed as an attempt to accurately match the known physics of water flow at a detailed level, whereas hydrological models can be viewed as being acknowledged simplifications of reality which gloss over the actual physics of the progress of water through catchments and channels because of the huge complexity involved in doing otherwise. There seems little merit in applying statistical simplification techniques to models which are themselves simplifications: if it is necessary to adopt an even simpler model in order that computations can be undertaken with little computer resources, or manually, it seems better to fit the simpler model directly to available observations.

However, it is possible to envisage developments of hydrological routing so as to become closer to representing important hydrodynamic modelling concepts, particularly in the channel routing components of gridded distributed models. This means that the initial conclusion above is not clear-cut. At some stage it may be worth attempting statistical simplification from such gridded models, in which case the set of considerations for this approach that was outlined for hydrodynamic models could be applied.

7 Real-time updating techniques

7.1 Overview

Real-time updating of forecasts is concerned with improving model forecasts by using real-time observations of river conditions to improve later forecasts. For example if a forecast of *current* flow made at a previous time-step is found to be an overestimate compared to the observed river flow, the model forecast at a *future* time-step can try to compensate for this by reducing the flow forecast accordingly. Usually this updating procedure is applied at locations where observations are available. However, if no measurements are available locally, the only way of improving model forecasts is to make use of real-time observations at other locations.

In many ways, model updating at an ungauged site can be considered as an extension to a simulation-mode model which relies on gauged observations elsewhere. In *simulation-mode*, a model for an ungauged site may be calibrated to historical observations (such as flow and rainfall) for another location, and then adjusted for the ungauged site. In *forecast-mode* the model makes a prediction at the other location, the prediction is compared to an observation at that site, and knowledge of the forecast error at the other location can be transferred across to the ungauged site in order to achieve the best possible forecast at that site.

Unfortunately there has been little documented research into the best methods of transferring forecast errors from one site to another. Some progress could be made by testing out schemes of this type by constructing forecasts for gauged locations as if they were ungauged. However, until these tests have been done, **the current recommendation is not to apply transferred-error (inferred-error) updating schemes** because of the risk of making basic forecasts for the ungauged site worse through ill-advised choice of transfer and updating parameters. However, it does seem worth using an inferred-error updating scheme in one specific type of application: this relates to cases where the target location is modelled using simple scaling or transposition (see Section 3.2); this is discussed in Section 8.2.

In the absence of available research into methods of transferring forecast errors from a gauged to an ungauged site, the following sections provide some possible approaches for future investigation.

7.2 Introduction

The purpose of Section 7 is to discuss ways in which forecasts can be improved on the basis of real-time observations of river conditions, with particular attention to dealing with ungauged locations for which there would be no telemetered observations. For completeness, one should note that there is potentially a much wider range of sources of real-time information that might improve model-forecasts. One such type of source would be catchment-wide estimates of soil-moisture or soil-temperature that are available on a real-time basis from satellite observations. A second type of source is direct measurement of soil-moisture or groundwater-level for a specific location. Use of such sources is not presently undertaken for real-time flood forecasting in the UK for gauged locations, although there is scope for this to be done. While treating such sources is apparently rather more complicated than when dealing with observations of river conditions, in fact the same underlying methods apply, and the same types of

extensions of the methodology to deal with ungauged locations can be foreseen. Thus, for the sake of clarity, it seems best to omit further explicit mention of updating based on non-river observations.

There is another limitation on the scope of the present section: it deals with forecasts based on structural approaches which aim to create forecasts for a series of time-points. A variety of approaches are available for constructing forecasts at a fixed lead-time with respect to a set of available observations: these could then be applied separately for a number of different lead-times. Such approaches can be characterised as involving an empirical forecasting rule for each lead-time. This type of approach has been discussed in Section 6. The disadvantage of treating lead-times separately is that the resulting time-series may behave erratically unless special efforts are made in structuring and fitting the forecasting schemes.

As discussed above, forecast-updating is concerned with improving forecasts by making use of real-time observations of river conditions to improve later forecasts. The usual application of updating techniques for real-time forecasting based on hydrological models has been to make use of real-time observations for a given location to update forecasts for that location only. In the case that a location is ungauged (*i.e.* has no telemetry observations), the only hope for improving modelled values is to make use of real-time observations at other locations. The possibilities for doing this depend on the type of model being used for the particular location.

The model-types which allow the most obvious approach to updating for ungauged locations are those which treat the ungauged location by indirect modelling (Figure 7.1). In this instance, values for the ungauged location are modelled as part of the representation of a more extensive model which is calibrated to observations at other gauged locations. If the model has a good physically consistent basis, it is to be hoped that state-updating methods applied to the more extensive model and based on real-time observations at the gauged locations will result in improved estimates at all ungauged locations (Figure 7.2 (a)).

More general but less direct approaches to forecast-updating are potentially available and might be applied even if indirect modelling for the target location has been adopted. Here forecast or modelling errors are evaluated at locations having telemetry and these are then "transferred" in some sense to the target location, after which the standard methods of forecast updating available for gauged locations can be applied directly (e.g. state-correction or error-prediction): a schematic of error-prediction is shown in Figure 7.2(b).

The main question is whether such a transfer of modelling-errors and their subsequent usage for forecast-updating will actually result in improved forecasts. It is clear that any transfer scheme would need to include the possibility of re-scaling the errors during the transfer process and thus such schemes could be configured to ensure that only relatively minor changes to forecasts would be made via this type of updating. Configuring these schemes for specific target locations is problematic since there would typically be no data available for the calibration of either transfer or updating parameters. Some progress could be made by testing out schemes of this type by constructing forecasts for gauged locations as if they were ungauged. Until such investigations have been made, it is possibly best not to apply transferred-error (inferred-error) updating schemes on the grounds of the effort required for implementation and the risk of making the basic forecasts for the ungauged site worse through ill-advised choice of transfer and updating parameters. It does seem worth using an inferred-error updating scheme in one specific type of application: this relates
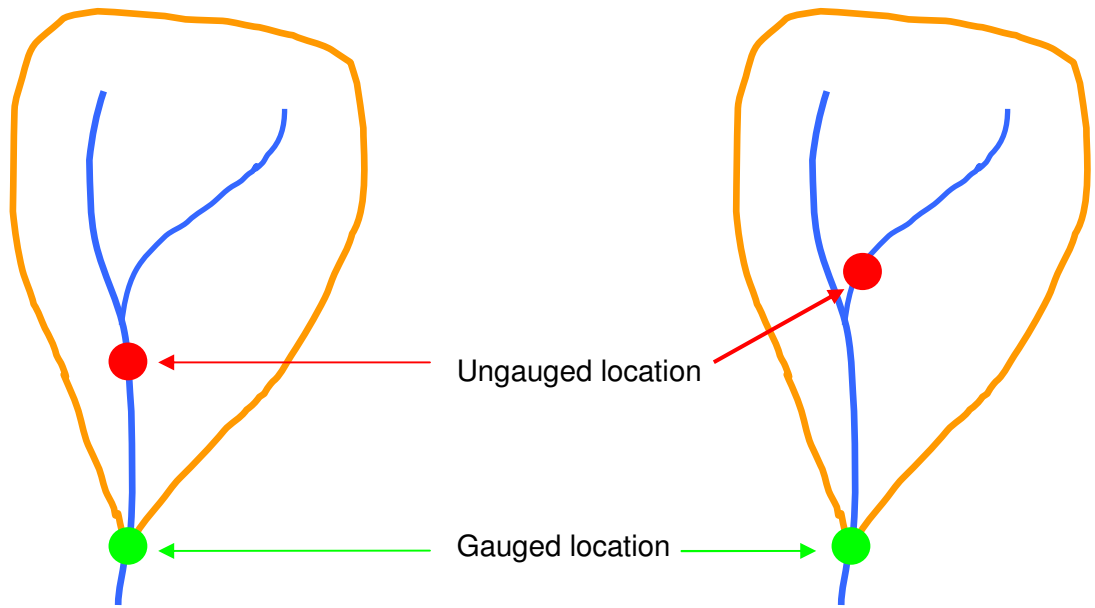
Catchment schematics
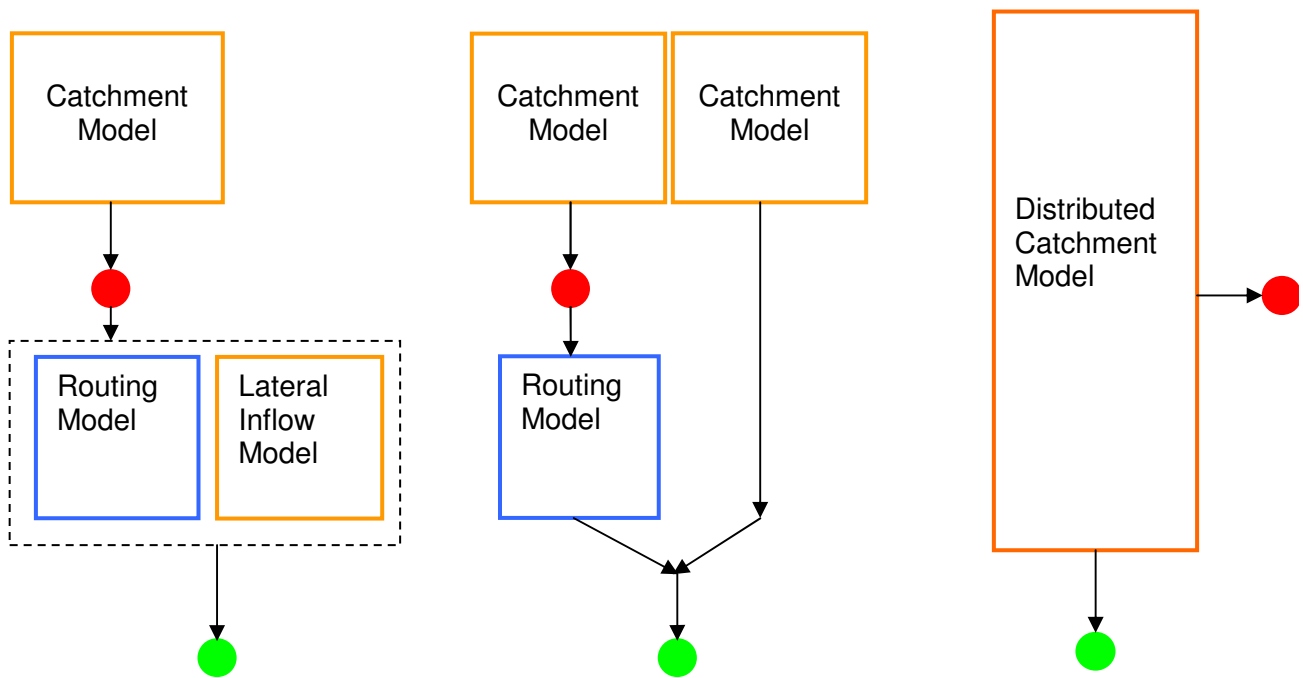
Direct modelling approaches for the ungauged locations

Indirect modelling for the ungauged location

Figure 7.1 Direct and indirect modelling for an ungauged location

(a) Updating using an indirect model
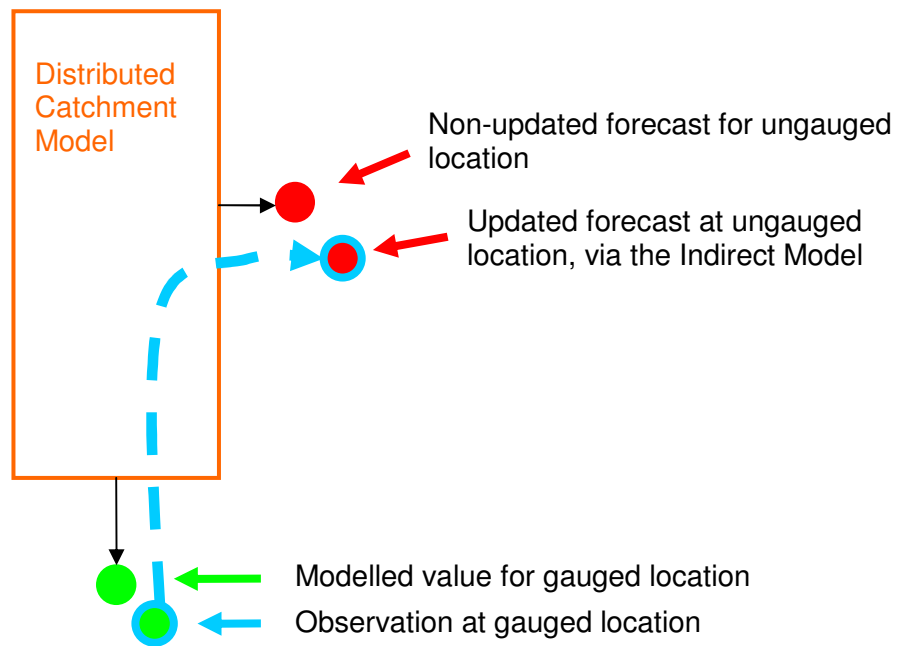
(b) Updating using a direct model with an external updating procedure
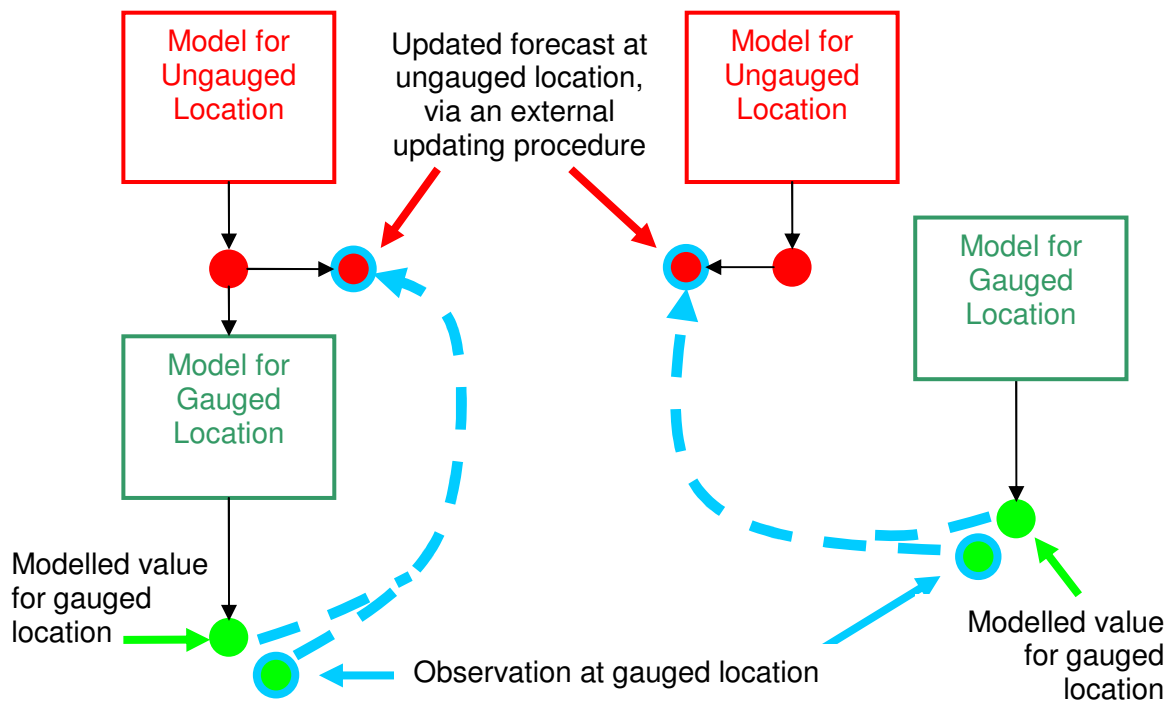
Figure 7.2 Forecast-updating for an ungauged location

Science Report – Rainfall-runoff and other modelling for ungauged/low-benefit locations (SC030227)

to cases where the target location is modelled using simple scaling or transposition (see Section 3.2); this is discussed in Section 8.2.

The following subsections outline some of the possible approaches to forecast-updating for when the target locations are ungauged. In principle, the underlying bases of these approaches are the same as those for gauged locations. However, the changed context does suggest that a wider range of variants of the basic methodologies need to be considered if a proper study of competing methods is to be made for the ungauged case. It may also be worth testing a number of these variants for the more standard case of updating at gauged sites since the methods presently being used in practice were established in the context of more limited computing resources than are now being used and when the emphasis was on simplicity and computational speed.

7.3 Off-line forecast improvement

In principle, the discussion of updating procedures would be restricted to ways of improving forecasts based on telemetered information. However, there are some important techniques of forecast improvement which have their basis in off-line procedures. Thus these procedures are potentially important to real-time forecasting for ungauged locations, since real-time data are not needed. However, the methods do require historical data for the calibration of the "improvements". The general basis of the methods is to identify consistent "biases" or other problems in a simulation-mode model, and to apply corrections for these in order to create improved forecasts. When real-time data are available, real-time versions of these forecast-improvement procedures are possible, based on calculating similar corrections based only on "recent" data. If a wide-enough interpretation is made of the classifications, such real-time improvements can be considered to be within the usual classes of error-prediction and state-correction forecast-updating procedures.

While it is possible to consider off-line forecast improvement schemes which don't make use of real-time data simply as special cases of the schemes which do use real-time data, it seems more appropriate to discuss these separately, for two reasons. Firstly, this reveals the conceptual basis of the improvement schemes. Secondly, it highlights the potential for considering the outcome of the forecast improvement scheme as a replacement for the initial version of the "simulation-mode" forecast created by an underlying model. Thus, some of the potential complexity of a forecast-updating scheme can be separated-off into a computational layer where the simulation-mode forecasts are "improved", before being updated.

Some simple examples of off-line forecast-improvement schemes are outlined here. These assume that an initial set of "simulation-mode" modelled values $\left\{\widetilde{Y}_t\right\}$ is available corresponding to quantities $\left\{Y_t\right\}$ for which forecasts are required. Examples of simple "improved" values are:

$$\breve{Y}_t = a + b\widetilde{Y}_t, \tag{7.1}$$

where this allows a correction for additive and scaling bias; and

$$\breve{Y}_t = \begin{cases} \widetilde{Y}_t & (\widetilde{Y}_t \le d), \\ \widetilde{Y}_t + c(\widetilde{Y}_t - d) & (\widetilde{Y}_t > d), \end{cases} \tag{7.2}$$

where this allows for a correction to high forecast values while leaving low forecasts unchanged. Here a , b , c and d are parameters of the improvement step which would be fitted using an objective function for calibration of the revised forecasting scheme. The inclusion of improvement steps of the above type will usually extend the range of possible outcomes from the underlying simulation-mode forecasts and hence the adjustment can lead to improved forecasts over the basic simulation-mode forecasts.

Implementation of adjustment schemes such as those outlined above should not be undertaken without careful consideration. The effect of such adjustments may be to reduce any high values of the simulation-mode forecasts, which may be undesirable. Automatic calibration of adjusted values will usually tend to concentrate on forecast-errors at individual time-points without recognising that there is at least some benefit from a forecast which gets the size of an event about correct even if there is a timing-error. There is some danger that, where a simulation-mode model is carefully calibrated by eye to account for such nebulous factors, this good work may be undone by calibration of an "improvement" to the simulation-mode forecast.

The "improvements" used as examples above are essentially based on adjusting a single time-point at a time. The possibilities are wider than this: for example, sharpening or attenuating filters might be applied in a time-series fashion. An additional important class of off-line forecast improvements is where an adjustment for a time-shift in the forecast is allowed, also known as phase-shifting. In this case an "improved" forecast might be formulated as:

$$\breve{Y}_t = a + b\widetilde{Y}_{t-\tau}, \tag{7.3}$$

where τ is an additional time-shift parameter (positive or negative) to be estimated by calibration.

7.4 Theoretical basis of updating methodologies

7.4.1 General

It is common to classify updating procedures into three types: error-prediction, state-correction and parameter-adjustment. In fact, all of these can potentially be treated within a single theoretical framework. In particular, error-prediction and parameter-adjustment can be reformulated so as to be included within the theoretical framework used for state-correction. Thus much the same discussion applies to all three approaches to forecast-updating. However, the three approaches have different underlying reasons for their use and different conceptual implications. "Parameter-adjustment" in the context of ongoing adjustments, rather than estimation starting from little information, is usually deprecated on the grounds that quantities which are model parameters should really be fixed values: if a forecasting approach appears to need "parameter-adjustment" then this indicates that the model-structure or model-conceptualisation are incorrect and should be improved. Error-prediction schemes are usually discussed separately from state-correction schemes because of the important special feature of error-prediction that it can be applied as an add-on to any model: state-correction must be applied as an intrinsic part, or revision, of the code for the model to which it is applied. Figures 7.3 and 7.4 illustrate the flow of information for error-prediction and state-correction methods and, in particular for the error-prediction scheme, the separation of the calculations into simulation-mode and error-prediction layers.
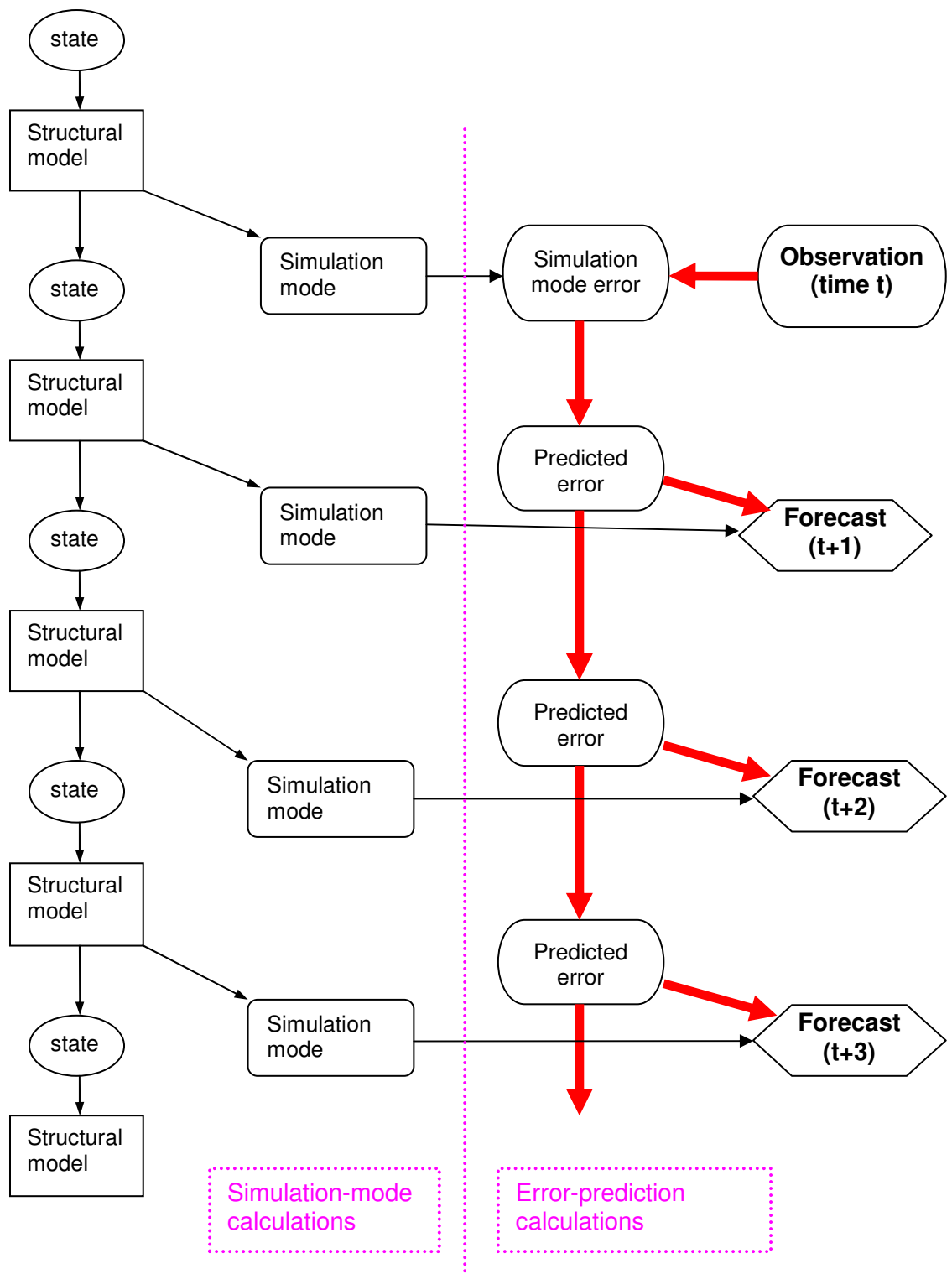
Figure 7.3 Error-prediction: flow of information from the last observation in creating a time-series of forecasts
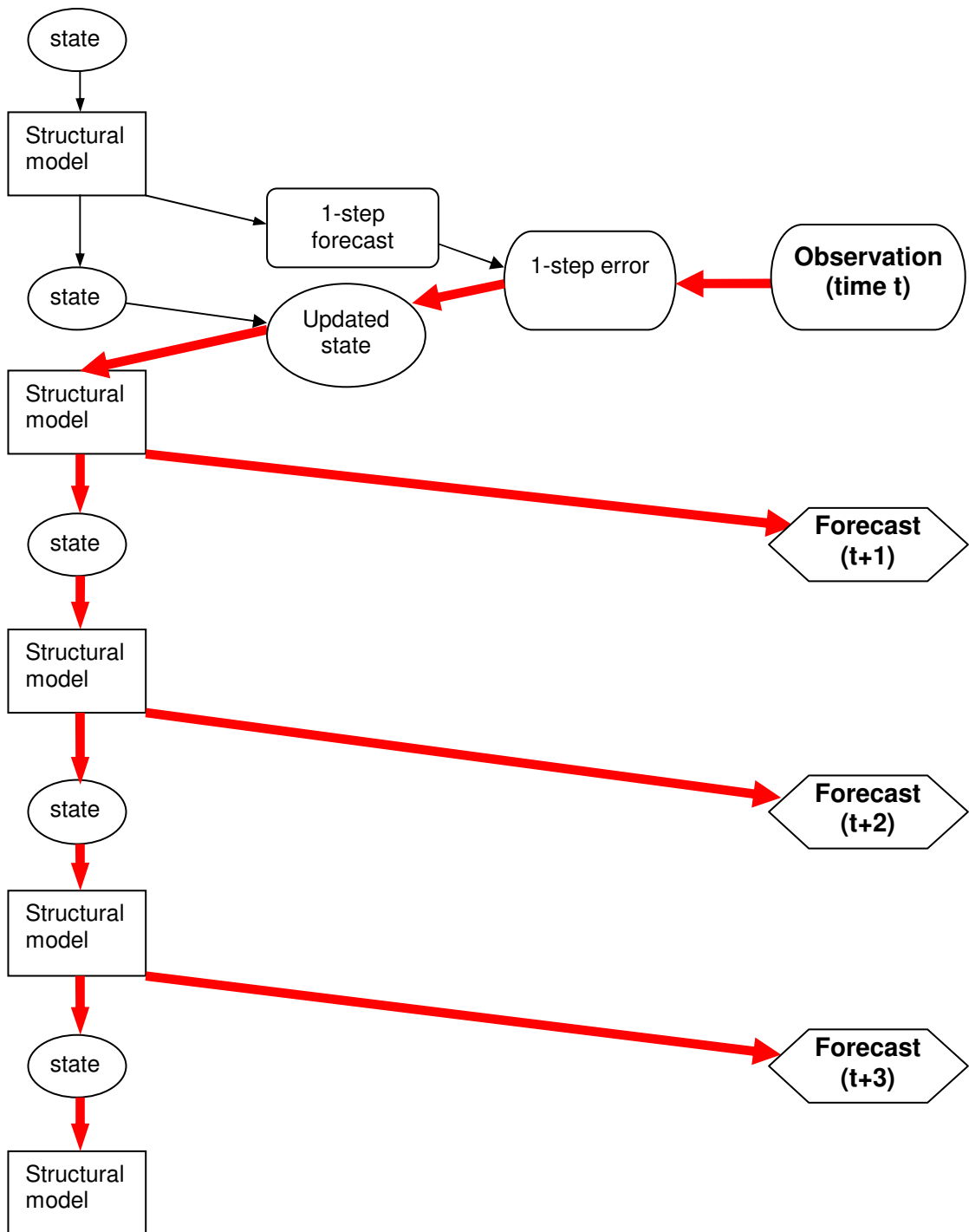
Figure 7.4 State-correction: flow of information from the last observation in creating a time-series of forecasts

The common feature of the updating methodologies that have been applied to real-time flow forecasting is that they are based on theories which say that a certain forecast-updating approach produces optimal forecasts if certain assumptions about statistical behaviour hold. In practice, it is known that the assumptions do not hold. However, the mathematical structure of the way that optimal updating is achieved when the assumptions hold is used as a guide to the way in which updated forecasts are calculated in practice when the assumptions do not hold. The updating procedures involve certain parameters which, if the theoretical assumptions could be assumed to hold, would be defined in terms of certain properties defined in the statistical description of the problem. When the underlying theory cannot be relied on to prescribe values for the updating parameters, their values are usually set in practice by a direct calibration procedure in which emulated updated forecasts are compared against the eventual outcomes. In this case much of the relevance of the underlying theory for the updating procedure is lost and the justification for the forecast-updating scheme becomes mainly that of having calibrated a moderately flexible scheme against observed data. However, the underlying theory for the updating procedure does play a significant role in having defined the way in which forecasts are updated. If improved forecasting procedures are to be devised it is likely that this will need to be done by re-evaluating and re-formulating the underlying theory to improve the realism of the assumptions made. Hopefully, this would improve the structure of the updating procedure in such a way that, when it is transferred into a real application where the improved assumptions don't hold, the forecasts resulting from applying the improved scheme after calibrating against real data will be better than those from the original scheme.

Not all applications of updating procedures are based on direct empirical calibration of the parameters of the procedure. In some instances the underlying theory is applied as if it was correct and "guessed" or "reasonable" values for the statistical properties defining the statistical model are supplied. In other cases, statistical techniques are used to fit the statistical model: this is a more onerous task than just fitting the parameters of the forecast-updating procedure derived from the statistical model. At the other extreme, when the updating procedure is particularly simple and when there are no data available for calibrating the updating procedure, it can be possible to set useable values of the updating parameters manually in order to achieve a reasonable behaviour for the updated forecasts. Here a subjective assessment would be made based on comparing the updated forecast with the non-updated forecast to ensure that the effect of an observed data-value lasts a reasonably long-time (which would depend on the context of the forecast) and is not particularly extreme: in particular, that the effect of including or excluding an observation from the dataset used for updating is reasonable.

For convenience, the description here uses a notation where it is assumed that both data-handling (availability of telemetry data for forecast-updating) and model calculations are done with the same time-step between data-points and the notation's time-unit is this basic time-step.

7.4.2 Updating using error-prediction

Error-prediction schemes are based on the following basic idea. An initial or "simulation-mode" set of modelled values $\{\tilde{Y}_t\}$ is available corresponding to quantities $\{Y_t\}$ for which forecasts are required. Observations of Y_t are available for a limited set of times (the past), while the simulation-mode values are available for all relevant times. A set of simulation-mode errors $\{\varepsilon_t\}$ are calculated for all times for which observations of Y_t are available. An example of an error-calculation is:

$$\varepsilon_t = Y_t - \tilde{Y}_t. \qquad (7.4)$$

Estimates of the errors likely to arise at times for which ε_t cannot be calculated are then formed: let these estimated (predicted) errors be denoted by $\{\hat{\varepsilon}_t\}$. Finally, the updated forecasts $\{\hat{Y}_t\}$ for times for which observations of Y_t are not available are defined by an equation corresponding to that used to define the simulation-model errors:

$$\hat{\varepsilon}_t = \hat{Y}_t - \tilde{Y}_t.$$

Thus, the updated forecasts are defined by

$$\hat{Y}_t = \tilde{Y}_t + \hat{\varepsilon}_t. \qquad (7.5)$$

A different example of an error-calculation is

$$\varepsilon_t = \log(Y_t / \tilde{Y}_t), \qquad (7.6)$$

for which the updating based on predicted errors is defined by

$$\hat{\varepsilon}_t = \log(\hat{Y}_t / \tilde{Y}_t), \qquad (7.7)$$

and hence the updated forecasts are defined by

$$\hat{Y}_t = \tilde{Y}_t \exp(\hat{\varepsilon}_t). \qquad (7.8)$$

The theoretical basis of this type of updating scheme relates to the way in which the predicted errors $\{\hat{\varepsilon}_t\}$ are constructed. The above outline has noted that there is some choice in the way that the error-calculation is defined (i.e. the definition of ε_t in terms of the observation and simulation-mode forecast). In practice such a choice should be influenced by the assumptions inherent in the underlying theoretical model for the updating approach since a closer validity for the assumptions should result in better updated forecasts.

The outline of the basis of the error-prediction scheme given above is very general, since any procedure for creating values for the predicted errors $\{\hat{\varepsilon}_t\}$ can be included. However, many practical instances of error-prediction schemes are based on using a simple linear structure for defining the predicted errors. Specifically, the calculation of

the predicted errors involves only linear combinations of the simulation-mode errors (at times when the observations of Y_t are available) and the predicted errors (at other times), and specifically does not involve the observations or simulation-mode forecasts other than via the simulation-mode errors. In principle, the usual schemes for error-prediction can be justified under two sets of rather different assumptions which are outlined below. The assumptions relate to the statistical properties of the simulation-mode errors, $\{\varepsilon_t\}$, and apply to the whole set of such errors including times at which these errors both have and have not been calculated.

Assumption Set A

The errors $\{\varepsilon_t\}$ are assumed to be a stationary, Gaussian, time-series which is statistically independent of the time-series of simulation-mode forecasts $\{\tilde{Y}_t\}$. Then one way of defining the best predictions of the as-yet unobserved errors in the series $\{\varepsilon_t\}$ is as the conditional mean of the unobserved values, conditioned on the observed data. Given the assumptions, this conditional mean does not depend on the simulation-mode forecasts and is a linear function of the observed values in the series $\{\varepsilon_t\}$. This linear combination is defined in terms of the mean and auto-covariance function of the time-series. If the predicted value used for the simulation-mode error is the conditional mean, this will ensure that the residual errors $\{a_t\}$, where

$$a_t = \varepsilon_t - \hat{\varepsilon}_t, \tag{7.9}$$

have the smallest possible mean square error. The implications of this for errors in the forecast depends on the particular type of error calculation being used. Thus, if an additive error formulation is being used, as in Equation (7.4), the final error can be defined as

$$e_t = Y_t - \hat{Y}_t = Y_t - (\tilde{Y}_t + \hat{\varepsilon}_t) = \varepsilon_t - \hat{\varepsilon}_t = a_t, \tag{7.10}$$

and hence the forecast of the observation has the minimum-mean-square-error property. If the logarithmic error calculation is being used, it is natural to use the same formulation for the final error:

$$\begin{aligned} e_t &= \log(Y_t / \hat{Y}_t) = \log\left(Y_t / \left\{\tilde{Y}_t \exp(\hat{\varepsilon}_t)\right\}\right) = \log(Y_t / \tilde{Y}_t) - \hat{\varepsilon}_t, \\ &= \varepsilon_t - \hat{\varepsilon}_t = a_t. \end{aligned} \tag{7.11}$$

Hence, in this case, the forecast again has the minimum-mean-square-error property, but the errors must be defined in the logarithmic sense. Under this set of assumptions, there is not strictly speaking a choice of whether or not to use arithmetic or logarithmic errors, or any other choice of definition of "error": the assumptions require that the simulation-mode errors $\{\varepsilon_t\}$ be formulated in such a way as to be statistically independent of the simulation-mode forecasts and this will be true for at most one formulation of "error".

Assumption Set B

> The errors $\{\varepsilon_t\}$ are assumed to be an ergodic time-series (i.e. there is an assumption that sample means, variances and covariances will converge to well defined values as sample size increases). The assumption is made that it is only necessary or only possible to consider predictions of the unobserved simulation-mode errors which are linear combinations of the observed simulation-mode errors (and not of the simulation- mode forecasts). Then, out of this class of predictors it is possible to determine the predictor which has the lowest mean-square-error. This predictor is determined by the mean and covariance properties of the simulation-mode errors. The "optimal" properties of the predictor are limited in the sense that the predictor is only optimal within a limited class of predictors, as determined by the assumption that this is all that will be considered. The relation of the prediction error of the forecasts of the observations to the prediction error of the simulation-mode errors is as outlined for Assumption Set A. However, in this case the choice of definition of "error" is open and the choice is usually made on pragmatic grounds.

Either set of assumptions places the problem within the context of "time series analysis" within statistical theory. This theory provides several different ways deriving the optimal forecasts. In practice it is most convenient to use the background of ARMA (AutoRegressive Moving Average) models: this provides set of tools that allow a structure for calculating the forecasts to be decided that is parameter-parsimonious without sacrificing accuracy of the forecasts. Typical applications of forecast-updating using error-prediction treat a single telemetry-site at a time, so that there is just a single time-series of observations and a single time-series of simulation-model errors. There is apparently no experience with error-prediction based on multiple series of telemetry observations, but the procedure is readily capable of implementation in this case, with the error-predictions being based on Multivariate ARMA models. This is an area of research that requires further work.

Real-time versions of off-line improvements

As already indicated, there is scope for extending the class of procedures usually counted as being "error-prediction" to include some where the series of simulation-mode forecasts is allowed to play a role other than via the simulation-mode errors. One possibility is to extend the class of predictors allowed to include linear-weighted functions of the simulation-mode forecasts. This approach would extend the class of predictors on the basis of a notional underlying model of the simulation-mode errors. An alternative approach to extending the class of error-predictors is provided by considering converting the type of off-line forecast improvement schemes discussed in Section 7.3 into real-time updating procedures. While it is easy enough to define calculation steps whereby the parameters of these off-line adjustments are estimated on the basis of a restricted time-period of the latest observations, it may still be necessary to extend the updating scheme to ensure that the observations and the "improved" simulation-mode forecasts blend together at the end of the observation period. The need for this would be similar to the justification of ordinary error-prediction as blending together the observations and the "unimproved" simulation-mode forecasts at the end of the observation period. The question of blending "improved" simulation-mode forecasts with observations may not have be researched previously, whereas real-time versions of off-line forecast improvements have been implemented as simple forecast-updating schemes.

It may be noted that an error prediction scheme deriving from the off-line improvements in Equations (7.1) and (7.2) would be linear in the unknown parameters (assuming d

is treated as known). Thus, these can be made to fit into the extended family of linear error-predictions. In contrast, the unknown time-shift parameter, τ, in Equation (7.3) introduces a particular type of nonlinear structure to the problem and hence extends the class of error-predictions to meet the requirements of certain applications where wandering time-shifts arise.

7.4.3 Updating using State-Correction

State-correction schemes are based on the following ideas. In the following, all quantities may be vectors. The underlying model or set of rules for calculating "simulation-mode" values is put into a "state-space" form: this involves the values, S_t, of the states of the model at a given time t, a function $g_t()$ representing both the structure of the model and the effects of any inputs driving the model, and a second function $h_t()$ representing how the observations relate to the model-states. The simulation-mode version of the model is then written in the form of two equations

$$S_t = g_t(S_{t-1}) \tag{7.12}$$
$$\tilde{Y}_t = h_t(S_t). \tag{7.13}$$

A state-corrected version of the model operates in a recursive fashion. Suppose that calculations have been done up to time $\tau - 1$, taking into account all observations Y_t available up to that time. The calculated states values available from the previous step are denoted by $S_{\tau-1|\tau-1}$, where the notation $X_{a|b}$ means the estimate of the value of X for the time a made using all observations for times up to and including time b. The first step is to calculate the one- step ahead forecast of the states, via an equation similar to

$$S_{\tau|\tau-1} = g_\tau(S_{\tau-1|\tau-1}), \tag{7.14}$$

and then to calculate the one-step-ahead forecast of the observation via an equation similar to

$$Y_{\tau|\tau-1} = h_\tau(S_{\tau|\tau-1}). \tag{7.15}$$

The phrase "via an equation similar to" has been included to cover some important variants of the approach: for the purposes of outlining the state-correction approach it is enough to understand the basic sequence of calculation steps, which consists of recursive application of calculation stages corresponding to: (i) pushing the model equation forward one step; (ii) derivation of one-step ahead forecasts of the observations, and (iii) correction of the model states to take account of errors in the one-step ahead forecast of the observation. This last stage is as follows. If an observation of Y is available for time τ, the one-step ahead error is calculated as

$$a_\tau = Y_\tau - Y_{\tau|\tau-1}, \tag{7.16}$$

and this is used to calculate the observation-adjusted value of the states as

$$S_{\tau|\tau} = S_{\tau|\tau-1} + k_\tau(a_\tau). \tag{7.17}$$

If no observation of Y is available for time τ, the observation-adjusted value of the states is given by

$$S_{\tau|\tau} = S_{\tau|\tau-1}, \qquad\qquad\qquad (7.18)$$

so that no adjustment is made. Here the function $k_\tau()$ is a "gain function" which controls the amount of adjustment made for a given size of forecast error. It is usual to concentrate on applications where the observations are known for all time-points up until a time T, and forecasts are requited for time-points after this. In this case, the recursive procedure is applied with state-correction up until time T, and then without error correction for later time-steps. The final set of forecasts $\{\hat{Y}_t\}$ for time after T is given by

$$\hat{Y}_t = Y_{t|t-1} = Y_{t|T} \qquad\qquad (t > T); \qquad\qquad (7.19)$$

that is, by the one-step ahead forecasts from the recursive procedure.

The intrinsic difference between error-prediction and state-correction schemes is that the latter are based on using the observation-adjusted (updated) set of states values in the recursive calculation in Equation (7.14), compared with the error-prediction approach which uses non-adjusted values of the states in Equation (7.12). However, it should be noted that, when state-correction is applied, the set of states may be an extended version of that used in the underlying simulation-mode model: this allows the overall model to represent modelling errors which are statistically dependent over time. Thus a comparison of error-prediction and state-correction schemes is not entirely straightforward.

The above outline description of state-correction has concentrated on calculation-stages which immediately relate to the construction of the forecast values in a structural sense, so that the difference between error-prediction and state-correction becomes more apparent. The underlying theory which justifies state-correction approaches is usually framed in such a way that it includes quantities representing how well the values of the states are known and the likely error in the one-step ahead forecasts of states and observations. In this case the "gain function", $k_\tau()$, is determined by calculations relating to these.

Filtering

A discussion of state-correction for use in the ungauged case is incomplete without mentioning the concept of filtering: forecasts for an ungauged location should strictly be based on the results from a filtering step with the state-correction scheme. The full scheme consists of 3 steps:

(i) forward state correction: recursively calculate $S_{\tau|\tau}$ for increasing τ up to the last observation time *t*;

(ii) forecasting step: recursively calculate $S_{\tau|t}$ for increasing τ up to the last forecast time-point required;

(iii) filtering step; recursively calculate $S_{\tau|t}$ for decreasing τ, back to the first forecast time-point required.

The forecasts for an ungauged location would then be based on $\{S_{\tau|t}\}$, where t is fixed as the time-point of the last observation available and where values are required for τ both before and after t. The relevance of filtering to hydrological modelling can be illustrated by considering the case of an ungauged location upstream of a gauged location and treated within the same model. In such a case there would naturally be a time-delay before any changes of flow noticed at the upstream site reach the downstream site. This delay would be represented within the state-evolution equation of a model represented in state-space form. Once a change has reached the downstream site, the observation there allows a corresponding inference to be made about the flow at the upstream site at an earlier time. The filtering operation allows this transfer of information back in time to made. In the context of flood-forecasting, this back-transfer of forecast-information may be entirely irrelevant, since the event has already happened. The combination of the forward state-correction steps with the forecasting step allows "optimal" estimates for ungauged locations to be calculated for the current time *t* and for all future times. However, applying the filtering step should allow the estimates of the time-series of values at the ungauged location to give a better representation of behaviour than could be achieved using the just the corrected states $S_{\tau|\tau}$ for times τ before the current time t. This may be important if there is a need to assess how long a flow or level threshold had been exceeded.

The simplest types of state-correction methods are based on a model formulation similar to Equations (7.12) and (7.13). The equations consist of a state-evolution equation, describing how the model states S_t change with time,

$$S_t = g_t(S_{t-1}) + u_t,\qquad(7.20)$$

and an "observation equation" describing how the observations Y_t relate to the model states,

$$Y_t = h_t(S_t) + v_t.\qquad(7.21)$$

Here u_t and v_t are random variables (or random vectors) representing model-error and observation-error respectively. More general types of state-correction procedures can be based on a continuous-time representation of the evolution of the model-states: here the state-correction formulation starts from a set of differential equations for the states, for example,

$$\dot{S}(t) = G_t(S(t)),\qquad(7.22)$$

and then represents the actual evolution, accounting for model-error, in the form of a stochastic differential equation

$$\dot{S}(t) = G_t(S(t)) + U(t).\qquad(7.23)$$

For simplicity these types of formulation will not be discussed further here.

Assumption Set A

> The random variables u_t and v_t are assumed to be Gaussian, independent over time and mutually independent: however elements within either or both of these vectors are allowed to be dependent. They are also assumed to be

independent of the model-states for time $t-1$. It is assumed that the means of the error vectors are zero and that the covariance matrices of u_t and v_t are known (but these covariances may vary with time). Then, in the case that the functions $g_t()$ and $h_t()$ in Equation (7.20) and (7.21) are linear functions, theory can be developed to provide the optimal (minimum mean square error) estimates of both the states and future observations. The equations for this are identical to those obtained if Assumption Set B is used: under Assumption Set A, the estimates are optimal among a much larger class of possible estimates. If the functions $g_t()$ and $h_t()$ are non-linear, theoretical expressions for how to proceed can be obtained, but these are usually of little immediate use. However, several procedures based on approximations are available.

Assumption Set B

The random variables u_t and v_t are assumed to be uncorrelated over time and mutually uncorrelated: however elements within either or both of these vectors are allowed to be correlated. They are also assumed to be uncorrelated with the model-states for time $t-1$. As for Assumption Set A, it is assumed that the means of the error vectors are zero and that the covariance matrices of u_t and v_t are known (but these covariances may vary with time). Then, in the case that the functions $g_t()$ and $h_t()$ in Equation (7.20) and (7.21) are linear functions, it is possible to find the best linear combinations of the observations and the previously-calculated estimates of states to provide the best (minimum mean square error) estimates of both the states and future observations.

In the standard theory-based approaches to state-correction, either set of assumptions lead to the same set of recursive equations (for increasing t) which is the usual form for practical calculations. This set of equations include expressions for the covariance matrices of the model-states and these are important in that these covariances are used in the calculation of the gain. All of these expression assume that the covariance matrices of u_t and v_t are known, and these matrices are used in the calculations. In practice these covariance matrices need to be estimated. Often a simple structure is imposed on the covariance matrices so as to reduce the number of parameters that need to be estimated or guessed. An important feature of both sets of assumptions is the need for u_t to be uncorrelated over time. This will usually be difficult to justify if the state-evolution equations are derived directly from an underlying hydrological or hydrodynamic model, since it is likely that modelling-errors will tend to be similar at adjacent times, at least if conditions are changing rapidly. This problem can be overcome by revising the formulation of the model so as to include new elements in the state vector whose role is to represent the actual modelling error: the state-evolution equations for these elements then allow the model to represent a simple type of statistical dependence over time, with the formal "model-error" now representing changes to actual modelling error. Clearly the effect of such revisions is to increase the overall number of states in the state-vector and it would usually also increase the number of unknown parameters that have to be estimated or guessed.

A non-standard approach to state-correction, known as "empirical state-correction" avoids some of the problems with providing and justifying particular covariance matrices of u_t and v_t It does this by noting that according to the standard theory, if the model doesn't contain any time-varying elements, if there are no missing observations before the latest observation, if a linearised model is used and if the calculations have

warmed-up sufficiently, the state-correction step is of the form

$$S_{\tau|\tau} = S_{\tau|\tau-1} + Ka_\tau .$$ (7.24)

Here K is a matrix that, in the standard approach would be calculated from the covariance matrices. The non-standard approach of "empirical state-correction" is to treat K as a parameter-matrix to be calibrated, and to not bother to determine values for the covariance matrices. The calibration is typically done by optimising the one-step ahead forecast error over a calibration-period. Notionally, the empirical state-correction approach requires fewer parameters to be defined and hence is simpler to apply. However this non-standard approach looses two of the important features available from the standard approach: (i) the variation of the gain in relation to the amount of information from recent observations (some of which may be missing); (ii) the quantification within the model of the uncertainty of the forecasts for any lead-time. Unfortunately, the possible extension of "empirical state-correction" to deal with the filtering step has not been investigated.

7.4.4 Choice between Error-Prediction and State-Correction

Section 7.4.1 mentioned the special distinction between error-prediction and state-correction: that the former can be applied as an add-on to any model (Figure 7.3) while the latter must be applied as an intrinsic part, or revision, of the code for the model to which it is applied. Thus lack of access to underlying model code may be one reason for choosing error-prediction. In addition, error-predictions has an intrinsic relative attraction related to the method's apparent simplicity. It has already been noted that, if the underlying simulation-mode form of a model were linear, then state-correction and linear error-prediction schemes could theoretically be formulated so as to give identical results for updated forecasts. It seems reasonable to believe that, where the underlying simulation-mode is non-linear, state-correction should produce better results than external error-prediction. The reason for this belief would be that state-correction allows the values of the model-states to be kept close to the "true" states-values and that applying the model's non-linear structure to more accurate states-values will produce better forecasts (Figure 7.4). Unfortunately, when applied to typical hydrological or hydrodynamic models, the number of locations having telemetered observations is very sparse compared to the overall number of model-states and thus one might think that there will be many states-values for which no benefit will be obtained from the observed values. One can also argue that, if either the underlying model structure, or the statistical extension to represent modelling errors, is wrong there is some danger that applying state-correction may actually produce worse results than if corrections were not applied at all. However, this danger is at least partly mitigated if the parameters controlling a state-correction scheme are calibrated on representative data from the actual application. There is need for further experience from case-studies comparing the performance of updated forecasts derived from the two basic approaches to forecast-updating.

The error-prediction and state-correction methodologies also differ regarding the ease with which it is possible to assess and deal with the importance of statistical dependence, over time, of the error-quantities on which forecast-updating is based. In the case of error-prediction, the relevant errors are immediately available and a direct statistical analysis can be applied to decide on a structure for the stochastic model representing the simulation-mode errors. Part of this analysis can readily assess the amount of benefit gained by moving from a simpler to a more complicated model for the errors. In contrast, the structure of a stochastic model for state-correction will involve error-quantities which are not directly observable: this makes it difficult to

decide on how to represent serial dependence in the modelling-errors. There seems to be no simple guidance as to how complicated the part of the model-structure representing stochastic errors needs to be. This leaves the question of model-structure to be decided by fully implementing and calibrating a number of competing structures and then comparing the results on validation data.

In terms of potential usefulness, state-correction methods share the same problems as the underlying models without updating, or with other types of updating. Specifically:

(i) It is unlikely that good forecasts of river level can be obtained unless either the forecasts are required for a location having an established rating or where the underlying model has at least some representation of hydrodynamic or backwater effects (so that river-levels are represented internally to the model in a realistic manner). Thus hydrodynamic models are a prime candidate for applying state-correction procedures for forecasting river-levels at ungauged locations. It may be that distributed hydrological models will eventually be developed so that the representation of river-channels includes sufficient hydrodynamic realism to provide at least indicative modelling of river-levels on widespread sets of minor channels that would not sensibly be modelled using a full hydrodynamic model. Then some type of state-correction might be attempted.

(ii) When the target quantity for an ungauged location is a river-flow, then updating may be successful where a hydrological model is being used and where good estimates of river flow are available at another location represented within the same model, usually via an established rating and based originally on telemetered river-levels. Thus rainfall-runoff models would generally be excluded. Updating for ungauged river-flows is potentially achievable for indirect modelling using hydrological routing models or hydrological routing within a distributed catchment model. In addition, updating for ungauged river-flows would be expected to work for hydrodynamic models, but there seems little point in this since the model would also produce updated forecasts of river-level which would usually be of more direct interest.

7.5 Potential updating methodologies for ungauged locations

7.5.1 General

Section 7.2 has outlined some of the issues with forecasting for ungauged locations, with the conclusion that it might well be possible to improve model-forecasts for an ungauged location by making use of telemetry at nearby locations as the basis of the forecast-updating procedure. However, except in the case of indirect modelling using a physically-consistent model, there is little reason to expect such updated forecasts to work well, partly because there have been no case-studies based on real data to assess the behaviour of this type of methodology.

Section 7.4 has outlined the theoretical bases of error-prediction and state-correction methodologies. The practical implementation of such schemes, even for gauged locations has up to now, not fully explored all the possibilities. In particular, the assumptions within the theoretical bases of the schemes may not hold and hence modified schemes may work better, or there may be practical concerns with computational resources that mean that it would be worthwhile considering sub-optimal

schemes provided that the loss of performance is not too great. These considerations apply to forecasting for gauged locations, but the ideas may well carry over to forecasting for ungauged locations.

The following subsections outline some possible approaches to forecast updating, with the emphasis on cases where there are no real-time observations for the target locations. Some of these approaches rely on there having been observations for the target location available for use when calibrating the updating scheme.

7.5.2 Error Prediction Methods

Error prediction with no nearby telemetry

The discussion of error-prediction schemes in Section 7.4.2 emphasised that the usual formulation of such schemes is based on an assumption that, once the simulation-mode errors are available, the simulation-mode forecasts from the underlying model are of no use when creating predictions of future simulation-mode errors. There is no particular reason why this assumption should be true. Certain combinations of model-structure with the objective function used for fitting the simulation-mode model, and with the objective function used for assessing the updated forecasts, would in fact lead to this assumption being true: however such cases do not arise in practice except for certain types of transfer-function model. The possibility of basing predictions of the simulation-mode error on the simulation-mode forecast means that it is possible to conceive of forecast-adjustment schemes that do not rely on using any real-time telemetry information.

Such adjusted forecasts are probably best discussed in a more direct way than as error-prediction schemes, in particular as off-line forecast-improvement schemes (Section 7.3). An example of a simple scheme is

$$\breve{Y}_t = a + b\widetilde{Y}_t. \tag{7.25}$$

This can be considered as an error-prediction scheme: for example, if the additive error definition of Equation (7.4) is being used, Equation (7.5) shows that the corresponding error-prediction would be

$$\hat{\varepsilon}_t = \breve{Y}_t - \widetilde{Y}_t. \tag{7.26}$$

In the case of forecast-updating for gauged locations, it would be possible to consider extending the usual error-prediction scheme so as to include the simulation-mode forecasts in the set of quantities available for use within the linear-weighting scheme for constructing the prediction of the simulation-mode error. An alternative is to use the initial set of simulation-mode forecasts to create a second set (the "improved" values) and to apply existing error-prediction methods to this set of simulation-mode forecasts.

Error prediction based on nearby telemetry

In cases where telemetered data are available from locations which are nearby and relevant to a target location which has no telemetry, but for which data for calibration purposes is available, an error-prediction approach is possible. Two basic approaches can be outlined. In the first, the approach is almost entirely empirical: the predicted error at the target site for a given lead-time ℓ from a time-origin t, denoted by $\hat{\varepsilon}_{t+\ell}^{(1)}$, is

defined to be calculated from the observed simulation-mode prediction errors, $\varepsilon_s^{(k)}$, at other sites indexed by the superscript k, by an equation of the form

$$\hat{\varepsilon}_{t+\ell}^{(1)} = \sum_{k=2}^{K} \left\{ a_0^{(k,\ell)} \varepsilon_t^{(k)} + a_1^{(k,\ell)} \varepsilon_{t-1}^{(k)} + \ldots \right\}. \tag{7.27}$$

Since observed values for the target location are always missing, it would usually be necessary to apply this equation with both positive and negative values of ℓ, and the outcome of the forecast-construction would be corrected values of the simulation-mode forecasts for the target site for times both before and after the "forecast-origin" which notionally relates to the gauged locations. In Equation (7.27), $\{a_j^{(k,\ell)}\}$ are sets of parameters to be estimated by calibration using historical data. In practice it would probably be necessary to prescribe $\{a_j^{(k,\ell)}\}$ via a family of parameterised functions in order to ensure that the behaviour of the forecasts $\hat{\varepsilon}_{t+\ell}^{(1)}$ is reasonable as the lead-time ℓ increases. The second general approach would be to fit a time-series model, such as a multivariate ARMA model to the collection of time-series $\{\varepsilon_t^{(k)}; k = 1, 2, \ldots\}$. While the theory of such time-series models is usually developed and applied for cases where observed values of all time-series are available up to some common forecast time-origin (and are all missing thereafter), the underlying theory can be developed and applied to more general patterns of missing values, including those where one time-series is always missing. Note that the theory here would typically lead to predictions of the simulation-mode forecast-errors for the target site which are linear combinations of the observed simulation-mode errors at the gauged locations, just as in Equation (7.27). In this approach, the time-series model provides an indirect way of specifying the coefficients $\{a_j^{(k,\ell)}\}$.

The following general points may be made:

(i) The approach is entirely general in that the various series of simulation-mode errors can be calculated from separate models for each location, or some of them can be from the same model, and the simulation models can even be of entirely different types. Further, the series of errors can, in principle, relate to different quantities and hence errors in modelling flow and level could be mixed.

(ii) The approach relies on there being a reasonable spatial coherence in the behaviour of the modelling errors at different locations, in order for it to be worthwhile attempting to transfer information between locations. It is unfortunate that there seems to be no relevant experience to suggest whether this is ever true, or in what circumstances the approach is worth considering.

(iii) The multivariate time-series approach extends the set of methods used in practice for error-prediction, which have typically dealt with error series singly. Thus the approach has the potential for improving on presently implemented forecast-updating schemes for gauged locations.

Inferred-error error-prediction

The discussion above applies to cases where a location which has no telemetry does have a historical record of (non-telemetered) data. If there are no data for calibration, such methods cannot be applied directly. If experience with the methods outlined under the heading "Error prediction based on nearby telemetry" is built up sufficiently, it is just

possible, but unlikely, that moderately complicated rules (similar to Equation (7.27)) for calculating predictions of simulation-mode errors will be justifiable for locations that do not have calibration data. It is more likely that simpler versions of the structure will be applicable: specifically ones involving relatively few parameters, which might be more meaningfully transferred from other case-studies, or guessed.

Where there are no data for calibration, it seems necessary to restrict possible applications of error-prediction to cases where gauged and ungauged locations have data of the same type (either river-flow or river-level) and where they are treated by essentially the same type of model, using similar sources of data to drive the models. If these restrictions apply it may then seem reasonable to assume that simulation-mode errors at the ungauged location will be similar to those at the gauged location, possibly shifted in time (for example where locations are on the same river). It may also be possible to construct scaling factors to relate errors at the different locations, possibly based on catchment areas and SAARs. Taking into account an overriding need for simplicity, the following is an outline of how inferred values of the simulation-mode errors at a target location might be constructed.

(i) For each gauged location (indexed by $k = 2, \ldots, K$), construct a "complete" set of values for estimated simulation-mode errors, $\left\{ \hat{\varepsilon}_t^{(k)} \right\}$, based on the model and observations for the given location. Specifically, $\left\{ \hat{\varepsilon}_t^{(k)} \right\}$ will include both observations of simulation-mode errors and estimated values using some error-prediction scheme.

(ii) Define an initial estimate of the errors for the ungauged location as

$$\tilde{\varepsilon}_t^{(1)} = (K-1)^{-1} \sum_{k=2}^{K} \beta_k \hat{\varepsilon}_{t-\tau_k}^{(k)}$$

(7.28)

where β_k are known (guessed) values of scaling factors and τ_k are known (guessed) values of relative timings.

(iii) Possibly apply a moving-average filter, or other smoother, to avoid transferring isolated errors which are unlikely to appear at another site. For example

$$\breve{\varepsilon}_t^{(1)} = (2L+1)^{-1} \sum_{\ell=-L}^{L} \tilde{\varepsilon}_{t+\ell}^{(1)} .$$

(7.29)

(iv) Define the final estimate by applying a downscaling factor, γ, whose value is guessed so as to be conservative in applying the correction:

$$\hat{\varepsilon}_t^{(1)} = \gamma \breve{\varepsilon}_t^{(1)} .$$

(7.30)

This is a case where the decision to apply a certain forecast-updating methodology might be affected by the use to which the forecast is being put. Specifically, it may be best to avoid using forecasts based on non-calibrated and unchecked adjustment procedures where the forecasts are used directly for making decisions about flood-warning *etc.*, where the forecast quantities would usually be river-levels. There may be a need for less caution where the forecasts are used as input quantities to other models, where the forecast-quantities are usually river-flows and where testing of the forecasts from the subsequent model can be used as a check on the adjustment procedure.

Hydrodynamic models may provide a particular class of models where inferred-error error-prediction for ungauged sites should be given special attention. Section 3.6 has already mentioned the possibilities of interpolating modelled levels externally to the model to provide values at ungauged locations and a similar approach to interpolating simulation-mode errors can readily be set down. For hydrodynamic models in particular, it seems reasonable to suppose that modelling errors will behave smoothly along river reaches, and thus that spatial interpolation of errors will perform well: however some allowance for temporal lags may be necessary. Further, implementations of hydrodynamic models where there are large numbers of gauged observations provide a good way of testing out forecast-updating strategies for ungauged locations by treating selected gauged locations as if they were ungauged. Note that multiple runs of the hydrodynamic model are not needed for testing such error-prediction schemes. Experience with model-configurations for which extensive calibration data are available is required as a basis for deciding when interpolation schemes are worthwhile. For example, there are questions as to whether error-interpolation will succeed across particular types of river structures, such as weirs, or across major tributary junctions.

7.5.3 State-correction methods

State-correction using Kalman filtering

Section 7.4.3 has outlined the basis of state-correction approaches to forecast-updating and has indicated the core sets of assumptions behind the basic approach which can be thought of as being Kalman Filtering in the standard terminology. Section 7.4.4 has mentioned some of the difficulties with the implementation of this type of scheme and with extended schemes. The present subsection considers the potential of the approach for flood forecasting. Some of this notional potential is limited in practice by the difficulties already mentioned and by other computational considerations. Later subsections outline some other varieties of state-correction which may overcome some of these problems but which do not formally derive from the theory of Kalman Filtering.

The major difficulties with state-correction schemes based on Kalman Filtering for flood forecasting are:

(i) nonlinearity of the model-structures;
(ii) potential statistical dependence of the modelling errors and the question as to how this should be treated;
(iii) complexity of computer code and computational resources required;
(iv) difficulty of estimating parameters of the updating procedure.

Statistical dependence of the modelling errors can potentially be dealt with by extending the number of states, with the extra elements in the states-vector representing values of the modelling errors. The state-transition function for these elements and the new modelling errors would then model a one-step Markov statistical model for the modelling errors of the original model. There are potential problems with this approach as the number of states can become rather large, possibly with no real gain in forecast performance. For example, a hydrodynamic model representing 300 model nodes would require about 600 states in its basic form (flow and level at each node). A direct modification of such a model to deal with one-step dependence would then need 1200 states and a higher-order dependence proportionately more. Some of this increase might be overcome by adopting a different approach, for example where modelling errors are dealt with explicitly at only a few river-locations and with other modelling-nodes being dealt with by interpolation.

The Kalman Filtering approach does provide one important advantage over other types of state-correction, assuming that the basic assumptions do hold. This advantage is that the theory provides for a self-consistent way of dealing with the question of filtering/smoothing. Here the final updated forecast for any unobserved data-value is based on all available observations, not just those available before or at the notional time of the data-value. This question has already been mentioned in Section 7.4.3. The point is important for updating for ungauged locations in ensuring that the trajectory of any forecast behaves smoothly. Calculations within the smoothing step implicitly take account of any time-delay within the model structure so that "future" values at the gauged location can be used to correct modelled values at an upstream ungauged location.

The "empirical state-correction" type of methodology, already mentioned in Section 7.4.3, is partly an attempt to overcome the difficulties outlined above, except that it does not attack the problem of statistical dependence in the modelling-errors. When the methodology is applied directly to an underlying model with calibration on historical data, it should yield something close to the optimal correction of the form given by Equation (7.24) if there is no serial dependence in the modelling errors, without relying on other statistical modelling assumptions: specifically, it is not necessary to specify covariance matrices for modelling and observational errors. There is again scope to extend the set of model states to take some account of serial dependence in the modelling errors. Discussion under the headings "Extended state-correction" and "Two-pass state-correction" below outline some other ways of modifying an empirical state-correction approach to take advantage of statistical dependence without too much extra computational complication.

Extended state-correction

Extended state-correction is a method that is based on the idea that, if there is reasonably strong statistical dependence in the modelling errors, then once the end of a time-series of observed values is reached the state-correction should continue to be made with corrections based on those corresponding to the last observation, but decreasing in time at a reasonable rate. This gives state-corrections of the form

$$S_{\tau|\tau} = S_{\tau|\tau-1} + Ka_{\tau|t},$$
(7.31)

where t is the last observation time, and the extended series of one-step ahead errors is given by

$$a_{\tau|t} = \beta a_{\tau-1|t}, \quad a_{t|t} = a_t.$$
(7.32)

The hope here would be to improve the performance of the multi-step-ahead forecasts based on observations up to time t, without the need to complicate the model-structure too much by explicitly modelling dependence.

Two-pass state-correction

It is conventional when dealing with state-space models to deal with state-correction using equations written in a particular way and making use of a formulation based on one-step ahead errors. This is convenient both mathematically and computationally. Where there are doubts about the basic assumptions behind the usual state-space forecast-updating schemes it may be worthwhile looking at other formulations that might achieve the objective of providing good forecasts. This might be justifiable on the grounds of avoiding restructuring a state-space model by adding additional states with no guarantee of improved forecasts. This subsection discusses a particular formulation of state-correction that is, in a sense, intermediate between error-prediction and more usual state-correction schemes. It may be appropriate if an ordinary state-correction scheme would be faced with dealing with serial-dependence of modelling errors. In addition, its formulation may be attractive in the situation where observations at gauged locations provide information which is time-delayed with respect to an ungauged target location: thus the extended calculations discussed under "filtering" in Section 7.4.3 might be avoided. A further feature of the approach is that it includes some aspects of continuing with the correction of model-states after the time of the last observation, as discussed previously under the heading "Extended state-correction".

This scheme can conveniently be described in terms of a two-pass set of calculations, although the idea can clearly be extended to multi-pass schemes: it is illustrated in Figure 7.5. In the first pass of the scheme the state-space model is run without state-correction to form the time-series of simulation-mode forecasts. For clarity the sets of states during this pass are indicated with a superscript of "(1)". Thus the calculations are formally a set of iterations over the equations:

$$S^{(1)}_{\tau|\tau-1} = g_\tau(S^{(1)}_{\tau-1|\tau-1}),\qquad(7.33)$$

$$S^{(1)}_{\tau|\tau} = S^{(1)}_{\tau|\tau-1}.\qquad(7.34)$$

$$\widehat{Y}^{(1)}_\tau = h_\tau(S^{(1)}_{\tau|\tau}),\qquad(7.35)$$

$$\widehat{Y}^{(1)}_\tau = h_\tau(S^{(1)}_{\tau|\tau}),\qquad(7.35)$$

(Note that the formulation used here is different from the ordinary state-correction formulation in that the estimate, $\widehat{Y}^{(1)}_\tau$, of the observation is based on the "corrected" state value $S^{(1)}_{\tau|\tau}$: there is no difference in the first pass but it is important for the second pass.) This then allows a set of estimated first-pass simulation-model errors to be formed. Thus there would be a time-series $\left\{\hat{\varepsilon}^{(1)}_t\right\}$ constructed using error-prediction techniques from the observed first-pass simulation-model errors $\left\{\varepsilon^{(1)}_t\right\}$ for which values are available for any time-point having an observation:

$$\varepsilon^{(1)}_t = Y_t - \widehat{Y}^{(1)}_t.\qquad(7.36)$$

Note specially that the series $\left\{\hat{\varepsilon}^{(1)}_t\right\}$ would be constructed for all time-points, with infilled values for missing observations in the past and predicted values for the future. The

Figure 7.5 Two-pass state-correction: the flow of information from the last observation. With this approach observations, and errors derived from these, can affect earlier times in the second pass of the calculations.

second pass includes state-correction based on the first pass estimated simulation-mode errors: it consists of a set of iterations over the equations:

$$S^{(2)}_{\tau|\tau-1} = g_\tau(S^{(2)}_{\tau-1|\tau-1}) \,, \tag{7.37}$$

$$S^{(2)}_{\tau|\tau} = S^{(2)}_{\tau|\tau-1} + \sum_k L_k \hat{\varepsilon}^{(1)}_{\tau+k} \,, \tag{7.38}$$

$$\widehat{Y}^{(2)}_\tau = h_\tau(S^{(2)}_{\tau|\tau}) \,. \tag{7.39}$$

Here the matrices L_k provide for weighting the estimated simulation-mode errors across a range of times with respect to the time of the calculation step: the estimated simulation-mode errors may be both before and after the time of the calculation step.

The intention would be to calibrate values for the matrices L_k based on matching the second-pass model values $\{\widehat{Y}^{(2)}_\tau\}$ to the set of observations $\{Y_\tau\}$. Careful choice of the structure of these matrices would be needed to avoid calibrating too many parameters and to ensure that time-delays were appropriate. The second-pass model values $\{\widehat{Y}^{(2)}_\tau\}$ might be treated as the final set of forecasts for the gauged locations, although an additional error-prediction step might be made. Forecasts for the ungauged locations would be derived from the corrected states $\{S^{(2)}_{\tau|\tau}\}$.

State-correction by input-selection

For certain types of model, particularly lumped and distributed rainfall-runoff models, it is arguable that the effect of errors in values of the quantities driving the model far outweigh the effects of structural modelling errors. In this case "errors" in the states values can be thought of as deriving directly from errors in these inputs. In certain types of forecasting system, errors in the inputs (often attributed the term "uncertainty") are dealt with by supplying the model with alternative sets of time-series for these inputs. In this situation a special type of state-correction procedure can be formulated, based on the idea of selecting the set(s) of inputs which gives the best match of its model-forecasts to the observations, and using the forecasts from these inputs as the final forecasts.

A generalisation of the scheme outlined briefly above would be to construct a set of weights for the various sets of inputs to reflect how well the model forecasts agree with the observations and to form a weighted average of the forecasts as the final forecast. The idea of "state-correction" plays an explicit role at the step in the overall forecasting scheme where a set (or sets) of states are saved from one forecast run to be used in the next run. Here the selection would naturally be made on the basis of the observations to ensure that "good" states are carried forward.

In addition to rainfall-inputs for rainfall-runoff models, there seems scope for applying input-selection methods to hydrological and hydrodynamic routing models in cases where there are relatively and slowly varying ungauged inflows.

There are doubts about the practicality of input-selection schemes. It seems plausible that they can only really be expected to perform properly if the errors in the inputs are relatively slowly changing over time, since this means that a relatively large number of observations can be used to help identify the "right" input series. In this case, the input-selection scheme may need to be implemented in combination with other forecast-

correction schemes in order to achieve good forecasts where other types of modelling error are changing more rapidly.

In an overall forecasting system where multiple sets of model-inputs are used to represent "uncertainty", the basic strategy of the design of the system may require that multiple sets of model-outputs (forecasts) should be generated for each model, with the variation between the sets of outputs again representing "uncertainty". This raises additional difficulties in relation to providing the means to ensure that such variation does reflect the actual uncertainty of the forecasts.

State-correction by model-subdivision

Model-subdivision is included here as relating to state-correction only for completeness. Consider a situation where a gauged location is on a river-reach modelled by a flow routing model or by a hydrodynamic model. If the location is such that the model can be split into two parts, upstream and downstream of the gauged location, many forecast systems are configured to do so. This would typically be undertaken only where there is no possibility of backwater effects resulting in conditions upstream of the gauged location being affected by conditions downstream.

In a situation such as that above, observations at the gauged location would typically be used to create a time-series of inputs to the downstream model consisting of observations, up to the current time, and forecasts into the future (derived from the upstream model). If this is compared to the alternative of treating the two models simultaneously, it is seen that subdividing this model in the above way has the effect of implementing a simple type of state-correction within the "downstream" part of the combined model (Figure 7.6).

A possible disadvantage of model-subdivision, when implemented in some forecasting systems, is that that the possibility of transferring forecast-updating information upstream may be overlooked. In practice, reaches that might be treated by hydrological flow routing have been subdivided at locations where telemetry already existed or where installation of telemetry was imminent. In normal operation, the time-delay resulting from the time-of-travel between sites would mean that nothing would be gained by attempting to transfer forecast-updating information to a gauged target location from a downstream site. However, if telemetry at a target location did go out of operation, the configuration of the forecasting system using model-subdivision may not allow such a transfer to occur when it would be beneficial.

Combined-model state-correction

Consideration of "state-correction by model-subdivision" has illustrated the potential advantage of subdividing a flow routing model at a location where telemetry is or will be available. In the case of an ungauged location, there is a potential advantage in combining together models upstream and downstream of an ungauged location. Errors in modelling values at the next location downstream of an ungauged target location arise partly due to errors in modelling at the target location. There is thus scope for using the observed errors at the downstream location to adjust modelled values at the target location. If the upstream and downstream models were combined into a single modelling unit there would be the possibility of applying state-correction methods to this new unit. If the models are not combined, some form of inferred-error updating method might still be applied for the target location. In most cases, such an inferred-error updating method would have the disadvantage of not having calibration data available for determining the parameters of
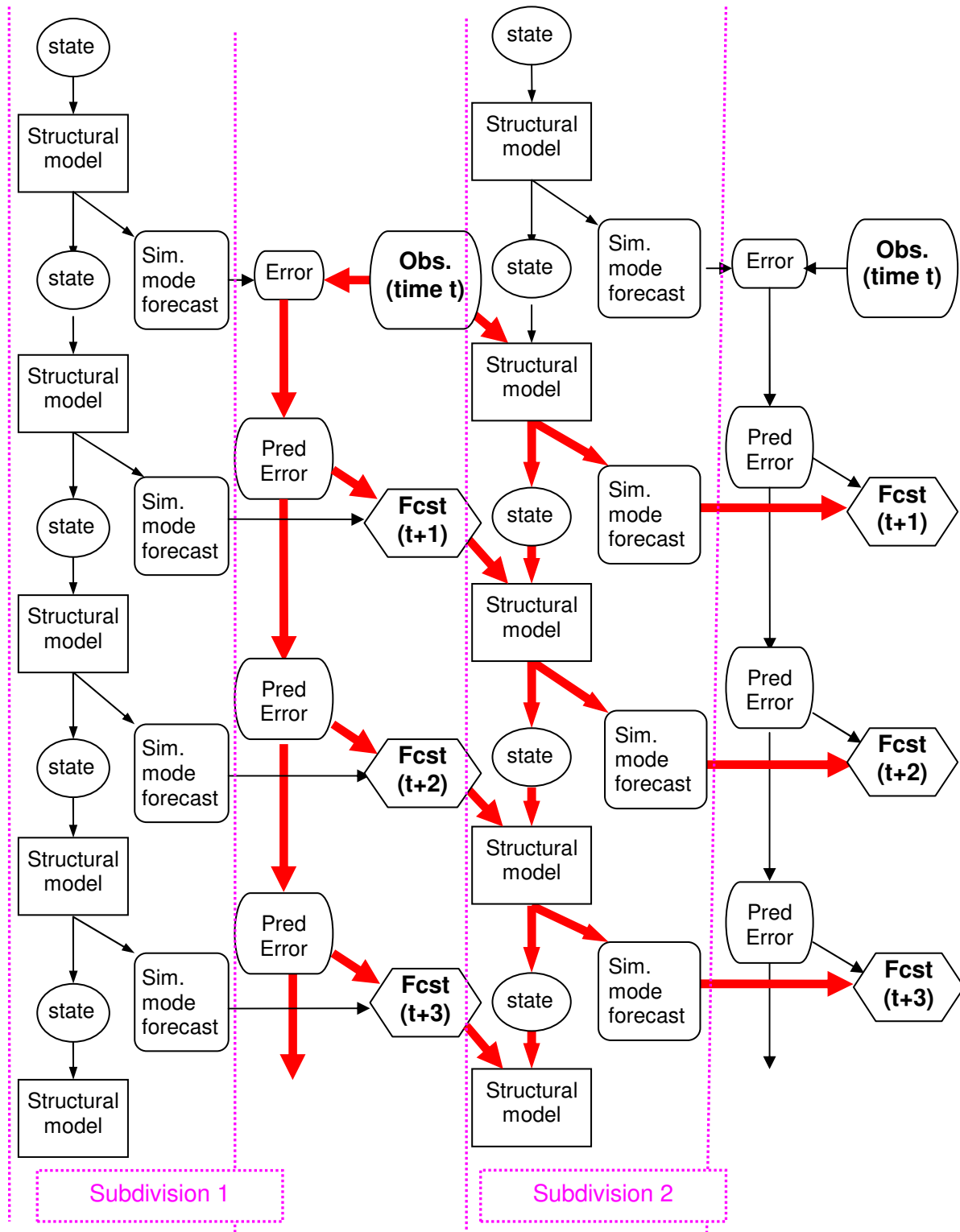
Figure 7.6 Model-subdivision: the flow of information from the last observation at an intermediate location in creating a time-series of forecasts at the downstream point. This example illustrates the effect on model states of using model-subdivision with error-prediction.

the updating method, whereas state-correction methods would be calibrated on the basis of improved forecasts for the gauged downstream location.

While it is easy to float the idea of combining models upstream and downstream of a target location into a single unit, there may be considerable practical difficulties in doing this. Notionally this would be easiest in cases where the two models are of the same basic type, such as a particular "brand" of hydrological routing model but even here the combination may not be easy because programs for such models have not been structured with this possibility in mind. More usually the models will be of different types. If a fully-fledged state-correction procedure were to be attempted special efforts would be required in one or both of the following directions.

> (i) Integration of program code into a unified whole;

> (ii) Restructuring of code to reflect a state-space formulation at a fundamental level.

This would usually be costly in terms of programming effort and may be practically impossible where proprietary code is involved.

An alternative to attempting a fully-fledged state-correction procedure is to combine the approaches of "two-pass state-correction" and "state-correction by model-subdivision" (which in this instance means not fully combining the two models). In the present instance, the "first pass" calculations would run the two models in succession, leading to a time-series of first-pass simulation-mode errors for the downstream location, to which error-prediction techniques are applied to extend the series into the future. These first-pass errors are then available for state-correction of both models on the second pass of calculations for both models. A variant of this would be to apply inferred-error methods based on the first-pass errors to the values for the target location, with these values being used as inputs to the second-pass of calculations for the downstream model only. This second pass of the downstream model might or might not incorporate internal state-correction steps: this would mean that the code for the downstream model could be used unchanged. As noted under the heading "State-correction by model-subdivision", the use of corrected values for the inputs to the downstream model has a type of state-correcting effect within the downstream model.

Updating methods which apply two-pass procedures to loosely-combined models in the ways outlined here will be referred to elsewhere in this report as "two-pass combined-model state-correction". The particular advantage of these procedures is that the forecast-updating part of the schemes can be objectively calibrated using existing records for the gauged downstream site.

State-correction by model-nudging

There is a wider field of data-assimilation methodologies outside those which are usually employed for updating hydrological and hydrodynamic models on observations of river-levels or flows. Often these methodologies are developed so as to adjust model-outputs to account for observations of quantities which are not the primary forecast quantities for the model. For example, observations of soil-moisture conditions may be available in an application where a lumped hydrological model would be applied. In the case of distributed models, sets of spatial observations may be available by remote sensing. In cases where models are thought of as having a direct connection with particular physical processes within a catchment, observations of quantities represented within a model should be of benefit to forecasts from the model.

The case of conceptual hydrological models may be problematic in this regard since any intermediate quantities with such models reflect combinations of behaviours and thus may not have any immediate counterpart in the real world.

Model-nudging techniques have been developed for applications where the basic model consists of differential equations for quantities varying in 3 spatial dimensions in addition to time. In this context, where there are effectively so many state-variables, it is difficult to implement "optimal" updating methods based on overall stochastic models which include modelling errors. Thus other updating/assimilation techniques have been sought. It is not clear that model-nudging (also called Newtonian nudging or Newtonian relaxation) strictly falls within an extended set of state-correction techniques since the basis of the method is not set out in that way. Rather, the basis of nudging methods is to alter the basic model equations that need to be solved. Thus if the basic differential equations for the model contain an expression of the form

$$\frac{\partial v}{\partial t} = F(v, x, t) \tag{7.40}$$

and a single observation of v were available for a given location x_0 and time t_0

$$v_0 = v(x_0, t_0),$$

then the "nudged" model would be

$$\frac{\partial v}{\partial t} = F(v, x, t) + G\, W(x - x_0, t - t_0)(v_0 - v(x, t)). \tag{7.41}$$

Here W is a time- and space-weighting function which distributes the effect of the observation "locally" to the observation ($W(0,0) = 1$) and G is an overall factor that determines the extent of the change. The effect of the adjustment to the equation is to tend to move the solution to the differential equation closer to the observed value in the vicinity of the observation. When there are many observations the adjusted equation contains a weighted sum of terms representing contributions from each observation.

The effect of the "nudging" procedure is to change the "state-values", v, from the values they would have been had there been no observations. In terms of forecasting, the effects of any observations will eventually diminish because the weight functions W are zero beyond a certain distance in time and space, and thus the trajectory of the forecasts will eventually be controlled by the basic model (Equation (7.40)). However, the effect of any observation would automatically appear within the model at times before the observation, because the weight functions W that are generally used are symmetric in time and hence the adjustment has effects for times before the observation-time. Thus the nudging procedure would incorporate certain of the features thought desirable when discussing modified state-correction procedures derived from "optimal" procedures (under the headings "Extended state-correction" and "Two-pass state-correction"), but allowing for serial dependence in the modelling errors.

State-correction by structural-error minimisation

A method of adjusting values of model states in response to observations arises most naturally in the case of hydrodynamic modelling, although it seems capable of implementation elsewhere. The relevant feature here of hydrodynamic models is that

these are usually structured as a number of mass and momentum balance equations which are, in principle, solved exactly at each time-step. For example, for a reach represented by N modelling nodes, the calculations require finding $2N$ values of flow and water-height, two of which are specified by the boundary conditions of the model leaving $2N-2$ unknown quantities. Each of the $N-1$ intervals between modelling nodes supplies 2 equations to be solved (the mass and momentum balance equations). There are therefore exactly as many unknowns as equations to be solved. When an attempt is made to force the modelled value of a water-height to agree with an observed value, this effectively introduces another equation into the models and means that the equation will usually contradict each other: the equations cannot be solved simultaneously. If observations were available at more nodes this would introduce more equations. The underlying principle of the particular method of state-correction discussed here is to carry over certain ideas from regression in statistics, where there are more equations (modelled value equals observed value) than there are free parameters (parameters of a regression line). In particular, the usual hydrodynamic model in principle provides two sets of equations to be solved:

$$A_j(\{Q_i\},\{h_i\}) = 0 ,$$
$$B_j(\{Q_i\},\{h_i\}) = 0 .$$

These are modified to

$$A_j(\{Q_i\},\{h_i\}) = \varepsilon_j^A ,$$
$$B_j(\{Q_i\},\{h_i\}) = \varepsilon_j^B ,$$

where $\{\varepsilon_j^A\}$ and $\{\varepsilon_j^B\}$ represent structural modelling errors introduced by not being able to solve all equations simultaneously. It is possible to introduce a further set of structural errors representing differences between modelled and observed values for those nodes which have observations available; otherwise these observations can be treated as providing exact values for selected members of the set of unknown values $\{Q_i\},\{h_i\}$. The idea is then to determine the modelled values of flow and water-height by minimising the sizes of the overall set of structural errors in some sense. This can be made more specific by constructing a weighted sum of squares of the structural errors and using this as an objective function to be minimised in determining $\{Q_i\},\{h_i\}$.

The potential need for weighting is revealed in the case of hydrodynamic models by the different units usually employed for the mass and momentum balance equations. More generally there is an apparent need for variable weighting of the structural errors along a reach to reflect the change in typical flow amounts as one progresses downstream along a river. There is considerable scope for experimentation with weighting schemes both for hydrodynamic models and for other types of models if this method of state correction is thought to be worthwhile.

8 Real-time updating techniques for specific model types

8.1 Introduction

This section discusses when there may be merit in forecast-updating for ungauged locations. The answer to this question is likely to depend on the importance of, and use for, any forecast being produced. The answer may also depend on the underlying type of model being used to create non-updated forecasts and on the possible availability of calibration data for non-telemetered locations. Other issues concern the hydrological and hydraulic relevance of gauged locations neighbouring to the target location at which a forecast is required.

8.2 Updating methods for simple scaling and transposition models

River-flow and level modelling methods using simple scaling and transposition approaches have been outlined in Section 3.2. These basic methods rely on a scaling or transposition rule, whereby the observed flow or level at a gauged location is used to infer a corresponding value an ungauged location. In these cases it is natural to apply the scaling or transposition to the forecast values after updating for observations at the gauged location. Thus, if the basic scaling model is established as

$$Q_T(t) = f \, Q_S(t),$$

(8.1)

and if a set of simulation-mode forecasts $\left\{ \tilde{Q}_S(t) \right\}$ are available for the "source" location, simulation-mode forecasts for the target location would be constructed using the equation:

$$\tilde{Q}_T(t) = f \, \tilde{Q}_S(t).$$

(8.2)

A similar equation can be used in a real-time context when telemetered observations at the "source" location are available for forecast-updating for that gauged location. If $\left\{ \hat{Q}_S(t) \right\}$ represents a "complete" time-series for the source location (i.e. a mixture of observations and updated forecasts), a similar series for the target location can be constructed using the equation

$$\hat{Q}_T(t) = f \, \hat{Q}_S(t).$$

(8.3)

The forecasts $\left\{ \hat{Q}_S(t) \right\}$ here need not arise from an error-prediction type of updating method. If they do, then the forecasts for the target site can also be viewed as error-prediction forecasts using a particular type of inferred-error method (Section 7.5.2). Thus

$$\hat{Q}_T(t) = \tilde{Q}_T(t) + \hat{\varepsilon}_T(t)$$

(8.4)

where

$$\hat{\varepsilon}_T(t) = f\,\hat{\varepsilon}_S(t)\,,\tag{8.5}$$

$$\hat{\varepsilon}_S(t) = \hat{Q}_S(t) - \tilde{Q}_S(t)\,.\tag{8.6}$$

Thus inferred-error methods are implicitly being used in practice, although not under that name.

In practice, simple scaling methods should not be applied in a real-time context without careful thought. One common use of scaled flow values is to represent ungauged catchment areas and the overall effect of the "source" values on the derived values is to scale-up any variations in the observed and modelled values for the "source" location. Thus any variations in the updated forecasts for the source location will be magnified within the forecast system and this may produce unrealistic results for locations further down the river network. There is thus some risk that poor forecasts caused by aberrant observations and/or an unstable forecasting methodology for the source location will have disastrous effects on forecasts elsewhere. In practice, this type of application of scaling methodology often occurs during an "input processing" stage of a hydrological or hydrodynamic routing model where its effects may not be obvious and where it may be difficult to take steps to mitigate the potential problem.

The above problem may be partly overcome by taking a more considered view as to how ungauged flow contributions should be treated. Some possible strategies are as follows.

(i) Limit the relative size of an ungauged area with respect to the size of the gauged area that will be used to provide representative values for it. A possible limit would be to say that the ungauged area should not be more than 1.5 times the size of the gauged catchment area.

(ii) Use several nearby gauged areas to create a weighted average as the modelled value for the ungauged area: this should reduce the effects of observations at individual sites.

(iii) Treat the simulation-mode forecasts for the ungauged location, as in Equation (8.2), as a separate model and apply some of the adjustments outlined in Section 7.5.2 to provide inferred error-predictions.

(iv) Model ungauged areas using rainfall-runoff models with care taken over any inferred-error scheme used to update forecasts on the basis of neighbouring observations.

8.3 Updating methods for lumped rainfall-runoff models

In the case of gauged locations, forecast-updating for lumped rainfall-runoff models has been implemented by both error-prediction and state-correction schemes. Both full state-correction and empirical state-correction methods have been reported in the hydrological literature, but usually in a research setting, while empirical state-correction has been implemented operationally for the PDM model.

For ungauged locations, there are two possibilities for updating based on neighbouring locations. The first of these possibilities would employ some type of inferred-error procedure, with the best hope of success arising where the same type of lumped model is used on similar neighbouring gauged catchments. Here "success" would usually need to be judged on the basis of results from a downstream model which uses the ungauged flows as an input. This downstream model would need to model a gauged location but the comparison would be between the observations and forecasts from the downstream model which do not make use of the observations from the downstream site. It seems possible that rainfall-runoff models for neighbouring catchments may be affected by similar local modelling errors, particularly if these arise from errors in rainfall inputs from the same source. Thus there is some hope that this approach may lead to good real-time corrections to all aspects of the flood hydrograph. Either error-prediction or state-correction seems a likely candidate for updating within the ungauged model. The second possibility would employ a downstream model (with a gauged target) as part of the updating scheme: in a sense the gauged output from the downstream model would provide a closure for the water balance of which the ungauged locations represent unknown components. Because of problems arising from the routing time-delay and attenuation within the downstream model, it seems likely that only relatively slowly changing effects could reasonably be hoped to be identified by this type of approach. Thus it may be possible to make real-time corrections to the baseflow and slow surface flow responses from an ungauged rainfall-runoff model. For this approach, a two-pass combined-model state-correction method seems likely to be the best choice.

For both of the above possibilities, the gauged values for the downstream model, run in non-updating mode, should provide a good basis for calibrating parameters of the updating step for the ungauged models. In real-time applications, the results from the downstream model would be subjected to the usual types of forecast-updating methods.

8.4 Updating methods for hydrological routing models

In the case of gauged locations, forecast-updating for hydrological routing models has been implemented by both error-prediction and state-correction schemes. Both full state-correction and empirical state-correction methods have been reported in the hydrological literature, but usually in a research setting, while error-prediction has been implemented operationally. The major "non-linear" feature of hydrological routing models may be thought of as being the ability to represent wave speeds which vary with the amount of flow. Thus a state-correction procedure may be expected to show better performance in matching the timing of peak flows than error-prediction if the basic routing-model specifically included the effect and if such a state-correction procedure could be established.

For ungauged locations, the best hope of successful modelling lies in an indirect modelling approach where the ungauged target location is treated within a more extensive model which can be calibrated against data from a gauged location downstream. Full state-correction methods are not commonly applied even for the gauged case. Therefore, when attempting to implement forecast-updating for ungauged locations based on telemetry at the downstream location, it seems that a reasonable approach would be to try a two-pass state-correction approach (Section 7.5.3). The first step should be to consider the likely sources of modelling errors. If there are a few comparatively large ungauged tributaries supplying concentrated lateral inflows, it may be best to structure the state-correction at the second pass of the calculations so as to restrict the state-correction to apply only at corresponding points

within the model. In contrast, if lateral inflows might be considered uniformly distributed along the main reach being modelled then this could be reflected in the correction scheme by applying similar corrections at all points within the model. While calibration of the updating scheme can be achieved using data for the gauged location, it would still be important to restrict the number of parameters required for the state-correction step. This can be achieved either by applying corrections at only a few modelling-node locations within the routing model, or by a parameterised rule applying to all modelling nodes or rules for subsets of nodes.

8.5 Updating methods for distributed hydrological models

If one excludes semi-distributed models (networks of simpler lumped rainfall-runoff and routing models), few if any distributed hydrological models have been applied for operational forecasting, even for gauged sites.

Since one reason for deploying distributed models is so that all (river) locations are modelled, it follows that the usual treatment of ungauged locations would be via indirect modelling of such sites based on calibration of the model to data at one or more gauged locations, both at the downstream point of the catchment being modelled, and at interior points.

There are substantial similarities between the questions of updating forecasts for ungauged locations for hydrological routing and distributed hydrological models, at least in so far as river locations are concerned. However, distributed hydrological models would usually contain a larger number of different types of model states within the model (nominally representing soil moisture and groundwater conditions as well as channel flows) than is the case for hydrological routing models. Once again it seems reasonable to attempt to apply a simple two-pass correction procedure for forecast updating. Because of the more complicated model structure (compared to hydrological routing) it is more difficult to assess likely sources of modelling errors. In some contexts it may be reasonable to assume that errors arise from measurements of rainfall and thus one may set out a state-correction scheme that results eventually in corrections to states throughout the whole model. This may seem too ambitious and there are possibilities of limiting corrections during the second pass of the model to states representing channel flow only. As for two-pass state-correction for hydrological routing models, there is a need to restrain the number of parameters controlling the state-correction steps so that calibration of the scheme can be achieved.

8.6 Updating methods for hydrodynamic models

In the case of gauged locations, forecast-updating for hydrodynamic routing models has been implemented by both error-prediction and state-correction schemes. Both full state-correction and empirical state-correction methods have been reported in the hydrological literature, but usually in a research setting, while error-prediction has been implemented operationally. One proprietary hydrodynamic model package (MIKE11) apparently contains an updating procedure based on a real-time version of an amplitude/phase correction procedure (briefly mentioned in Section 7.4.2 under "real-time versions of off-line improvements"), which is grouped in this report under the heading "error-prediction". This, and some other, error-prediction schemes require real-time observations at the target location and are thus of no immediate relevance to ungauged locations, except where transposition of forecasts can be employed.

For ungauged locations, direct transposition or interpolation of updated forecasts for gauged locations are straightforward ways of determining forecasts. These have advantages regarding the ability to ensure that forecasts for locations along a river reach behave in a reasonable manner. An alternative approach could be based on the interpolation of simulation-mode errors in an inferred-error scheme (Section 7.5.2).

9 Monitoring, forecasting and warning

9.1 Introduction

This section aims to review, in broad terms in relation to their relevance to forecasting for the ungauged case, the following topics: areal rainfall estimation, remote sensing prospects, stage-discharge relations for level-only sites, emerging technologies for low-cost river level sensing, and identification of flood warning triggers for ungauged locations. The review of these topics will aim to ensure that relevant existing work in each of these areas is identified and documented. At the same time, any shortcomings and gaps in existing knowledge that requires to be filled through further research will be highlighted.

9.2 Use of radar and raingauge networks for areal rainfall estimation over ungauged areas

Whilst modelling for ungauged locations is the main concern of this Guidelines Report, a major influence on the performance of rainfall-runoff models is the estimation of the rainfall input. The traditional information sources are networks of raingauges and radars. The former are associated with relatively good point accuracy whilst the latter are able to delineate the spatial pattern of rain with some success but with sometimes significant errors in rainfall magnitude. These characteristics have led to methods for radar correction and for combining the two sources. The state-of-the-art in the UK provides Nimrod QC (quality-controlled) products from the Met Office in real-time. These are received and processed by Hyrad within the Environment Agency, supporting visualisation of the radar images and onward transmission to flood forecasting and modelling systems.

Research suggests that there is still advantage to be gained by combining raingauges available within a region with radar data. However, this is not done operationally except in Thames Region within the Cascade System using Hyrad kernel software. Appendix C provides a review of methodology, based on multiquadric surface fitting, for areal rainfall estimation using raingauge-only estimates and estimates that combine raingauge and radar data. It is shown that the methods reduce to a set of linear weights on the raingauge values for the spatial areas of integration (catchments or grid-squares) for raingauge-only methods. For combining radar and raingauge data, the methods reduce to linear weights on the gauge-adjustment factors for each grid-square. This gauge-adjustment surface is applied to the radar field to obtain gauge-adjusted radar rainfall estimates. Procedures such as these should be considered when applying rainfall-runoff models in lumped or distributed form to ungauged areas, where more than one raingauge in the vicinity and/or radar coverage are available.

9.3 Remote sensing prospects

A major value of remote sensing for ungauged forecasting relates to the derivation of digital datasets, particularly of elevation and land cover. Developments here, of relevance to the configuration and parameterisation of flood forecasting models, have

been reviewed in Section 5. Whilst such datasets for practical purposes can be regarded as static, there are also temporally-varying spatial datasets produced as satellite-derived products. Examples such as spectroradiometer estimates of Leaf Area Index, snow cover and flood inundation extent from MODIS (1km resolution, global coverage, 8 day update) and synthetic aperture radar estimates of soil moisture have been reviewed in Section 5.3. The use of remote-sensing for river-level sensing is discussed in the next section.

9.4 Emerging technologies for low-cost river-level sensing

Satellite remote sensing of river discharge is still at an early stage of development. A recent review of methods and a feasibility study for the Yangtse River in China using QuickBird-2 optical imagery is given by Zhang *et al.* (2004). The method proposed is based on making remote sensing measurements of river width at a monitoring site, chosen to have a trapezoidal section so that a width-stage relation can be established that is sensitive to width changes. A target site with non-trapezoidal section is used to estimate flow from the estimated stage, using a relationship established from historical records. The latter implies the availability of some historical records, although a modelling approach could be used to help develop a relation if channel geometry information is available. A related approach is to use remote sensing to measure water-surface area and, with an estimate of reach length, to infer an "effective width" and from this discharge. The efficacy of such approaches is constrained in part by image resolution, image frequency and cost, and cloud cover for optical systems. More direct measurement of water level variations using radar altimetry or interferometery, capable of resolving down to the centimetre scale, is possible. However, the latter process is complex and the former has poor spatial spatial resolution (3-5 km for TOPEX/Poseidon). In general, the greatest applicability of remote-sensing of river level and discharge is for the larger rivers of the world. For UK conditions and in terms of relevance to forecasting for the ungauged case, satellite remote-sensing of discharge has little applicability at the present time.

The RiGHt (River level Monitoring using GPS Heighting) Foresight Project, and its successor FURLONG (Future Real-time Location and Navigation study), aimed to explore the potential of satellite global positioning systems (GPS) to monitor river level. The basic idea is to mount a GPS on a tethered floating buoy to sense water level fluctuations and to communicate readings to a data centre for use in flood warning. It was recognised that the current GPS constellation cannot provide the required levels of accuracy, reliability and availability. The limits of application derive from a combination of available positioning data from multiple satellite sources and communication techniques, especially where these have to be satellite-based. FURLONG explored the potential of future satellite positioning systems – Galilieo and next generation GPS – to give height estimates with centimetre accuracy, through simulation. It highlighted that river locations in gorges (using Ironbridge as an example) precluded use of satellite communication; also isolated rural areas might have no terrestrial wireless service. This emerging technology appears to be viable at some future time when satellite developments allow.

9.5 Stage-discharge relations for ungauged and level-only sites

Stage-discharge relations, or rating curves, define a relationship between water level and river flow. They are defined at gauging stations via weir formulae for gauging structures and developed from velocity measurements for a range of discharges (using a current meter or Acoustic Doppler Current Profiler (ADCP)) and cross-section survey for natural sections (velocity-area stations). Ultrasonic and electromagnetic stations provide continuous measurements of river level and flow. The hydrometry of flow measurement is well reviewed in established texts (Ackers *et al.*, 1978; Herschy, 1999).

An ungauged site of interest may have no measurement at all or a measurement of river level but no rating curve (a level-only site). In the former case, this guideline report has presented a variety of methodologies, ranging from simple scaling of measurements for a similar gauged site to more sophisticated model-based schemes. These methodologies are often flow-based and still require a rating curve to infer river level. In the case of level-only sites, a rating curve is required to infer river flow. River flow may be required, for example, for flood forecasting using rainfall-runoff or channel flow routing models.

The Environment Agency's best practice guidance manual on "Extension of rating curves at gauging stations" (Ramsbottom and Whitlow, 2003) provides a convenient reference source for developing rating curves. Whilst specifically written for rating curve extension, there is much of relevance to developing a rating curve for sites with none. The methods fall into two categories: simple hydraulic techniques and computational hydraulic models. In the first category are simple extension and extrapolation of the rating curve, extrapolation of velocity against stage or hydraulic radius or of flow against geometric properties of the Manning equation, and slope-area methods. Modelling approaches include consideration of 2- and 3-D formulations in addition to the 1-D model of St. Venant considered here.

CEH's suite of models, within the CEH Model Calibration environment, provide facilities to embed an unknown rating curve within the model formulation. This is most useful for the KW channel flow routing model applied to river reaches with a level-only station at one end and a gauging station at the other, particularly when ungauged lateral inflows do not dominate the reach water balance. The facility is also available for rainfall-runoff models – the PDM and PSM (TCM and IEM) – but is generally less reliable as the catchment water balance components are not as well defined.

9.6 Identification of flood warning triggers for ungauged locations

A best practice guide to the use of trigger mechanisms in flood warning has been produced for the Environment Agency by Cadman and Moore (1998) in draft form. A trigger mechanism is used to stimulate action in advance of flooding occurring. Threshold levels are identified that are relevant to flood warning, such as bankfull discharge or level. A trigger is a condition set to initiate action in advance of a threshold being crossed. The trigger may be based on observations or forecasts of the condition. Threshold levels normally relate to a physical quantity that can be obtained from survey, lidar or experience for an ungauged site.

The trigger mechanism to use could be one of the methodologies for ungauged forecasting outlined in this report. Or it might use methodology for level or flow estimation at an ungauged site, in preference to a trigger condition set in terms of less certain forecast values. A trigger mechanism might embrace a range of trigger conditions stimulating actions of different severity.

Advances in best practice should be seeking to accommodate estimates of uncertainty, and costs of alternative actions, into the decision-making process within which the flood warning triggers lie. This implies providing uncertainty estimates for methodologies concerned with ungauged site flow/level estimation.

10 Overview of operational guidelines

10.1 Introduction

This Section aims to provide an overview of approaches for modelling at ungauged locations that can serve as operational guidelines for Environment Agency use. The emphasis is on the types of problem commonly encountered and the general approaches that can be considered when addressing them. Whilst rainfall-runoff models are the main focus of attention, broader discussion encompasses hydrological channel flow routing models and hydrodynamic river models; simpler empirical models including level-to-level correlation methods are also considered.

Even for specific rainfall-runoff model types, it is unusual for a methodology to be sufficiently well established for its application to be routine for ungauged forecasting purposes. The overview first focuses on the nature of the ungauged problem and the modelling approaches available when considered at a generic level. Subsequent discussions of specific model types serve to illustrate how some of these approaches have been applied and their shortcomings. Possible opportunities for improvement are identified.

An important aspect of ungauged modelling is the ability to utilise digital spatial datasets on properties of the terrain, land cover, soil and geology that will influence the hydrological response. The more useful datasets for use in modelling are highlighted.

Although not a natural choice for application to ungauged locations, the scope for using purely statistical (empirical) modelling approaches, such as level-to-level and structure function methods, is considered. Similarly, the application of real-time updating techniques at ungauged locations is not immediately obvious, but a number of methods of transferred-error updating are identified as deserving of future attention.

Opportunities are considered for improved flood warning at ungauged locations relating to advances in monitoring and uncertain triggers for warning. Topics addressed encompass improved methods of areal rainfall estimation, remote-sensing of land surface properties and river height and width, stage-discharge curve derivation, and flood warning trigger mechanisms incorporating uncertainty and costs of alternative actions.

A final section considers practical examples of model transfer to ungauged locations using case studies from upland and lowland Britain. The detail is presented in a separate appendix.

10.2 Modelling Approaches for Ungauged Locations

Definition of "ungauged" and data availability

An ungauged catchment may have different *levels of data availability*. Classically absence of river level measurement at the catchment outlet defines an ungauged catchment. The presence of rainfall measurements in the catchment would not normally affect such a classification. This guideline recognises different degrees of

"ungauged", including consideration of: stage-discharge relations for flow estimation, past historical records but no current ones, the presence of telemetry for real-time data access and availability of data from neighbouring catchments. These levels of data availability impact on the choice of modelling approach, both in terms of process model selection and method of updating. These issues have been outlined in Section 2.

Ungauged modelling approaches

The *direct modelling* of gauged catchments gives way to *indirect modelling* of *target* ungauged catchments. This involves some form of *information transfer* (of data or model parameters) from donor (neighbouring, nested, downstream or "similar") catchments to the ungauged catchments of interest. The method of transfer may be called the *inference model.* An inference model may relate to the process model, updating method or both. It may also embrace the method of rainfall estimation (such as Thiessen polygon interpolation) used in the construction of the model input. The process model may take a lumped or distributed form. For example, a lumped rainfall-runoff model and a method of parameter regionalisation may constitute the inference model. In the case of a distributed model configured using spatial datasets, this may typically combine runoff production and flow routing schemes on a grid for a prescribed area that embraces some gauged sites, providing a natural inference model for forecasting at ungauged sites. A distributed model of this form is referred to as an *area-wide model* to distinguish it from a *distributed catchment model* that is configured to a bounding river basin. Both can be used as inference models for forecasting at target ungauged sites. For the case of *forecast updating*, errors in the forecasts at gauged sites can be transferred to ungauged sites using either model state-correction or an error-prediction based inference model. There will be a need to down-weight the adjustments to reflect the uncertainty of transfer from gauged to target sites.

Choice of modelling approach

The nature of the catchment will influence the choice of modelling approach to use. Considerations include catchment size, location within a river basin (headwater, middle reach, lower reach), steepness and the influence of tides, backwater or river gate controls. Headwater catchments of small or moderate size are natural candidates for rainfall-runoff models using transferred parameters, or scaled versions of model forecasts from neighbouring or similar catchments. Techniques for use on the middle to lower reaches of more major rivers may vary from simple level-to-level correlation methods or hydrological storage-routing models (extrapolated from gauged sites), to hydrodynamic river models (using survey data for configuration and model parameters transferred from "similar" gauged reaches). Tidally-influenced rivers may use hydrodynamic approaches or simpler tabular forecasts linked to observations and tide/surge predictions at gauged locations along the river, estuary or coast. Distributed hydrological models have the ability to mix rainfall-runoff and routing models in an integrated way to allow a unified transfer of information from gauged to ungauged sites whilst using spatial datasets on terrain, soil, land use and geology to support model configuration. They are potentially flexible to the type of catchments being targeted but may not incorporate the detailed modelling capability of hydrodynamic river models developed for tidal- and backwater-influenced rivers.

Under the five minor headings that follow, a set of modelling approaches for flow forecasting at ungauged locations are outlined for different types of model. Figure 3.1 provides a useful structural overview of these approaches. It serves as a guide to where more detail can be found, through number reference to specific sections of this report.

Simple scaling and transposition methods

A distinction can be made between simple scaling and transposition methods. *Simple transposition* involves direct use of gauged flow values for a *source location* at a nearby *target location.* River level values may also be transposed in some instances although a datum adjustment may be required. Proximity and similarity are key factors to the success of simple transposition. One example application is the use of gauged flow to trigger a warning at a nearby flood-prone site.

Simple scaling involves transformation of the gauged values for the source location to the target location to make them more representative. A commonly used scaling factor to use is the ratio of the source and target catchment drainage areas. A refinement of this might use the Standard Average Annual Rainfall (SAAR) as a further ratio factor. Further possibilities, including offset and time-shift forms, have been outlined in Section 3.2.

Lumped conceptual rainfall-runoff models

A rainfall-runoff model developed for a gauged catchment can be used as the basis of information transfer to a target ungauged catchment. Different approaches present themselves. *Simple model transfer* involves the direct transfer of the model and its parameters, only changing the catchment area and input rainfall to that of the target catchment. This may be appropriate for catchments that are very similar in location, area, terrain, soil, land cover and geology. It may prove better than simple scaling, particularly at times of spatially-varying rainfall for which good areal estimates are available for both source and target catchments.

Where rainfall-runoff models can be calibrated for a variety of gauged catchments, it is tempting to develop regression relations linking model parameters to catchment properties. The approach of *relating model parameters to catchment properties* has proved a popular method of model transfer to ungauged catchments because of its apparent simplicity. In practice, careful attention needs to be given to: (i) possibilities for model simplification to achieve a degree of parameter independence, (ii) choice of appropriate catchment property measures, and (iii) the form of regression methodology to use. The approach can be criticised for its lack of a physical basis, it can be time-consuming to apply in a rigorous manner, and model performance for some target locations may be disappointing. A variant of this approach employs a *transfer function parameter link to catchment properties*. The functional form of the transfer functions and the catchment properties they relate to are predefined and parameters estimated in a one-step calibration process across all gauged catchments. This contrasts with the conventional two-step "model calibration and parameter regression" approach. It may prove more robust and faster to apply. An alternative to the parameter regression on catchment properties approach is to estimate the model parameters for the target site as a weighted combination of those at "similar sites". This *site-similarity approach* uses the catchment properties to define *similarity* or *distance* (in the catchment property space) *measures* between the target catchment and potential source catchments. These measures are used to identify a set of similar catchments to use as source catchments (the pooling group) and to establish the weights in the weighted average of parameters across the source catchments used to estimate the model parameters at the target site. All these model parameter transfer approaches employ an essentially empirically-based link to catchment properties and are not physically-based.

A scientifically more rigorous approach is to formulate a rainfall-runoff model from the outset that has a structure and parameters that can be linked in a conceptual-physical way to spatial datasets on topography, soil, land cover and geology. The approach of

establishing conceptual-physical linkages to model structure and parameters has considerable appeal for application to ungauged catchments. Either lumped or distributed forms of model can be developed, lumped models usually being derived from a distributed form that establishes the links to the spatial datasets. Such models normally have a small set of *regional parameters* that allow mapping onto a much larger set of model parameters with the support of the spatial datasets. Gauged sites in the region can be used for calibration of these regional parameters and the overall model used to forecast at ungauged locations in a natural way. Models are normally formulated as distributed hydrological models either in source-to-sink or grid-to-grid form. *Source-to sink models* are formulated to simulate flow at a catchment outlet (the sink), with runoffs generated from distributed source areas being translated directly to the outlet. In contrast, *grid-to-grid models* route runoff from grid-cell to grid-cell across a predefined area that would generally not correspond to a specific catchment or river basin. For this reason they can be described as *area-wide models*. Using either form of model, it is possible to calibrate the model parameters at gauged locations within the modelled area and to extract flows for interior ungauged locations for forecasting purposes. Such models, whilst essentially distributed in form, can be used as lumped rainfall-runoff models for specific locations. An important advantage is that their model structure and parameters have been derived using property datasets in spatial form as opposed to using empirical relations with catchment-aggregated properties.

Distributed hydrological models

Distributed models arguably provide the most natural way of flood forecasting at ungauged sites across a region. They embrace runoff-production and flow routing components within a unified framework. The modelled domain can encompass gauged sites supporting model calibration, forecast assessment and updating and ungauged sites requiring flood forecasts. *Physics-based distributed models* classically employ partial differential equation representations of water movement and storage in soil, aquifer and channel systems. Such detailed mathematical description can prove illusory because of (i) the spatial complexity of such systems, (ii) the interest in aggregated flows from larger scale elements (hillslope, catchment, river basin), and (iii) the difficulty of spatial characterisation and measurement of the properties of the propagating media, especially underground. Simpler *conceptual-physical formulations* are commonly sought for forecasting applications for such reasons and because of ease of application and performance issues. Irrespective of the type of distributed model in question, experience suggests that in many situations it is hard to outperform lumped conceptual models in operational use for flood forecasting. Whilst this arguably still applies for gauged catchments, the prospect for improvements in flood forecasting for ungauged catchments via a distributed modelling approach seems much greater.

The *area-wide distributed models* developed for atmospheric modelling purposes, in support of weather forecasting and climate prediction, have emphasised vertical water and heat transfers with the atmosphere. These *land surface schemes* have been developed for national and global application and have elements, supported by global datasets on soil and land cover, that are of some interest to the ungauged problem. However, the focus on vertical transfers of water to the exclusion of horizontal transfers under topographic control means they do not provide a natural starting point for flood forecasting at ungauged sites.

Channel flow routing models

Channel flow routing models are used to translate a flow hydrograph from an upstream site to one downstream. The situation where the downstream flow influences this translation via backwater control is treated separately under hydrodynamic river

models. A modelled river reach is normally sub-divided into sub-reaches with nodes at their boundaries. Assigning a boundary node to a target ungauged location provides a simple example of the use of a channel flow routing model as an indirect modelling approach for ungauged forecasting. Ungauged lateral inflows commonly bring further complexity and lessen forecast accuracy. Simple scaling methods or rainfall-runoff models may be used to represent such ungauged lateral inflows.

A lesser form of "ungauged problem" is where only river level measurements are available and a stage-discharge relation cannot readily be established via a current metering field programme. The stage-discharge relation may be embedded within the channel flow routing model and its form and parameters calibrated along with those of the routing model.

Some channel flow routing models can be linked directly to the St. Venant equations of open channel flow and through them to the properties of the river channel and its floodplain. This can provide a direct basis for application to ungauged sites but, on account of the simplifications involved, is likely to benefit greatly from experience gained in modelling similar river reaches that are gauged.

Hydrodynamic river models

Hydrodynamic river models, through their direct link to channel and floodplain form and formulation as equations in terms of both flow and level, at first sight appear immediately suited to the ungauged forecasting problem. They are particularly suited to rivers under backwater influence from tides, river confluences and river controls. Simplification of processes, reduction to one dimension, poor definition of lateral inflows and roughness parameters requiring a degree of calibration are some of the reasons for application not being straightforward for ungauged sites. Experience of model application for similar river reaches will invariably prove invaluable. The simplest and most successful use of hydrodynamic models for ungauged forecasting will be for model node locations within a river reach gauged at its upstream and downstream boundaries, and without significant ungauged lateral inflows. Standing water level on the floodplain, off the main river channel, may also form a target ungauged forecast requirement. The extent of the modelled region may be extended to encompass tributaries under the backwater control of the main river with ungauged locations requiring flood forecasts.

10.3 Some Specific Modelling Tools

Figure 4.1 provides an overview of the specific modelling tools considered here within the structure of the modelling approaches summarised in Figure 3.1. These figures provide a useful guide to where further information can be found in this report, relating to the overview that follows, through number reference to sub-sections.

Simple scaling methods

Simple scaling methods, typically involving Area/SAAR weighting factors for the gauged source catchment and ungauged target catchment, are rather general in nature and are not discussed further with respect to specific modelling tools.

Lumped rainfall-runoff models

Specific rainfall-runoff models in use by the Environment Agency for flood forecasting include: the Thames Catchment Model (TCM or Catchmod, and available within the

Penman Store Model or PSM), the Midlands Catchment Runoff Model (MCRM), the PDM (Probability Distributed Model), the Isolated Event Model (IEM, and available within the PSM), the ISO (Input-Storage-Output) model, forms of Transfer Function (TF) model, and the NAM model.

It is not commonplace for specific models like the above to have well defined procedures for routine application to ungauged sites. Rather, there are methodologies that can be utilised to develop such procedures for particular applications and geographical areas. For forecasting applications and over England and Wales, such methodologies have rarely been invoked in a comprehensive way.

Some lumped rainfall-runoff models are more suitable than others for application to ungauged sites. However, many share common elements and are rather similar with regard to their suitability and approach for application to ungauged catchments. This report has reviewed each of the above models in terms of its suitability for ungauged catchments, and others. Some models, such as the TCM, appear more complex and having large numbers of model parameters. However, they can be reduced to simpler forms and a smaller set of dominant parameters, albeit at the expense of flexibility in the modelled response. The more complex forms may have closer ties to measurable quantities, and map information, that can support model configuration and calibration and application to ungauged catchments. Experience with their application across a region will give the modeller increasing confidence to formulate models for similar ungauged catchments, in terms of choice of configuration and parameter values.

Regional application of the "regression of model parameters on catchment properties approach" in the case of the MCRM, led to identifying subsets of sensitive parameters for this 22 parameter model, invoking a stepwise regression procedure, and using judgement to guide the development of plausible relations and the rejection of outlier catchments. An earlier attempt focussed on model simplification to reduce model parameters, simplifying the regression step, and resulting in the "Simple MCRM". In both cases, the results failed to be convincing overall for operational use on ungauged catchments, although good results were obtained in some situations with the Simple MCRM.

Notwithstanding these difficulties, a similar approach was attempted for design application at ungauged sites for the PDM model. The research focussed on model simplification, different regression techniques (including sequential regression) and choice of catchment properties. The simplified form compromised performance overall and use of regression relations for parameter estimation at ungauged sites caused further deterioration. Rather similar results were obtained using a site-similarity approach for parameter estimation instead of regression. Whilst rather straightforward to apply, it is not clear that the performance of these empirical approaches would be acceptable for flood forecasting and warning purposes.

The physical-conceptual nature of the PDM and its intermediate level of complexity do offer the prospect of using the approach of "establishing conceptual-physical linkages with model structure and parameters". Such an approach could capitalise on the use of spatial datasets on terrain, soil, land cover and geology at their basic resolution rather than via catchment-aggregated properties used in the regression approach. To date, this approach has not been pursued although some first steps are considered here. The use of a distribution function of absorption capacity in the PDM to control water storage and runoff production lends itself to explore links to terrain, soil and land cover data. One formulation is based on invoking a linear relation between terrain slope and absorption capacity which leads to a Pareto distribution of absorption capacity defined through slopes calculated from a Digital Terrain Model. An alternative

approach is to use soil survey data, such as the Integrated Air Capacity of the Soil Survey, to characterise absorption capacity and its spatial distribution. The canopy component of absorption capacity, if judged important, can be introduced through use of land cover data. Hybrid forms of these approaches can be considered.

Flow routing in the PDM, via fast (typically channel) and slow (typically groundwater) pathways, is represented by variants of the Horton-Izzard equation including simple linear storages in series. A body of theory exists that links the time constants and power exponents in these equations to properties of the channel and aquifer units involved. Some of the relevant theory has been summarised here to point the way forward in support of application to ungauged catchments. However, there are problems to be overcome in the appropriate use of spatial data on relevant properties, particularly on account of the lumped catchment-aggregated form of the PDM's routing functions. One approach is to consider distributed routing formulations as a means of arriving at effective parameters for the lumped routing components used in the PDM.

Similar considerations are relevant to applying the IEM and ISO models to ungauged catchments as their model structures encompass forms of the Horton-Izzard equation. The IEM with only four model parameters is arguably a good candidate for the "regression of model parameters on catchment properties" approach, although this has yet to be undertaken. The shortcomings of this empirical approach need to be borne in mind to avoid false expectations and possible disappointment in a forecasting context.

The NAM model has 16 parameters and the User Guide does not offer advice on its application to ungauged catchments. Remarks made already for the MCRM are probably as applicable to the NAM and parameter/property regression approaches are likely to encounter similar difficulties. Experience of applying it on gauged catchments is likely to provide a "feel" for how to apply it to similar ungauged catchments, as discussed for the TCM.

The TF (Transfer Function) model, including UH (unit hydrograph) forms, when viewed purely as black-box models do not appear to be immediately suited for application to ungauged catchments. However, they can be subject to conceptual-physical interpretation as deriving from configurations of linear storages allowing links to be established with physical properties. Parameter parsimonious forms, including ARMA (autoregressive-moving average) and triangular UH functions, can also ease the task of establishing parameter regressions on catchment properties. However, in their restricted forms they only address the routing process and usually require add-ons to accommodate the runoff production mechanism and its control on flood volumes. The triangular UH of the Flood Study Report (FSR) and Flood Estimation Handbook (FEH) developed for use in design provides a good example. This has recently been revised to have a kink in the recession limb and combined with a PDM type of runoff production function and a linear reservoir representation of groundwater. This revision is called the ReFH model and is provided with explicit parameter regressions on catchment properties for application to ungauged catchments. In some cases the parameter regressions on catchment properties are rather weak and the overall approach may not be good enough for flood forecasting purposes. It is possible that the regressions might prove a useful guide for modellers trying to apply the PDM, and forms of TF and UH model, to ungauged catchments.

Distributed hydrological models

The classical *physically-based distributed models* in hydrology employ nonlinear partial differential equation descriptions of key physical processes that are solved numerically using, for example finite difference or finite element schemes. Well known examples

are the SHE (Systéme Hydrologique Européean) and the IHDM (Institute of Hydrology Distributed Model). The fundamental equations employed are the Richard's equation for subsurface flow, the Boussinesq equation for groundwater flow and the St. Venant equations for overland and channel flow. Their success as useful tools for flood forecasting applications has been limited. Reasons for this include the real complexity of hydrological systems, much of which is unobservable below ground, issues of scale of representation, and the necessary approximations involved in process representation and numerical solution. For gauged catchments, simpler formulations are easier to apply and model calibration can result in as good if not better performance. Even for ungauged catchments, the complexity of model formulation can raise false expectations of model accuracy. The utility of distributed hydrological models is greater in design and planning contexts where the hydrological response to a change in catchment conditions needs to be understood.

The difficulties associated with classical physics-based distributed hydrological models have led to simpler *physical-conceptual models* being developed and linked to spatial datasets on controlling properties. These commonly use simpler, aggregated representations of key processes. Examples are the Grid Model (developed by CEH for the Environment Agency for flood forecasting purposes) and the Grid-to-Grid Model (developed by CEH for the Ministry of Defence for indicative area-wide flow forecasting and for Defra in support of climate change flood impact studies). These two models provide contrasting examples of source-to-sink and grid-to-grid (area-wide) approaches to distributed hydrological modelling. Both have structures well-suited to the ungauged problem and can accommodate the effects of topography, soil, land cover and geology in physically sensible ways. The Grid Model's source-to-sink method of routing is computationally more efficient than grid-to-grid routing and can more readily utilise terrain data at sub-grid resolutions. The Grid-to-Grid Model area-wide formulation offers a more flexible approach to forecasting at any grid outlet location, gauged or ungauged. There are significant opportunities to develop either approach as a basis for ungauged flood forecasting.

A further category of distributed hydrological model is offered by the *land surface scheme models* developed for interfacing to atmospheric models for national, regional and global application. A good example is offered by MOSES (Met Office Surface Exchange Scheme) and its development as MOSES-PDM to incorporate a Probability-Distributed Model of soil water capacity as an extension of the Richard's equation control of soil moisture. It has also been coupled to the Grid-to-Grid Model routing scheme to obtain area-wide indicative estimates of river flow. A strength of this approach for ungauged flood forecasting is that its formulation naturally lends itself to employ soil property information although this has not been fully exploited in practice. However, the model's use of a rather detailed vertical description of water movement, no explicit link to topographic control on runoff production, and absence of groundwater representation makes it of limited interest as an approach for ungauged flood forecasting purposes at catchment scales. The UK-wide grid-square estimates of runoff and river flow may have value in a Flood Watch context for providing a spatial indication of potential "hotspots", although at a coarse resolution. A more hydrologically-tailored distributed model approach is clearly called for to meet the requirements of flood forecasting for ungauged catchments.

A unified approach based on a kinematic wave representation of lateral soil drainage, saturation overland flow, channel flow and groundwater is being considered as one way forward, invoked as a variant of the Grid-to-Grid Model. The formulation allows for direct use of spatial datasets on properties of terrain, soil, land cover and geology. Model equations reduce to a simple nonlinear reservoir form applied within each grid-cell with parameters defined as physical properties appropriate to the process being

represented. Prototyping of this approach is in progress as a possible area-wide approach to flood forecasting for gauged and ungauged locations. Appendix D.7 presents some provisional results.

Channel flow routing models

Hydrological and hydrodynamic approaches to channel flow routing can usually be shown to have a common basis in the St. Venant equations, and though them to the physical properties of the river channel and its floodplain. As a consequence, application to ungauged river channels has a natural physical basis. However, even for the most refined hydrodynamic river model, channel geometry simplification and the inherently empirical nature of roughness normally means there is benefit in model calibration for gauged sites and transfer of the experience gained for application to ungauged reaches. Hydrological approaches combine simple mass balance water storage accounting with a simplified momentum equation linking channel storage to water level or flow. The simplifications involved can make the links to channel properties less direct in physical terms, but can ease practical application and the building up of experience for use in modelling ungauged reaches. Simpler hydrological approaches are normally preferred where backwater influences from tides, river controls and confluences are not dominant. The hydrodynamic approach is sometimes distinguished by models providing estimates of both river flow and level for situations where there is no unique relation between these two quantities. However, the distinction between hydrological and hydrodynamic (hydraulic) approaches is largely artificial with a spectrum of levels of simplification.

A popular method of hydrological routing is provided by the Muskingum scheme in which reach storage is a linear function of a weighted combination of the reach inflow and outflow. It is possible to relate this back to the underpinning St. Venant equation and in this way establish relations with channel properties applicable to ungauged reaches. There are different ways of doing this leading to different variants. For example, the Muskingum-Cunge method chooses a weighting that matches the numerical and physical diffusion whilst the mixing-cell approach uses a variable space-step to eliminate the diffusion term. As previously discussed, experience gained with "calibration" at similar gauged reaches will benefit application at ungauged reaches. Kinematic wave routing schemes can also be linked back to channel properties.

Hydrodynamic models

A number of off-the-shelf hydrodynamic models have been employed by the Environment Agency, but only ISIS and Mike11 are used in real-time to support flood warning. Whilst channel and floodplain property information can be used to set up a model for an ungauged reach, much can be gained from experience of model configuration and calibration for gauged reaches. This is particularly true of roughness parameters, initially inferred from field inspection in relation to published tables and photographs, where parameter calibration can prove of great benefit. This may also apply to other essentially empirical parameters such as weir, bridge and gate contraction coefficients.

Care needs to be exercised when transferring a hydrodynamic model developed for design studies to use in real-time, for both gauged and ungauged reaches. The full range of flows should be adequately modelled, computational problems should not arise at very low flows or during rapid fluctuations of river level, and opportunities for simplifying the model configuration need to be borne in mind.

Of major relevance to ungauged forecasting using hydrodynamic models is the need to pay appropriate attention to the modelling of ungauged lateral inflows. A false expectation of accuracy from the detailed configuration of a hydrodynamic model may arise if ungauged lateral inflows are significant and poorly represented. Methods for their estimation encompass the scaling, rainfall-runoff and channel flow routing approaches discussed previously.

Flood mapping tools

Flood mapping tools facilitate the mapping of water levels continuously over an area so the ungauged location is most typical. The tool may serve wholly as a visual display facility with the information mapped deriving from observed (remotely-sensed imagery) and/or modelled sources. The mapping tool may be provided as an intrinsic component of a 1-D or 2-D hydrodynamic river modelling system.

There is a developing opportunity for area-wide hydrological models to map inundation extent and depth at an indicative level and with UK coverage. The river flow volume along the entire river network can also be mapped in intensity-coded line form. Simple geomorphological relations on channel geometry linked to grid-to-grid flow routing models and DTMs provide the modelling support to such products.

10.4 Digital datasets to support modelling ungauged locations

Over the last decade the increased availability of digital spatial datasets on terrain and properties of soil, land cover and geology has revolutionised what is possible in hydrological modelling. The old practice of using time-consuming mapwork to derive properties, usually simplified to "catchment characteristics" to make the task bearable, had a huge influence on what could be done. Ungauged modelling approaches tended to be limited to lumped rainfall-runoff models and parameter regressions on catchment characteristics, which proved arduous but practical. As digital datasets became increasingly available, particularly Digital Terrain Models (DTMs), the first applications focussed on automating catchment characteristic derivation. There was inertia in moving on from the parameter regression approach which was now much easier to implement and opened up many opportunities to invent new characteristics aggregated to the catchment scale. The complexity of physics-based distributed models and disappointments in their performance for forecasting purposes were further reasons for digital datasets not being used as fully as possible in model formulation. There are now great opportunities to explore new conceptual-physical formulations linked directly to spatial datasets rather than to derived characteristics at the catchment scale.

Tables 5.1, 5.2 and 5.3 provide an inventory of spatial datasets that may be of value in support of modelling for ungauged flood forecasting purposes. These concern datasets on soil and geology, land cover and terrain respectively. The most useful soil datasets with England and Wales coverage are held by the National Soil Resources Institute (NSRI). Those of most interest to a physics-conceptual approach to modelling concern the more basic soil properties of saturated hydraulic conductivity, water content at field capacity, pore space, Integrated Air Capacity, and van Genuchten parameters. The HOST (Hydrology of Soil Types) are of lesser interest and emerged as a requirement of the "catchment characteristic" era of ungauged flood modelling, for which they continue to have value. Notable omissions from the list of advertised products are total soil depth and residual soil moisture content. These datasets are available at resolutions of 1, 2 or 5 km but only under license. Hydrological modellers only able to

utilise free products, or with global modelling interests, usually turn to the IGBP soil dataset with ~9 km resolution over the UK. This contains soil water content at field capacity and wilting point, available water capacity, saturated hydraulic conductivity and van Genuchten parameters. Model performance at the catchment scale in flood forecasting applications is likely to be compromised if the NSRI datasets are not used.

For land cover, the CEH land cover dataset available at 25m or 1 km resolution would be the first choice for use over England and Wales. Spatial-temporal datasets on remotely-sensed land properties are becoming available from operational satellites. Of particular interest to hydrological modelling is the MODIS/Aqua Leaf Area Index, updated every 8 days on a 1 km grid. This can have value in modelling seasonal variations in evaporation loss, for example from growing crops, that impact on the water balance and runoff production.

For terrain data, the natural choice for hydrological modelling over England and Wales is the IHDTM (Integrated Hydrological Digital Terrain Model). It is provided on a 50m grid and includes elevation, flow directions, cumulative drainage area and surface type. For hydrodynamic river modelling and floodplain mapping purposes the Environment Agency's LIDAR elevation dataset at 2m resolution has great value. The new NEXTMAP DTM at 5m resolution is of potential interest, and its utility for modelling requires investigation.

10.5 Statistical methods for forecasting

Statistical methods of forecasting are understood here to be empirical approaches leading to flexible forecasting rules with parameters that are calibrated using available data. They cover level-to-level correlation schemes, more generalised empirical forecasting schemes (including autoregressive flow predictors and neural network approaches) and the statistical simplification of hydrodynamic models (e.g. predictors based on tabulated "structure functions" obtained from a hydrodynamic river model) and hydrological models. Statistical forecasting methods are not natural candidates for forecasting at ungauged locations, since they depend on observations for parameter calibration and forecast construction. They are not considered further here.

10.6 Real-time updating techniques

Observations of river flow in real-time allow modelled flows for future times to be improved upon via real-time updating techniques. The most popular approaches are *state-correction* (where forecast errors are used to adjust model state values to achieve better agreement with observations) and *error prediction* (where dependence in errors over time is used to predict future errors). Updating normally requires observations being available for the target forecast site. However, it is feasible to consider the transfer of information from a gauged site to an ungauged target forecast site. This may involve the transfer of forecast errors at the gauged site to adjust forecasts from a model at the ungauged target site. There is clearly a risk in applying such *transferred-error* (inferred-error) updating schemes. In general, such schemes are best avoided until some successful experience in their use is first gained; a number of research opportunities have been identified.

An important exception to the above general advice is where a simple scaling or transposition approach is used as the inference model. The simple scaling of past flow observations and updated forecasts at a source gauged location to provide flow estimates at an ungauged target location is straightforward, but needs to be

undertaken with care and caution. The scaling factor can be defined in terms of the relative areas of the two catchments (and possibly SAARs). If the scaling factor is large, then the danger of amplifying forecast errors is likely to be greater and argue against use of the method.

The situation where transferred-error updating schemes are most likely to work is where an indirect modelling approach is used for the target ungauged location, where this location forms only part of a more extensive modelled area also containing river gauging stations. Any correction to modelled states for gauged sites are likely to form a useful basis for adjustment at ungauged sites, particularly if there is a physical basis to the model.

One updating approach identified as particularly deserving of further investigation, and applicable to transferred-error updating for ungauged locations, is the *two-pass state-correction* approach. This has potential for both rainfall-runoff and hydrological flow routing models. The approach is in some ways intermediate between error-prediction and state-correction schemes, and as such is particularly suited to situations where errors from conventional state-correction schemes are correlated over time (i.e. serially-correlated). The approach can also continue to correct model-states forward in time from the forecast time-origin. In the first pass, the model is run without state-correction to obtain simulation-mode error forecasts. The second pass includes state-correction based on an additive adjustment to the current state-set using a weighted sum of these simulation-mode errors. The corrected model states are used in the construction of forecasts at an ungauged location for which a similarly structured simulation model is applied.

10.7 Monitoring, forecasting and warning

Whilst the main attention here relates to modelling for ungauged locations, a few topics related to monitoring and flood warning deserve special mention in relation to ungauged areas. These concern areal rainfall estimation, remote-sensing, stage-discharge relations and trigger mechanisms for flood warning.

The method of *areal rainfall estimation* for catchment and grid-square domains can be of significant importance to forecast accuracy, for both gauged and ungauged areas. One aspect is the monitoring of rainfall by raingauge and weather radar networks, their quality control (QC) and their best use as separate or combined sensors of rainfall. A further, and related, aspect is the method of interpolation over space used to construct catchment and grid-square estimates of rainfall needed as input to lumped and distributed hydrological forecasting models. The Met Office Nimrod QC product provides a state-of-the-art rainfall product for Environment Agency use whilst CEH's Hyrad system provides facilities to visualise and to interface this rainfall product to modelling and forecasting systems. Methodologies for areal rainfall estimation, based on multiquadric surface fitting (and with links to Kriging methods), have been reviewed and shown to reduce to simple linear weightings of the rainfall sensor values for the spatial areas of interest (catchments or grid-squares).

Weather radar is a ground-based form of *remote sensing* configured for rainfall measurement. There are other important forms of monitoring by remote-sensing that are satellite-based. Some have already been commented on, especially as a source of elevation and land cover data. Whilst these datasets are often considered static, there is now increasing availability of time-history spatial datasets of leaf area index, snow cover, area of flood inundation and surface soil moisture. These have relevance both to the monitoring and modelling/forecasting of ungauged areas.

An exciting prospect is the ability to remotely sense river level (and width) from which to develop flow discharge estimates. However, the state-of-the-art suggests some progress with optical imagery for the larger rivers of the world but probably limited applicability for the scale of river encountered in the UK. A combination of GPS (global positioning system) technology and a tethered floating buoy has been investigated in field trials and through computer simulation of anticipated satellite position systems. This is now seen as emerging technology that has potential use for some ungauged locations in the UK as the supporting satellite network improves.

Stage-discharge relations for ungauged locations have importance in a number of situations, including their potential use with the remote sensing of river levels discussed above. Flow from a hydrological model of an ungauged site may require conversion to river level for flood warning purposes. A rating may need to be inferred from a hydrological model for a "level-only site" in order to calibrate the model and to use the levels for forecast updating in real-time. Procedures for embedding a stage-discharge relation within a hydrological model are available within CEH's Model Calibration environment. Standard procedures for extending rating curves at gauging stations, by hydraulic-geometry extrapolation and using hydrodynamic river models, have been reviewed by HR Wallingford for the Environment Agency. These procedures also have relevance for developing ratings at ungauged locations.

A key component of the flood warning operation is the *trigger mechanism* used to stimulate action in advance of flooding occurring. The mechanism might involve the crossing of a critical condition (e.g. bankfull discharge) at a location that is ungauged. The action may be to disseminate a flood warning or to upgrade the level of flood surveillance. The quality of the methods of forecasting for an ungauged site will clearly impact on the success of the action. Knowledge of the *uncertainty* associated with the forecast and consideration of the *costs of alternative actions* can form the scientific basis of effective *decision-making* for flood warning operations. Developing such an approach to decision-making is seen as an important future challenge and relevant to both gauged and ungauged locations at threat from flooding and requiring effective warning.

10.8 Practical illustration of some ungauged forecasting methods

To conclude this overview of operational guidelines, it is pertinent to consider providing an illustration of the practical application of selected methods of model transfer to ungauged catchments. The focus of the report has been on reviewing existing methods, as well as considering new improved ones, and not in providing examples of their practical application. To provide more practical guidance, Appendix D considers a selection of methods of model transfer to ungauged catchments and uses case study catchments to illustrate their application. This appendix thereby serves to provide practical guidance on the application of a selection of methods considered in this report, some in prototype form. It does not aim to be comprehensive and is limited to examples of rainfall-runoff model transfer and their simulation performance, excluding consideration of the real-time updating of flood forecasts by transfer methods.

11 Conclusions and recommendations

This section provides a thematic summary of the main conclusions of the report relevant to flood forecasting at ungauged locations. Some of these conclusions are in the form of recommendations for operational practice or for further research.

Modelling approaches for ungauged locations

(1) The appropriate choice of modelling approach will depend on the nature of the ungauged location and the extent and type of data available.

(2) Simple scaling and transposition approaches are well established, routinely used and may suffice in some situations.

(3) Application of rainfall-runoff models to ungauged locations for flood forecasting is not routine. Well developed methodologies are rare.

(4) Simple transfer of rainfall-runoff models from neighbouring or similar sites can prove practical. Experience needs to be gained through trial transfers, using gauged sites as if they are ungauged, for given areas of application.

(5) Relating rainfall-runoff model parameters to catchment properties via regression is a popular method used in flood design applications. However, the performance may not be acceptable for use in flood forecasting and warning, particularly for more complex responding catchments. This results from model simplification and often rather weak empirical regression relations. Using a site-similarity-approach, in place of regression, makes little difference.

(6) Rainfall-runoff models developed to have more direct physical-conceptual links to land properties (terrain, land cover, soil, geology) are seen as the way forward. Such model formulations do not suffer from the need to start with catchment-aggregated properties commonly referred to as "catchment characteristics".

(7) Physical-conceptual distributed models employing a grid-to-grid flow routing structure and kinematic representations of lateral soil drainage, surface and subsurface runoff and channel flow are naturally suited for area-wide hydrological forecasting across both gauged and ungauged locations. It is recommended that further research on this type of model should be undertaken.

(8) Channel flow routing models normally result from simplifications of the St. Venant equations for open channel flow. This provides a theoretical basis for relating model structure and parameters to properties of the river channel and its floodplain for application to ungauged river reaches. However, on account of the simplifications involved and the essentially empirical nature of roughness, there is a need to complement the theory with experience of a model's application to similar river reaches.

(9) Hydrodynamic river models are normally applied where backwater influences are significant, such as in tidal rivers, in the vicinity of river controls and where a forecast location is on a tributary under the backwater control of the receiving river. Models of

this type are configured to make direct use of geometry and material properties of the river and are naturally suited to application to ungauged river reaches. However, experience with gauged reaches is likely to prove very valuable in setting roughness parameters and for compensating for simplifications in model configuration.

(10) The accuracy of channel flow routing and hydrodynamic river models can be greatly influenced by the method of estimation of ungauged lateral inflows. Suitable methods may include simple scaling of a nearby gauged tributary inflow or a rainfall-runoff model for the ungauged inflow catchment.

Some Specific Modelling Tools

More specific conclusions and recommendations can be made in relation to specific models, especially those in operational use by the Environment Agency and reviewed here in more detail. They are treated thematically under the headings: lumped rainfall-runoff models, distributed hydrological models, channel flow routing models and hydrodynamic river models. Flood mapping tools are treated under a separate heading.

(a) Lumped rainfall-runoff models

(1) The main rainfall-runoff models employed for flood forecasting by the Environment Agency, and given special attention here, are: Thames Catchment Model or TCM, Midlands Catchment Runoff Model (MCRM), the PDM (Probability Distributed Model), the Isolated Event Model (IEM), the ISO (Input-Storage-Output) Model, the NAM model, and forms of Transfer Function Models. Some rainfall-runoff models developed for design use in the UK - associated with the Flood Studies Report, Flood Estimation Handbook and follow-on work – have also been given special consideration.

(2) Many brand-name rainfall-runoff models share common elements. Thus rather general conclusions relating to their suitability for application to ungauged areas can be made.

(3) Conceptual rainfall-runoff models that can accommodate a range of hydrological behaviours normally contain a reasonable number of parameters. These parameters are often interdependent and only weakly related to aggregated catchment properties ("catchment characteristics"). Simple empirical "regionalisation" procedures - based on forms of regression or site-similarity methods linking model parameters to catchment characteristics – can be limited in the performance they can achieve, particularly for more complex catchments. Such methods have been applied to simplified forms of the MCRM and PDM models.

(4) Only one of the models considered in detail, the TCM, is configured to have spatial response zones within which a hydrological response model operates. This formulation is used to represent parallel flow responses from say aquifer, clay and riparian areas. The result is an overall model with many parameters and having great interdependency across zones. However, application to ungauged areas is less difficult than might be imagined as the response zones can be made to operate in hydrological sensible ways in the hands of an experienced modeller. Transfer of experience from modelling similar catchments in the same region can prove particularly valuable. Digital datasets can be used to support assignment of response zone areas.

(5) The physical-conceptual nature of the PDM and its intermediate level of complexity offer some hope of successful application to ungauged sites. Each of the model parameters has a clear physical meaning that invites attempts to establish physically-

based linkages with data on soil and geological properties, land cover, topography and stream network topology. However, to date, there has been no systematic attempt to do this. Only simple empirical regionalisation approaches using aggregated catchment properties have been considered: these have achieved some success, but usually where the catchment response is relatively simple. Some ideas for advancement have been set down in this Report and are recommended for further investigation. These ideas also have relevance to other forms of conceptual rainfall-runoff model, both of lumped and distributed form.

(6) The Transfer Function or TF model when viewed as a pure black-box model is arguably the antithesis of a suitable model for ungauged catchments. However, simple forms of TF model can be related to physical-conceptual models representing the storage and release of water in soils, groundwater and river channels. This can be used to support parameter estimation using properties of soil, geology and topography. Also simple forms of TF model, including certain unit hydrograph (UH) forms, are characterised by a small number of basic characteristics that lend themselves to empirical regionalisation approaches. However, progress is more likely to be made by recognising that TF and UH models provide the storage routing function of a more complete conceptual rainfall-runoff model incorporating runoff production and the principle of water mass balance. The ReFH, as a reformulation of the FSR and FEH rainfall-runoff method for design use, provides a good example of such an approach. It combines a simple kinked-triangle UH routing function with a PDM-type runoff production function. However, empirical regionalisation of the ReFH parameters has proved rather weak.

(b) Distributed hydrological models

(1) Physically-based distributed models, such as the SHE and the IHDM, employ nonlinear partial differential equation descriptions of key physical processes that are solved numerically on a finite difference grid or finite element mesh. Their performance will necessarily be constrained by the real complexity of hydrological systems above and below ground, the data support available, and the approximations involved in the process representation and numerical solution. Experience with models of this type indicates their value is greatest where there is a need to understand the impact of some future change within a catchment, particularly relating to land cover or land management. Application of such models for real-time flood forecasting is less likely to prove worthwhile. The complexity of model formulation can raise false expectations of model accuracy. Simpler physical-conceptual distributed models are easier to apply, can give as good if not better performance, and are generally preferred for flood forecasting application.

(2) The CEH Grid Model is a distributed physical-conceptual rainfall-runoff model configured on a regular square grid. It uses a source-to-sink formulation in which water flows are routed directly to the basin outlet: it is efficient to apply to specific catchments. In contrast, the CEH Grid-to-Grid Model uses an area-wide formulation in which water flows are routed from grid to grid making it easy to output water flows at any set of locations, gauged or ungauged. In other respects the models are similar and provide modelling environments within which alternative runoff production functions operating within each grid-square can be formulated and trialled. Both flow routing and runoff production formulations are chosen to be physical-conceptual in nature so that they can be supported by digital datasets on elevation, soil and geological properties, and land cover. When configured on the weather radar network grid, such models can exploit the benefits of grid-square radar rainfall estimates to the full. Models of this type provide an attractive way of addressing the ungauged forecasting problem. It is recommended that further work is undertaken on alternative formulations leading to a

prescription for operational use. Some ideas for improved model formulations, relating especially to lateral drainage and groundwater, have been identified as deserving of further research.

(3) The land surface scheme, MOSES-PDM, used in combination with the Grid-to-Grid flow routing scheme provides estimates of soil moisture, evaporation, runoffs and routed river flows with UK-coverage on an operational basis. Although not well-suited to the ungauged forecasting problem at a detailed level, these estimates are likely to prove of value in a Flood Watch context.

(4) Ideas for improved runoff production and flow routing schemes that enjoy physically based linkages with topography (though the influences of terrain slope and water pathway topology), soil properties and land cover have been considered in some detail. New kinematic representations of lateral soil drainage, surface runoff and channel flow together with consideration of groundwater transfers need to be investigated within the Grid-to-Grid modelling framework. This is an area where real progress on the ungauged forecasting problem can be made. It can be seen as a move away from the empirical regionalisation approaches towards one with a sounder scientific basis and more robust and accountable performance.

(c) Channel flow routing models

(1) Channel flow routing models have a common basis in the St. Venant equations and their simplification. This provides a formal link to channel properties, concerning geometry and resistance (roughness), and a sound basis for application to ungauged channel reaches. Simplifications of representation and of channel geometry, together with the essentially empirical nature of roughness, means that their will normally be benefit in model calibration at gauged sites and transfer of this experience to ungauged sites. This applies even for the most refined hydraulic models.

(2) A new Mixing–Cell variant of the Muskingum Method is introduced as a good example of a simplified routing scheme derived from the St. Venant equations that is well suited for application to ungauged river reaches. The model is configured using the following channel properties: bottom slope, roughness, cross-section shape and reach length. The practical application of this method deserves further investigation, and compared with the commonly used Muskingum-Cunge method.

(d) Hydrodynamic models

(1) The Environment Agency has commissioned a number of investigations under the "Benchmarking of Hydraulic Models" project to which the reader is referred for more detail of the differences between different model codes. The main model codes adopted for use by the Environment Agency are ISIS, Mike-11 and HEC-RAS. The main differences, apart from computational methodology, affect the handling of river channel water transfers, sinuosity, static water bodies, channel roughness, wind drag, river structures and out-of-bank flows. Because of their sound physical basis, they are well suited for application to ungauged rivers. However, the simplification of flow process representation and configuration combined with the essentially empirical nature of roughness makes model calibration desirable at gauged sites, transferring the experience gained to ungauged site applications.

(2) The method of estimation of ungauged lateral inflows to river reaches represented by a hydrodynamic model may prove critical to forecast performance, if these inflows account for a significant water volume in relation to those in the receiving stream. The

detail of the hydrodynamic modelling may raise false expectations of model performance in such situations.

(3) Special considerations need to be applied when transferring a hydrodynamic model configured for design use to one to be used in real-time flow forecasting. This includes ensuring good performance is maintained over the full flow range, possibly requiring the addition of nodes and river structures to deal with low river-levels, and the removal of detail important only to the design study.

(e) Flood mapping tools

(1) Animated spatial displays of observed and modelled water levels are useful to depict the spatial extent and severity of flood inundation. It is common for some form of GIS (Geographical Information System) to be used to provide this functionality. The degree to which the GIS itself is used for inference of mapped information or an external model or observations will depend on the detail of the application.

(2) While flood mapping tools are commonly used with 1-D, 2-D and 3-D hydrodynamic model outputs, there is also great scope to use distributed hydrological forecasting model outputs to produce spatial maps of river flow, flood inundation and related quantities over time. Some early prototyping of these opportunities has been done using the Grid-to-Grid hydrological model. Model outputs in gridded form are exported to HYRAD and displayed as animated images of river flows propagating down the modelled river network along with fields of soil moisture deficit and local runoff. Also, time-series hydrographs can be extracted and viewed for any location (gauged or ungauged) down the river network. Further work leading to operational implementation is recommended here.

Digital Datasets to Support Modelling Ungauged Locations

(1) A key growth area is the use of spatial digital datasets on elevation, soil and geology properties and land cover to underpin the configuration and parameterisation of process-based hydrological forecasting models, making them suited for application to ungauged locations. A review of relevant spatial datasets is provided in support of this modelling activity. These extend to include certain space-time datasets from satellite sensors: for example leaf area index (relevant to seasonal land cover effects on water balance) and processed images of flooded areas (useful for inundation model assessment purposes).

Statistical methods for forecasting

(1) Statistical methods for forecasting are understood here to involve empirical model building resulting in a flexible forecasting rule with parameters that are calibrated using available data. They are essentially empirical methods, in contrast to the hydrological and hydrodynamic process-based mathematical models. Because of their dependence on observed data, they are not immediately applicable to ungauged forecasting: methods of transfer to the ungauged target site are required.

(2) Level-to-level correlation is arguably one of the best known and simplest statistical methods for forecasting, and usually focuses on forecasting peak river levels. When applied to gauged reaches upstream and downstream of a target ungauged location, a transfer method based essentially on interpolation (possibly incorporating a datum adjustment and time shift) can be devised for ungauged forecasting.

(3) Empirical forecast rules need not be limited to those based on linear functions, and may extend to embrace neural network methods for example.

(4) A hydrodynamic model configured for a river reach using known channel properties can be used to produce river level/flow outputs for ungauged locations from which a simplified empirical forecasting model may be derived. The simple predictive relationships so-derived may be of value in bringing computational savings or as the basis of a back-up manual forecasting procedure. The methodology can also be used to extend the range of extremes experienced beyond those contained in historical records. Tabular "Structure Functions" derived from hydrodynamic model runs can be of value in forecasting peak water levels along a tidal estuary from upstream river flow and downstream peak tidal level.

Real-time updating techniques

(1) Transferring forecast errors from gauged to ungauged catchments is not recommended for routine use at the present time. Research is required on possible techniques leading to recommendations for operational use. One exception to this is the use of transferred-errors where the target location is modelled using a simple scaling or transposition approach. Even in this case, care needs to be exercised in the choice of suitable situations and the method of application.

(2) Research needs to be carried out on transferred-error updating schemes to gain experience that can be carried through to operational use. A particular priority is to investigate the two-pass state-correction approach to forecast updating. This provides an intermediate approach between error-prediction and state-correction and can be used to continue to correct states forwards in time from the time-origin of the forecast. It is applicable to both rainfall-runoff and channel flow routing models.

(3) The promise of improved forecasting at ungauged locations using physical-conceptual distributed models configured on a gridded domain encompassing gauged sites argues for research on real-time updating techniques for such models. There has been little progress to date in this challenging area.

Monitoring, Forecasting and Warning

(1) The method of areal rainfall estimation can be a major influence on the performance of rainfall-runoff models. Correction (quality-control) of radar data and their combination with raingauge data can significantly improve the robustness and accuracy of rainfall estimates for catchment and grid-square areas. Some procedures for combining raingauges alone, and radar data in combination with raingauges, are reviewed here for guidance when applying rainfall-runoff models.

(2) Remote sensing has proved particularly valuable in providing elevation and land cover data with wide-area coverage and improved resolution and accuracy. These data are invaluable to the configuration and parameterisation of flood forecasting models in ungauged areas. Some space-time satellite datasets can be of value to model assessment (flood inundation extent for example) and in support of time-varying parameterisations (leaf area index for example).

(3) The remote sensing of water level offers the prospect of remotely inferred river levels and flows of use in flood forecasting for any location. There has been some

progress of use for the larger rivers of the world but the approach has little applicability for UK conditions at the present time. GPS technology used in combination with a tethered buoy offers the potential of a low-cost gauging method: satellite developments in the future may eventually make this worth considering for application in the UK.

(4) An ungauged site may have no measurement at all or a measurement of river level but no rating curve (a level-only site). Where a rating is required then the Environment Agency's best practice guidance manual on "Extension of rating curves at gauging stations" provides a convenient reference source for developing rating curves using simple hydraulic techniques or computational hydraulic models. The CEH Model Calibration Environment supporting the KW, PDM and PSM (TCM and IEM) models also provides facilities to embed an unknown rating curve within the model formulation.

(5) The Environment Agency's "A best practice guide to the use of trigger mechanisms in fluvial flood warning" provides advice on setting a trigger mechanism to stimulate action in advance of a flood. The information used may concern observations and/or forecasts of river level or flow. Such information may be provided for ungauged sites using the methodologies outlined in this report, with the appropriate degree of caution. This highlights the need for research on assessing the uncertainty of forecasting at ungauged sites, on the costs of alternative actions, and on placing decision-making for flood warning on a sounder scientific footing.

Closing remarks

The ungauged flood forecasting problem is at the heart of hydrological science and its application. As such, it is a problem that is being addressed by many researchers and practioners across the globe in different ways. A recent perspective on issues in flood forecasting for ungauged basins, with UK applications, was presented at the Kovacs Colloquium on 'Frontiers in Flood Research' (Moore *et al.*, 2006).

One mechanism for co-ordinating this global activity has been provided by the International Association of Hydrological Sciences (IAHS) declaring 2003-2012 as the IAHS Decade on Predictions in Ungauged Basins with the acronym PUB. The PUB forum provides an opportunity to share ideas at specialist workshops, such as that held in Perth in February 2004 (Franks *et al.*, 2005). Conclusions of this workshop, of particularly relevance here, were the need for (i) data at nearby or similar sites, (ii) improved process-based models to reduce the reliance on data elsewhere, (iii) intercomparison and integration of diverse techniques as a means of improving estimation, and (iv) quantification of uncertainty of estimates to assess their worth for application.

Of especial interest to improvements in modelling is the DMIP (Distributed Model Intercomparison Project) in the USA (Smith *et al.*, 2004) which has now entered a second phase.

In the UK, the Natural Environment Research Council's FREE (Flood Risk from Extreme Events) initiative has ungauged flood forecasting as an important component of its 5 year Science Plan with implementation starting in 2006.

It will be important to engage in and monitor such national and international activities to ensure knowledge transfer of useful outcomes to operational practice in flood forecasting and warning for ungauged locations.

References

Abbott, M.B., Bathurst, J.C., Cunge, J.A., O'Connell, P.E. & Rasmussen, J. 1986. An introduction to the European Hydrological System - Système Hydrologique Europèen "SHE", 2: Structure of a physically-based distributed modelling system. *Journal of Hydrology*, **87**, 61-77.

Balascio, C.C. 2001. Multiquadric equations and optimal areal rainfall estimation. *J. Hydrologic Engrg.*, 6(6), 498-505

Barnes 1967. Roughness characteristics of natural channels. US Geological Survey, Water Supply Paper No. 1849, US Government Press.

Bell, V.A. and Moore, R.J. 1998a. A grid-based distributed flood forecasting model for use with weather radar data: Part 1. Formulation. *Hydrol. Earth System Sci.*, **2(2-3),** 265-281.

Bell, V.A. and Moore, R.J. 1998b. A grid-based distributed flood forecasting model for use with weather radar data: Part 2. Case Studies. *Hydrol. Earth System Sci*, **2(2-3)**, 283-298.

Bell, V.A. and Moore, R.J. 2004. *A flow routing and flood inundation facility for Nimrod/CMetS.* Report to the Met Office, CEH Wallingford, 56 pp.

Bell, V.A., Moore, R.J. and Jones, R.G. 2004. *Flow Routing for Regional Climate Models: UK application*. Final report to the Hadley Centre, CEH Wallingford, 124pp.

Benning, R.G. 1995. *Towards a new lumped parameterisation at catchment scale.* Report 54, Department of Water Resources, Agricultural University, Wageningen, 60pp plus Appendices and Tables.

Beven, K. 1985. Distributed models. In: *Hydrological Forecasting* (Ed. M.G. Anderson and T.P. Burt), Chapter 13, J. Wiley, 405-435.

Blyth, E. 2002. Modelling soil moisture for a grassland and woodland site in south-east England. *Hydrol. Earth System Sci.*, **6(1)**, 39-47.

Boorman, D.B., Hollis, J.M. and Lilly, A. 1995. Hydrology of soil types: a hydrologically based classification of the soils of the United Kingdom. *IH Report No. 126*, Institute of Hydrology, Wallingford, 137pp.

Box, G.E.P. and Jenkins, G.M. 1970. *Time series analysis forecasting and control*, Holden-Day.

Brakenridge, G. R., Tracy, B. T., and Knox, J. C. 1995. Orbital SAR remote sensing of a river flood wave. *International Journal of Remote Sensing*, **19**, 1439-1445.

Brooks, R.H. and Corey, A.T. 1964. Hydraulic properties of porous media. Hydrol. Paper 3, Colorado State University, Fort Collins, USA.

Brunsdon, G.P. and Sargent, R.J. 1982. The Haddington flood warning system. Advances in Hydrometry (Proc. Exeter Symp.), *IAHS Publ. no. 134*, 257-272.

Cadman, D. and Moore, R.J. 1998. *A Best Practice Guide to the Use of Trigger Mechanisms in Fluvial Flood Warning*. EA File Ref: 674/14, Version 3, Draft Final, Flow & Level Forecasting Project, Environment Agency, 27pp.

Calver, A., Crooks, S., Jones, D., Kay, A., Kjeldsen, T. and Reynard, N. 2005. National river catchment flood frequency method using continuous simulation. Volume 1: Main Report. *R&D Technical Report FD2106*, Research Contractor: CEH Wallingford, Defra/EA Flood and Coastal Defence R&D Programme, Department for Environment, Food & Rural Affairs, 136pp.

Calver, A., Lamb, R., Kay, A.L. and Crewett, J. 2001. *The continuous simulation method for river flood frequency estimation.* Defra Project FD0404 Final Report, CEH Wallingford.

Central Water Planning Unit 1977. *Dee Weather Radar and Real-time Hydrological Forecasting Project*. Report by the Steering Committee, 172 pp.

CEH Wallingford, 2005a. *KW Channel Flow Routing Model.* Version 2.2, Centre for Ecology & Hydrology, Wallingford. (Includes Guide, Practical User Guides, User Manual and Training Exercises).

CEH Wallingford, 2005b. *PDM Rainfall-Runoff Model*. Version 2.2, Centre for Ecology & Hydrology, Wallingford. (Includes Guide, Practical User Guides, User Manual and Training Exercises).

CEH Wallingford, 2005c. *PSM Rainfall-Runoff Model*. Version 2.2, Centre for Ecology & Hydrology, Wallingford. (Includes Guide, Practical User Guides, User Manual and Training Exercises)

Chaudhry, M.H. 1983. *Open-channel flow*. Prentice-Hall, New Jersey, 483pp.

Chow, V.T. 1959. *Open-channel hydraulics*. International Student Edition, McGraw-Hill, 680pp.

Clapp, R.B. and Hornberger, G.M. 1978. Empirical equations for some soil hydraulic properties. *Water Resour. Res*., **14(4)**, 601-604.

Cox, P.M., Betts, R.A., Bunton, C.B., Essery, R.L.H., Rowntree, P.R. and Smith, J. 1999. The impact of new land surface physics on the GCM simulation of climate and climate sensitivity. *Climate Dynamics*, **15**, 183-203.

Crowder, R.A., Pepper, A.T., Whitlow, C., Sleigh, A., Wright, N. and Tomlin, C. 2004. Benchmarking of hydraulic river modelling software packages: Project Overview. *R&D Technical Report W5-105/TR0*, Environment Agency, Bristol, 14pp plus Appendix.

Cunge, J.A. 1969. On the subject of a flood propagation computation method (Muskingum Method). *J. Hydaulic Res.*, **7(2)**, 205-230.

De Roo, A.P.J, Bartholmes, J., Bates, P.D., Beven, K., Bongioannini-Cerlini, B., Gouweleeuw, B., Heise, E., Hils, M., Hollingsworth, M., Holst, B., Horritt, M., Hunter, N., Kwadijk, J., Pappenburger, F., Reggiani, P., Rivin, G., Sattler, K., Sprokkereef, E., Thielen, J., Todini, E. and Van Dijk, M. 2003. Development of a European Flood Forecasting System. *International Journal of River Basin Management,* **1**, 49-59.

Ding, J.Y. 1967. Flow routing by direct integration method. *Proc. Int. Hydrology Symp., Fort Collins*, 1, 113-120.

Dooge, J.C.I. 1973. Linear theory of hydrologic systems. *Technical Bulletin No. 1468*, Agriculture Research Service, United States Department of Agriculture, U.S. Government Printing Office, Washington, DC20402, USA, 327 pp.

Dooge, J.C.I. and O'Kane, J.P. 2003. Deterministic methods in systems hydrology. IHE Delft Lecture Note Series, A.A Balkema Publishers, 309pp.

Dunne, T. and Leopold, L.B. 1978. *Water in Environmental planning.* W.H. Freeman, San Francisco, 818pp.

Fekete, B.M., Vörösmarty, C.J. and Lammers, R.B. 2001. Scaling gridded river networks for macroscale hydrology: Development, analysis, and control of error. Water Resources Research, 37(7), 1955-1967.

Franks, S.W., Sivapalan, M., Takeuchi, K. and Tachikawa, Y. (eds.) 2005. Predictions in ungauged basins: international perspectives on the state of the art and pathways forward. *IAHS Publ. 301*, 348pp.

Fread, D.L. 1985. Channel routing. In: *Hydrological Forecasting* (Ed. M.G. Anderson and T.P. Burt), Chapter 14, J. Wiley, 437-504.

Greenfield, B.J. 1984. *The Thames Water Catchment Model.* Internal Report, Technology and Development Division, Thames Water, UK.

Nash, J.E. 1960. A unit hydrograph study with particular reference to British catchments. *Inst. Civil Engin. Proc.*, 17, 249-282.

Harpin, R., Webb, D.R., Whitlow, C.D., Samuels, P.G. and Wark, J.B. 1995. Benchmarking of Hydraulic Models: Stage One - Final Report. *R&D Project Record 508/ST/2*, National Rivers Authority, Bristol, 129pp.

Herschy, R.W. 1999. *Hydrometry. Principles and Practices.* 2nd edition, Wiley, 376pp.

Horton, R.E. 1938. The interpretation and application of runoff plot experiments with reference to soil erosion problems. *Soil Sci. Soc. Am., Proc.*, **3**, 340349.

Horton, R.E. 1945. Erosional development of streams and their drainage basins: hydrophysical approach to quantitative morphology. *Bull. Geol. Soc. America*, **56**, 275-370.

Houghton-Carr, H. 1999. *Flood Estimation Handbook. Volume 4 Restatement and application of the Flood Studies Report rainfall-runoff method.* Institute of Hydrology, 288pp.

Hundecha, Y. and Bardossy, A. 2004. Modeling of the effect of land use changes on the runoff generation of a river basin through parameter regionalisation of a watershed model. *J. Hydrol.*, **292**, 281-295.

Jones, D.A. and Moore, R.J. 1980. A simple channel flow routing model for real-time use. Hydrological Forecasting, Proc. Oxford Symp., April 1980, *IAHS Publ. No. 129*, 397-408.

Kjeldsen, T.R., Stewart, E.J., Packman, J.C., Folwell, S.S. and Bayliss, A.C. 2005. Revitalisation of the FSR/FEH Rainfall-Runoff model. *R&D Technical Report FD1913*, Joint Defra/EA Flood and Coastal Erosion Risk Management R&D Programme, Department for Environment, Food & Rural Affairs, 234pp.

Lambert, A.O. 1972. Catchment models based on ISO-functions. *J. Instn. of Water Engineers*, **26**, 413-422.

Liu, Z. Martina, M.L.V. and Todini, E. 2005. Flood forecasting using a fully distributed model: application of the TOPKAPI model of the Upper Xixian Catchment. *Hydrol. Earth System Sci.*, **9(4)**, 347-364.

Liu, Z. and Todini, E. 2002. Towards a comprehensive physically-based rainfall-runoff model. *Hydrol. Earth System Sci.*, **6(5)**, 859-881.

Mandeville, A.N. 1975. *Non-linear conceptual catchment modelling of isolated storm event*, PhD thesis, University of Lancaster.

Moore, R.J. 1985. The probability-distributed principle and runoff production at point and basin scales. *Hydrol. Sci. J.*, **30(2)**, 273-297.

Moore, R.J. 1986. Advances in real-time flood forecasting practice. *Symposium on Flood Warning Systems*, Winter meeting of the River Engineering Section, Inst. Water Engineers and Scientists, 23 pp.

Moore, R.J. 1999. Real-time flood forecasting systems: Perspectives and prospects. In: R. Casale and C. Margottini (eds.), *Floods and landslides: Integrated Risk Assessment*, Chapter 11, 147-189, Springer.

Moore, R.J. 2006. The PDM rainfall-runoff model. *Hydrol. Earth System Sci.*, **10**, in press.

Moore, R.J. and Bell, V.A. 2001. Comparison of rainfall-runoff models for flood forecasting. Part 1: Literature review of models. *Environment Agency R&D Technical Report W241*, Research Contractor: Institute of Hydrology, September 2001, Environment Agency, 94pp.

Moore, R.J. and Bell, V.A. 2002. Incorporation of groundwater losses and well level data in rainfall-runoff models illustrated using the PDM. *Hydrol. Earth System Sci.*, **6(1)**, 25-38.

Moore, R.J., Bell, V.A. and Carrington, D.S. 2000. Intercomparison of rainfall-runoff models for flood forecasting. In: M. Lees and P. Walsh (eds.), *Flood forecasting: what does current research offer the practitioner?* Occasional Paper No. 12, British Hydrological Society, 69-76.

Moore, R.J., Cole, S.J., Bell, V.A. and Jones, D.A. 2006. Issues in flood forecasting: ungauged basins, extreme floods and uncertainty. In: I. Tchiguirinskaia, K. N. N. Thein & P. Hubert (eds.), Frontiers in Flood Research, 8th Kovacs Colloquium, UNESCO, Paris, June/July 2006, *IAHS Publ. 305*, 103-122.

Moore, R.J. and Jones, D.A. 1978. An adaptive finite-difference approach to real-time channel flow routing. In: Vansteenkiste, G.C. (ed.), *Modelling, Identification and Control in Environmental Systems*, North-Holland, Amsterdam, The Netherlands, 153-170.

Moore, R.J., Watson, B.C., Jones, D.A. and Black, K.B. 1989. *London weather radar local calibration study: final report.* Contract report prepared for the National Rivers Authority Thames Region, Institute of Hydrology, 85pp.

Morris, D.G. and Flavin, R.W. 1990. A digital terrain model for hydrology. *Proc. 4th Internat. Symp. on Spatial Data Handling*, 23-27 July, Zürich, Vol. 1, 250-262.

NERC 1975. *Flood Studies Report. Volume 1 Hydrological Studies.* Natural Environment Research Council, 550pp.

O'Connor, K.M. 1982. Derivation of discretely coincident forms of continuous linear time-invariant models using the transfer function approach, *J. Hydrol.*, **59**, 1-48.

Oliver, F., Famiglietti, J. and Asante, K. 2000. Global-scale flow routing using a source-to-sink algorithm. *Water Resour. Res.*, **36(8)**, 2197-2207.

Or, D. and Wraith, J.M. 2002. Soil water content and water potential relationships. In: Warrick, A.W. (ed.), *Soil physics companion*, CRC Press, Boca Rouge, 49-84.

Pegram, G. C. and Pegram, G. G. S. 1993. Integration of rainfall via multiquadric surfaces over polygons. *J. Hydr. Engrg.*, 119(2), 151-163

Ramsbottom, D.M. and Whitlow, C.D. 2003. Extension of rating curves at gauging stations. Best Practice Guidance Manual. *R&D Manual W6-061/M*, Research Contractor: HR Wallingford in association with Eden Vale Modelling Services, Environment Agency, 254pp

Rossiter, D.G. (2004). Digital soil resource inventories: status and prospects. *Soil Use & Management,* **20 (2),** in press.

Singh, V.P. (ed.) 1995. *Computer models of watershed hydrology.* Water Resources Publications, Colorado, USA, 1130.

Smith, R.N.B., Blyth, E.M., Finch, J.W., Goodchild, S., Hall, R.L. and Madry, S. 2006. Soil state and surface hydrology diagnosis based on MOSES in the Met Office Nimrod nowcasting system. *Meteorol. Appl.*, **13**, 89–109.

Smith, M.B., Georgakakos, K.P., and Liang, X.(eds.) 2004. The Distributed Model Intercomparison Project (DMIP). Special Issue, *J. Hydrol.*, **298**(1-4), 1-334.

Smith, R.E and Hebbert, R.H.B. 1983. Mathematical simulation of independent surface and subsurface hydrologic processes. *Water Resources Research*, **19(4)**, 987-1001.

Soile, P. 2004. Optimal removal of spurious pits in grid digital elevation models. *Water Resour. Res.*, **40**, W12509, 10.1029/2004WR003060.

Sturm, T.W. 2001. *Open channel hydraulics.* McGraw-Hill, 493pp.

Todini, E. 1995. New trends in modelling soil processes from hillslope to GCM scales. In: H.R. Oliver and S. A. Oliver (eds.), *The role of water and the hydrological cycle in global change.* NATO ASI Series, Vol. I 31, 317-347, Springer-Verlag.

Van Genuchten M.T. 1980. Predicting the hydraulic conductivity of unsaturated soil. *Soil Sci. Soc. Am. J.* **44,** 892–898.

Wagener, T., Wheater, H.S. and Gupta, H.V. 2004.Rainfall-runoff modelling in gauged and ungauged catchments. Imperial College Press, London, 306pp.

Wang, G.-T., Yao, C., Okoren, C. and Chen, S. 2006. 4-point FDF of Muskingum method based on the complete St Venant equations. *J. Hydrol.*, **324**, 339-349.

Werner, P.H. and Sundquist, K.J. 1951. On the groundwater recession curve for large watersheds, Proc. AIHS General Assembly, Brussels, Vol. II, *IAHS Pub. No. 33*, 202-212.

Zhang, J., Xu, K., Watanabe, M., Yang, Y. and Chen, X. 2004. Estimation of river discharge from non-trapezoidal open channel using QuickBird-2 satellite imager. *Hydrol. Sci. J.*, 49(2), 247-260.

Appendix A Probability-distributed runoff production scheme for grid models

A.1 Introduction

This appendix sets down the probability-distributed runoff production scheme employed within the Grid Model (Bell and Moore, 1998) and currently used within the Grid-to-Grid Model. The scheme is based on the use of a probability-distributed store within a model grid-square to control runoff production, soil water storage, drainage and evaporation. The basic Grid Model runoff-production scheme is first outlined in Section A.2. The probability-distributed scheme is developed as a variant of this in Section A.3.

A.2 Basic runoff production scheme

For a given grid square, the following linkage function is used to relate the maximum water storage capacity, S_{max}, and the average topographic gradient, $\overline{g}$, within the grid square:

$$S_{max} = c_{max}\left(1 - \frac{\overline{g}}{g_{max}}\right), \tag{A.1}$$

for $\overline{g} \le g_{max}$. The parameters g_{max} and c_{max} are upper limits of gradient and storage capacity respectively and act as "regional parameters" for the runoff-production model. An estimate of mean slope for each grid square can be obtained from a DTM. In turn, this allows values for the structural parameter S_{max} for all grid squares to be determined using only the two regional parameters, g_{max} and c_{max}.

The soil column loses water as runoff, drainage and evaporation, as indicated in Figure A.1. If the column is fully saturated from previous rainfall, then further addition of rain
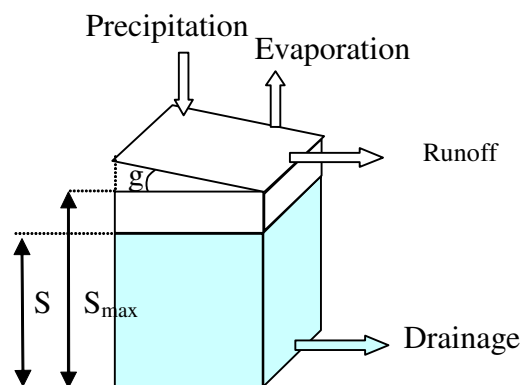
Figure A.1 A typical grid-box storage illustrating the components of the water balance

spills over as runoff and is routed via fast pathways. Drainage from the base of the column is dependent on the volume of water stored, S, and is routed via slow pathways. Finally, water is lost from the top of the column via evaporation.

Specifically a water balance is maintained for each grid square and time interval (ignoring time and space subscripts for notational simplicity) as follows. Evaporation loss from the soil column occurs at the rate, E_a, which is related to the potential evaporation rate, E, through the relation

$$E_a = E\left\{1 - \left(\frac{S_{max} - S}{S_{max}}\right)^2\right\} \tag{A.2}$$

where S is the depth of water in store. Drainage from the grid-box occurs at the rate

$$d = \begin{cases} k_d(S - S_t)^\beta, & S - S_t > 0, \\ 0, & S - S_t \le 0, \end{cases} \tag{A.3}$$

where the regional parameters are k_d a storage rate constant, S_t a soil tension threshold below which there is no drainage and β an exponent of the relation (often set to 3). If $S_{max} < S_t$ then drainage from that grid square can never occur.

Finally, the (potential) water storage is given by the update equation

$$S = \max(0, S + p\Delta t - E_a\Delta t - d\Delta t), \tag{A.4}$$

where p is the rainfall rate. The direct runoff rate contributing to the fast pathways is then calculated as

$$q = \max(0, S - S_{max}), \tag{A.5}$$

and the water storage S reset to S_{max} if direct runoff is generated.

The inflows to the flow-routing scheme of equation (B.5), u_r or u_l, and u_{rb} or u_{lb}, comprise the surface and sub-surface runoff terms, q and d, in equations (A.5) and (A.3), depending on whether the grid-square is assigned land or river.

A.3 Probability-distributed runoff production scheme

In order to introduce heterogeneity of soil storage within a grid square, the probability-distributed soil moisture (PDM) formulation developed by Moore (1985, 1999) has been applied to an individual grid-square. A perceived benefit of introducing this additional level of complexity is that a certain proportion of the grid square is assumed to be saturated and generating runoff, even when rainfall amounts are small. Under the basic formulation of Section A.2, an entire grid-square has to become saturated before it generates runoff.

The probability-distributed extension to the basic runoff production scheme is developed as follows. Consider the simple empirical relation between gradient, g, and storage capacity, c, at a point

$$c = (1 - g/g_{max})c_{max},$$ (A.6)

where g_{max} and c_{max} are the maximum regional gradient and storage capacity values. For a given distribution of gradient within a grid-square, equation (A.6) can be used to derive the distribution of storage capacity over the square in terms of the parameters defining the distribution of gradient.

The choice of distribution can be guided by constructing frequency curves of topographic slope from DTM data, both for within-grid square areas and for whole regions. Particular distributions, such as truncated exponential or power, can be fitted to the slope frequency curve data. Parameters defining these distributions may then be used in the derived distribution for store capacity. The probability distributed formulation presented by Moore (1985) can then be used to obtain the proportion of each grid square which is saturated and in turn the volume of runoff generated.

The distribution function of store capacity for a power distribution of slope may be derived as follows. Consider slopes in the range $0 \le g \le g_{max}$ which follow a power distribution of the form

$$F(g) = \text{Prob}(\text{slope} \le g) = \left(\frac{g}{g_{max}}\right)^b \qquad 0 \le g \le g_{max}$$ (A.7)

with the exponent b related to the mean slope $\bar{g}$ by

$$b = \frac{\bar{g}}{g_{max} - \bar{g}}.$$ (A.8)

The distribution function of storage capacity may be derived assuming equation (A.6) to hold, and takes the Pareto distribution form

$$F(c) = 1 - \left(1 - \frac{c}{c_{max}}\right)^b \qquad c \le c_{max}.$$ (A.9)

From the PDM methodology (Moore, 1985) it then follows that the soil moisture storage S and the critical capacity C^* are related by

$$S = \frac{c_{max}}{b+1}\left[1 - \left(1 - \frac{C^*(t)}{c_{max}}\right)^{b+1}\right].$$ (A.10)

The critical capacity is that below which all stores of smaller capacity are full and generating surface runoff during rainfall. Note that the maximum possible value of soil moisture storage over the grid-square is given by

$$S_{max} = \frac{c_{max}}{b+1} \, ,$$
(A.11)

which is also the mean store capacity, $\bar{c}$. It is this Pareto-based formulation that constitutes the probability-distributed variant of the basic runoff production scheme.

Note that the constraint $S_{max} \geq \bar{c}_{min}$ can be imposed to prevent any grid-square having a zero maximum storage capacity; here $\bar{c}_{min}$ is the minimum mean store capacity of a grid-square that is allowed and is treated as a regional parameter. For grid squares where this constraint applies, c_{max} is recalculated using (A.1) with $S_{max} = \bar{c}_{min}$.

Appendix B Grid-to-Grid flow routing scheme

B.1 The basic 1-D scheme

The 1-D kinematic wave equation relates channel flow, q, and lateral inflow per unit length of river, u, by

$$\frac{\partial q}{\partial t} + c\frac{\partial q}{\partial x} = cu \,, \tag{B.1}$$

where c is the kinematic wave speed and x and t are distance along the reach and time respectively. Consider time, t, and space, x, to be divided into discrete intervals Δt and Δx such that k and n denote positions in discrete time and space. Invoking difference approximations to the derivatives in (B.1) gives the discrete formulation

$$q_k^n = (1-\theta)q_{k-1}^n + \theta\left(q_{k-1}^{n-1} + u_k^n\right) \tag{B.2}$$

where the dimensionless wave speed $\theta = c\,\Delta t / \Delta x$ and $0 < \theta < 1$. This is a recursive formulation which expresses flow out of the n'th reach at time k, q_k^n, as a linear weighted combination of the flow out of the reach at the previous time with inflow to the reach from upstream (at the previous time) and the total lateral inflow along the reach (at the same time).

An alternative derivation of equation (B.2) can be sought from a simple hydrological storage approach. The n'th reach can be viewed as acting as a linear reservoir with its outflow related linearly to the storage of water in the reach such that

$$q_k^n = \kappa\, S_k^n, \tag{B.3}$$

where κ is a rate constant with units of inverse time. If S_k^n is the storage in the reach just before flows are transferred at time k, then continuity gives

$$S_k^n = S_{k-1}^n + \Delta t\left(q_{k-1}^{n-1} - q_{k-1}^n + u_k^n\right) \tag{B.4}$$

and the equivalence to (B.2) follows, given $\theta = \kappa\,\Delta t$ with $\kappa = c/\Delta x$.

It is the above 1-D scheme that forms the basis of CEH's KW channel flow routing model (Moore and Jones, 1978; Jones and Moore, 1980) and is invoked to represent fast and slow pathway routing in the Grid Model of Bell and Moore (1998). It is a scheme based on a discrete approximation of the 1-D kinematic wave equation with lateral inflow as expressed by equation (B.2)

B.2 The 2-D Grid-to-Grid scheme

In the Grid-to-Grid Model it is assumed that a runoff-production scheme first partitions precipitation and evaporation fluxes into water stored in the soil and canopy, and water generated as surface and sub-surface runoff. The above kinematic routing scheme is then applied separately to these runoffs so as to represent parallel fast ("surface") and slow ("subsurface") pathways of water movement. The routing scheme also allows for different formulations over land and river pathways (initially just a different wave speed). The scheme as used for the Grid-to-Grid Model differs in two distinct ways from that implemented for the Grid Model. The first is that water is explicitly transferred from one grid to another based on topographic control. (In contrast, the Grid Model maps runoff from each grid onto a cascade of routing reaches defined via isochrones inferred from the DTM.) Secondly, a *return flow* term allows for flow transfers between the subsurface and surface pathways representing surface/sub-surface flow interactions on hillslopes and in river channels.

The Grid-to-Grid routing scheme equations in 1-dimension are:

$$\frac{\partial q_l}{\partial t} + c_l \frac{\partial q_l}{dx} = c_l (u_l + R_l)$$

$$\frac{\partial q_{lb}}{\partial t} + c_{lb} \frac{\partial q_{lb}}{dx} = c_{lb} (u_{lb} - R_l)$$

$$\frac{\partial q_r}{\partial t} + c_r \frac{\partial q_r}{dx} = c_r (u_r + R_r)$$ (B.5)

$$\frac{\partial q_{rb}}{\partial t} + c_{rb} \frac{\partial q_{rb}}{dx} = c_{rb} (u_{rb} - R_r)$$

where q_l is flow over land pathways, q_r is flow over river pathways, R_l and R_r denote land and river return flow, and u_l and u_r are inflows for land and river, which include runoff generated by a runoff-production scheme. The additional subscript b denotes sub-surface ("baseflow") pathways. The wave speed c can vary with the pathway and surface-type combination as indicated by the suffix notation.

The four partial differential equations are each discretised using a finite-difference representation similar to equation (B.2), but extended to include the return flow term R_k^n, such that

$$q_k^n = (1-\theta)q_{k-1}^n + \theta\left(q_{k-1}^{n-1} + u_k^n + R_k^n\right).$$ (B.6)

For application to two dimensions, the q_{k-1}^{n-1} term, which represents inflow from the preceding grid-cell in space, is given by the sum of the inflows from adjacent grid-cells.

In practice, the routing is implemented in terms of an equivalent depth of water in store over the grid square, S_k^n, where $q_k^n = \kappa S_k^n$, and the inflow and return flow are also parameterised as water depths. The return flow to the surface is given by $R_k^n = r S_k^n$, where S_k^n is the depth of water in the subsurface store and r is the return flow fraction. This fraction takes a value between zero and one since it represents the proportion of

the sub-surface store content that is routed to the surface, and can differ for land and river paths. For sub-surface routing, the return flow term is modified to subtract from water in store. Note that whilst return flow is normally positive, it can take negative values to represent influent, rather than the more normal effluent "stream" conditions. The flow-routing scheme allows for different values of the dimensionless wave speed, θ, for the different pathway (surface or subsurface) and surface-type (land or river) combinations.

Appendix C Multiquadric surface fitting and areal rainfall estimation

C.1 Introduction

Multiquadric surface fitting can be applied to raingauge totals (over 15 minute time intervals) to infer the spatial distribution of rainfall across a region under consideration (for example, see Moore *et al.*, 1989). A brief summary of the multiquadric surface fitting technique is given in Section C.2. Having derived the fitted surface, it is possible to integrate the inferred rainfall totals over a catchment to calculate the catchment average rainfall total. Indeed, any area of interest can be considered. For example, an area may be assigned a grid and areal estimates for each grid-square obtained. The assigned grid may be defined as the 1 km radar grid so as to mirror radar datasets.

It will be shown, following Balascio (2001), that the catchment (or grid) average rainfall total is in fact equivalent to applying a set of (constant) linear weights to the set of raingauge totals. A formula and method for calculating these linear weights are presented in Sections C.3 and C.4 respectively. The original motivation for deriving these sets of linear weights is their use in lumped, catchment-based, conceptual rainfall-runoff models such as the PDM. However, Section C.5 presents a new application for these weights in constructing spatio-temporal rainfall datasets for use as input to distributed rainfall-runoff models configured on a grid. This includes both raingauge-only datasets and those that combine radar and raingauge measurements.

C.2 Multiquadric surface fitting techniques

C.2.1 Introduction

The classical problem of surface fitting is to find a surface $s(\underline{x})$ which passes exactly through N data values, z_i, specified at the N points, $\underline{x}_i = (x_i, y_i)$. The multiquadric calibration surface is defined as the weighted sum of N distance, or basis functions centred on each of the N data locations; that is

$$s(\underline{x}) = \sum_{j=1}^{N} a_j \; g(\underline{x} - \underline{x}_j) + a_0 \tag{C.1}$$

where $\{a_j, j = 0, 1, 2, \ldots, N\}$ are parameters of the surface. There are many choices for the form of the distance function. The three examples presented here are all based on the simple Euclidean distance

$$d = \| \underline{x} \| = \sqrt{(x^2 + y^2)}. \tag{C.2}$$

The example distance functions are defined as:

Cone: $\quad g(\underline{x}) = d$, $\hspace{6cm}$ (C.3a)

Exponential: $\quad g(\underline{x}) = \exp(-d/l)$, $\hspace{4.5cm}$ (C.3b)

Reciprocal: $\quad g(\underline{x}) = 1/(1+d/l)$. $\hspace{4.5cm}$ (C.3c)

For the exponential and reciprocal distance functions, equations (C.3b-c), l is an additional constant parameter, referred to as the scaling length, which is prescribed prior to the surface fitting procedure. When using just the Euclidean distance, equation (C.3a), the surface defined by (C.1) is constructed from a set of N right-sided cones, each centred on one of the N data locations $\underline{x}_i$.

Evaluation of the surface parameters $\{a_j, j = 0, 1, 2, \ldots, N\}$ is achieved by imposing the condition that the fitted surface should take the values z_i at the points $\underline{x}_i$ for $i = 1, \ldots, N$. Formally the N equations are

$$s(\underline{x}_i) = \sum_{j=1}^{N} a_j \, g(\underline{x}_i - \underline{x}_j) + a_0 = z_i \qquad (i = 1, 2, \cdots, N) \hspace{2cm} \text{(C.4)}$$

which when expressed in matrix form results in

$$\underline{\underline{G}}\,\underline{a} + a_0 \underline{1} = \underline{z} \hspace{6cm} \text{(C.5)}$$

where $\underline{\underline{G}}$ is an N by N matrix with the (i, j)'th element given by $G_{ij} = g(\underline{x}_i - \underline{x}_j)$, $\underline{1}$ is a unit vector of order N, $\underline{z}$ is the vector containing the N data values z_i, $i = 1, \ldots, N$ and $\underline{a}$ is the vector containing the N surface parameters $\{a_j, j = 1, 2, \ldots, N\}$. The distance functions used here mean that the matrix $\underline{\underline{G}}$ is symmetric and this assumption is used later. Equation (C.5) provides N constraints towards evaluating the $N+1$ surface parameters $\{a_j, j = 0, 1, 2, \ldots, N\}$. The remaining constraint can be applied in two forms, both of which are detailed below.

C.2.2 Flatness at large distance

One approach to fully define the surface fitting procedure is to include the additional constraint that the slope of the surface should be zero for large distances from the surface fitting points. This ensures that the surface neither continually increases nor decreases at large distances (note that the limiting surface value may well be different in different directions). When the Euclidean distance function (C.3a) is used, the zero-slope constraint is

$$\underline{a}^T \underline{1} = 0. \hspace{6cm} \text{(C.6)}$$

This additional constraint can be used to complete the specification of the surface fitting problem for other distance functions as well. However, the application of condition (C.6) to other distance functions usually leads to either the quickest approach to a constant value at large distances or to the least rapid increase or decrease. More

importantly, constraint (C.6) arises in a different way when a surface-fitting procedure is required to be strictly additive. That is, if a constant value is added to all observations the fitted surface is obtained by adding the same constant to the original surface. This is known as additive invariance.

Solution of equation (C.5) subject to constraint (C.6) for the surface parameters $\{a_j, j = 0, 1, 2, \ldots, N\}$ gives

$$a_0 = \left(\underline{1}^T \underline{\underline{G}}^{-1} \underline{z}\right) / \left(\underline{1}^T \underline{\underline{G}}^{-1} \underline{1}\right), \tag{C.7a}$$

$$\underline{a} = \underline{\underline{G}}^{-1}\left(\underline{z} - a_0 \underline{1}\right). \tag{C.7b}$$

C.2.3 Fixed value at large distance

An alternative way of fully defining the surface fitting problem is to force the fitting surface to approach a given fixed value at large distances from the surface fitting points. This constraint is only suitable for distance functions which approach a finite limit for large distances. For the examples encountered so far, this approach is appropriate for the exponential and reciprocal distance functions, where the finite limit is zero, but is not suitable for the Euclidean distance since $d \to \infty$ for large distances.

Suppose that the limiting value of the distance function for large distances is zero, as is the case for the exponential and reciprocal distance functions. Then, if b is the required limiting value for the surface, this additional parameter constraint leads to $a_0 = b$ and then the surface fitting parameters $\{a_j, j = 1, 2, \ldots, N\}$ are given by

$$\underline{a} = \underline{\underline{G}}^{-1}\left(\underline{z} - b\underline{1}\right). \tag{C.8}$$

Equation (C.8) is analogous to equation (C.7b) and completes the specification of the surface.

C.2.4 Offset parameter, K

For some applications it is appropriate to relax condition (C.4) to not force the fitted surface to pass exactly through the surface fitting data. Instead the fitted surface is only required to pass *near* to the surface fitting data and a smoother surface results. This is achieved by introducing an offset parameter, K. The distance functions (C.3) are then modified to take the following zero distance values:

Cone: $\quad \tilde{g}(\underline{0}) = -K$, $\tag{C.9a}$

Exponential: $\quad \tilde{g}(\underline{0}) = 1 + K$, $\tag{C.9b}$

Reciprocal: $\quad \tilde{g}(\underline{0}) = 1 + K$, $\tag{C.9c}$

where $\tilde{g}$ is the modified distance function. Note that when this modification is used, the fitted surface formally has point discontinuities at each of the fitting points; however

this problem is avoided by using the unmodified form of the basis function for surface evaluation.

These modified distance functions can be used with either the 'Flatness at large distance' condition, Section C.2.2, or the 'Fixed value at large distance', Section C.2.3. The former condition has the following interpretation when using an offset parameter. The modified distance function satisfies the constraint,

$$z_i = \sum_{j=1}^{N} a_j \; \tilde{g}\left(\underline{x}_i - \underline{x}_j\right) + a_0 \quad \left(i = 1, 2, \cdots, N\right). \tag{C.10}$$

However, the surface value (evaluated using the unmodified distance function g) at the point $\underline{x}_i$ will be

$$z_i^* = \sum_{j=1}^{N} a_j \; g\left(\underline{x}_i - \underline{x}_j\right) + a_0 = \sum_{j=1}^{N} a_j \; \tilde{g}\left(\underline{x}_i - \underline{x}_j\right) + a_0 \pm K a_i \tag{C.11}$$

where the sign depends on the distance measure used. Therefore

$$z_i - z_i^* = \mp K a_i \tag{C.12}$$

and the flatness constraint $\underline{a}^T \underline{1} = 0$ will ensure that these 'errors' or 'discrepancies' add up to zero.

C.3 Estimation of areal average rainfall totals

C.3.1 Introduction

A method of calculating time-series of catchment average rainfall totals is required for use as input to lumped conceptual rainfall-runoff models such as the PDM. The following method of areal average estimation is based on the work of Balascio (2001). Formally the catchment average rainfall P is defined as follows. Let the function $f(x, y)$ be the rainfall total at every point (x, y) within the catchment under consideration. Let R denote the catchment region with associated (horizontal) surface area A. Then the catchment average rainfall total is defined as

$$P = \frac{1}{A} \iint_R f(x, y) \, dx \, dy \qquad \text{where} \qquad A = \iint_R dx \, dy. \tag{C.13}$$

Of course the function $f(x, y)$ is unknown. However, we may estimate the function $f(x, y)$, and in turn the catchment average rainfall total, by fitting a multiquadric surface $s(\underline{x})$ to a given network of N raingauge totals. In this context $\underline{x}_i = (x_i, y_i)$ represents the location of the i th raingauge and z_i represents the rainfall total (over 15 minute intervals) at the i th raingauge.

Therefore the estimated catchment average rainfall total $\hat{P}$ obtained using the multiquadric surface is

$$\hat{P} = \frac{1}{A} \iint_R s(\underline{x})\, dx\, dy \qquad = \frac{1}{A} \iint_R \left\{ \sum_{j=1}^{N} a_j\, g(\underline{x} - \underline{x}_j) + a_0 \right\} dx\, dy$$

$$= \frac{1}{A} \iint_R \sum_{j=1}^{N} a_j\, g(\underline{x} - \underline{x}_j)\, dx\, dy + a_0 . \tag{C.14}$$

Since $s(\underline{x})$ is a linear combination of the distance functions $g(\underline{x} - \underline{x}_j)$, the summation in equation (C.14) may be integrated term by term. Let $\underline{v}$ be a vector of order N comprising of the distance functions $g(\underline{x} - \underline{x}_j)$ such that

$$\underline{v} = \begin{pmatrix} g(\underline{x} - \underline{x}_1) \\ \vdots \\ g(\underline{x} - \underline{x}_N) \end{pmatrix}. \tag{C.15}$$

This definition allows equation (C.14) to be rewritten as

$$\hat{P} = \frac{1}{A} \iint_R \underline{v}^T \underline{a}\, dx\, dy \; + \; a_0 . \tag{C.16}$$

Recalling that the vector $\underline{a}$ is a constant, the only dependence on x and y in equation (C.16) enters through the distance functions contained in $\underline{v}$ which can be separated out. Integrating $\underline{v}$ term by term yields the volume vector $\underline{V}$:

$$\underline{V} = \iint_R \underline{v}\, dx\, dy . \tag{C.17}$$

Separating the x and y dependence out of equation (C.16) and using the definition (C.17), the estimated catchment average rainfall total becomes:

$$\hat{P} = \frac{1}{A} \underline{V}^T \underline{a} + \; a_0 . \tag{C.18}$$

Depending on the form of the distance function and catchment boundary, $\underline{V}$ can be calculated explicitly. For example, Pegram and Pegram (1993) derive a solution for the conic distance function over a polygon boundary. Their method could be applied to the DTM-derived catchment boundaries. Alternatively, Balascio (2001) describes a method for the conic distance function using 3-D CAD software. However, within the present study, a general numerical scheme has been developed which can be applied to a range of basis functions over polygon boundaries. This generalised scheme is detailed in Section C.4.

C.3.2 Flatness at large distance

Recall from Section C.2.2 that the condition of flatness at large distances is achieved by adding the constraint $\underline{a}^T \underline{1} = 0$. Substituting the resulting solutions for $\underline{a}$ and a_0 (see equation (C.7)) into equation (C.18) yields:

$$\hat{P} = \frac{1}{A}\left[\underline{V}^T \underline{\underline{G}}^{-1} + \frac{\left(A - \underline{V}^T \underline{\underline{G}}^{-1}\underline{1}\right)}{\underline{1}^T \underline{\underline{G}}^{-1}\underline{1}} \underline{1}^T \underline{\underline{G}}^{-1}\right] \underline{z}.$$ (C.19)

Equation (C.19) implies that the catchment average rainfall total, derived by integrating the multiquadric surface over the region, is equivalent to applying a set of constant linear weights to the raingauge totals *regardless* of the actual value of $\underline{z}$. To see this explicitly, let w_i be the constant linear weighting coefficient for the ith raingauge. Then equation (C.19) can be rewritten as

$$\hat{P} = \underline{w}^T \underline{z}$$ (C.20a)

where

$$\underline{w} = \frac{\underline{\underline{G}}^{-1}}{A}\left[\underline{V} + \frac{\left(A - \underline{V}^T \underline{\underline{G}}^{-1}\underline{1}\right)}{\underline{1}^T \underline{\underline{G}}^{-1}\underline{1}} \underline{1}\right].$$ (C.20b)

This is equivalent to equation (17) of Balascio (2001) (except for a typographical error). Clearly $\underline{w}$ is a constant vector and it is trivial to show that the sum of the weights equals one, i.e. $\underline{1}^T \underline{w} = 1$. Since the sum of the weights is equal to one, multiquadric surfaces give an *unbiased* estimate of the catchment average rainfall total when the constraint of flatness at large distance (or of additive invariance) is applied. Note that in deriving (C.20), use has been made of the matrix rules that $(\underline{\underline{D}}\underline{\underline{E}})^T = \underline{\underline{E}}^T \underline{\underline{D}}^T$ and that if $\underline{\underline{F}}$ is symmetric then $\underline{\underline{F}}^T = \underline{\underline{F}}$.

C.3.3 Fixed value at large distance

As discussed in Section C.2.2, the constraint of fixed value at large distance is only appropriate if the distance function tends to a finite value at large distances from the raingauge network. Without loss of generality, consider the case when the fixed value is zero (i.e. $a_0 = b = 0$) since any other choice can be recast in this form by replacing z_i with $z_i - b$. For the case $a_0 = b = 0$ the vector $\underline{a}$ is given by:

$$\underline{a} = \underline{\underline{G}}^{-1}\underline{z}.$$ (C.21)

Substituting (C.21) and $a_0 = b = 0$ into equation (C.18) yields:

$$\hat{P} = \frac{1}{A}\underline{V}^T \underline{\underline{G}}^{-1} \underline{z}.$$ (C.22)

This implies, as in Section C.3.2, that the catchment average rainfall total is equivalent to applying a set of constant linear weights to the raingauge totals, z_i, regardless of their values. Let w_i be the constant linear weighting coefficient for the ith raingauge. Then equation (C.19) can be rewritten as

$$\hat{P} = \underline{w}^T \underline{z}$$ (C.23a)

where

$$w = \frac{1}{A} \underset{=}{G}^{-1} \underline{V} \ .$$

<div align="right">(C.23b)</div>

Once again $\underline{w}$ is clearly constant. However, for the constraint of a fixed value at large distances, the sum of the weights is not necessarily equal to one and therefore the weights give a *biased* estimate of the catchment average rainfall. The estimators are unbiased in the special case that the "fixed value at large distance" is specified to be equal to the long-term mean rainfall.

C.3.4 Offset parameter, K

When an offset parameter, K, is used (see Section C.2.4), the weighting definitions derived above are still valid. However, care must be taken over which distance measure is used for defining $\underline{V}$ and $\underset{=}{G}$. The correct method is to use the unmodified distance function g when calculating $\underline{V}$ whilst using the modified distance function $\tilde{g}$ when defining $\underset{=}{G}$.

# C.4 Outline of method for calculating the volume vector $\underline{V}$

The aim of this section is to outline the method used to calculate the volume vector $\underline{V}$ (see equation (C.17)) which is required to derive the linear weighting coefficients $\underline{w}$.

To illustrate the method, consider integrating a function $h(x, y)$ over a polygon boundary. Let R denote the catchment region. Let $\underline{x}_0$ be a fixed point (e.g. a raingauge location) that can lie inside or outside the polygon boundary and let the vertices of the polygon boundary be numbered in a clockwise sense from $\underline{x}_1$ to $\underline{x}_M$, where M is the total number of vertices. This configuration is presented in Figure C.1 for a simple catchment boundary. Then the following steps allow the function $h(x, y)$ to be integrated over the boundary.
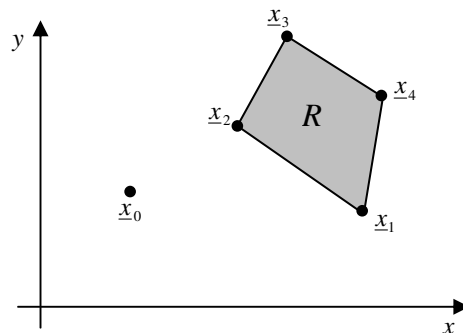
Figure C.1 Configuration of a simple catchment region R within a polygon boundary with vertices $\underline{x}_1$ to $\underline{x}_4$ and with a raingauge located at $\underline{x}_0$

Step 1: Starting at the first edge of the polygon boundary between $\underline{x}_1$ and $\underline{x}_2$ construct a triangle with the fixed point $\underline{x}_0$. This has area T_1 and is illustrated in Figure C.2.
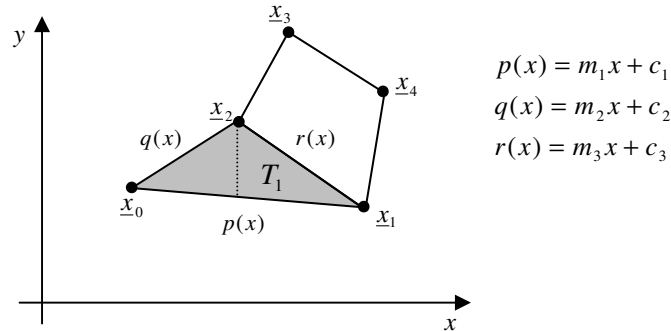
Figure C.2 Construction of triangle T_1

Step 2: T_1 is then split into two smaller triangles by a vertical line emanating from the vertex of T_1 whose x position lies between the others: in the current example it is $\underline{x}_2$. Simple geometry gives the equations of the lines that form the triangle T_1, namely $p(x)$, $q(x)$ and $r(x)$. Let I_1 be the integration of $h(x,y)$ over T_1 which is equivalent to integrating over the two smaller triangles. For the current example,

$$I_1 = \iint\limits_{T_1} h(x,y)\,dx\,dy = \int_{x=x_0}^{x=x_2}\int_{y=p(x)}^{y=q(x)} h(x,y)\,dy\,dx + \int_{x=x_2}^{x=x_1}\int_{y=p(x)}^{y=r(x)} h(x,y)\,dy\,dx. \quad \text{(C.24)}$$

The integration over the smaller triangles can be estimated by a numerical scheme. In this study Gaussian quadrature has been used.

Step 3: The integral I_1 is then multiplied by a rotation factor r_1 where

$r_1 = 1$ if moving from $\underline{x}_1$ to $\underline{x}_2$ results in a clockwise rotation about $\underline{x}_0$,
$r_1 = -1$ if moving from $\underline{x}_1$ to $\underline{x}_2$ results in a anti-clockwise rotation about $\underline{x}_0$.

                                                          (C.25)

This rotation can easily be determined from basic geometry. For example, let θ_1 be the rotation of $\underline{x}_1$ about $\underline{x}_0$ with respect to the y direction and let θ_2 be the rotation of $\underline{x}_2$ about $\underline{x}_0$. Then

$r_1 = 1$ if $\theta_2 - \theta_1 > 0$,
$r_1 = -1$ if $\theta_2 - \theta_1 < 0$.   (C.26)

For the current example $\theta_2 - \theta_1 < 0$, see Figure C.3, and so $r_1 = -1$.
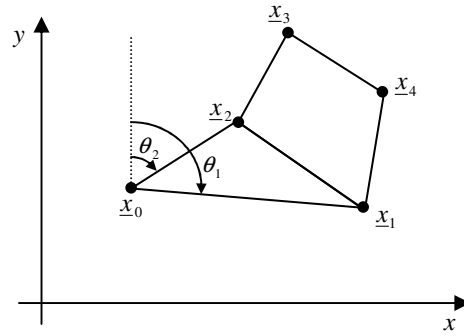
Figure C.3 Evaluation of rotation factor r_1

Step 4: Repeat steps 1 to 3 for the next edge of the boundary, e.g. edge $\underline{x}_2$ to $\underline{x}_3$ with associated triangle T_2, integration I_2 and rotation factor r_2. Repeat until the final edge of the boundary, edge $\underline{x}_M$ to $\underline{x}_1$, is reached. Then the integration of $h(x, y)$ over the region R, bounded by the polygon boundary is given by

$$
\begin{aligned}
I = \iint\limits_{R} h(x, y)\, dx\, dy \quad &= r_1 \iint\limits_{T_1} h(x, y)\, dx\, dy + \cdots + r_M \iint\limits_{T_M} h(x, y)\, dx\, dy \\
&= r_1 I_1 + \cdots + r_M I_M \\
&= \sum_{j=1}^{M} r_j I_j
\end{aligned}
\tag{C.27}
$$

Note that $R = \sum_{j=1}^{M} r_j T_j$. The triangles and rotation factors derived using this method for the example are illustrated in Figure C.4.

Once the volume vector $\underline{V}$ has been calculated by this method, it is simple to calculate the constant weighting coefficient vector $\underline{w}$ from either (C.20b) or (C.23b) depending on the additional constraint used.

However, it is important to stress that this method does not guarantee that the raingauge weights are all positive. If negative weights do occur, the recommendation is to remove the raingauge in question from the network and repeat the method. Note that this only involves eliminating the appropriate elements from $\underline{V}$, $\underline{G}$ and $\underline{z}$ and then recalculating $\underline{w}$.
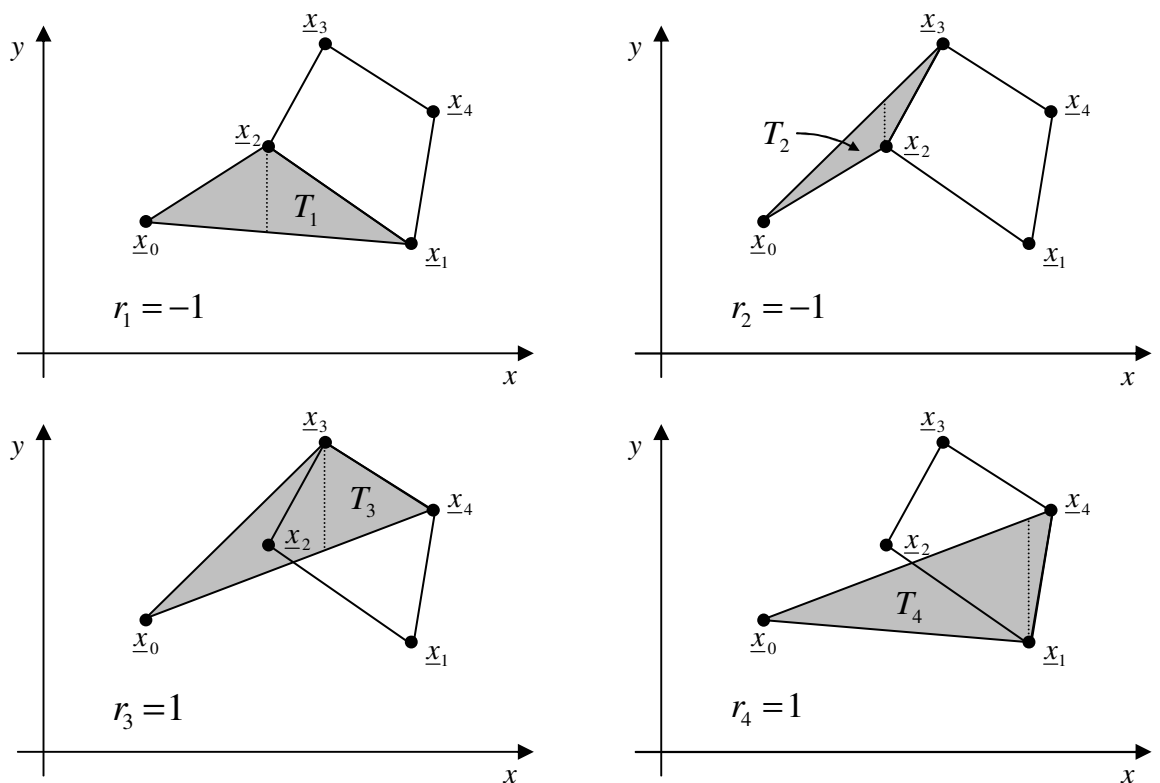
Figure C.4 Illustration of method for calculating the volume vector $\underline{V}$

C.5 Application for distributed rainfall-runoff models on a grid

Up to this point the main emphasis has been to derive a set of linear raingauge weights for a particular catchment. These weights may then be used to combine values from the set of raingauges for use by lumped conceptual rainfall-runoff models. However, a different requirement arises for rainfall input to area-wide spatially distributed models. In contrast to the catchment-based focus of lumped conceptual rainfall-runoff models, area-wide distributed models require rainfall estimates on a grid. The model's full area coverage allows river flows to be estimated and extracted for any location of interest.

The types of rainfall input available fall into three main categories:

  (i)   Raingauge based estimations,
  (ii) Radar based estimations,
  (iii) Estimations combining radar and raingauge data.

Types (i) and (iii) are well suited to surface fitting techniques and their implementation for distributed rainfall-runoff models on a grid are discussed below.

C.5.1 Raingauge-only rainfall estimation

When the precipitation input to a distributed hydrological model is provided by a network of raingauges, the key question posed is how to infer the spatial distribution of the rainfall total and, in particular, how to construct the grid-square average rainfall totals required by the model? One option is to fit a multiquadric surface to the observed raingauge totals at each model time-step and then calculate, for each grid-square, the grid-square average rainfall total. However, Section C.3 indicates that the average rainfall total for a given grid-square will be the same linear combination of raingauge totals for every time-step: that is the weights will be the same regardless of the actual raingauge values being combined. Therefore, it is far more efficient to simply calculate the linear set of raingauge weights for each grid-square in turn at the outset and then use these weights at each time-step to construct the grid-square average rainfall totals required by the distributed rainfall-runoff model. In practice these weights (but not the volumes as these remain constant and only need to be calculated once) are recalculated each time a raingauge in the network comes in to or out of service.

Depending on the extent of the region of interest it may not be appropriate to use the entire network of raingauges for all grid squares. The approach used for deriving the weights for a given grid square is outlined in the decision flowchart presented in Figure C.5.

The raingauge values can be transformed, using a modified logarithmic form, before the grid-square averages are calculated. Then the inverse transformation is applied and any negative rainfall that results is set to zero. Moore *et al.* (1989) have found that this can provide improved spatial rainfall estimates.

Specifically, let R_g^i denote the rainfall rate for the ith raingauge and $\hat{R}_g^i = f(R_g^i)$ the transformed rainfall, where f is a rainfall transformation function. The transformed rainfalls, used as the data points z_i in the multiquadric surface fitting techniques discussed earlier, are given by:

$$\hat{R}_g^i = f(R_g^i) = \begin{cases} \log(R_g^i) & \\ \log(R_0) + \dfrac{R_g^i}{R_0} - 1 & \end{cases} \quad \text{for} \quad \begin{aligned} R_g^i &> R_0 \\ R_g^i &\le R_0 \end{aligned} \tag{C.28}$$

where R_0 is a parameter empirically estimated from the data. The inverse transformation

$$f^{-1}(\hat{R}_g^i) = \begin{cases} 10^{\hat{R}_g^i} & \\ \max\left\{ R_0 \left(\hat{R}_g^i + 1 - \log(R_0) \right), 0 \right\} & \end{cases} \quad \text{for} \quad \begin{aligned} \hat{R}_g^i &> \log(R_0) \\ \hat{R}_g^i &\le \log(R_0) \end{aligned} \tag{C.29}$$

then gives the required estimate of the rainfall rate.
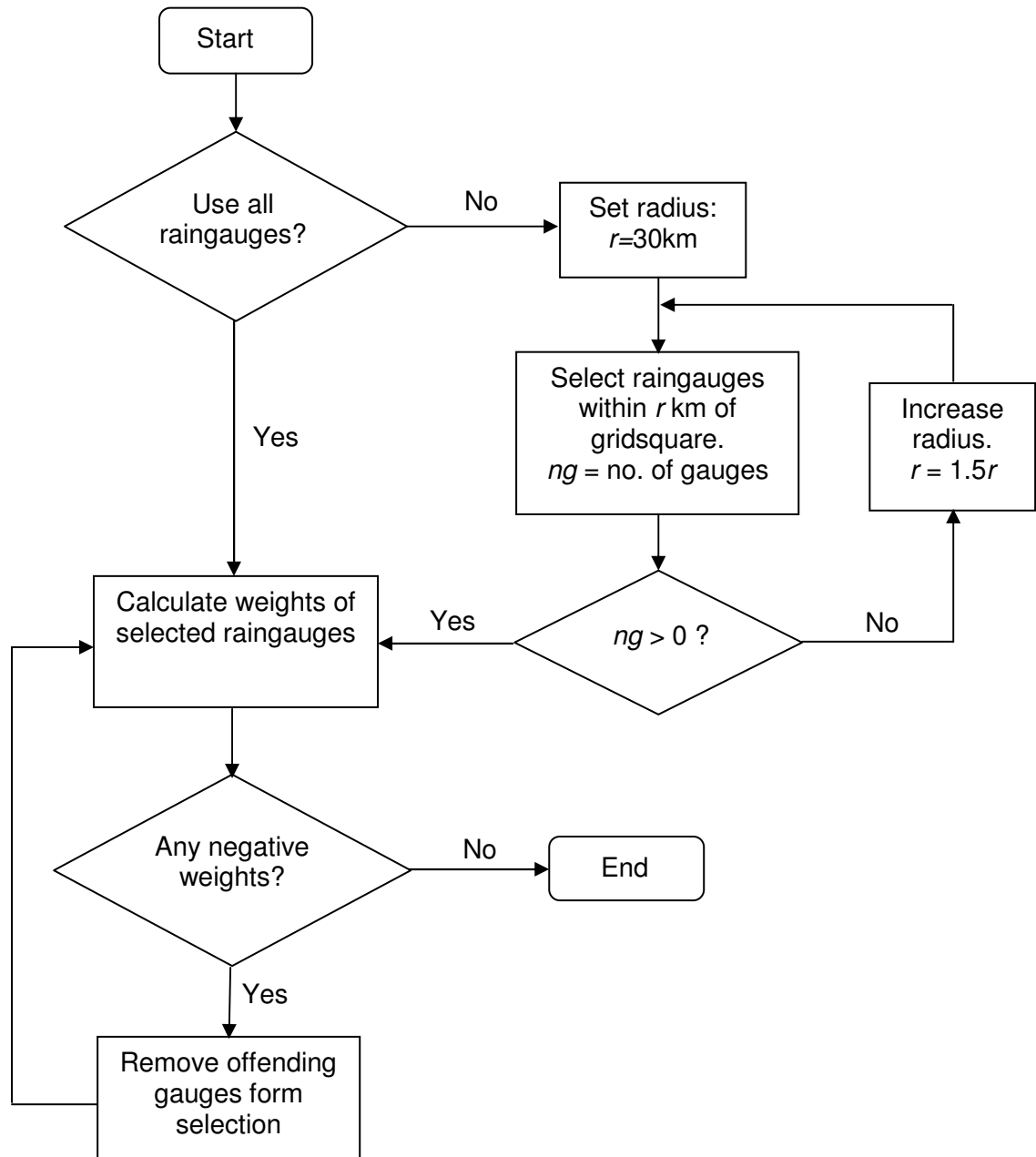
Figure C.5 Flowchart for deriving raingauge weights for a given grid-square

C.5.2 Combined radar and raingauge rainfall estimation

Radar estimates of rainfall capture the spatial variability of rainfall well, in comparison to the point estimates of a raingauge network (unless a very dense network is available). However, the accuracy of an estimate of rainfall from radar for a gauge location is significantly less than that provided by the raingauge itself. Therefore, there is merit in combining the two information sources in an attempt to obtain a more accurate spatially-varying rainfall field with obvious benefits for distributed modelling.

Static gauge-adjustment

This approach attempts to improve the radar data by identifying the long-term bias of a radar dataset with reference to information from a raingauge network and then correcting for it. This is known as *static gauge-adjustment*, as a single adjustment factor is applied to the entire radar dataset. For the i th raingauge the long-term bias, B_i, is defined to be the arithmetic mean ratio calculated over n time-frames:

$$B_i = \frac{1}{n} \sum \frac{R_g^i}{R_r^i} \qquad \text{(C.30)}$$

where R_r^i is the radar estimate for the grid-square coincident with the i th raingauge. In practice, the ratio is only calculated if both R_r^i and R_g^i are greater than 1 mm h^{-1}. This minimises discretisation errors and the influence of anomalous propagation. Averaging this over the N raingauges gives the long-term bias, B, of the radar

$$B = \frac{1}{N} \sum B_i \; . \qquad \text{(C.31)}$$

Applying this as an adjustment factor to the entire radar dataset gives the static gauge-adjusted radar rainfall estimates.

Dynamic gauge-adjustment

For the case of dynamic gauge-adjustment of radar data, the data points z_i that the multiquadric surface is fitted to are gauge-adjustment factors. This is known as dynamic gauge-adjustment as the surface is constructed at each time-step. There are several options for the form of the gauge-adjustment factor. In this study two related forms are considered. The first is defined as a modified ratio of the rainfall at the i th raingauge, R_g^i, to the radar estimate, R_r^i, for the grid-square coincident with the raingauge, such that

$$z_i = \frac{R_g^i + \varepsilon_g}{R_r^i + \varepsilon_r} \qquad \text{(C.32)}$$

where ε_g and ε_r are positive constants such that the ratio is defined for all values of R_g^i and R_r^i. This form was found to be most effective in previous studies (Moore *et al.,* 1989) and is referred to as *standard dynamic gauge adjustment of radar*.

An extended form (Wood *et al.,* 2000) that takes account of the long-term bias can also be considered that modifies the gauge-adjustment factor (C.32) to

$$z_i = \frac{R_g^i + \varepsilon_g}{\kappa R_r^i + \varepsilon_r} \qquad \text{(C.33)}$$

where κ is the long-term static gauge-adjustment factor (B in (C.31)). In this case $\varepsilon_g = \varepsilon_r = \varepsilon$. This is referred to as *dynamic adjustment of radar including mean bias*. An important point is that, for this form of adjustment factor, the long term bias is

accounted for and therefore the surface fitted should tend to an adjustment factor of 1 (i.e. no adjustment) at large distances. As such only the exponential form of the Euclidean distance and the inverse distance measures should be used along with the no adjustment at large distances boundary condition.

For both forms of dynamic gauge adjustment of radar, once the surface of calibration factors has been derived it can be applied to the (raw) radar estimate to obtain the raingauge adjusted radar estimate. Note that unlike the raingauge-only case the raingauge rainfall is kept in its original form. The derivation of the weights required for the grid-square average adjustment factors follows the same procedure as the raingauge-only case, outlined in Figure C.5.

Appendix D Case study applications of ungauged forecasting methods

D.1 Introduction

This appendix provides case study applications to illustrate different approaches to forecasting at ungauged sites using rainfall-runoff models. Four approaches have been selected for illustration:

(i) simple transfer of a lumped, conceptual rainfall-runoff model from a neighbouring or similar site;

(ii) transfer by relating the parameters of a simplified form of lumped, conceptual rainfall-runoff model to catchment properties via a regression or a site-similarity-approach;

(iii) transfer of a simple distributed grid-based rainfall-runoff model, configured using elevation data, to neighbouring or internal sites; and

(iv) transfer of a simple distributed grid-based rainfall-runoff model, configured using soil properties and elevation data, to neighbouring or internal sites.

The four approaches are described in detail in Sections 3 and 4 of the main body of the report. The aim here is to illustrate the application of these approaches using case study catchment areas from both upland and lowland Britain.

The next section provides descriptions of the case study catchments as a precursor to the modelling applications that follow. To demonstrate the method of transfer to ungauged catchments, certain gauged locations will be taken to be ungauged allowing their flow records to be used for independent assessment of the success of the method. However, note that the purpose of the case studies is to illustrate the application of an approach, in some cases using models in prototype form. A formal intercomparison of approaches would require a more extensive study and further model development. Also the illustrations are limited to forecasts in simulation-mode: they do not extend to consider transfer of model errors from gauged sites to construct updated forecasts for target ungauged locations.

D.2 The case study catchments

Case study catchments have been selected from upland and lowland Britain. Two upland catchments have been selected: the River Kent and the River Darwen, both in Northwest Region. For the lowland case study, two catchment areas sharing a common watershed have been chosen: the River Stour in Midlands Region and the Upper Thames in Thames Region. Figure D.1 provides a location map of the case study catchments. The remainder of this section provides details of the catchments and supporting hydrometry as background to the examples of model transfer that follow.
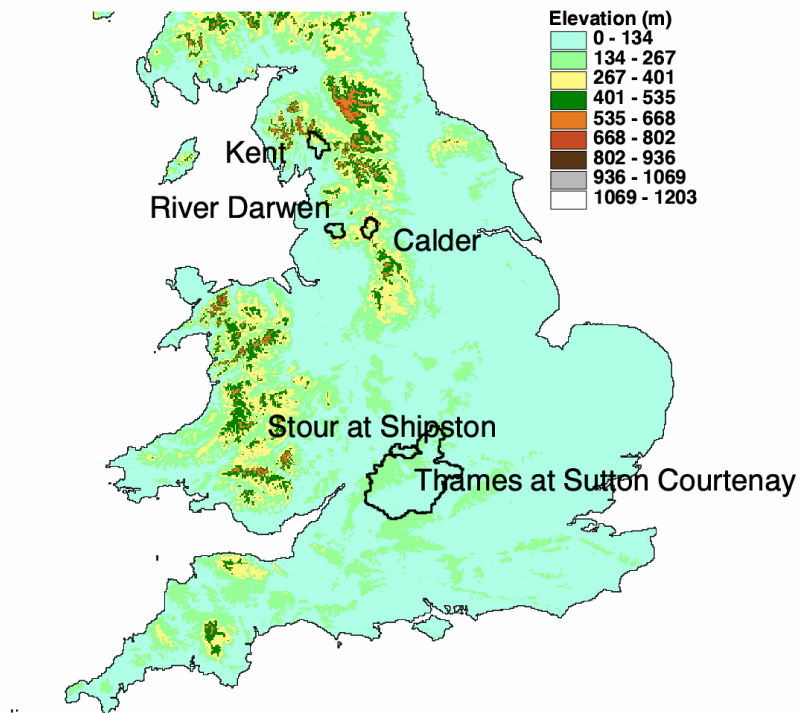
Figure D.1 Locations of the case study catchments

D.2.1 River Kent, North West Region

The River Kent rises in the southeast part of the Cumbrian Hills with the river eventually feeding into Morecambe Bay. For the purposes of this case study, the River Kent is taken to comprise the catchment upstream of the gauging station at Sedgwick, encompassing an area of 212 km^2 with an altitude ranging from 19 to 812 m.

This case study is concerned with modelling river flows at five locations within the Kent catchment to Sedgwick, each corresponding to an established river gauging station. Figure D.2 maps the station locations and the position of the Kentmere Reservoir in relation to the river network. Also shown are the boundaries of their drainage areas and the locations of the telemetry raingauges. The station at Bowston is on the River Kent upstream of Kendal. Gauging stations at Sprint Mill and Mint Bridge are on tributaries to the River Kent whose confluences with the River Kent are also upstream of Kendal. The station at Victoria Bridge is within Kendal on the River Kent.

The upper reaches of the River Kent and its tributaries descend steeply to Kendal (SD 515 927), the only major town within the catchment, and are fast flowing. The upper reaches also have very high relief and are generally wet. The very northern part of the catchment consists of volcanic and low-grade metamorphic rocks of Ordovician age. Moving south to Kendal these are overlain by a wide tract of rocks of Silurian age, comprising of slates and grits, which are predominantly impermeable and covered by heather moorland and peat. From Kendal southwards a Carboniferous Limestone Series occurs: this consists of thick limestone layers interbedded with low-permeability shales and mudstones and provides good grazing. The only significant reservoir within

the catchment is the Kentmere Reservoir (NY 447 078) at the head of the River Kent with a drainage area of 5.02 km^2.

Table D.1 lists the location, station number, catchment area and Standard Average Annual Rainfall for each gauging station in terms of total drainage area and natural drainage area (i.e. excluding the Kentmere Reservoir drainage area). The latter is most appropriate for modelling purposes. Note that the total catchment areas are those given by the Environment Agency whilst the naturally draining areas have been derived
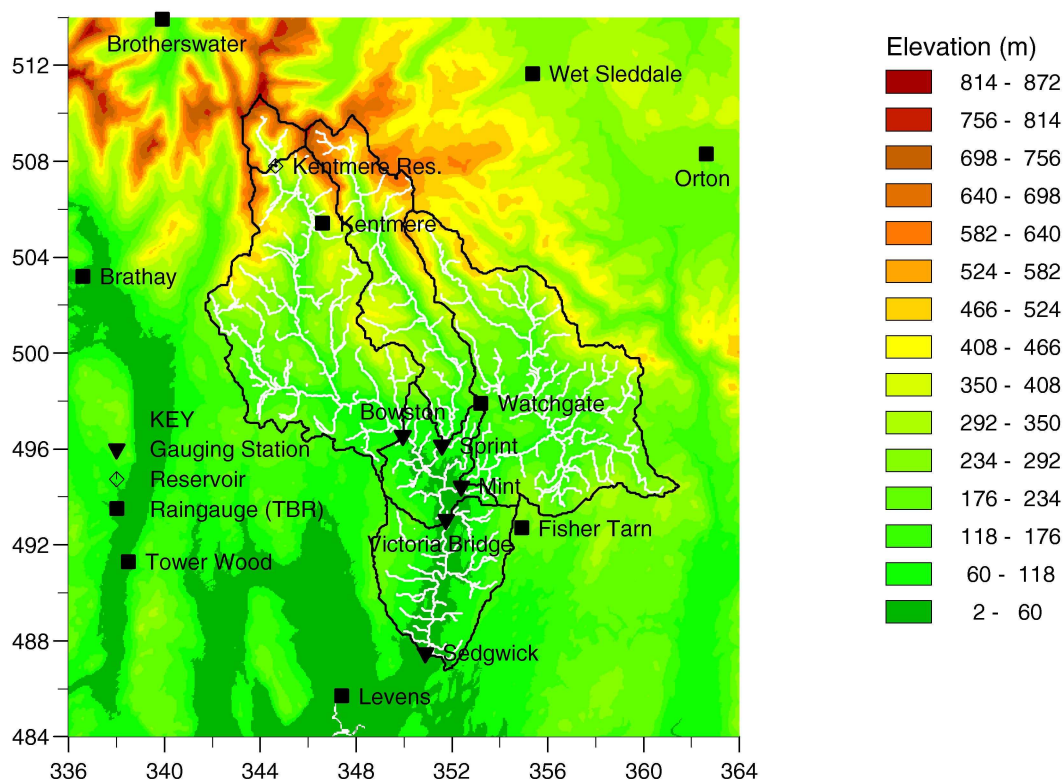

Figure D.2 Map of relief for the Kent catchment and surrounding area.
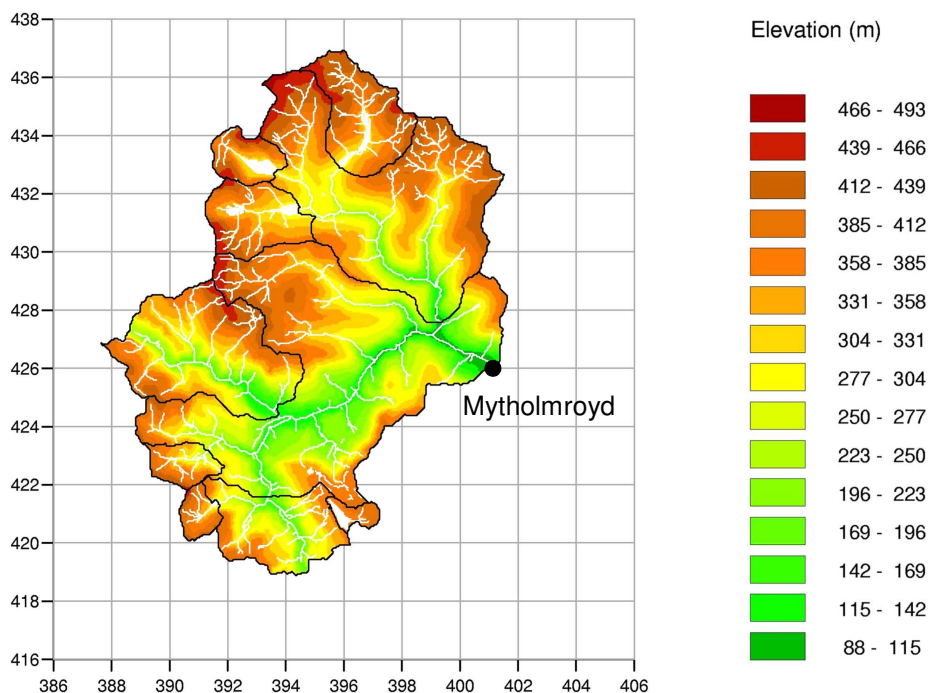
Table D.1 River gauging stations in the Kent catchment

Station	National Grid Reference	Station Number	Total Catchment		Naturally Draining	
			Area (km^2)	SAAR (mm)	Area (km^2)	SAAR (mm)
River Kent at Bowston	SD 4994 9653	730120	70.61	1925	64.78	1868
River Sprint at Sprint Mill	SD 5148 9610	730203	34.60	2019	34.60	2019
River Mint at Mint Bridge	SD 5241 9447	730404	65.80	1599	65.80	1599
River Kent at Victoria Bridge	SD 5181 9307	730507	183.0	1786	179.71	1761
River Kent at Sedgwick	SD 5088 8742	730511	209.0	1727	207.31	1705

using the CEH Digital Terrain Model. River level measurements at 15 minute intervals are available for conversion to flows using rating equations derived from historical current meter readings made at a range of flows.

D.2.2 River Calder, Northeast Region

The Upper Calder river basin (Figure D.3) is located in the Southeast Pennines, in West Yorkshire. For the purposes of this study the Upper Calder is taken to comprise the catchment upstream of Mytholmroyd gauging station, draining an area of 147 km^2 with altitude ranging from 88m to over 400m.

The catchment lies entirely on Carboniferous rocks of Millstone Grit and Coal Measures, with the former predominating in the high moorland areas. The river and its tributaries flow through steep and relatively narrow valleys. About 18% (26 km^2) of the area drains to reservoirs. Typically these are reservoirs for direct water supply, releasing only compensation flows unless spilling at times of flood. The natural flow regime has also been modified by various channel improvements and flood defences. Table D.2 lists the location, station number, catchment area and SAAR for Mytholmroyd in terms of total drainage area and the natural drainage area (i.e. excluding the reservoir drainage areas).

Figure D.3 Map of relief for the Calder catchment to Mytholmroyd.

Table D.2 Gauging station details for the Calder catchment to Mytholmroyd

Station	National Grid Reference	Total Catchment		Naturally Draining	
		Area (km^2)	SAAR (mm)	Area (km^2)	SAAR (mm)
Calder at Mytholmroyd	SE 012 260	147.03	1365	120.67	1354

D.2.3 River Darwen, Northwest Region

The River Darwen has its source in the Southwest Pennines in Lancashire. The case study focuses on the catchment to the river gauging station at Blue Bridge, draining an area of circa 136 km^2 with an altitude range between 11m and just over 400m (Figure D.4). A second gauging station within the catchment at Ewood drains an area of about 39 km^2. The headwaters are steep and contain several small reservoirs draining about 15% (20 km^2) of the catchment area to Blue Bridge. Table D.3 provides a summary of the catchment and reservoir areas and the areas that are naturally drained. The Darwen catchment and its surrounding area is served by a network of 8 telemetry tipping-bucket raingauges (Figure D.4).

The catchment is underlain mainly by Carboniferous grits except near Blue Bridge where the bedrock is Permo-Triassic sandstone. Superficial deposits are predominantly glacial clays and gravel. The upper catchment is almost entirely urbanised by the towns of Blackburn and Darwen whilst the lower half is mainly agricultural.
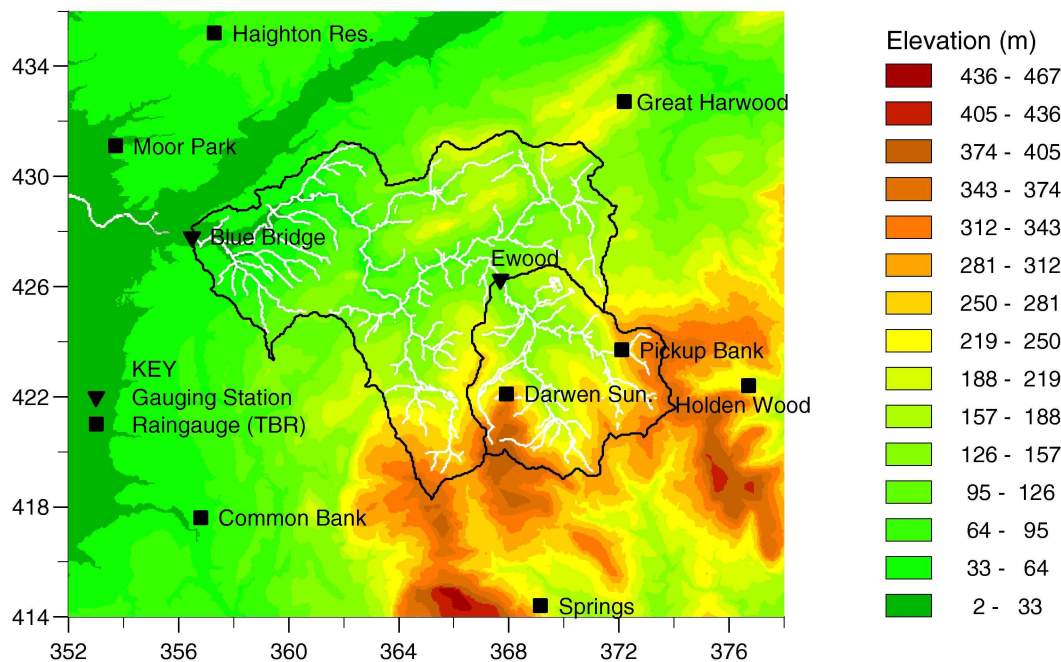

Figure D.4 Relief map of the Darwen catchment showing the river network, catchment boundaries and the hydrometric network.

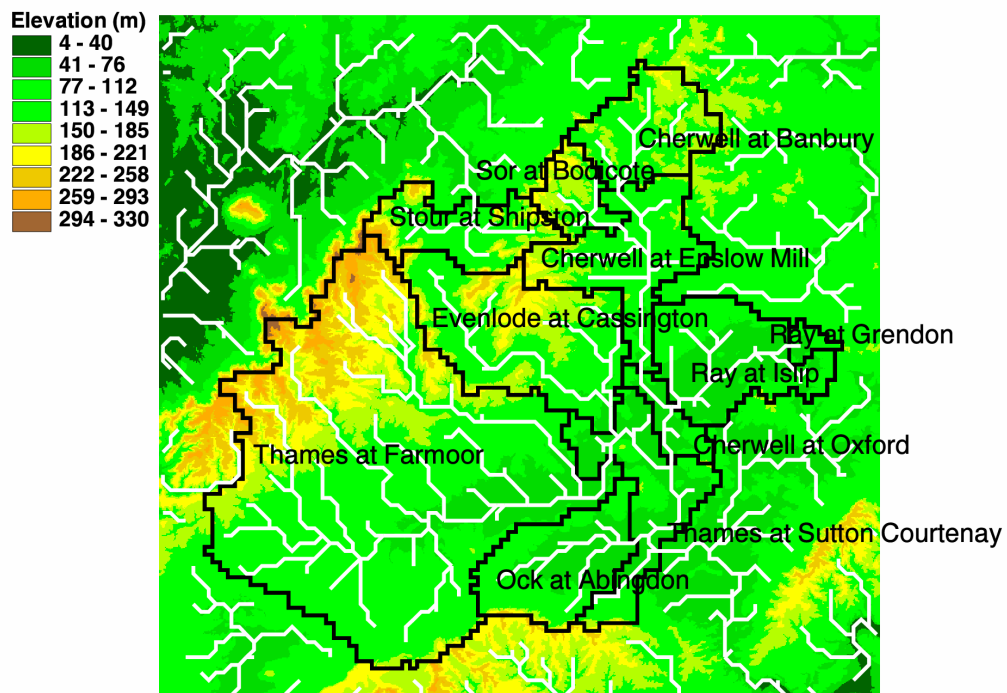**Table D.3 River gauging stations in the Darwen catchment**

Station (Station Number)	National Grid Reference	Total Catchment		Naturally Draining	
		Area (km^2)	SAAR (mm)	Area (km^2)	SAAR (mm)
Darwen at Ewood (713120)	SD 677 262	38.99	1339	29.66	1322
Darwen at Blue Bridge (713122)	SD 565 278	135.68	1198	116.09	1171

D.2.4 Upper Thames and Stour catchments, Thames and Midland regions

Ten catchments which contribute to flow in the Thames at Sutton Courtenay are considered here, together with an adjacent catchment to the north, the Stour to Shipston within Midlands Region. A complete list of catchments is presented in Table D.4 whilst they are mapped in Figure D.5. The River Cherwell rises at Charwelton in Northamptonshire, flows southward through Banbury and eventually joins the Thames at New Hinksey, South Oxford. During its southward passage it is joined by several tributaries including Sor Brook, gauged at Bodicote. Sor Brook rises in the relatively steeply sloping Cotswolds Hills with the catchment to Bodicote ranging in altitude from 225m to 90m and draining an area of approximately 89km^2. The Cherwell to Banbury covers a similar altitude range, from 224m to 90m, but drains a larger area of circa 202km^2 and has less steep tributaries.

The northern catchments are underlain by Liassic formations with a majority being clay, in particular Lower Lias clay to the North of Banbury. Apart from the town of Banbury the catchments are mainly rural in character but flow regimes are affected by abstraction. The flow at Banbury is affected by intakes and returns from the Oxford Canal and by a sewage treatment works. For two of the catchments, the Ray at Islip and the Cherwell at Oxford, flow records are of poor quality and exhibit spurious fluctuations. However, they have been included for completeness as they provide some indication of how well the model performs across a range of subcatchments. The Ray at Grendon Underwood is considered to be largely unaffected by artificial disturbance and provides a good record of natural flows.

Figure D.5 Catchment map and DTM-derived river network for the Thames catchments draining to Sutton Courtenay and the Stour to Shipston.

Table D.4 River gauging stations in the Upper Thames and Stour catchments

Station	Station ID	Area (km^2)	Comments
Stour at Shipston	54106	185.2	Open channel station with cableway, gauge no longer operational. Soils originate predominantly from Keuper Marl
River Cherwell at Banbury	39026	199.4	Asymmetrical compound Crump style weir. Maximum gauged level (flow) is 2m (56 m^{3}s^{-1}). Peak levels estimated as level floats can jam during flood events. River flows also diminished by a large u/s abstraction (Grimsbury). Lias Clays.
Sor Brook at Bodicote	39144	87.7	Crump weir. Abstraction upstream of weir. Peak flows affected by upstream level float 'jamming' during floods, although little evidence in hydrograph.
Evenlode at Cassington	39034	430.0	Compund Crump and single Crump with high level overfall. Mixed geology, oolites in lower reaches.
Cherwell at Enslow Mill	39021	551.7	Asymmetrical compound Crump. Measured high flows unreliable due to bypass of flows. Runoff reduced by public water supply abstraction. Mixed geology with Liassic formations.
Thames at Farmoor	39129	1608.6	Ultrasonic gauge. Significant bypassing on left bank at high flows. Levels affected by gates, abstractions and lock movements. Mixed geology.
Ray at Grendon	39017	18.8	Flat V gauging station. Occasional small fluctuations in levels. Negligible artificial disturbance to the very responsive flow regime. Flat, impermeable Oxford Clay, rural.
Ray at Islip	39140	290.1	Ultrasonic gauge located within "wingwalls" of moveable sluices. Rapid changes in measured flow as a result of sluice movements. Relatively flat, impermeable (Oxford Clay).
Cherwell at Oxford	39139	906.8	Many spurious 'blips' – evident in hydrographs
Ock at Abingdon	39081	234.0	Crump weir, part of which is subject to non-modular conditions. Possible influence from Thames. Mixed geology with 50% clays and chalk. Significant abstraction and recharge. Contributing area exceeds topographical catchment.
Thames at Sutton Courtenay	39046	3414.0	Ultrasonic gauge. Influenced by downstream sluices and lock movements. Mixed geology: Oolitic Limestone headwaters, Oxford Clay below.

D.3 Rainfall data for model calibration and assessment

The catchment descriptions in Section D.2 indicate the numbers and locations of raingauges and flow stations in the study catchments. For all catchments, several raingauges are available for estimating rainfall. Both lumped conceptual and distributed rainfall-runoff models require accurate estimates of rainfall; in the case of lumped models, estimates of catchment average rainfall are required whilst spatially-distributed models can take advantage of spatially-distributed rainfall estimates in grid-square form. In order to provide a consistent rainfall input to both types of model, multiquadric surface fitting has been used to obtain areal rainfall estimates from raingauge data for catchment and grid-square areas as described in Appendix C. The surface-fitting method reduces to a set of linear weights on the raingauge values for the spatial areas of integration (catchments or grid-squares). Table D.5 lists the periods for which model calibration and assessment has been undertaken.

Table D.5 Periods used for model calibration and assessment

Hydrological case study	Calibration period	Evaluation Period
River Kent	25 Oct – 30 Dec 2003	29 Jan - 8 Feb 2004
River Darwen	17 Feb - 9 Mar 2002 26 Jul – 16 Nov 2002	26 Jul – 16 Nov 2002
River Stour	8 Jan - 8 Apr 1990	6 April - 19 April 1998
Upper Thames	1 Sep 2000 – 1 Jun 2001	6 April - 19 April 1998

D.4 Method 1: Simple transfer of lumped, conceptual rainfall-runoff models from neighbouring or similar sites

Transferring modelling information (parameters or data) from one site to another leads to *indirect modelling* of the target site. Information leading to a flood forecast at the target site is assumed to be transferred from a neighbouring, nested, or larger site. Models can be applied directly to the target site, or indirectly through measurement and model application at another site. The method used to transfer information, such as model parameters or data, from the indirectly modelled site to the target site has been termed the *Inference Model*. Common examples of inference models include forms of parameter regionalisation (sometimes called parameter generalisation) explored in Section D.5. The Thiessen polygon method, and other methods used for estimating catchment average rainfall from a network of raingauges, can also be thought of as inference models.

The methodology explored in this Section uses model parameter inference to transfer information from one site to another. The model used here is the standard PDM, a lumped conceptual rainfall–runoff model.

Implementation of the simple model transfer process has involved the steps set down below.

1. *Rainfall inference*

   A multiquadric surface is fitted to the point rainfalls recorded across the telemetry raingauge network in the vicinity of the target catchment. Catchment average rainfalls are then calculated from the fitted surfaces for the target site. All catchments used in this illustration of Method 1 have reasonable raingauge coverage.

2. *Model setup*

   - The rainfall factor parameter, f_c, is set to 1 for all target sites, regardless of the value at the donor site, as the fitted rainfall surface is assumed to be a good estimator of catchment rainfall. If using a single raingauge, an adjustment based on the ratio between catchment and raingauge SAAR would be appropriate.

   - The returns/abstraction parameter, q_c, is set to zero for all target sites, regardless of the value used at the donor site. A non-zero value should only be used if there is a known amount of returns and/or abstractions which affect the catchment.

   - The target site catchment area is used.

The PDM has been independently calibrated for a majority of the catchments used in this illustration of the transfer method; the associated R^2 results are referred to as *calibrated PDM* results. For completeness, the calibrated parameters are listed in Section D.8. The periods chosen for analysis are split into *calibration periods* (i.e. they were used for model calibration) and *evaluation period* as indicated in Table D.5. These results act as a useful reference to judge the performance of transferred model parameters, without the benefit of calibration.

D.4.1 PDM model transfer applied to the River Kent

The River Kent to Sedgwick constitutes a moderate to large headwater catchment and envelops four moderate size headwater sub-catchments. The network of river gauging stations (Figure D.2) makes the River Kent catchment an ideal candidate for illustrating application of the simple transfer of lumped conceptual rainfall–runoff model parameters.

Three simple model transfers have been performed and are detailed below.

Case 1. Calibrated PDM parameters from Sedgwick, the largest catchment, have been transferred to the four sub-catchments.

Case 2. Calibrated PDM parameters from Sprint Mill have been transferred to 2 neighbouring catchments (Bowston and Mint Bridge) and 2 downstream catchments (Victoria Bridge and Sedgwick).

Case 3. Another catchment, the River Calder at Mytholmroyd, is thought to have a similar response to the River Kent catchments and has a comparable total drainage area (140.7 km^2). The calibrated PDM parameters from the Calder are transferred to the five River Kent catchments.

The model simulation results are presented in Table D.6 in terms of R^2 statistics with the best results for each catchment highlighted in bold. These show that all three transfers have performed well and highlight some subtle trends. The transferred Sedgwick parameters (Case 1) perform best for the two larger catchments (Bowston and Victoria Bridge) whilst the Sprint Mill parameters (Case 2) perform best for the neighbouring catchments of comparable size, Mint Bridge and Bowston. The worst results are achieved by transferring the Sedgwick parameters to the two smaller sub-catchments Sprint Mill and Mint Bridge. These trends are due to the catchments becoming flashier with decreasing area and so the Sedgwick parameters respond too slowly for the smaller catchments whilst the Sprint Mill parameters are too flashy for the larger catchments. These trends are evident in the model simulations presented in Figure D.6. However, the simulation results using either set of parameters (Case 1 and 2) are very good and would have clearly been of value had any of the locations been ungauged.
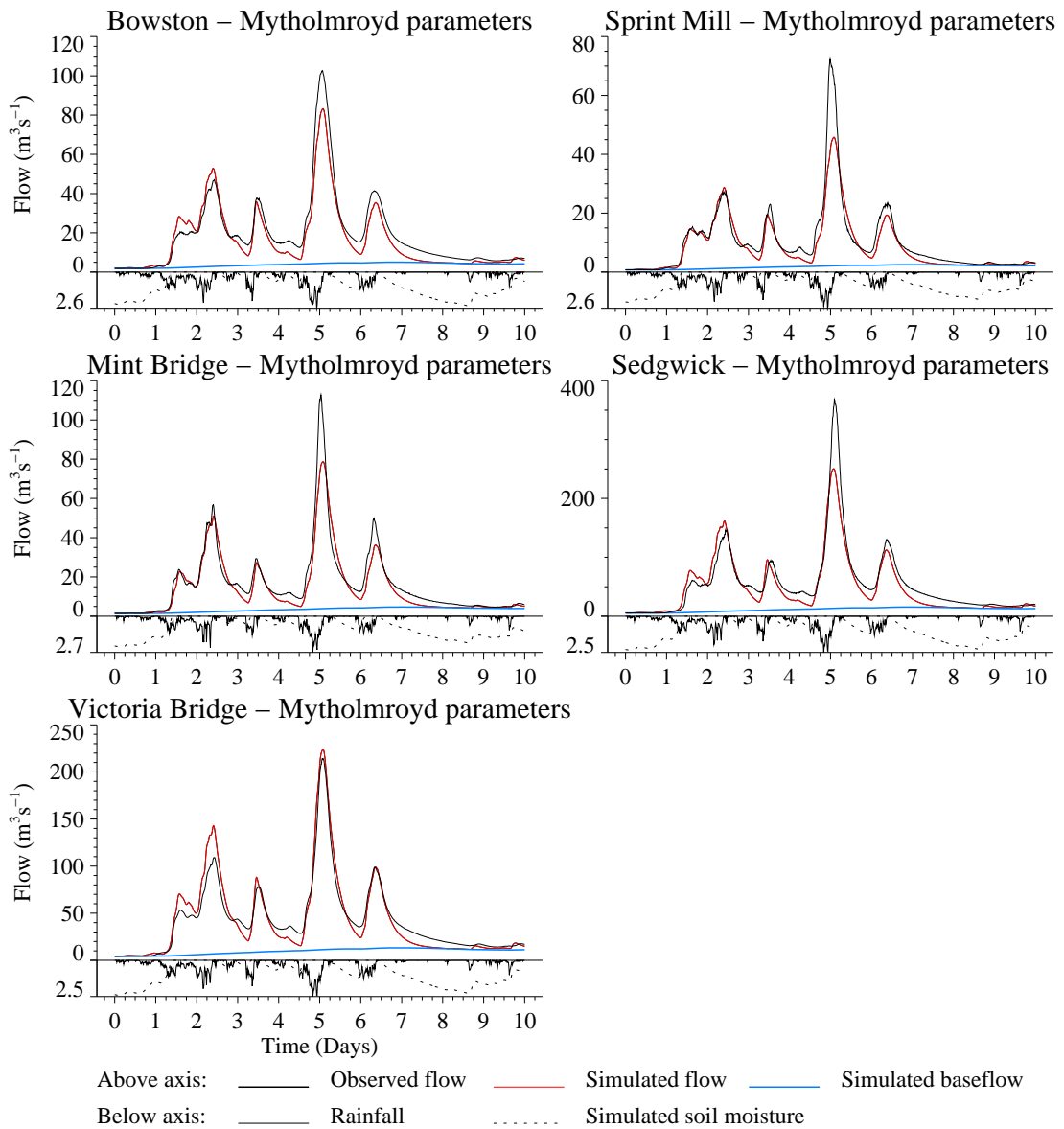
Model transfer using the parameters from the River Calder at Mytholmroyd (Case 3) is exceptionally good considering the spatial distance between it and the Kent catchment. This shows how local hydrological knowledge of catchment response can be extremely useful in identifying appropriate donor catchments and is very encouraging. The model simulations for all catchments over the evaluation period are presented in Figure D.7 and confirm the success of the model transfer.

Table D.6 Simple PDM model transfer: R^2 model simulation results for the Kent catchments

Catchment (Area, km^2)	Case 1: Sedgwick parameters	Case 2: Sprint parameters	Case 3: Mytholmroyd parameters	Calibrated PDM
Calibration Event				
Sprint Mill (34.6)	0.885	N/A	**0.922**	0.962
Bowston (64.8)	**0.956**	0.929	0.931	0.968
Mint Bridge (65.8)	0.912	**0.954**	0.948	0.964
Victoria Bridge(179.7)	**0.930**	0.861	0.885	0.967
Sedgwick (207.3)	N/A	0.873	**0.898**	0.968
Evaluation Event				
Sprint Mill (34.6)	0.744	N/A	**0.852**	0.891
Bowston (64.8)	0.867	**0.926**	0.898	0.912
Mint Bridge (65.8)	0.746	**0.929**	0.890	0.927
Victoria Bridge (179.7)	0.868	0.867	**0.922**	0.952
Sedgwick (207.3)	N/A	**0.896**	0.874	0.879
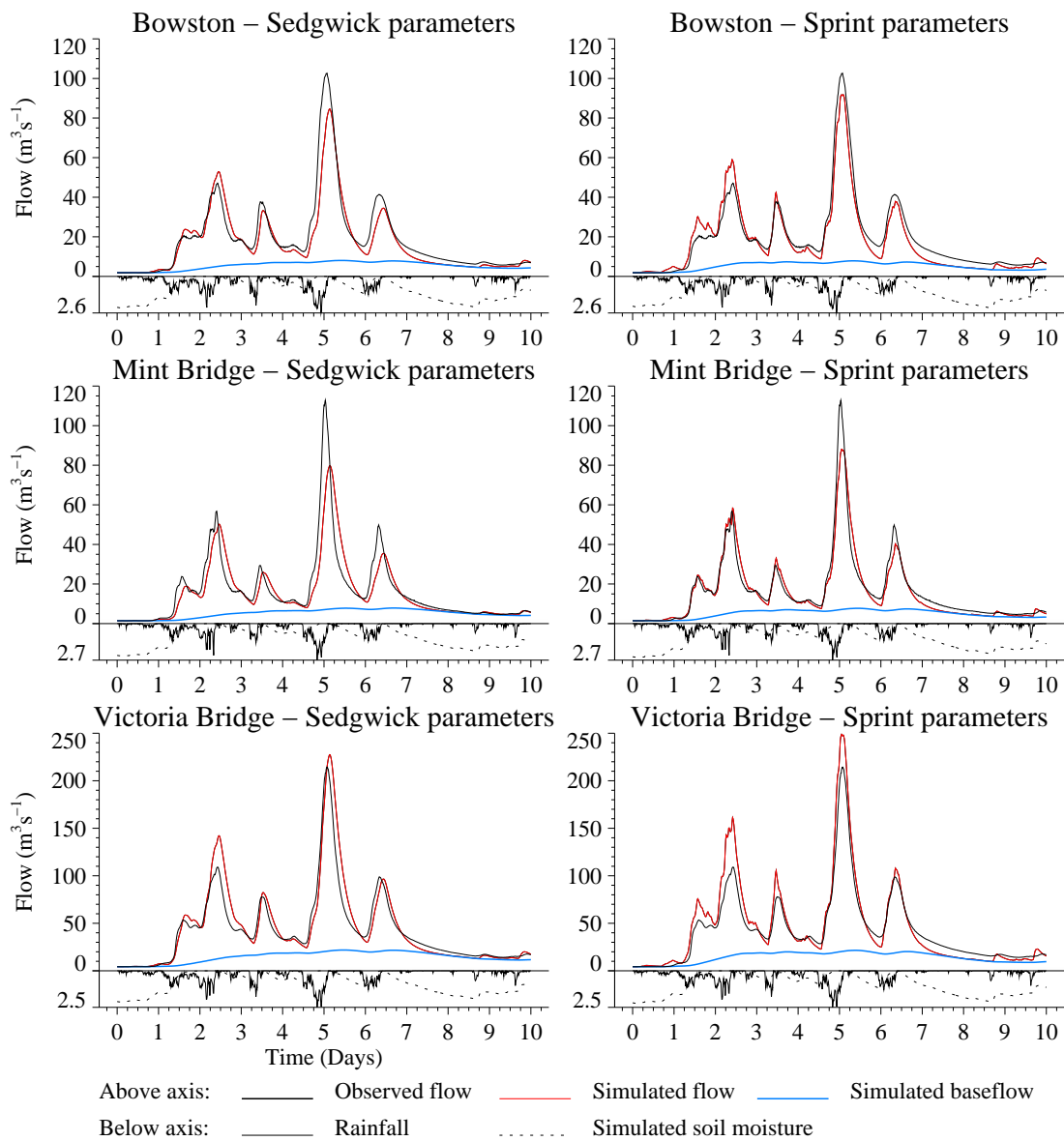
Figure D.6 Flow hydrographs over the evaluation period for three Kent sub-catchments. Parameters transferred from Sedgwick are used in the left-hand column and parameters transferred from Sprint Mill in the right-hand column.

Figure D.7 Flow hydrographs over the evaluation period for all the Kent catchments using parameters transferred from the River Calder at Mytholmroyd.

D.4.2 PDM model transfer applied to the Upper Thames and Stour

Three neighbouring lowland headwater catchments are considered here: the Stour at Shipston, the Sor at Bodicote and the Cherwell at Banbury (see Section D.2.4 for catchment descriptions). The spatial proximity of the catchments makes them a sensible choice for illustrating the method of simple model transfer of lumped conceptual rainfall-runoff parameters. Also they provide a contrast to the responsive upland catchments used for the River Kent example in the previous section.

Two cases of model transfer have been performed and are detailed below.

Case 4. Calibrated PDM parameters for the Kent at Sedgwick (Northwest Region) are transferred to the three target catchments: the Stour at Shipston, the Sor at Bodicote and the Cherwell at Banbury.

Case 5. Calibrated PDM parameters from one target catchment to another, e.g. transfer the calibrated PDM parameters from the Stour at Shipston to the Sor at Bodicote and the Cherwell at Banbury, etc.

An assessment of model simulation performance for both cases is summarised in Table D.7 in terms of the R^2 efficiency measure. The best transfer results are highlighted in bold. Model simulations for the evaluation event, which covers the severe Easter 1998 floods, are presented in Figure D.8 and Figure D.9. The results show reasonable model transfer to some target sites but poor results at others. This is not surprising as a challenging set of target sites have been chosen. Inspection of the observed hydrographs shows that the Stour responds quickest to rainfall, followed by Banbury whilst the Sor at Bodicote is appreciably slower. These differing responses reflect differences in soil and geology between catchments: see Section D.7 for more details.

Table D.7 Simple PDM model transfer: R^2 performance of model simulations for the Upper Thames and Stour catchments

Catchment (Area, km^2)	Case 4: Kent parameters	Case 5: Cherwell parameters	Case 5: Sor parameters	Case 5: Stour parameters	Calibrated PDM
Calibration Event					
Stour (185.2)	0.705	0.680	**0.760**	N/A	0.913
Cherwell (199.4)	0.162	N/A	**0.523**	0.361	0.752
Sor (87.7)	-2.684	-1.729	N/A	**-1.534**	0.907
Evaluation Event					
Stour (185.2)	**0.694**	0.146	0.105	N/A	0.676
Cherwell (199.4)	-0.499	N/A	0.291	**0.892**	0.848
Sor (87.7)	-8.125	**-0.938**	N/A	-1.006	0.715
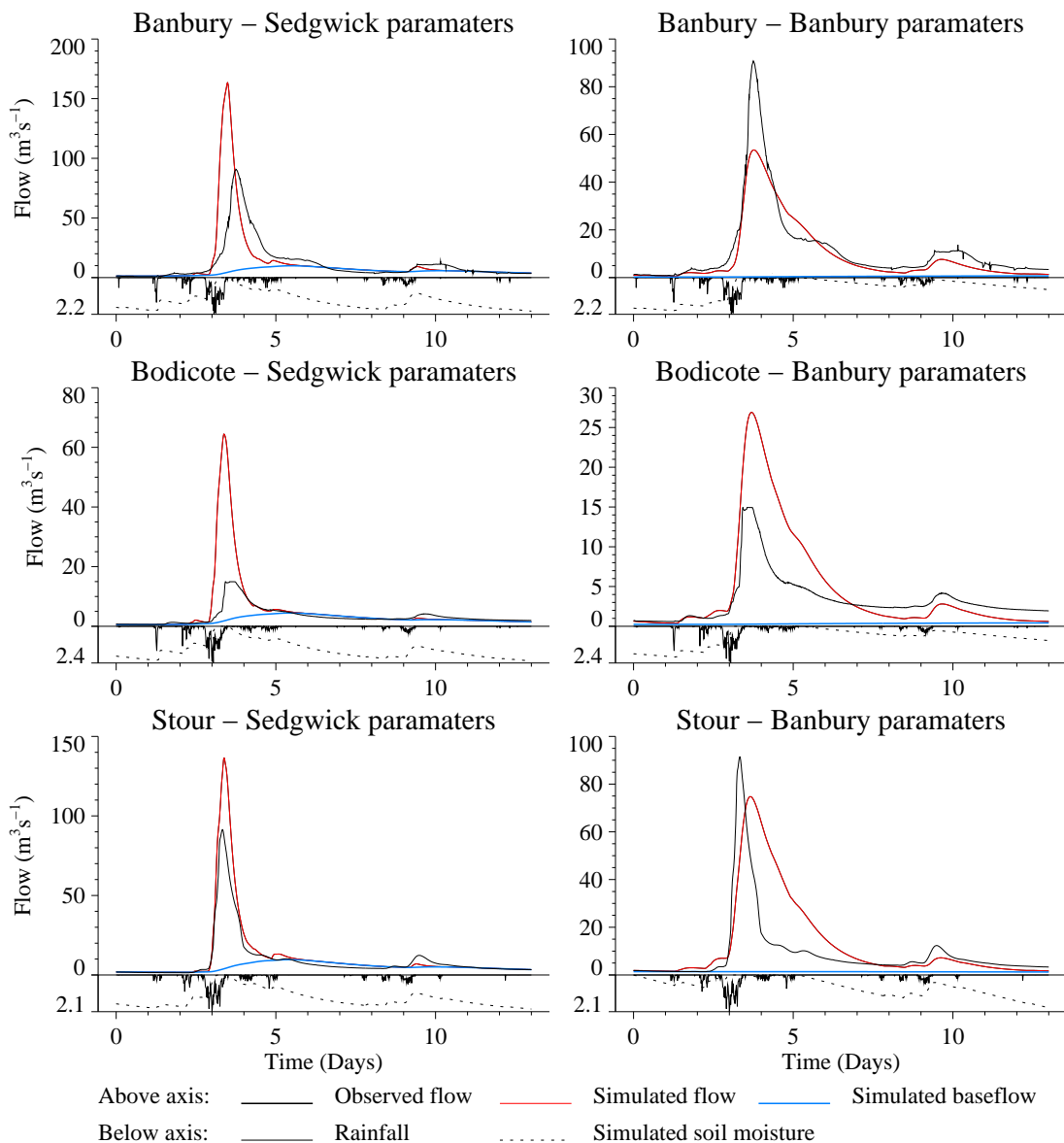
Figure D.8 Flow hydrographs over the evaluation event for the Upper Thames and Stour catchments. Parameters transferred from the Kent at Sedgwick are used in the left-hand column and parameters transferred from the Cherwell at Banbury in the right-hand column.

The results show that the PDM parameters from Sedgwick, a quickly responding upland catchment, transfer well to the Stour, the quickest responding target site, but less well to the other target sites with slower responses. Model transfer from Stour to Banbury and vice versa is reasonable. However, model transfer from either the Stour or Banbury to the neighbouring catchment at Bodicote results in very poor simulations, despite the close spatial proximity of the donor and target sites. This highlights the care needed in selecting appropriate donor sites and that spatial proximity alone will not guarantee good model transfer. Local hydrological knowledge and consideration of key catchment properties should be used to ensure that "similar" donor and target sites are selected.
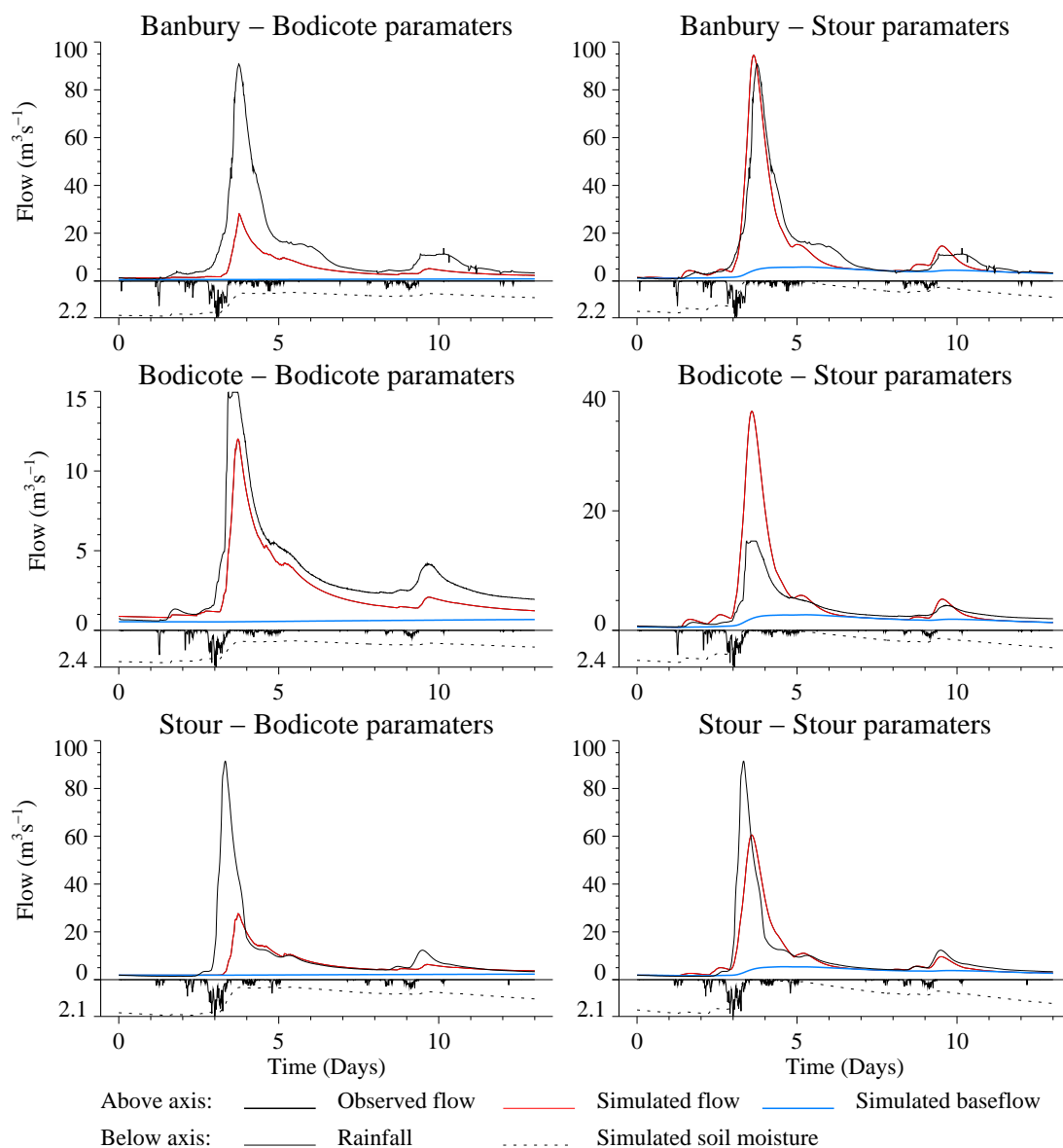
Figure D.9 Flow hydrographs over the evaluation event for the Upper Thames and Stour catchments. Parameters transferred from the Sor at Bodicote are used in the left-hand column and parameters transferred from the Stour at Shipston in the right-hand column.

D.5 Method 2: Relating rainfall-runoff model parameters to catchment properties via regression or a site-similarity approach

Here, the inference model used to transfer information from one site to another is a form of parameter regionalisation (sometimes called parameter generalisation). The rainfall-runoff model used is a simplified form of the PDM, termed the parameter-generalised PDM, described in Section 4.3.4. The full PDM has a number of different formulations, but for use in the continuous simulation approach to flood frequency analysis a simplified version was configured aimed at giving better spatial-generalisation of the five model parameters that remained. The aim of regionalisation (spatial generalisation) is to allow the application of rainfall-runoff models at sites where there is insufficient flow data for model calibration. Instead, the values of model parameters are inferred for ungauged sites using derived relationships to catchment properties. These properties have been chosen to be readily and reliably calculable across the country. For instance, they may describe land cover, soil type, catchment topography or the river network.

Here, parameter values for the study catchments have been estimated using two spatial generalisation approaches.

(i)   *Sequential regression.* Predictive equations for model parameters are derived in a sequence, rather than independently, in order to try to account for the effect that already-generalised parameters have on the remainder of the parameter set.

(ii)   *Site-similarity.* An approach in which rainfall-runoff model parameters are weighted by means of parameter values from a set of catchments of similar hydrological response, as characterised by key catchment properties.

For the parameter-generalised PDM model the site-similarity approach (reviewed in Section 3.3.4) was found to be marginally superior to the catchment property regression approach. For illustrative purposes, the application of both approaches is presented here. Table D.8 presents the parameter-generalised PDM model parameter values obtained for the study catchments using both regression and site-similarity procedures. These parameters are: f_c, a volume adjustment factor; c_{max}, the maximum depth at any point within the soil store; k_1 and k_b, the respective time constants of the fast and slow flow stores; and α, the split of the direct runoff between the fast and slow flow stores. Note that in the tables, sequential regression is denoted "Regression" whilst the site-similarity approach is denoted "Similarity".

Values for the f_c parameter, the rainfall volume adjustment factor, tend to be greater than the ideal value of 1.0 for the Kent and Darwen catchments. This is a symptom of the flood estimation project for which the parameters were derived (Calver *et al.*, 2005). This application put particular emphasis on accurate estimation of high flood peaks, and can result in relatively high values of the rainfall adjustment factor for some catchments. Other parameters, c_{max}, k_1, k_b and α vary from catchment to catchment. It is worth noting that values for α, the runoff partitioning factor in the parameter-generalised PDM which is based on the value for the baseflow index, show little variation in the Kent and Darwen catchments. This contrasts with the Thames catchments, for which α is more variable reflecting a changing baseflow regime.

Table D.8 Parameter-generalised PDM model parameters
(a) Kent catchments

Catchment	Station ID	Area, km²	Method	Parameters required by parameter-generalised PDM				
				f_c	c_{max}	k_1	k_b	α
Bowston	730120	64.78	Similarity	1.440	120.81	12.865	98.611	0.434
			Regression	1.389	150.498	9.038	112.491	0.434
Sprint Mill	730203 (73009)	34.6	Similarity	1.439	113.7438	9.670	110.567	0.445
			Regression	1.392	160.454	4.750	128.346	0.445
Mint Bridge	730404 (73011)	65.8	Similarity	1.300	139.01	16.514	92.944	0.368
			Regression	1.388	167.378	6.685	97.716	0.368
Victoria Bridge	730507	179.71	Similarity	1.374	112.704	16.556	106.451	0.397
			Regression	1.380	135.295	8.008	134.625	0.397
Sedgwick	730511 (73005)	209.0	Similarity	1.372	112.46	13.784	145.97	0.381
			Regression	1.382	124.66	8.260	180.84	0.381

(b) Darwen catchments

Catchment	Station ID	Area, km²	Method	Parameters required by parameter-generalised PDM				
				f_c	c_{max}	k_1	k_b	α
Darwen at Ewood	713120	29.66	Similarity	1.326	129.711	7.748	92.357	0.367
			Regression	1.259	116.923	6.976	176.719	0.367
Darwen at Blue Bridge	713122	116.09	Similarity	1.399	124.538	8.063	114.855	0.387
			Regression	1.236	96.770	9.112	193.520	0.387

(c) Stour at Shipston

Catchment	Station ID	Area, km²	Method	Parameters required by parameter-generalised PDM				
				f_c	c_{max}	k_1	k_b	α
Stour at Shipston	2092	185.16	Similarity	1.112	232.067	14.850	151.793	0.413
			Regression	1.078	257.020	14.136	78.964	0.413

(d) Upper Thames catchments

| Catchment	Station ID	Area, km²	Method	Parameters required by parameter-generalised PDM				
				f_c	c_{max}	k_1	k_b	α
Sor at Bodicote	39144	88.8	Similarity	0.948	248.720	34.916	273.613	0.233
			Regression	0.938	282.751	22.596	170.059	0.233
Cherwell at Banbury	39026	199.4	Similarity	0.999	233.109	17.397	49.821	0.427
			Regression	1.057	264.315	20.199	55.521	0.427

The parameter transfer procedure is very straightforward, and simply requires the PDM to be run on the target catchments, for the periods of interest, using the parameters derived with the regionalisation procedure. Parameters derived using the two spatial generalisation approaches, site-similarity and regression, were used in the parameter-generalised simplified form of the PDM. A further set of experiments was performed using an f_c value of 1.0, in order to test whether the relatively large values of this parameter was adversely affecting model performance. A summary of model performance is presented as tables of R^2 statistics, comparing observed and modelled flows for selected periods, together with flow hydrographs. The performance of the parameter-generalised PDM is also compared to a typical PDM model which has been directly calibrated to observed flows for the "calibration event". This comparison is rather unfair on the parameter-generalised PDM, which has not been exposed to the calibration event before; however, it does provide an informal benchmark against which model performance can be compared. Results are now presented for each case study.

D.5.1 Parameter-generalised PDM results for the Kent catchments

PDM model simulation performance is summarised in Table D.9 in terms of the R^2 statistic. Best parameter-generalised PDM results for each catchment are highlighted in bold. Neither method of deriving parameter-generalised PDM parameters seems better than the other; also there appears to be little benefit from setting the f_c value to unity. In general, the standard calibrated PDM performs better, but the performance of the parameter-generalised PDM is generally respectable for these simply responding catchments. In one case, the evaluation event for Mint Bridge, the parameter-generalised PDM performed marginally better than the PDM calibrated in the standard way. A set of example hydrographs comparing observed and modelled flows is presented in Figure D.10 and Figure D.11. A model simulated hydrograph for the longer calibration period has been included here as it highlights the overall good performance of the parameter-generalised PDM on this catchment.

Table D.9 Model performance assessed using the R^2 statistic for the Kent catchments

| Catchment	Station ID	Area, km^2	Method	Calibration event: 25 Oct – 30 Dec 2003			Evaluation event: 29 Jan - 8 Feb 2004		
				Derived f_c	f_c = 1	Standard PDM	Derived f_c	f_c = 1	Standard PDM
Bowston	730120	64.78	Similarity	0.782	0.786	0.970	0.826	0.579	0.918
			Regression	**0.800**	0.767	0.970	**0.856**	0.564	0.918
Sprint Mill	730203 (73009)	34.6	Similarity	**0.755**	0.611	0.962	**0.649**	0.380	0.891
			Regression	0.743	0.567	0.962	0.607	0.293	0.891
Mint Bridge	730404 (73011)	65.8	Similarity	0.819	0.749	0.964	0.927	**0.934**	0.927
			Regression	**0.821**	0.795	0.964	0.791	0.533	0.927
Victoria Bridge	730507	179.71	Similarity	0.765	**0.824**	0.967	0.664	0.629	0.952
			Regression	0.737	0.800	0.967	**0.794**	0.666	0.952
Sedgwick	730511 (73005)	207.31	Similarity	**0.791**	0.737	0.968	0.657	0.400	0.879
			Regression	0.743	0.698	0.968	**0.685**	0.393	0.879
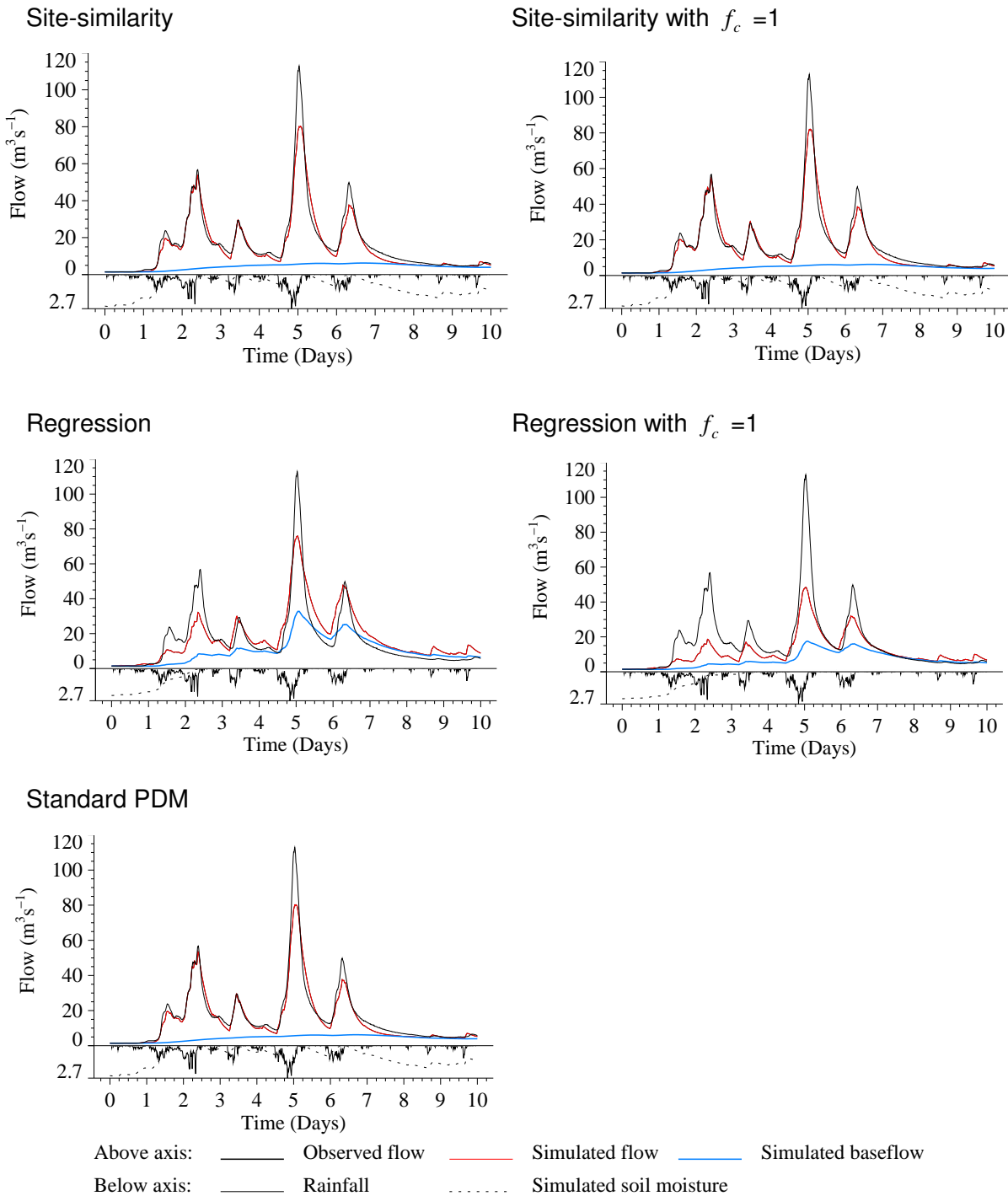
Figure D.10 Flow hydrographs for the Kent to Mint Bridge comparing model performance obtained from the parameter-generalised and standard PDM
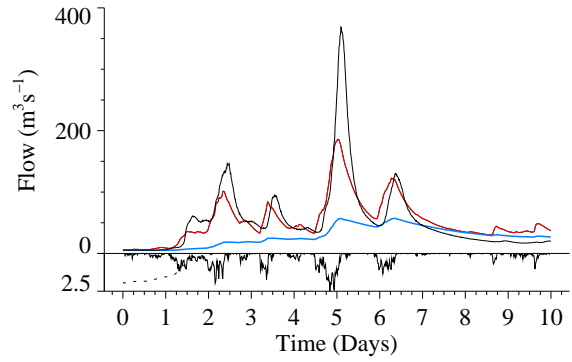
Calibration event: parameter-generalised PDM using site-similarity
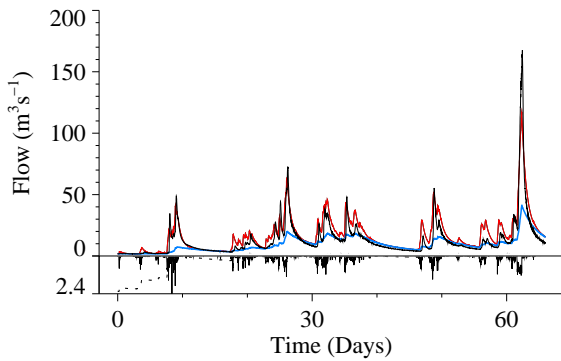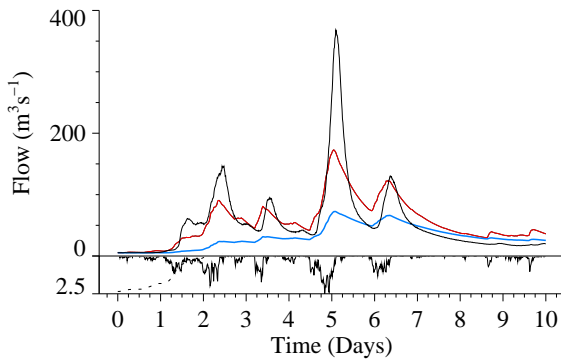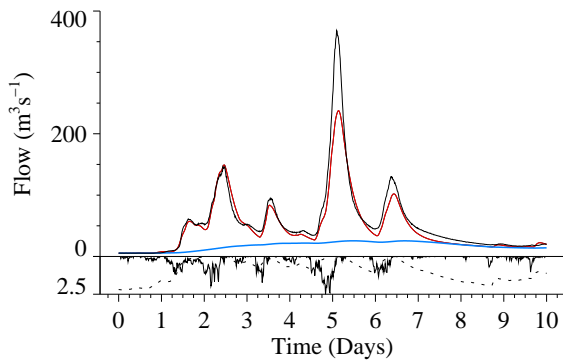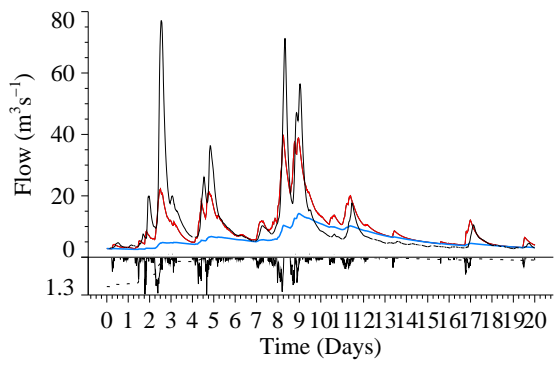

Evaluation event
Site-similarity

Regression

Standard PDM

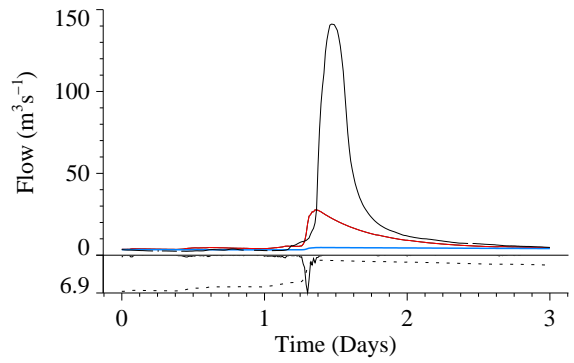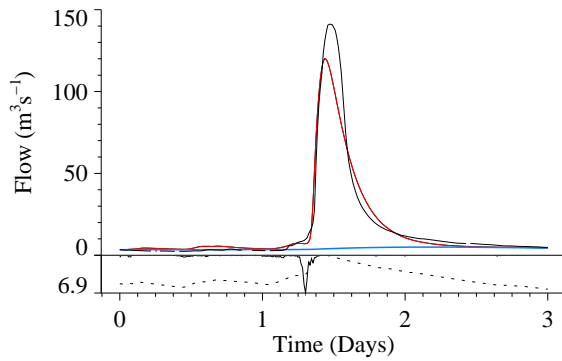| Above axis: | ——— | Observed flow | ——— | Simulated flow | ——— | Simulated baseflow |
| Below axis: | ——— | Rainfall | ······· | Simulated soil moisture | | |

Figure D.11 Flow hydrographs for the Kent to Sedgwick comparing model performance obtained from the parameter-generalised and standard PDM

D.5.2 Parameter-generalised PDM results for the Darwen catchments

PDM simulation results are presented in Table D.10 in the form of values of R^2. Best generalised PDM results for each catchment are highlighted in bold. For both events, parameters obtained through the method of site-similarity gave better results. There also appears to be little benefit from setting the f_c value to unity. The standard calibrated PDM performed substantially better for both events. A set of example hydrographs comparing observed and modelled flows is presented in Figure D.12. Although the performance of the generalised PDM is poor for the evaluation event, the hydrograph for the three week calibration period indicates that the model broadly simulates the response of the catchment to rainfall, but tends to partition too much runoff to baseflow leading to underestimated flow peaks.

Table D.10 Model simulation results for the River Darwen

Catchment	Station ID	Area, km^2	Method	Calibration event: R^2			Evaluation event: R^2		
				Derived f_c	$f_c = 1$	Standard PDM	Derived f_c	$f_c = 1$	Standard PDM
Darwen at Ewood	713120	38.99	Similarity	**0.530**	0.314	0.954	**0.150**	0.039	0.778
			Regression	0.459	0.287	0.954	0.140	0.049	0.778
Darwen at Blue Bridge	713122	135.68	Similarity	**0.597**	0.328	0.972	**0.175**	0.003	0.934
			Regression	0.502	0.331	0.972	0.111	0.007	0.934

Calibration event: Site-similarity

Evaluation event
Site-similarity   Regression
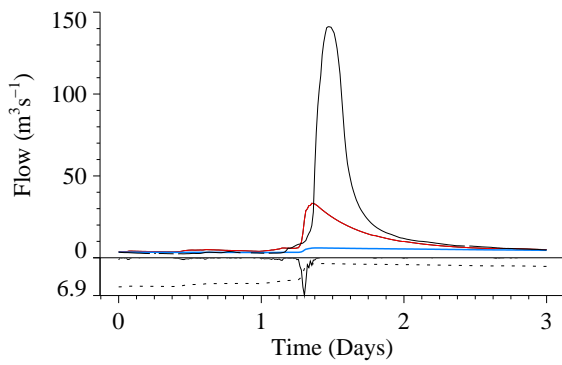
Standard PDM

| Above axis: | _____ | Observed flow | _____ | Simulated flow | _____ | Simulated baseflow |
| Below axis: | _____ | Rainfall | . . . . . . | Simulated soil moisture | | |

Figure D.12 Flow hydrographs for the Darwen to Blue Bridge comparing model performance obtained from the parameter-generalised and standard PDM

D.5.3 Parameter-generalised PDM results for the Stour to Shipston

Model simulation performance for the parameter-generalised PDM is summarised in Table D.11, in terms of the R^2 statistic, with the best performance for each catchment highlighted in bold. The performance of the standard PDM is given for comparison.

Table D.11 Model simulation performance (R^2 statistic) for the Stour to Shipston

Catchment	Area, km^2	Method	Calibration event: 8 Jan - 8 Apr 1990			Evaluation event: 6 April - 19 April 1998		
			Derived f_c	$f_c = 1$	Standard PDM	Derived f_c	$f_c = 1$	Standard PDM
Stour to Shipston	185.1	Similarity	0.737	0.680	0.913	0.539	0.455	0.676
		Regression	**0.742**	0.671	0.913	**0.562**	0.499	0.676

For both events, parameters obtained through the method of regression give slightly better results. There also appears to be little benefit from setting the f_c value to unity. The standard calibrated PDM performs better, but the performance of the parameter-generalised PDM is respectable. The evaluation event consists of the Easter 1998 flood event, which can be considered an extreme event. Both formulations of the PDM perform less well on this event, as shown in Figure D.13; however, problems with measurement of both rainfall and river flow under such extreme conditions are likely to be contributory causes of poorer performance.

D.5.4 Parameter-generalised PDM results for the Thames catchments

PDM model simulation performance is summarised in Table D.12 in terms of the R^2 statistic. Best parameter-generalised PDM performance for each catchment is highlighted in bold. Neither method of estimating parameter-generalised PDM parameters seems better than the other, but for these catchments there can be some benefit from setting the f_c value to unity (however, the f_c values obtained from the spatial generalisation methods are not overestimated for these catchments, so this change is not greatly justified). In general, the standard calibrated PDM performs better, but the performance of the parameter-generalised PDM is generally respectable. A set of example hydrographs comparing observed and modelled flows is presented in Figure D.14.

Table D.12 Model simulation performance (R^2 statistic) for Thames catchments

| Catchment	Station ID	Area, km^2	Method	Calibration event: 1 Sep 2000 – 1 Jun 2001			Evaluation event: 6 April - 19 April 1998		
				Derived f_c	$f_c = 1$	Standard PDM	Derived f_c	$f_c = 1$	Standard PDM
Sor at Bodicote	39144	88.8	Similarity	**0.831**	0.788	0.907	0.204	0.299	0.715
			Regression	0.743	0.641	0.907	0.301	**0.423**	0.715
Cherwell at Banbury	39026	199.4	Similarity	0.444	0.444	0.752	0.554	0.554	0.848
			Regression	0.468	**0.527**	0.752	**0.569**	0.506	0.848

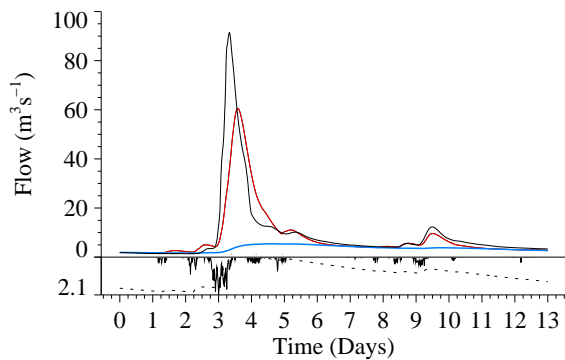Calibration event: Generalised PDM using Site-similarity
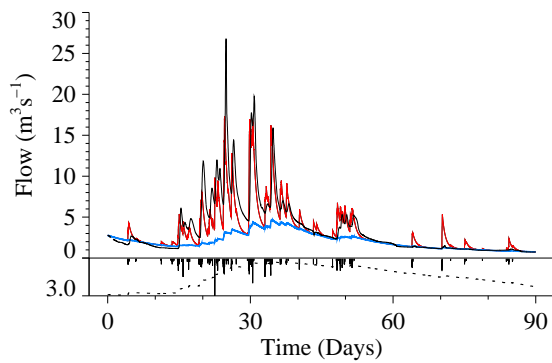
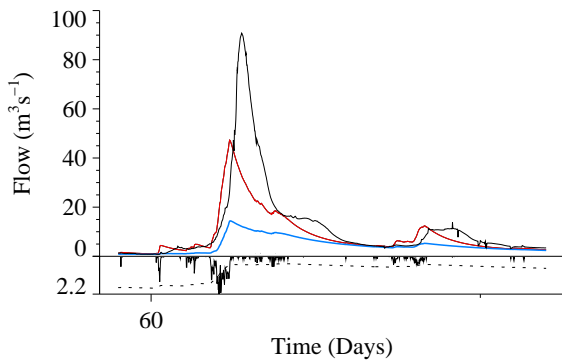Evaluation event: Generalised PDM
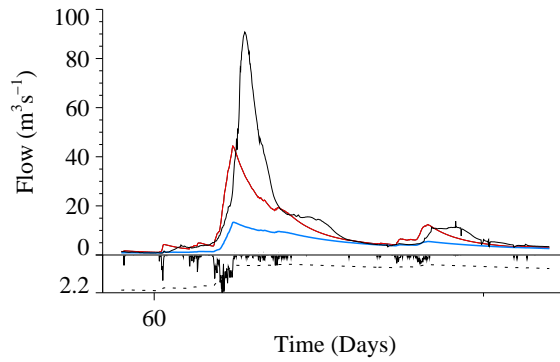Site-similarity
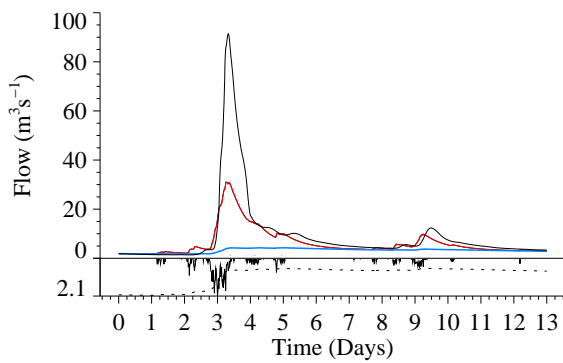
Regression
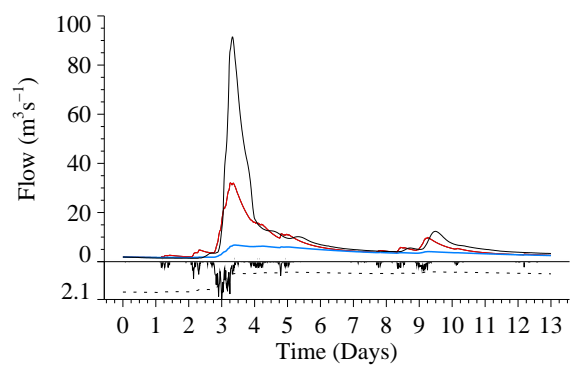
Standard PDM

| Above axis: | ——— | Observed flow | ——— | Simulated flow | ——— | Simulated baseflow |
| Below axis: | ——— | Rainfall | .... | Simulated soil moisture | | |

Figure D.13 Flow hydrographs for the Stour to Shipston comparing model performance obtained from the parameter-generalised and standard PDM
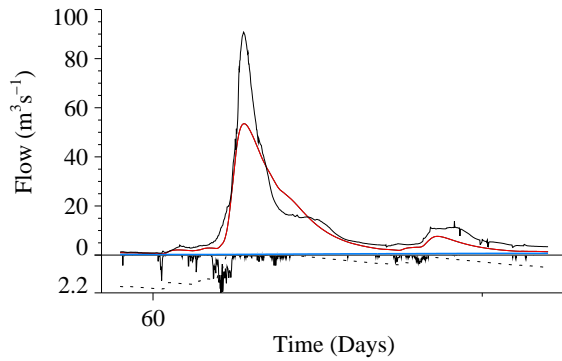
Figure D.14 Flow hydrographs for the Cherwell to Banbury comparing model performance obtained from the parameter-generalised and standard PDM

D.6 Method 3: Transfer of a simple grid-based rainfall-runoff model (configured using elevation data alone) to neighbouring or internal sites

This section considers methods of transfer applied to a simple distributed rainfall-runoff model, the Grid-to-Grid Model or G2G. In its basic form, the G2G uses digital terrain data to support its configuration and parameterisation, and this is used to underpin the method of model transfer. The Grid-to-Grid model requires three elevation-derived gridded datasets:

1. *flow directions* - required to configure the routing scheme;
2. *area draining to every grid-cell* - used in model configuration to determine whether a grid-cell is land or river; and
3. *mean slope within each grid-square* - required by the parameterisation of the runoff-production scheme operating within each grid-square.

All these datasets can be derived from digital elevation data. Here, the IHDTM (Morris and Flavin, 1990) has been used as the basis for most of the datasets.

D.6.1 The digital datasets

Deriving flow path directions and drainage areas for the Grid-to-Grid model

The process of deriving routing pathways from a DTM is summarised in the diagram below.
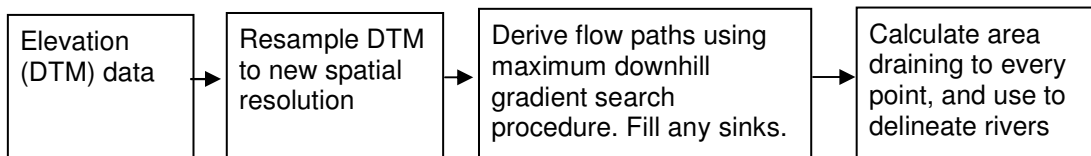
The process of creating a network of routing pathways involves automated search procedures that iteratively calculate flow paths, correcting them by artificially raising or lowering elevations to remove sinks. This process will usually lead to a network of flow paths that has no sinks and bears some resemblance to the actual river network which, if required, can be further refined by hand correction. Occasionally automated procedures produce unrealistic river networks and, although techniques exist to correct them in a semi-automated way, it can often be straightforward to manually "burn" more realistic river flow paths into the terrain.

With the aim of combining the accuracy of high resolution flow paths and the computational efficiency of lower resolution grid cells, a scheme to automatically identify flow directions and catchment areas on a low resolution grid (1km) using flow directions on a finer grid (e.g. 50m) has been investigated by Fekete *et al.* (2001). This method divides a larger grid cell into a block of $n \times n$ smaller grid cells for which flow directions and accumulated areas are known. The flow directions of the larger cells are determined from the magnitude (and sometimes the position) of the maximum value of the accumulated areas of the smaller cells in the $n \times n$ block.

Here the automated procedure of Fekete has been implemented to derive an initial set of flow directions. The method determines flow directions of the 1km cells from the magnitude of the maximum value of the accumulated areas of the 50m cells, taken from the IHDTM, in the 1×1km block. Once a set of flow directions has been identified, the catchment area draining to any point can be determined. Table D.13 shows the catchment areas derived from the Fekete flow paths compared to the 50m resolution catchment areas. Values of percentage error are given in brackets. Use of the Fekete method to derive flow networks generally results in reasonable agreement between derived and observed catchment areas, though there are significant errors for some catchments.

Although good agreement in terms of catchment area was achieved by the automated Fekete method for a majority of the catchments studied, closer examination and comparison with 50m flow directions revealed that the 1km flow directions for all catchments might benefit from a degree of hand correction in order to achieve a satisfactory water-balance for the catchment. By way of illustration, Fekete-derived and hand corrected 1km flow directions and boundaries for the catchments draining to the River Kent are presented in Figure D.15, together with the detailed 50m elevation, flow directions and catchment boundaries. The map highlights the deficiencies of the automated method for the smaller River Kent catchments. Figure D.16 shows the improvement provided by hand correction.

Table D.13 Comparison of observed and DTM-derived catchment areas

| Catchment | Derived Area (km^2) and percentage error | | |
	50m DTM	1km Fekete Method	Hand corrected 1km Fekete Method
River Kent			
Sedgwick	212.3	212 (0%)	212 (0%)
Victoria	184.7	188 (2%)	185 (0%)
Bowston	69.8	69 (-1%)	70 (0%)
Mint	65.5	49 (-26%)	67 (+2%)
Sprint	34.5	45 (+29%)	36 (+3%)
River Stour			
Shipston	185.2	185 (0%)	185 (0%)
River Thames			
River Cherwell at Banbury	201.9	205 (+2%)	202 (0%)
Sor Brook at Bodicote	88.8	98 (+10%)	88 (-1%)
Evenlode at Cassington	427.2	436 (+2%)	428 (0%)
Cherwell at Enslow Mill	555.4	565 (+2%)	556 (0%)
Thames at Farmoor	1608.6	1637 (+2%)	1609 (0%)
Ray at Grendon	21.2	25 (+19%)	22 (+4%)
Ray at Islip	290.0	258 (-11%)	289 (0%)
Cherwell at Oxford	906.8	903 (0%)	916 (+1%)
Ock at Abingdon	185.2	185 (0%)	185 (0%)
Thames at Sutton Courtenay	3425.7	3424 (0%)	3426 (0%)
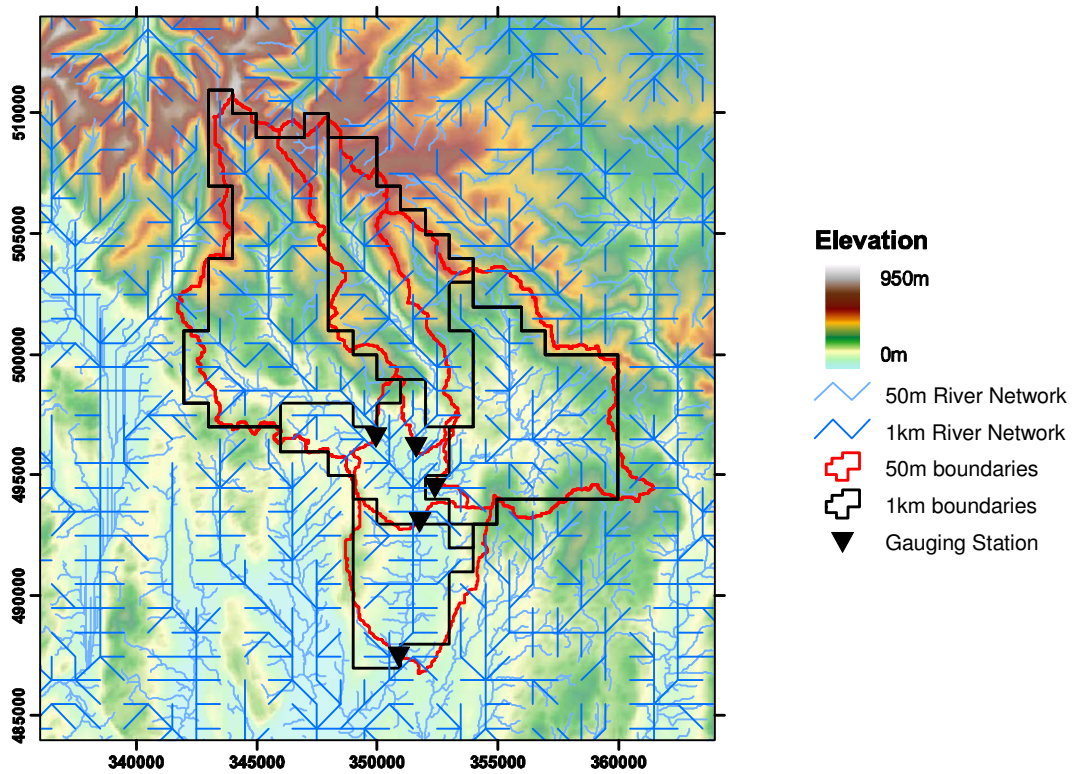
Figure D.15 Fekete derived 1km and IHDTM 50m resolution flow directions and catchment boundaries: River Kent catchment.
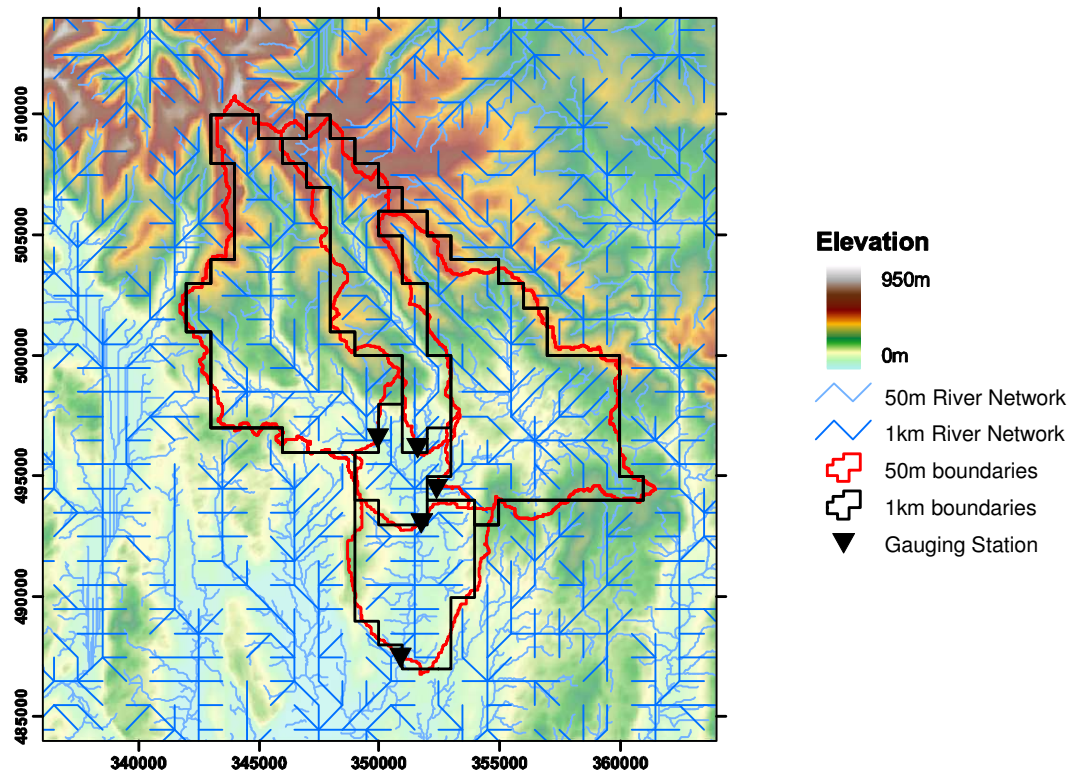

Figure D.16 Hand corrected 1km and IHDTM 50m resolution flow directions and catchment boundaries: River Kent catchment.

Topographic slope dataset

For the River Kent (Case 1 below) the mean slope of a grid square has been calculated using HYDRO1K elevation data by constructing 1km resolution flow paths and then calculating the gradient between connected 1km grid squares.

With the availability of 50m resolution DTMs it is possible to calculate a better estimate of the mean slope for a grid square by constructing 50m resolution flow paths, calculating the gradient between connected 50m squares and then averaging these over the 1km grid squares. For the Upper Thames (Case 2 below) the IHDTM has provided the 50m elevation data and the mean slope for each 1km grid square is presented in Figure D.17.
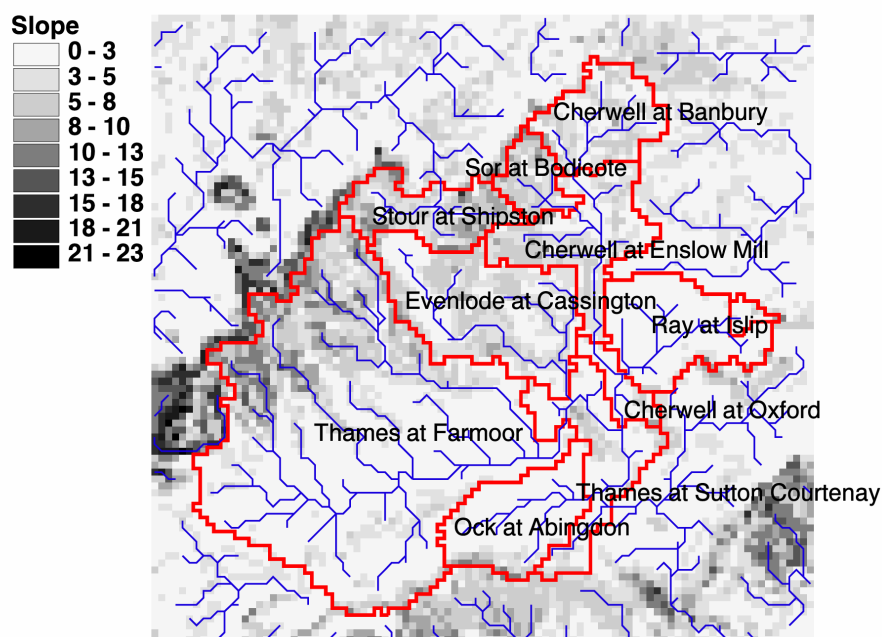

Figure D.17 Map of 1km resolution slope for the Upper Thames and Stour

D.6.2 Model transfer to internal sites: River Kent, Northwest Region

The River Kent basin has a reasonably dense gauging network as shown in Figure D.2. The Grid-to-Grid model has been manually calibrated using flow records from the furthest downstream gauging station at Sedgwick. Since the Grid-to-Grid model is an area-wide distributed model, river flow estimates can be obtained for any grid-square in the modelled domain. This allows simulated flow to be compared to gauged flow for all stations upstream of Sedgwick. This constitutes model transfer to internal sites.

Model simulation performance is presented in Table D.14 in terms of the R^2 statistic. The PDM performance obtained from calibration to each station are given for comparison and show how well the Grid-to-Grid model has worked over the entire River Kent basin. The good performance of the Grid-to-Grid model is confirmed by the model simulations over the evaluation event presented in Figure D.18. The success of the Grid-to-Grid model transfer in this upland area is probably due to the dominant topographic control on flow response. It also shows the great benefits a single

distributed model of simple form can bring to forecasting at multiple ungauged locations within an area where topography provides the dominant control on flow response.

Table D.14 Simple Grid-to-Grid model transfer: R^2 model simulation performance for the Kent catchments

| Model	Target catchment				
	Bowston	**Sprint**	**Mint**	**Victoria**	**Sedgwick**
Calibration Event					
Grid-to-Grid calibrated at Sedgwick	0.912	0.937	0.930	0.901	0.942
Calibrated PDM (at each catchment)	0.968	0.962	0.964	0.967	0.968
Evaluation Event					
Grid-to-Grid calibrated at Sedgwick	0.921	0.894	0.918	0.887	0.900
Calibrated PDM (at each catchment)	0.912	0.891	0.927	0.952	0.879

D.6.3 Model transfer to neighbouring sites: Upper Thames

In this example only two neighbouring catchments in the Upper Thames are considered, namely the Sor at Bodicote and the River Cherwell at Banbury. The Grid-to-Grid model has been calibrated for each catchment separately and then the model parameters transferred from one catchment to the other.

Model simulation performance is summarised in Table D.15 in terms of the R^2 statistic. The PDM performance obtained from calibration to each station is given for comparison and shows that the Grid-to-Grid model calibrated at each site compares well with the PDM results. However, the results clearly show that the transfer of Grid-to-Grid model parameters from the Cherwell to the Sor or vice versa give poor results. This is emphasised in the model simulations for the calibration event presented in Figure D.19 and Figure D.20. As in Section D.4.2, this is attributed to the very different soil/geology controls for the two catchments causing differing catchment responses despite their close proximity. This is because a very simple form of Grid-to-Grid model has been used, using only topographic information in its formulation and not also datasets of soil/geology. This highlights that the simple distributed model formulation can be improved upon by making use of other spatial datasets: this is pursued in Section D.7.

Note that an initial attempt to calibrate a single Grid-to-Grid model for both the Cherwell and the Sor was abandoned because of the contrasting responses observed. The site calibrations presented here need to be taken into account when considering their performance in relation to the results of Section D.7, which employ a single parameter set for several catchments, including the Cherwell and the Sor.
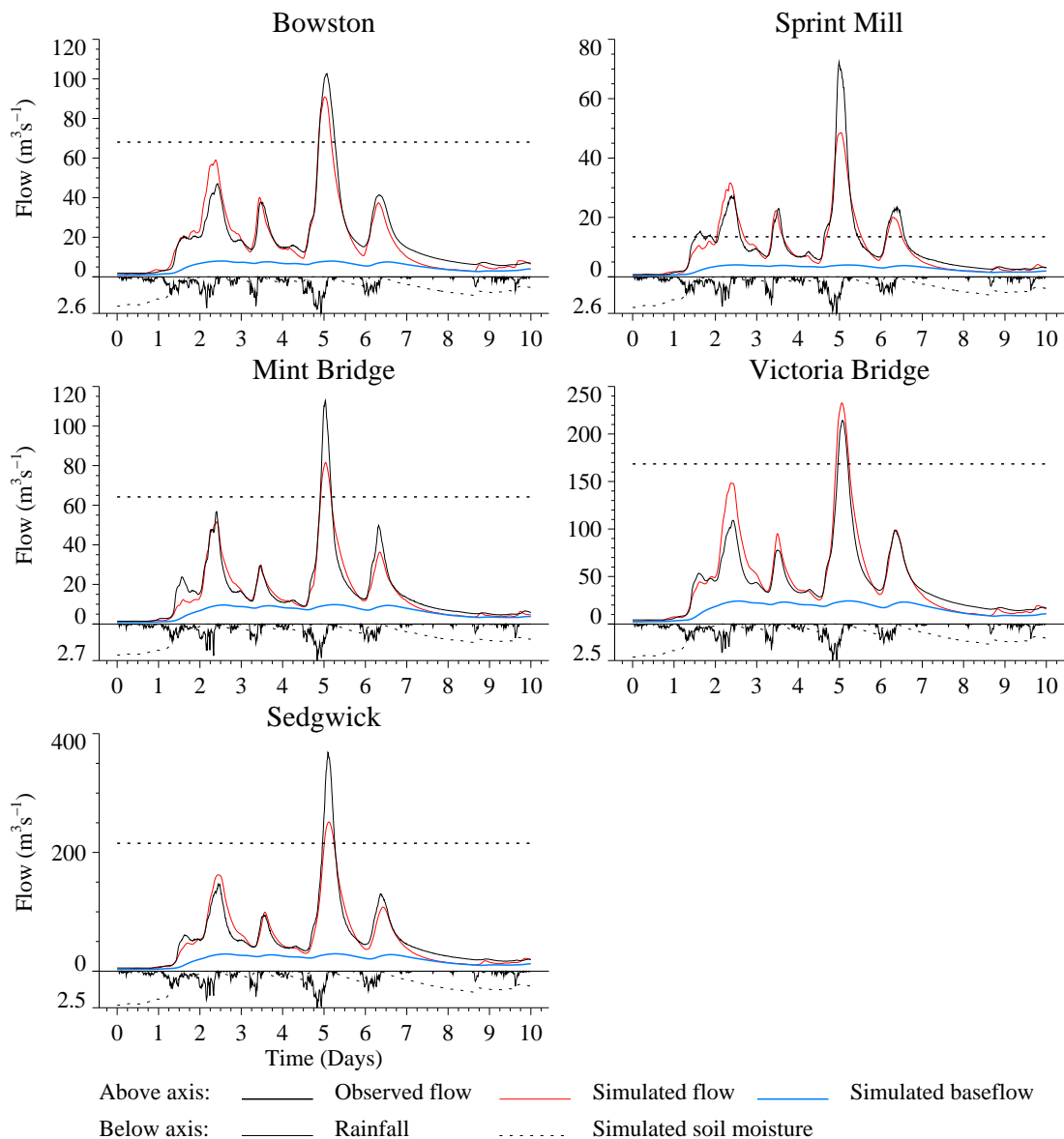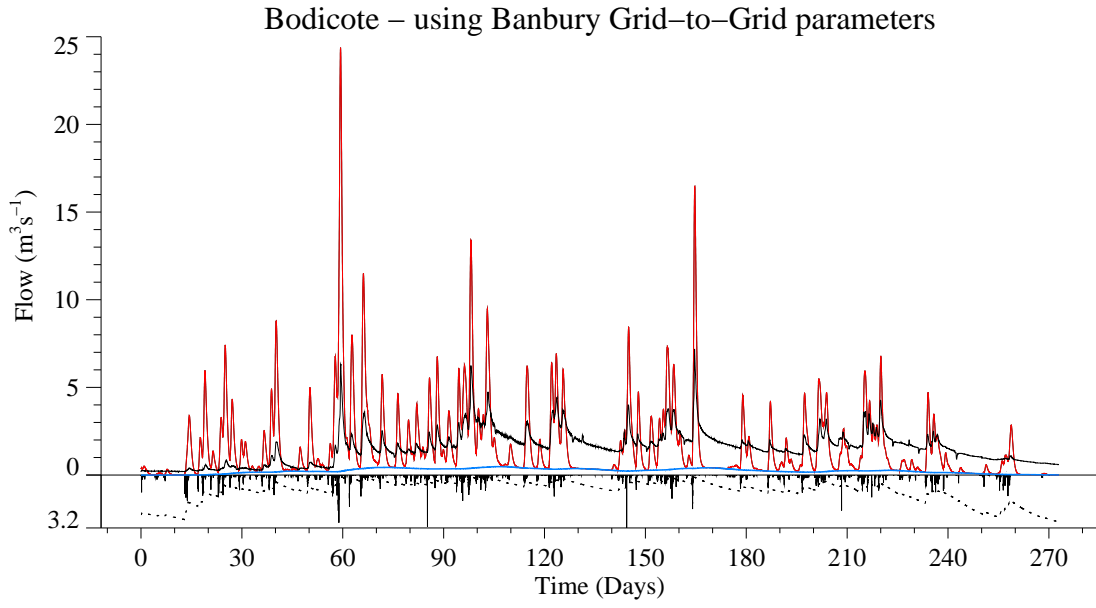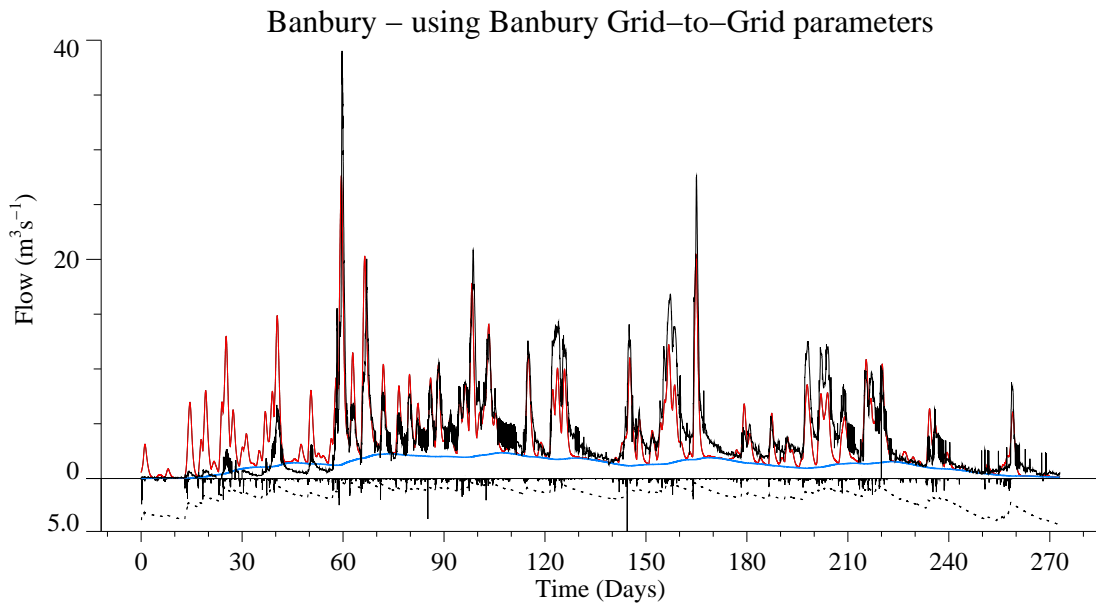
Figure D.18 Flow hydrographs for the Grid-to-Grid model over the evaluation event for the River Kent. Note that the model has only been calibrated at Sedgwick. The dashed line above the axis indicates the flow associated with the maximum stage used to derive the rating equation for that catchment.

Table D.15 Simple Grid-to-Grid model transfer: R^2 **model simulation performance for the Upper Thames catchments**

Catchment	Calibration Event			Evaluation event		
	Banbury G2G parameters	Bodicote G2G parameters	Calibrated PDM	Banbury G2G parameters	Bodicote G2G parameters	Calibrated PDM
Cherwell at Banbury	0.666	-2.663	0.752	0.811	-0.048	0.848
Sor at Bodicote	0.347	0.890	0.907	-1.972	0.662	0.715

Figure D.19 Flow hydrographs for the Grid-to-Grid model over the calibration event for the Upper Thames. Note that the model has been calibrated at Banbury.
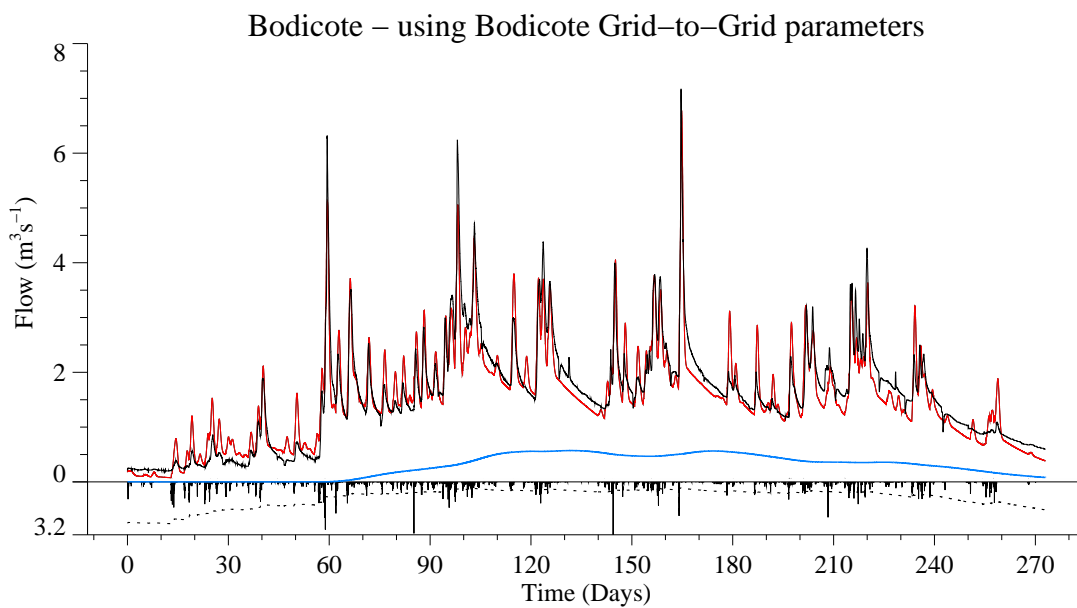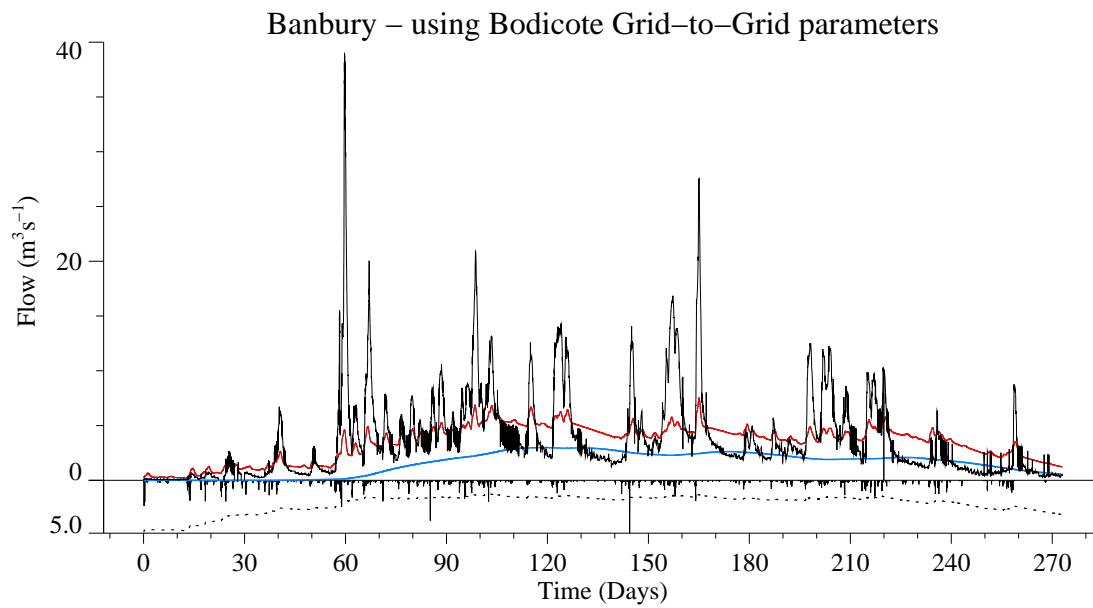
Figure D.20 Flow hydrographs for the Grid-to-Grid model over the calibration event for the Upper Thames. Note that the model has been calibrated at Bodicote.

D.6.4 Calibrated Grid-to-Grid model parameters

For completeness, the Grid-to-Grid model parameters calibrated for the Kent and Upper Thames case studies are presented below.

Table D.16 Calibrated Grid-to-Grid model parameters

Parameter name	Case study		
	Kent	Banbury	Bodicote
Wave Speeds			
Surface land, c_l	0.05	0.04	0.04
Surface river, c_r	1.1	0.2	0.2
Sub-surface land, c_{lb}	0.05	0.005	0.005
Sub-surface river, c_{rb}	0.55	0.005	0.005
Return Flows			
Land, r_l	0.07	0.0005	0.0005
River, r_r	0.07	0.0005	0.0005
Runoff generation			
c_{max} Regional maximum	55	100	380
$\bar{c}_{min}$ Regional minimum	10	10	10
S_t	0	15	150
k_d	1.5×10^{-4}	1.5×10^{-5}	9.0×10^{-6}
Land/River designation			
Accumulated area threshold, a_0	2	4	5
Routing time-step (mins)	5	15	15

Calibration of the Grid-to-Grid model at Banbury and Bodicote was aided by invoking a soil tension storage capacity, S_t, which increases the effect of evaporation on the water balance. Note that for a given grid square, if S_t is greater than the maximum storage capacity S_{max} then at all times water from the soil storage can only be lost through evaporation and not drainage.

D.7 Method 4: Transfer of a distributed rainfall-runoff model, configured using soil properties in addition to elevation data, to neighbouring or internal sites

This section considers a method of model transfer based on the use of a distributed rainfall-runoff model that is formulated to employ both terrain and soil datasets. These digital datasets are used to configure and parameterise a grid-based model of runoff-production, lateral flow generation and flow-routing across a landscape. The additional sources of landscape information might be expected to diminish the reliance of the rainfall-runoff model on traditional model parameters estimated by calibration to a specific location. They serve to impose a spatial structure on the model that has a physical basis.

This section considers a general approach to rainfall-runoff modelling based on a simple kinematic wave model foundation, as described in Section 4.4.5. The prototype model described here allows the influence of soil physical properties to be introduced into the model in a physically-based way and using available digital datasets. The prototype model employs formulations for lateral soil drainage, surface runoff and recharge that can make use of datasets on soil properties and topography, instead of using site-calibrated parameters. The nature and limited availability of certain soil properties has necessitated the use of various approximations in applying the prototype model formulation. Improvements to the nature and availability of spatial datasets for soil/geology/land-cover properties will strengthen the model's underpinning by properties, rather than calibrated model parameters, in the future.

Digitised soil datasets

A derived quantity called the HOST (Hydrology of Soil Types) class is available with UK coverage. This classification has 29 classes and encompasses soil type, hydrological response and substrate hydrogeology (Boorman *et al*., 1995). The database for England and Wales, which is available at a 1km resolution, is based on the soil-survey 1:250,000 maps produced by the Soil Survey and Land Research Centre. A map of HOST classes covering the case study catchments in the Upper Thames and Stour is presented in Figure D.21.

Although this classification only provides an integer identifier for 29 different soil types, a database of derived soil attributes supports the derivation of these classes and consists of properties such as air capacity, parent material, depth to gleying and depth to slowly permeable layer. These derived soil attributes are not generally made available, but may be available under licence. Highly derived soil properties have been extracted from the soil properties database, SEISMIC, available from the National Soil Resources Institute (NSRI). In SEISMIC, soil series are analysed down to a depth of 1.5 m. There are normally several horizons present in a given series. An upper and lower depth and some other soil properties are available for each horizon.
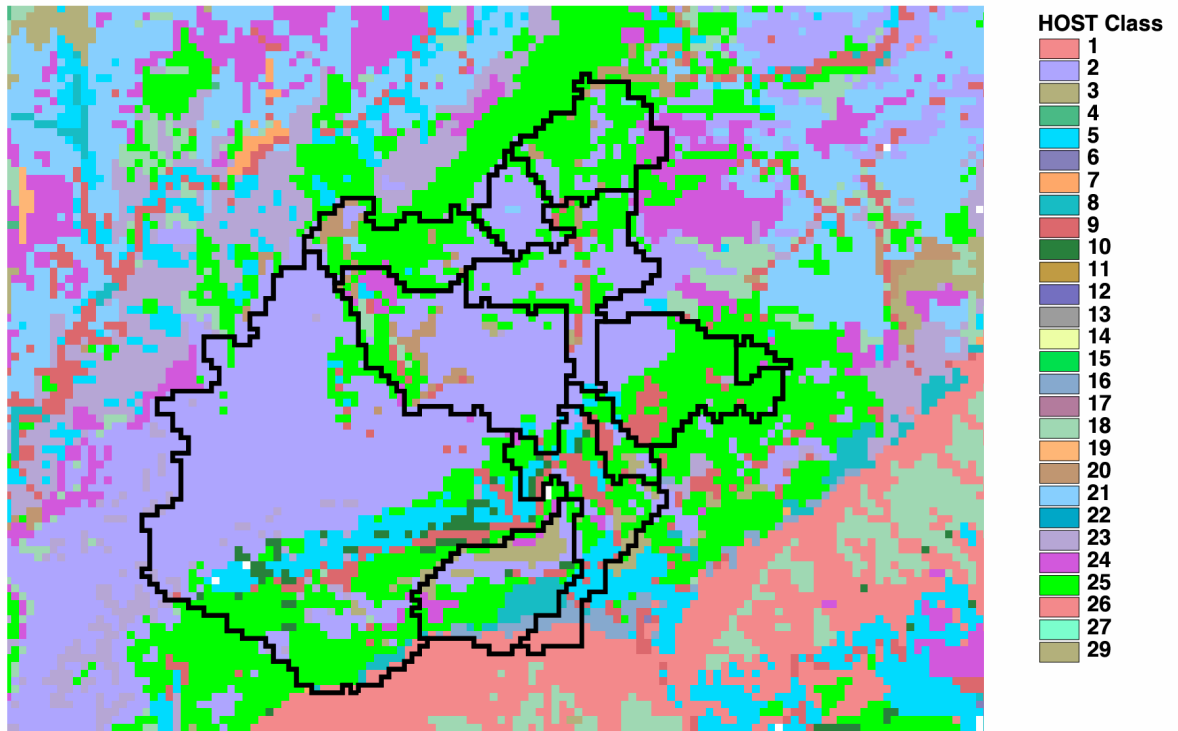
Figure D.21 Map of HOST classes covering the Upper Thames and Stour catchments.

By comparing information from SEISMIC with the HOST dataset, Ragab *et al.* (pers. comm.) associated statistics for values of five soil properties with each of the 29 HOST classes. These properties are as follows:

- water content at field capacity, θ_{fc}: fractional volume at 5KPa

- residual water content, θ_r: half the fractional volume at 1500KPa

- porosity, φ: fractional volume

- hydraulic conductivity at saturation : k_s (cm d^{-1})

- depth to "C" and "R" horizons (cm).

Mean values for these soil properties for each HOST class are presented in Table D.17. The depths to "C" and "R" horizons consist of two values. The SEISMIC User Manual defines the C-layer as "mineral substrate, relatively unweathered 'soft' unconsolidated material, gravel or rock rubble", and the R-layer as "relatively unweathered, coherent rock". The depth to the R-layer has been used here as a surrogate for soil depth. Where a value for depth to the R-layer is not available, the depth to the C-layer is used instead. In many cases (but not all), depth to the R-layer for each soil type is greater than the depth to the C-layer. Figure D.22(a) presents a map of soil depth for the Thames Region derived from SEISMIC values for the depth to "C" and "R" horizons.

**Table D.17 Soil properties associated with each HOST class**

HOST class	Water content		Porosity, φ (% volume)	Hydraulic conductivity, k_s (cm d^{-1})	Average depth to R-layer (cm)
	at 5 kPa (field capacity, θ_{fc})	at 1500 kPa (2 × residual, $2\theta_r$)			
1	0.381	0.178	0.504	132.	77.
2	0.394	0.182	0.533	151.	95.
3	0.255	0.082	0.474	383.	47.
4	0.373	0.147	0.536	229.	71.
5	0.258	0.088	0.472	367.	72.[*c]
6	0.371	0.175	0.477	85.	39.[*c]
7	0.252	0.085	0.469	367.	63.[*c]
8	0.359	0.160	0.486	143.	42.[*c]
9	0.417	0.209	0.520	101.	10.
10	0.326	0.132	0.517	319.	65.[*c]
11	0.326*	0.156*	0.517*	156.*	100.[*c]
12	0.346	0.156	0.477	156.	100.[*c]
13	0.330	0.142	0.459	138.	62.
14	0.344	0.158	0.436	58.	14.
15	0.346	0.121	0.540	322.	65.
16	0.352	0.162	0.469	108.	52.
17	0.396	0.175	0.531	138.	35.
18	0.353	0.174	0.442	64.	59.
19	0.361	0.126	0.547	302.	66.
20	0.420	0.230	0.467	29.	50.
21	0.391	0.207	0.459	29.	78.
22	0.405	0.158	0.602	333.	106.
23	0.447	0.260	0.495	18.	48.
24	0.376	0.198	0.452	51.	39.
25	0.429	0.248	0.469	24.	27.[*c]
26	0.408	0.201	0.490	57.	80.
27	0.488	0.229	0.688	329.	132.
28	0.488*	0.229*	0.688*	329. *	132. *
29	0.488*	0.229*	0.688*	329. *	132. *

* Indicates missing property values, now replaced by an estimated value for similar soil types.
[*c] Indicates soils for which there is no value for depth to R-layer, so the value for depth to C-layer has been used instead.

The residual soil water content, θ_r, and the saturated hydraulic conductivity, k_s, can be used directly in the runoff production scheme with lateral soil water drainage described in Section 4.4.5. The water content at field capacity, θ_{fc}, represents the water content below which drainage becomes negligible. As a rule of thumb, $\theta_{fc} = \theta_s/2$, where θ_s is the water content at saturation (Or and Wraith, 2002). An estimate of θ_s is required for the runoff-production scheme and this might be seen to provide a convenient approximation. However, values for θ_{fc} in Table D.17 range from 0.25 to 0.49 and seem rather large compared to literature values ranging from 0.1 for fine sand to 0.39 for clay (Dunne and Leopold, 1978). For the present purposes it will be assumed that $\theta_s = 1.25\,\theta_{fc}$, which results in values of θ_s ranging from 0.31 to 0.61. Figure D.22(b)

(a) Soil depth, L (cm)
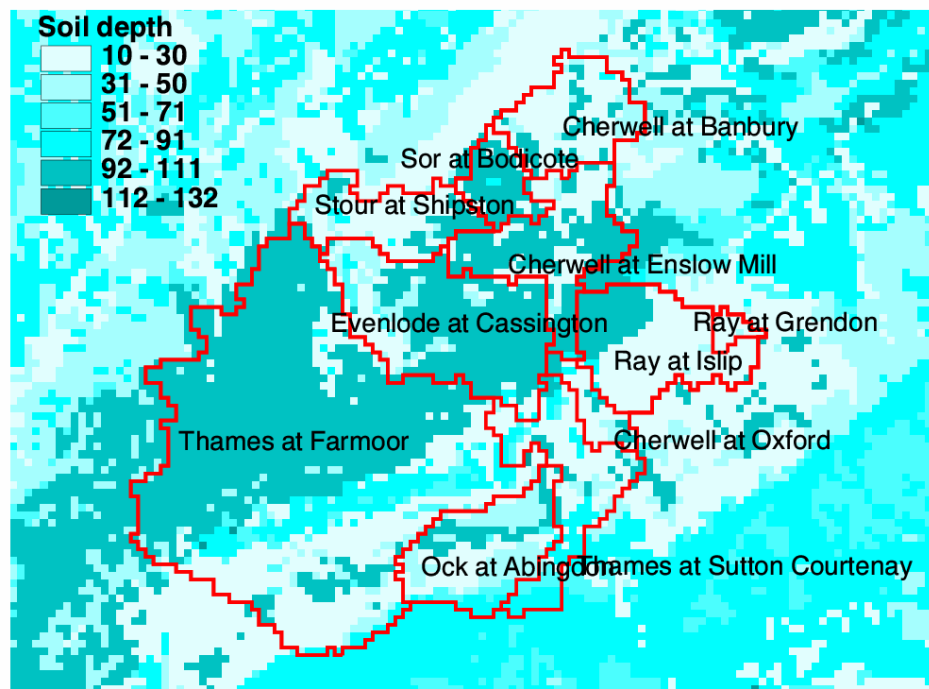
(b) Field capacity (1000 θ_{fc})
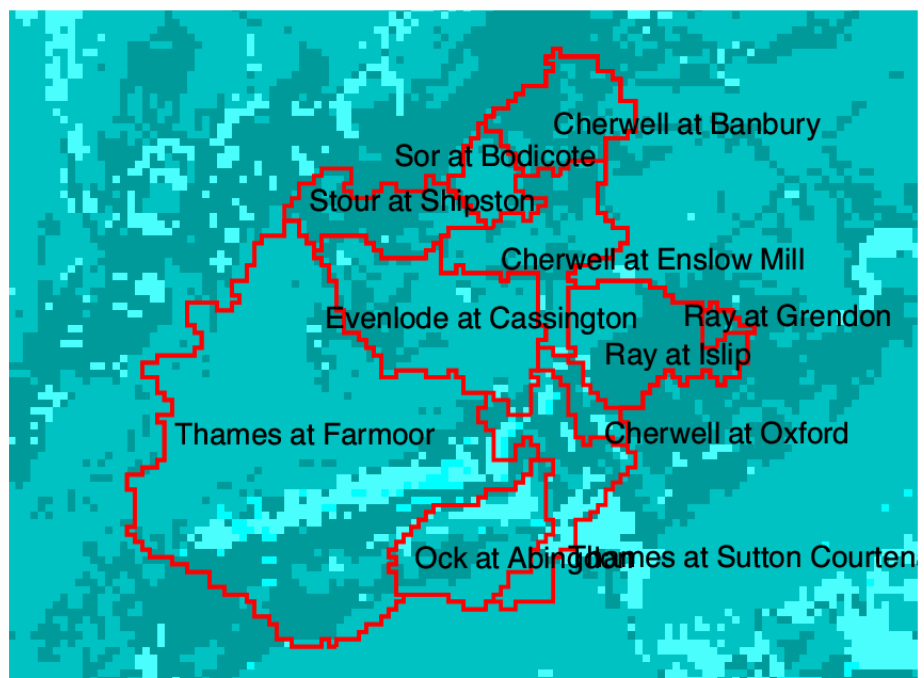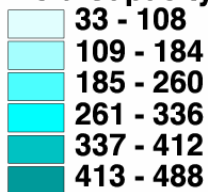
Figure D.22 Maps of soil properties over the Upper Thames and Stour derived from HOST/SEISMIC.

presents a map of HOST/SEISMIC derived field capacity over the Upper Thames and Stour catchments.

The detailed maps presented in Figure D.22 show considerable spatial heterogeneity which is consistent with observed soils and geology at a 1km resolution. Figure D.23 highlights the benefits of using this 1km dataset in comparison to a widely available 10km resolution global dataset, IGBP (International Geosphere Biosphere Programme). The maps show variation in saturated hydraulic conductivity, k_s, obtained from the two data sources. It is evident that the 1km HOST dataset provides considerably more spatial detail than the 10km IGBP dataset, particularly over South East England.

(a) HOST/SEISMIC 1km resolution dataset
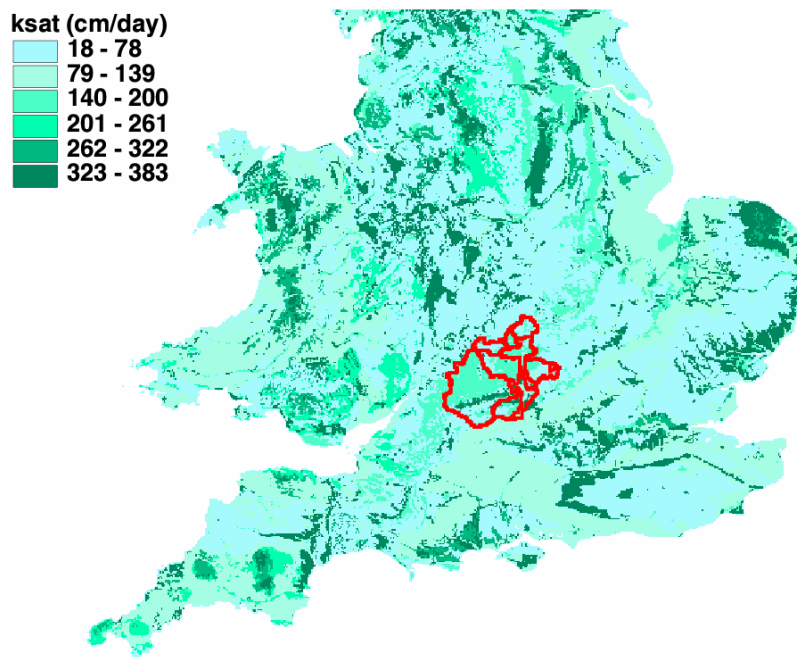
(b) IGBP 10km resolution dataset
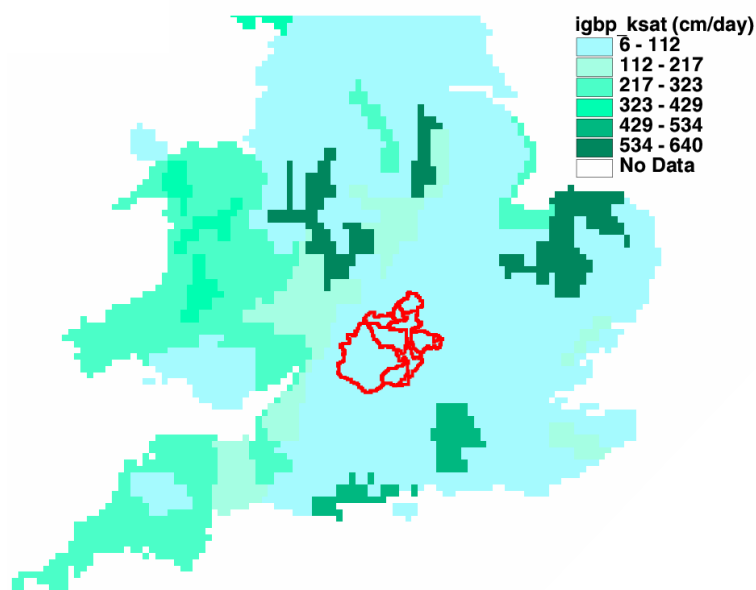
Figure D.23 Maps comparing estimated saturated hydraulic conductivity (cm d^{-1}) derived from two different sources of soil data.

D.7.1 Enhanced Grid-to-Grid Model formulation

Runoff production scheme with lateral soil water drainage

Consider a sloping soil column of depth L and slope s_0 subject to precipitation falling at a rate p (ms^{-1}) as shown in Figure D.24.

The actual and maximum water contents (m) in the column are given by

$$S = (\theta - \theta_r)L \tag{D.1}$$

$$S_{max} = (\theta_s - \theta_r)L, \tag{D.2}$$

where θ_s is the content at saturation and θ_r is the residual content, estimated from HOST/SEISMIC data.
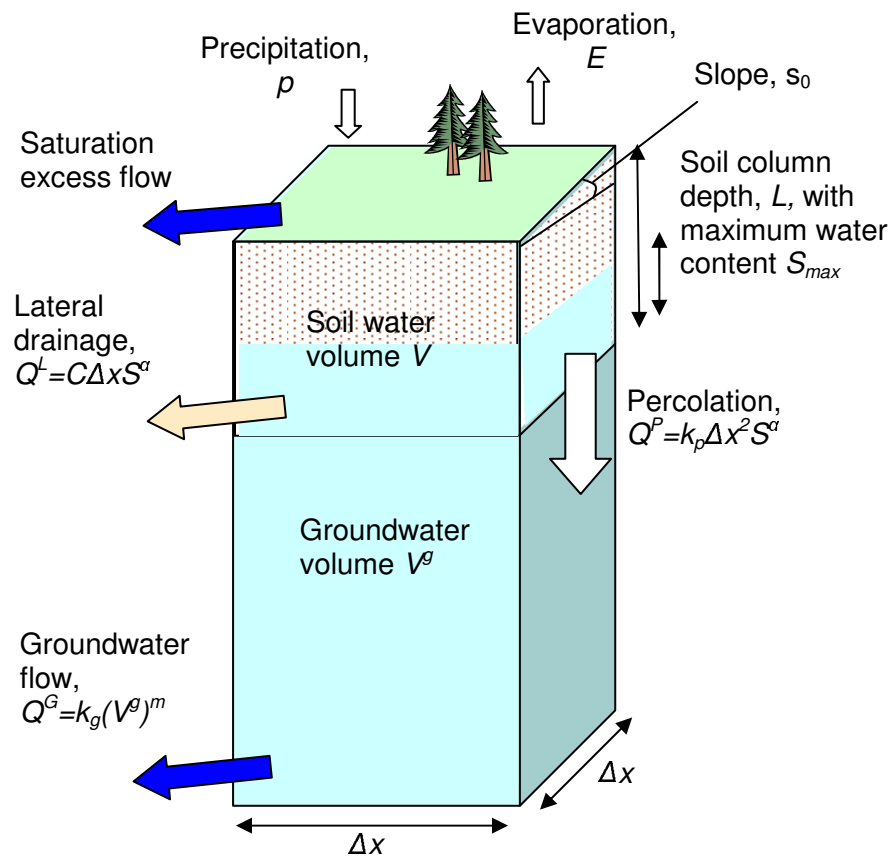
Figure D.24 Conceptual diagram showing runoff production and lateral drainage in a 1-D soil column.

Let $V = \Delta x^2 S$ denote the volume of water stored in the unsaturated layer of the i th soil column. From continuity, the rate of change in water volume is given by

$$\frac{dV}{dt} = p\Delta x^2 + Q^I - Q^L - Q^P,$$ (D.3)

where, Q^I is the inflow to cell i from contributing upstream cells, Q^L is the lateral drainage from the cell and Q^P is the downward percolation (drainage) to the saturated zone.

Lateral drainage, Q^L is given by

$$Q^L = \frac{C\,\Delta x}{\Delta x^{2\alpha}} V^\alpha = C\,\Delta x S^\alpha.$$ (D.4)

C is the conveyance term given by $C = Lk_s^L s_0 / S_{max}^\alpha$, where s_0 is the local slope, derived from digital elevation data. The lateral saturated hydraulic conductivity, k_s^L is unknown but is assumed to be related to the vertical k_s taken from HOST/SEISMIC data via the relation $k_s^L = 1000 k_s$. The parameter α is linked to the Brooks and Corey relation for hydraulic conductivity and typical values lie between 3 and 4, although a value of 1 has been used for the initial model formulation described here.

Percolation (a vertical downward flow, m³s⁻¹), Q^P, is represented as a simple power law function of the soil water volume V, expressed as a fraction of the saturated water volume V_{max},

$$Q^P = k_P \Delta x^2 \left(\frac{V}{V_{max}}\right)^{\alpha_P} = k_P \Delta x^2 \left(\frac{S}{S_{max}}\right)^{\alpha_P},$$ (D.5)

where k_P is a vertical saturated hydraulic conductivity of the soil (ms⁻¹) and α_p is the exponent of the percolation function. Spatially varying estimates for k_P are not routinely available, so k_P is assumed to be linearly related to k_s, i.e. $k_p = \lambda k_s$, where λ is treated as a spatially invariant model parameter. Clapp and Hornberger (1978) indicate, on the basis of soil experiments, that α_p can vary from circa 11 for sand to 25 for clay. Here a constant value for α_p of 15 has been assumed.

A soil water balance for a time-step $(t_0, t_0 + \Delta t)$ gives the saturation excess flow volume as

$$q = \max\{[V'(t_0 + \Delta t) - \min(V'(t_0 + \Delta t), V^{max})], 0\}$$ (D.6)

where V^{max} is the saturated soil water storage.

The storage at the end of the interval is

$$V(t_0 + \Delta t) = \min(V'(t_0 + \Delta t), V^{max}) - E_a \Delta x^2,$$

(D.7)

where E_a is the actual evaporation.

It is assumed that percolation freely drains as recharge to the groundwater saturated zone (for the cell), so that recharge $Q^R \equiv Q^P$. Let V^g denote the groundwater volume (m³) stored in the cell and s_b the slope of the underlying bedrock in the flow direction.

Continuity for the groundwater volume is

$$\frac{dV^g}{dt} = Q^P - Q^G$$

(D.8)

where Q^G is the lateral groundwater flow from the cell.

Darcy's law gives the lateral groundwater flow out of the cell to a reasonable approximation by the linear relation

$$Q^G = \frac{k_g s_b}{\Delta x} V^g$$

(D.9)

where k_g is the horizontal hydraulic conductivity of the aquifer. However, suitable values for bedrock slope, s_b, and conductivity, k_g, are not straightforward to obtain. One approach is to assume that bedrock slope mirrors the surface topographic slope which can be estimated from digital terrain data. Conductivity information may be obtained from geology datasets but obtaining meaningful values for the present scale of application may present difficulties. For the present prototyping purposes geological datasets have not been used. Instead, a nonlinear storage function relating groundwater flow to volume has been invoked, such that

$$Q^G = k(V^g)^m, \; k > 0, \; m > 0,$$

(D.10)

where k is a rate constant with units of inverse time and m is the nonlinear power. For this application, a cubic storage function has been assumed ($m = 3$), and k is treated as a spatially invariant parameter for estimation.

D.7.2 Estimation of river flows using the Grid-to-Grid routing model

Runoff from the soil column is considered to consist of the saturation excess flow volume, q_i, and groundwater flow, Q^G. These values of gridded runoff form the lateral inflows to the Grid-to-Grid routing model, which consists of a kinematic wave formulation for routing both surface and sub-surface gridded runoff to estimate river flow.

The routing model equations in 1-dimension are as follows:

$$\frac{\partial q_l}{\partial t} + c_l \frac{\partial q_l}{dx} = c_l(u_l + R_l)$$

$$\frac{\partial q_{lb}}{\partial t} + c_{lb} \frac{\partial q_{lb}}{dx} = c_{lb}(u_{lb} - R_l) \qquad \text{(D.11)}$$

$$\frac{\partial q_r}{\partial t} + c_r \frac{\partial q_r}{dx} = c_r(u_r + R_r)$$

$$\frac{\partial q_{rb}}{\partial t} + c_{rb} \frac{\partial q_{rb}}{dx} = c_{rb}(u_{rb} - R_r)$$

where q_l is flow over land pathways, q_r is flow over river pathways, R_l and R_r denote land and river return flow, and u_l and u_r are inflows for land and river, which include runoff generated by the runoff-production scheme. The additional subscript b denotes sub-surface ("baseflow") pathways.

The four partial differential equations are each discretised using a finite-difference representation. Time, t, and space, x, are divided into discrete intervals Δt and Δx such that k and n denote positions in discrete time and space. Invoking forward difference approximations to the derivatives in (D.11) gives the discrete formulation

$$q_k^n = (1-\theta)q_{k-1}^n + \theta\left(q_{k-1}^{n-1} + u_k^n + R_k^n\right) \qquad \text{(D.12)}$$

where the dimensionless wave speed $\theta = c\,\Delta t / \Delta x$ and $0 < \theta < 1$. This is a simple, explicit numerical formulation for the kinematic wave equation extended to include the return flow term R_k^n. This numerical scheme has the advantage of introducing diffusion (albeit numerically) and so more closely represents the propagation of actual flow in rivers. Figure D.25 summarises the key features of the coupled runoff-production and routing scheme.

In practice, the routing is implemented in terms of an equivalent depth of water in store over the grid square, S_k^n, with $q_k^n = \kappa S_k^n$ and where $\kappa = c/\Delta x$ is a rate constant with units of inverse time and Δx is the grid-cell size. The inflow and return flow are also parameterised as water depths. Return flow to the surface is given by $R_k^n = r\,S_k^n$

where S_k^n is the depth of water in the subsurface store and r is the return flow fraction.
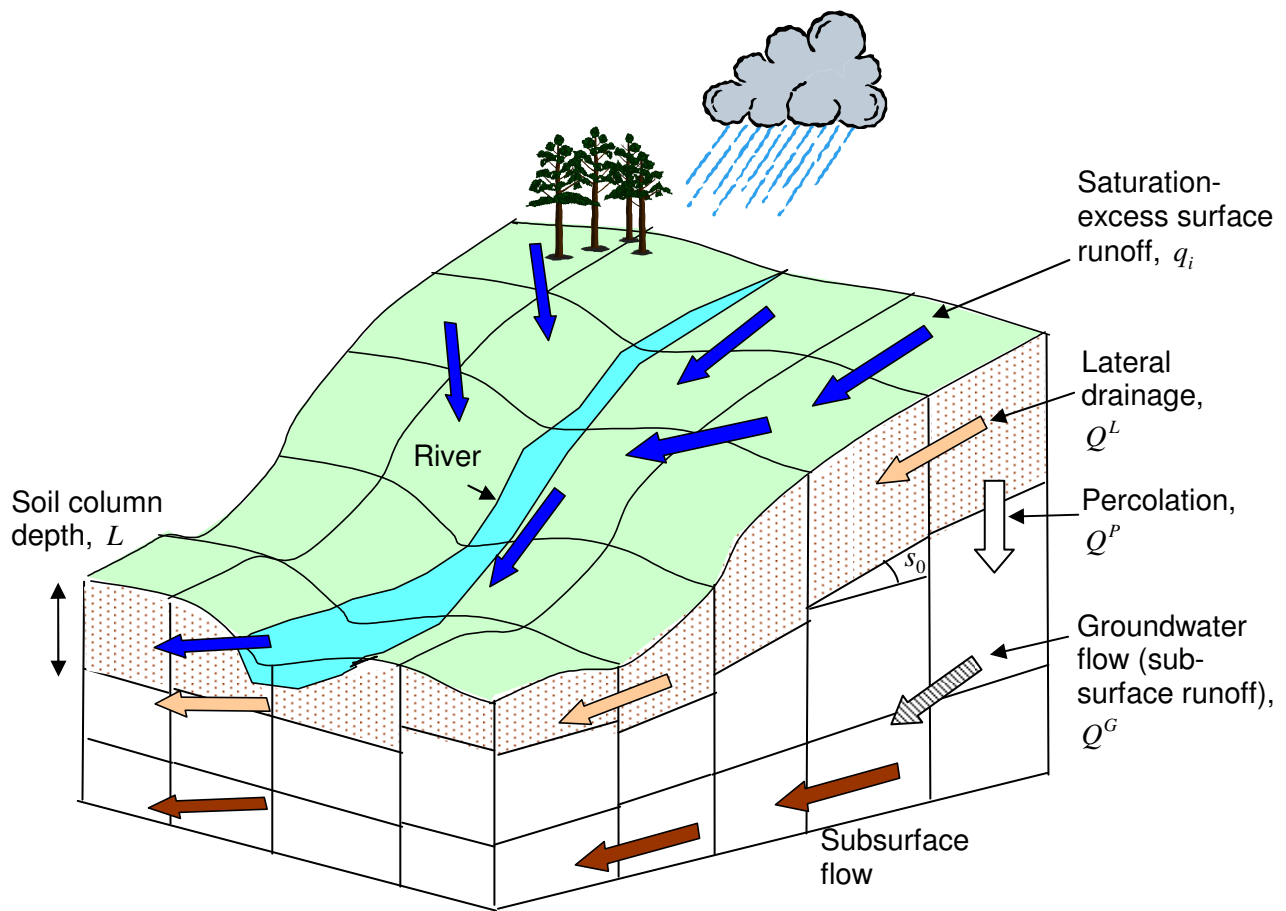
Figure D.25 Key features of the coupled runoff-production and routing scheme.

D.7.3 Model Configuration

The Grid-to-Grid routing model requires the two DTM-derived datasets:

    (i) flow directions (each grid-cell can drain in only one of 8 directions),

    (ii) area draining to each 1 km grid-cell,

whilst the runoff production scheme with lateral soil water drainage currently requires the following five digital datasets:

    (iii)   average slope,

    (iv)   residual soil water content, θ_r,

    (v)   saturated soil water content, θ_s,

    (vi)   saturated hydraulic conductivity, k_s,

    (vii)   soil depth, L.

However, values for soil properties such as bedrock slope, s_b, horizontal hydraulic conductivity of the aquifer, k_g, vertical saturated hydraulic conductivity of the soil, k_P, lateral saturated hydraulic conductivity, k_s^L, and the exponents of the percolation function, α_p, and lateral drainage function, α, are currently not available as gridded

datasets and have had to be estimated through parameterisation. Improved availability of datasets such as these should lead to a more physically-based formulation and less reliance on parameter adjustment.

Catchment average values of soil properties currently used by the model are presented in Table D.18, together with values for the maximum soil water content, $S_{\max}$, derived from soil depth and soil water content (residual and field capacity) properties using equation (D.2) and the modified rule-of-thumb between field capacity and saturated values.

Table D.18 Catchment average values of soil properties for the Upper Thames and Stour catchments

Catchment	Area (km^2)	Water content		Depth (cm)	k_s (cm/day)	$S_{\max}$ (cm) range of values in brackets
		at 5 kPa (field capacity, θ_{fc})	at 1500 kPa ($2\times$ residual, $2\theta_r$)			
Stour at Shipston	185.2	0.418	0.229	46.9	55	24.0 (14.5-46.8)
Cherwell at Banbury	199.4	0.416	0.229	43.4	53	22.2 (5.2-46.8)
Sor at Bodicote	87.7	0.402	0.198	78.4	118	38.9 (14.5-46.8)
Evenlode at Cassington	430.0	0.397	0.195	73.6	118	36.2 (5.2-46.8)
Cherwell at Enslow Mill	551.7	0.407	0.210	61.0	94	30.5 (5.2-46.8)
Thames at Farmoor	1608.6	0.389	0.189	72.3	143	34.7 (5.2-80.5)
Ray at Grendon	18.8	0.427	0.246	27.5	25	14.6 (14.5-18.3)
Ray at Islip	290.1	0.416	0.224	43.4	70	22.0 (5.2-46.8)
Cherwell at Oxford	906.8	0.410	0.215	54.3	87	27.1 (5.2-46.8)
Ock at Abingdon	234.0	0.368	0.178	51.5	149	23.5 (5.2-46.8)
Thames at Sutton Courtenay	3414.0	0.392	0.194	64.7	127	31.2 (5.2-80.5)
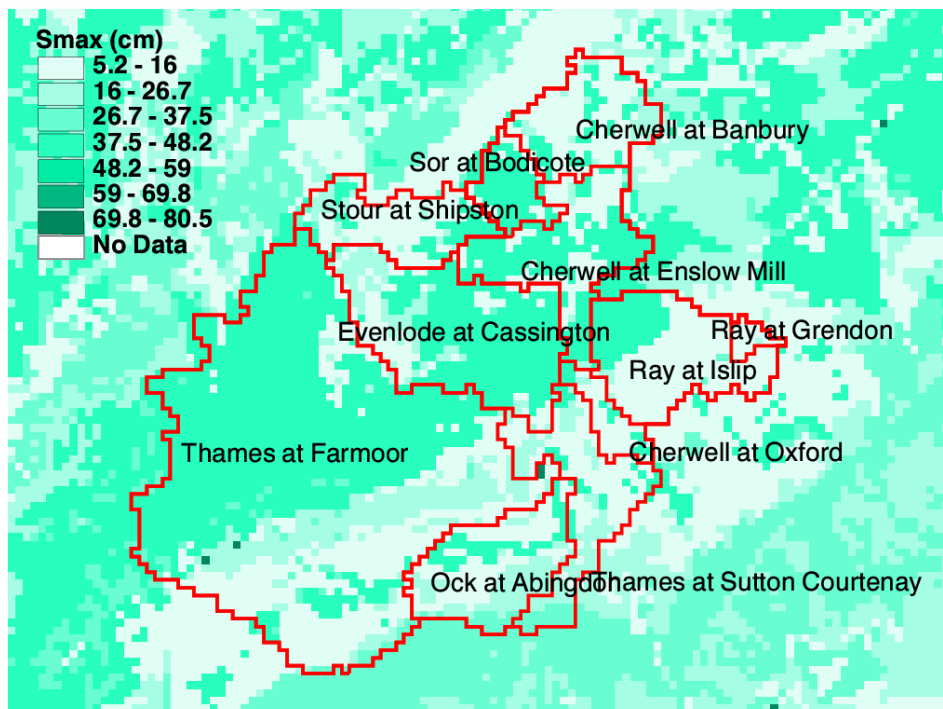
Figure D.26 Map of maximum soil water content, $S_{\max}$, derived from soil properties for the Upper Thames and Stour

D.7.4 Model calibration and assessment

The Grid-to-Grid model has been designed for area-wide application, providing estimates of flow for rivers throughout a region, irrespective of catchment boundaries. Where possible, the Grid-to-Grid model is configured to a region, in this case the Upper Thames and Stour, using gridded datasets to represent spatial heterogeneity of hydrological response across grid-cells. A small number of parameters are set at a regional level and are treated as parameters for model calibration. These control the overall runoff response and flow translation of the model and are used, along with the gridded datasets, to derive the grid-cell parameter values.

The model parameters have been manually adjusted for the period 1 September 2000 to 1 June 2001 for which 15 minute rainfall observations are available. In practice, calibration was undertaken on just three catchments: the Ock at Abingdon, the Cherwell at Banbury and Sor at Bodicote. These catchments were selected on the basis of geographic proximity and variation in hydrological response to rainfall.

Table D.19 presents a single set of routing and runoff-production model parameters for the whole region of application, in this case the Upper Thames and Stour.

Table D.19 Parameter values for the enhanced Grid-to-Grid model

Parameter name	Symbol	Units	Typical value	Description
Routing model parameters:				
Surface wave speeds:				
Land:	c_l	ms^{-1}	0.2	Related to the flow velocity
River:	c_r	ms^{-1}	0.25	
Sub-surface wave speeds:				
Land:	c_{lb}	ms^{-1}	0.15	Usually less than the surface
River:	c_{rb}	ms^{-1}	0.15	wave speed
Return flow factors:				
Land:	r_l	-	0.00	Proportion of the sub-surface store
River:	r_r	-	0.008	that is routed to the surface/river
Runoff model parameters:				
Drainage storage rate constant	k_p	s^{-1}	0.00002	Regulates drainage from the soil store into the saturated groundwater store
Baseflow storage rate constant	k_g	s^{-1}	5×10^{-7}	Regulates drainage from the groundwater store into sub-surface runoff

The parameters have been adjusted manually in order to obtain the best match between modelled and observed flows for the three catchments used for model calibration. These parameters were then applied to the whole region, and resulted in reasonably accurate flow estimates for the eight other catchments, taking into account artificial influences on observed river flows.

Model performance for the calibration and assessment periods is summarised in terms of the R^2 statistic in Table D.20. Note that a single set of model parameters has been used to estimates flows for all catchments. Both calibration and evaluation periods were preceded by a two month "warm-up" period which has not been included in the performance evaluation. The purpose of this two month period is to minimise the effect that incorrect initialisation of the model states may have on model performance. Model performance for the calibration period is variable, and surprisingly good for some catchments such as the Thames at Sutton Courtenay and the Cherwell at Oxford, for which calibration was not explicitly undertaken. Modelled and observed flow hydrographs for the Thames and Stour catchments are presented in Figure D.27 and Figure D.28 respectively. The set of hydrographs indicates that the prototype distributed model is able to broadly reproduce a wide range of hydrological behaviour in catchments which have very different responses to rainfall. For example, the Ray at Grendon Underwood is a highly responsive catchment overlying flat, impermeable Oxford Clay, whereas the Thames at Sutton Courtenay and the Thames at Farmoor have a mixed geology, are less responsive and have a substantial baseflow component to the river flow. For both types of catchment, the model produces a realistic response to rainfall, even though it does not always estimate peak flows correctly. Model simulations for the slower responding catchments also indicate that the hydrograph recession is too steep resulting in underestimation of the slow component of flow following a flow peak. Further model development may well overcome some of these deficiencies. The evaluation period, 6-19 April 1998, consists of the extreme flood event of Easter 1998. Accurate simulation of extreme events can be a challenge even for established models, and flow and rainfall measurements can also be in error. Flow simulation accuracy for this prototype enhanced Grid-to-Grid model is presented in column three of Table D.20 for those catchments for which flow observations are available.

**Table D.20 Summary of model performance for the enhanced Grid-to-Grid model**

Catchment	R^2	
	Calibration period 1 September 2000 – 1 June 2001	Evaluation period 6-19 April 1998
Ock at Abingdon	0.590	0.792
Cherwell at Banbury	0.592*	0.506
Sor at Bodicote	0.676*	0.438
Evenlode at Cassington	0.516*	0.588
Cherwell at Enslow Mill	0.363	-
Thames at Farmoor	0.675	0.054
Ray at Grendon Underwood	0.340	-
Ray at Islip	0.381	-0.414
Cherwell at Oxford	0.847	-0.144
Thames at Sutton Courtenay	0.850	0.383
Stour at Shipston	0.524[1]	0.455

*In practice calibration has been undertaken on these catchments alone.
[1]The calibration period used for the Stour to Shipston was 1 November 1991 to 1 May 1992
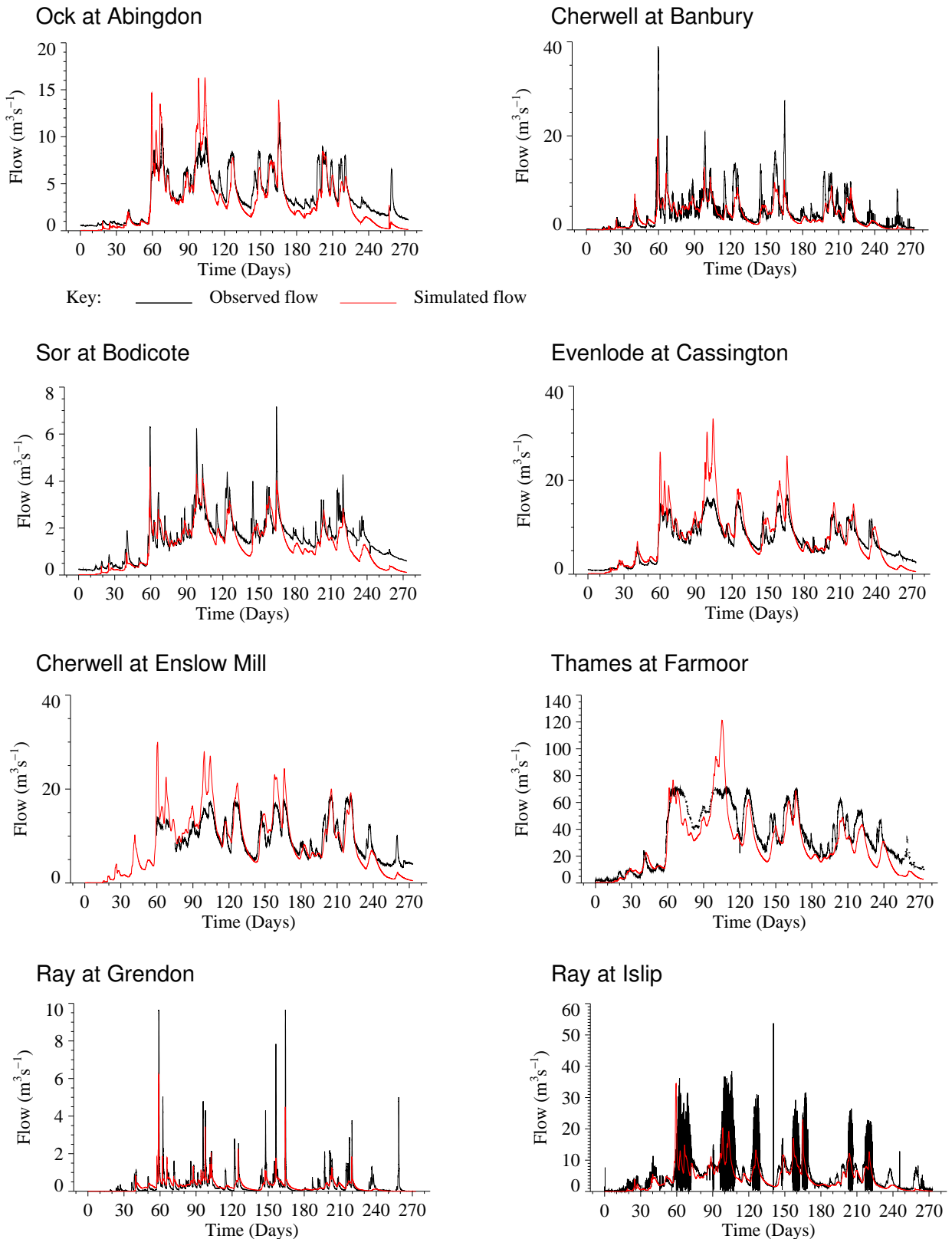
**Figure D.27 Flow hydrographs for the Thames catchments comparing model
performance obtained from the enhanced G2G model: 1 September
2000 – 1 June 2001**

Cherwell at Oxford   Thames at Sutton Courtenay

Key: —— Observed flow   —— Simulated flow
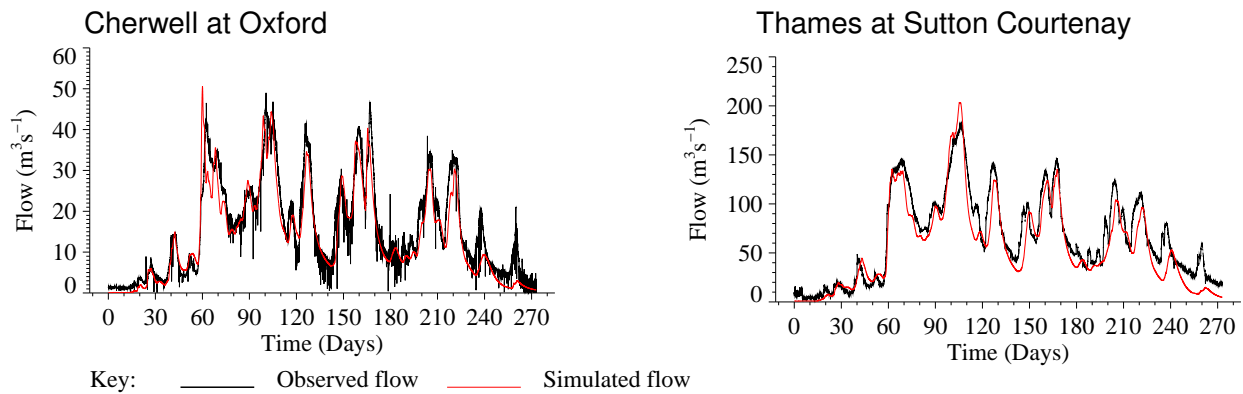
Figure D.27 (continued…) Flow hydrographs for the Thames catchments
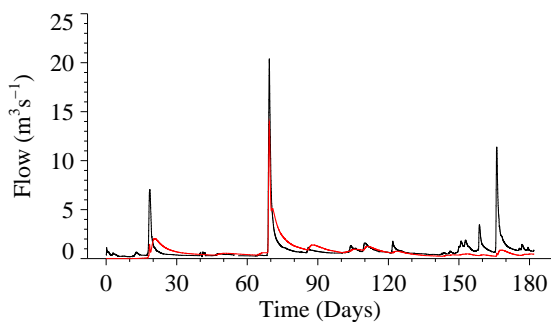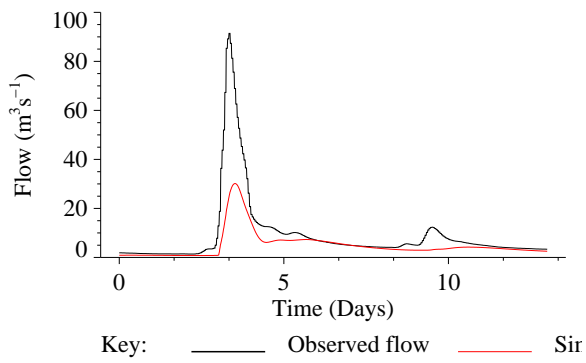

Figure D.28 Flow hydrographs for the Stour to Shipston comparing model performance obtained from the enhanced G2G model

Model performance for the Ray at Islip and the Cherwell to Oxford is particularly poor: however, the flow hydrographs in Figure D.29 reveal that the flow gauge was not working well during the extreme event, resulting in spurious/intermittent flow observations. For those catchments for which good flow records are available, and which recorded a high flow peak, the model simulations were disappointing, as they underestimated the flow peak significantly. Further model development may overcome some of these deficiencies, though it is worth noting that the parameter-generalised PDM also underestimated the flow peak for this event, as shown in Figure D.11. However, the standard PDM, which had been calibrated to this catchment, performed rather better, indicating that poor model performance could not entirely be attributed to error in the rainfall estimates.
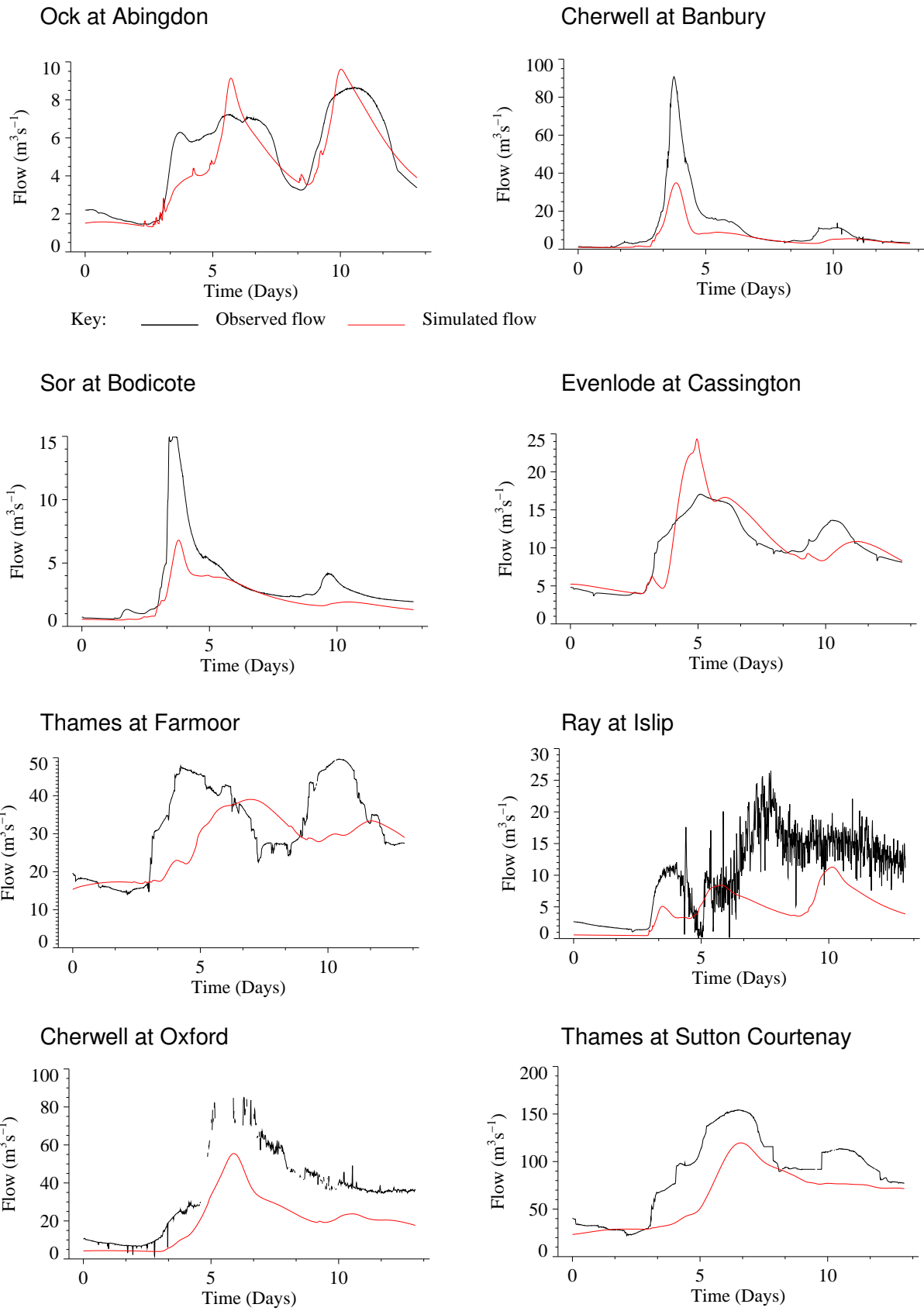
Figure D.29 Flow hydrographs for the Thames catchments comparing model performance obtained from the enhanced G2G model: 6-19 April 1998

Figure D.30 Flow hydrographs for the Stour to Shipston comparing model performance obtained from the enhanced G2G model: 6-19 April 1998

D.8 Calibrated PDM parameters

For completeness, this section lists the PDM parameters calibrated at each river gauging station site in the case study catchments. The performance of the flow simulations using these parameters have served as a useful benchmark when assessing the various ungauged methods illustrated here.

Table D.21 Calibrated PDM model parameters: River Kent catchments

Parameter name	Catchment				
	Bowston	**Sprint**	**Mint**	**Victoria**	**Sedgwick**
Rainfall factor					
f_c	1.010	0.963	0.980	0.930	0.913
Time Delay					
τ_d	2.151	1.890	1.301	2.192	2.156
Soil Moisture					
c_{min}	35.9	27.1	31.3	25.0	26.9
c_{max}	80.2	70.3	69.46	65.41	64.06
b	1.342	1.995	1.918	2.085	1.743
Evaporation function					
b_e	2.5	2.5	2.5	2.5	2.5
Recharge function					
k_g	2140	1203	1483	1007	1495
b_g	2.093	2.183	2.015	2.205	2.156
S_t	26.55	22.65	20.61	19.87	18.43
Surface routing					
k_1	7.568	5.699	6.791	7.816	6.417
k_2	0.017	0.008	0.005	0.137	1.236
Base flow storage (cubic)					
k_b	53.53	31.99	50.87	55.00	54.38
Returns/abstractions					
q_c	0.276	0.276	0.179	0.814	0.946

Table D.22 Calibrated PDM model parameters: River Darwen catchments

Parameter name	Catchment	
	Blue Bridge	**Ewood**
Rainfall factor		
f_c	1.110	1.100
Time Delay		
τ_d	1.211	0.280
Soil Moisture		
c_{min}	0	0
c_{max}	27.595	41.06
b	0.335	0.306
Evaporation function		
b_e	2.5	2.5
Recharge function		
k_g	302.9	628.0
b_g	1.650	1.571
S_t	5.0	5.0
Surface routing		
k_1	4.103	3.039
k_2	0.937	0.524
Base flow storage (cubic)		
k_b	32.70	0.004
Returns/abstractions		
q_c	0	0

Table D.23 Calibrated PDM model parameters: Upper Thames and Stour catchments

Parameter name	Catchment		
	Stour at Shipston	Sor at Bodicote	Cherwell at Banbury
Rainfall factor			
f_c	0.840	1.000	0.900
Time Delay			
τ_d	3.120	9.000	3.000
Soil Moisture			
c_{min}	0.0	20.0	20.0
c_{max}	84.8	225.0	90.0
b	0.340	0.350	0.300
Evaporation function			
b_e	2.5	2.5	2.5
Recharge function			
k_g	97596	80000	10000
b_g	2.240	1.900	1.500
S_t	0.00	60.0	40.0
Surface routing			
Cascade of 2 linear reservoirs			
k_1	6.080	N/A	5.000
k_2	6.080	N/A	25.000
A single cubic store			
k_1	N/A	25.000	N/A
Base flow storage (cubic)			
k_b	5.0	300.0	25.0
Returns/abstractions			
q_c	0.000	0.000	0.000

D.9 Closing remarks on methods for model transfer to ungauged catchments

The results from the case studies highlight that, for catchments with a simple response, PDM model transfer can be quite successful using informal transfer of model parameters from a "similar" catchment. Knowledge of catchment form and response can be very useful in guiding the choice of "donor" catchment judged to be similar to the "target" catchment; spatial proximity may not be important. Also, empirical regionalisation methods (regression or site-similarity) used with a reduced-form PDM can be successfully used for transfer to ungauged basins having a very simple flood response, such as is the case for the Kent catchments. Results for the Darwen catchment, however, suggest that the performance can be much worse than using the standard PDM (but with calibration). Application of the regionalisation methods is straightforward. Regression and site-similarity approaches to parameter estimation can give rather different results and it is worth comparing them. Catchments with a "simple response" are typically upland catchments where topographic controls dominate flood hydrograph formation and soil/geology controls act in an homogeneous way or are weak.

The success of using a single set of regional parameters in the Grid-to-Grid model to forecast river flows at all 5 sites in the Kent catchment highlights the appeal of this area-wide model: a model that can be used to forecast at all locations within the modelled domain. It achieves comparable performance to the standard PDM calibrated at each site in the very simply responding Kent catchment.

Lowland basins can be very challenging to model transfer, particularly where heterogeneous soils and geology dominate over topographic controls on flood response. A search for a suitable "similar" donor catchment may prove difficult and the results of model transfer can be unreliable. Trial transfers using gauged catchments can help guide the choice of donor catchment and give an indication of confidence in the likely success.

The Stour catchment is a simpler, quicker responding lowland basin and informal transfer of the Kent (at Sedgwick, and of similar area: circa 200 km^2) PDM parameters proves remarkably successful. The more complex and slowly responding Upper Thames catchments (Cherwell at Banbury and Sor at Bodicote), whilst in close proximity, reveal contrasting behaviours reflecting differences in areal extent and soil/geology controls. The Sor is most different with the slowest response and smallest area (circa 100 km^2).

Use of a common set of regional parameters by the simple Grid-to-Grid model served to highlight the differences in response of these two upper Thames catchments. This contrast pointed to the need for an enhanced model incorporating soil/geology control in addition to topographic control. Catchment-specific calibration of the Grid-to-Grid Model achieved comparable performance to the standard PDM, but pointed to the difficulty of model transfer. Application of the parameter-generalised PDM to these two catchments achieves mixed success, being quite good for the Sor but only moderate for the Cherwell (results for the Easter 1998 "evaluation event" are difficult to interpret because of its extreme nature and hydrometric measurement uncertainties).

A prototype Grid-to-Grid Model, enhanced to have a runoff production component capable of exploiting soil datasets, achieved some stabilisation of performance using a

single regional parameter set across the two catchments. Whilst the performance for the Cherwell was better than the parameter-generalised PDM (R^2 of 0.59 compared to 0.53) this was not the case for the Sor (R^2 of 0.68 compared to 0.83) whilst the site-calibrated standard PDM gave the best R^2 performance of 0.75 for the Cherwell and 0.91 for the Sor. However, the parameter-generalised PDM for the Sor performed worst of all for the extreme "Easter 1998" evaluation event. The soil properties for the Cherwell and Sor highlight the differences between the two catchments (Table D.18). On average, the soil depth is almost twice as deep for the Sor (78 compared to 43 cm), the saturated hydraulic conductivity twice as fast (118 compared to 53 cm/day) and the maximum soil water content almost twice as large (39 compared to 22 cm). The larger water storage capacity per unit area of the Sor is clearly responsible for its slower response, despite the catchment area being half that of the Cherwell (circa 88 compared to 200 km^2). It is the deep soil depth in the Sor catchment, rather than differences in porosity, that dominate the different hydrograph responses of the two catchments.

In terms of HOST class, the Sor is largely Class 2 (SPRHOST=2%, BFIHOST=1) whilst the Cherwell is largely Class 25 (SPRHOST=49.6%, BFIHOST=0.17), highlighting the contrasting soil classes for the two catchments (see Figure D.21). This information is coming through to the parameter-generalised PDM using regression primarily via SPRHOST, which determines the surface-runoff/baseflow partition parameter α and partially determines $c_{\max}$ and k_1; BFIHOST exerts some influence on k_b. Note that using BFIHOST to determine α would seem a more natural choice; use of SPRHOST implies a volume adjustment that is the purpose of f_c, the rainfall factor. Seeking physical insights using these HOST class associations to catchment descriptors is not straightforward, lacking a physical basis for interpretation. Note that hydrogeology and drift information given for both catchments in the National Surface Water Archive are similar and described largely as very low permeability with little drift cover.

Improved use of soil and geology datasets in forms of model like the extended Grid-to-Grid model, developed here only in prototype form, is seen as deserving further research leading to operational implementation. The case study of the Upper Thames and Stour catchments, embracing 11 target catchments, demonstrates how easily and widely the model can be applied to address the ungauged forecasting problem at any location within the chosen modelled domain.

We are The Environment Agency. It's our job to look after your environment and make it **a better place** – for you, and for future generations.

Your environment is the air you breathe, the water you drink and the ground you walk on. Working with business, Government and society as a whole, we are making your environment cleaner and healthier.

The Environment Agency. Out there, making your environment a better place.